


5-1-2016

Perchlorate Bioremediation: Controlling Media Loss in Ex-Situ Fluidized Bed Reactors and In-Situ Biological Reduction by Slow-Release Electron Donor

Sichu Shrestha

University of Nevada, Las Vegas, sichu103@gmail.com

Follow this and additional works at: <https://digitalscholarship.unlv.edu/thesesdissertations>

 Part of the [Civil Engineering Commons](#), and the [Environmental Engineering Commons](#)

Repository Citation

Shrestha, Sichu, "Perchlorate Bioremediation: Controlling Media Loss in Ex-Situ Fluidized Bed Reactors and In-Situ Biological Reduction by Slow-Release Electron Donor" (2016). *UNLV Theses, Dissertations, Professional Papers, and Capstones*. 2744.
<https://digitalscholarship.unlv.edu/thesesdissertations/2744>

This Dissertation is brought to you for free and open access by Digital Scholarship@UNLV. It has been accepted for inclusion in UNLV Theses, Dissertations, Professional Papers, and Capstones by an authorized administrator of Digital Scholarship@UNLV. For more information, please contact digitalscholarship@unlv.edu.

PERCHLORATE BIOREMEDIATION: CONTROLLING MEDIA LOSS IN EX-SITU
FLUIDIZED BED REACTORS AND IN-SITU BIOLOGICAL REDUCTION BY SLOW-
RELEASE ELECTRON DONOR

By

Sichu Shrestha

Bachelor of Engineering in Civil Engineering,
Institute of Engineering, Tribhuvan University, Nepal
2004

Master of Science in Civil and Environmental Engineering
Carnegie Mellon University
2011

A dissertation submitted in partial fulfillment
of the requirements for the

Doctor of Philosophy- Civil and Environmental Engineering

Department of Civil and Environmental Engineering and Construction
Howard R. Hughes College of Engineering
The Graduate College

University of Nevada, Las Vegas
May 2016

Copyright 2016 by Sichu Shrestha
All Rights Reserved



Thesis Approval

The Graduate College
The University of Nevada, Las Vegas

April 21, 2016

This thesis prepared by

Sichu Shrestha

entitled

Perchlorate Bioremediation: Controlling Media Loss in Ex-Situ Fluidized Bed Reactors
and In-Situ Biological Reduction by Slow-Release Electron Donor

is approved in partial fulfillment of the requirements for the degree of

Doctor of Philosophy- Civil and Environmental Engineering
Department of Civil and Environmental Engineering and Construction

Jacimaria R. Batista, Ph.D.
Examination Committee Chair

Kathryn Hausbeck Korgan, Ph.D.
Graduate College Interim Dean

Daniel Gerrity, Ph.D.
Examination Committee Member

Sajjad Ahmad, Ph.D.
Examination Committee Member

David James, Ph.D.
Examination Committee Member

Eduardo A. Robleto, Ph.D.
Graduate College Faculty Representative

ABSTRACT

The main concern of perchlorate exposure through drinking water is its effects on the production of thyroid hormone, which is important for human metabolism and child's brain development. The US Environmental Protection Agency (EPA) has listed perchlorate in the contaminant list as well as in the Unregulated Contaminant Monitoring rule.

The extent of perchlorate contamination can be categorized by the level of contamination into parts per million (ppm) levels, typically in locations where perchlorate was manufactured, and parts per billion (ppb) levels where perchlorate was used for various purposes. Ion-exchange is generally adopted for treating ppb levels of perchlorate while biological reduction, bioremediation, is preferred for treating ppm level contamination.

This dissertation focuses on two important but not completely researched issues related to ex-situ and in-situ perchlorate biodegradation: (a) Use of digital image as a tool to determine appropriate backwashing frequency for fluidized bed reactor (FBR) used to treat perchlorate contaminated waters, (b) Feasibility of using a slow release electron donor, emulsified oil, to support in-situ degradation of perchlorate in groundwater with slow and fast hydraulic conductivities.

To address the first issue, two FBRs were built using five feet long and half inch diameter transparent plexiglass columns. Activated carbon was used as media and synthetic solutions containing 100 ppb, 100 ppm, and 10 ppm perchlorate were used. A high resolution camera was mounted targeting the operating zone of the FBR and pictures were taken at interval of 1.5 hours. The digital pictures were analyzed using the image processing tool, ImageJ. A biofilm model was developed and its simulated results were used to determine theoretical frequencies to backwash the filters so to avoid media loss. To address the second issue, four 5-foot long and

2.5-inch diameter column bioreactors were used to simulate saturated groundwater zones with fast and slow groundwater velocities. Soil and plastic rings were used as media to simulate slow and fast velocities, respectively.

The results revealed that the biofilm model predicted backwashing times that were very close to those observed using digital imaging. For the first FBR run, backwashing time forecasted using biomass growth, in perchlorate fed batch bioreactors, was in agreement with the other two methods used. However, the biomass growth data was unable to simulate similar backwashing for the second and third runs in the FBRs.

The result of FBR operation indicates that images processed with the ImageJ closely represented the height of the expanded media in the FBR, and hence it can be used to decide backwashing frequency. A good agreement was found between the backwashing needs encountered in the FBR runs and those forecasted using the biofilm model.

For the testing of slow release electron donor, emulsified oil was proven to be an effective slow release electron donor to degrade nitrate and perchlorate in saturated groundwater zones. The removal of perchlorate required acclimation time while nitrate degraded almost immediately. Perchlorate degradation was highly impacted by high hydraulic conductivities (i.e. smaller contact time). Perchlorate degradation commenced after nitrate levels decreased to less than 0.5 mg/L. On the other hand, once a significant amount of biomass has been built into the system, degradation of both perchlorate and nitrate took place. It was found that the extent of degradation is dependent upon the relative amounts of perchlorate and nitrate present, the amount of electron donor present, and the residence time.

ACKNOWLEDGEMENTS

I would like to first and foremost thank my supervisor, Dr. Jacimaria Batista, for her inspiration and encouragement throughout this study. My work would not have been what it is now without her guidance and support. She has provided immense support and motivation during the entire course of my graduate study.

I would like to extend my sincere gratitude and appreciation to my committee members, Dr. Sajjad Ahmad, Dr. Daniel Gerrity, Dr. David James, and Dr. Eduardo Robleto for their constructive and invaluable suggestions to finalize my work. I am very grateful to Mr. Peter Fraught for his assistance in the laboratory and for helping me with the experimental set-up. I would like to mention Ms. Julie Bertoia and Winnie David for their support and help. I am thankful to Mr. R. Marsh Starks for his assistance in setting up the camera.

I would like to appreciate the support and opportunities that I received as a graduate student at UNLV, from the entire Civil and Environmental Engineering and Construction family, and also to the Fulbright S&T for the opportunity and supporting my study. My gratitude is to the Southern Nevada Water District for giving me the opportunity to work as intern, and learn about the emerging contaminants and other challenges that a drinking water sector is facing.

I want to thank all my colleagues of Environmental Laboratory for their direct or indirect contributions and encouragement. Special thanks go to Erica, Mayra, Kazim, Mennah, Charles, Olivier, Yesika, Miguel, Bany and Caroline. It was pleasure working with you all. Thanks to the Nepalese community in Las Vegas for making me feel at home and giving me a memorable time at UNLV.

Last but not the least; I would like to thank all my family members for their love and blessings. No words can express my gratitude to my parents, in-law parents, Mr. Gyanendra

Khadka and Ms. Naradevi Shrestha Khadka, sister Dr. Sinora Shrestha Joshi, brother in-law, Dr. Biswas Joshi, and in-law brother, Milan Khadka, for their support and constant inspiration to work harder. Special thanks to my husband, Mr. Mukesh Khadka, for being patient and supportive throughout this journey. It would not have been possible without his help and moral support. To my daughter, Aadya Khadka, thank you for being such an understanding and wonderful little girl. My words cannot convey suffice her efforts to cheer me up, give me hope and unconditional love, and her patience to give me the time I needed to complete my work. To my nephew, Aryav Joshi, your smile is the world best stress-busters for me.

Lastly, I would like to dedicate this work to my parents who gave their all to make me who I am today.

TABLE OF CONTENTS

ABSTRACT.....	iii
ACKNOWLEDGEMENTS.....	v
TABLE OF CONTENTS.....	vii
LIST OF TABLES.....	xi
LIST OF FIGURES.....	xiii
LIST OF ACRONYMS.....	xvi
CHAPTER 1 PROBLEM STATEMENT.....	1
1.1 Background.....	1
1.2 Objectives and Hypotheses.....	4
CHAPTER 2 STATE OF KNOWLEDGE.....	6
2.1 Perchlorate Contamination Sites - Case Studies.....	6
2.1.1 Basic Management Industrial Complex, Nevada.....	6
2.1.2 Naval Weapons Industrial Reserve Plant, McGregor, Texas.....	7
2.1.3 Equivalent Hydraulic Conductivity at Sites with Multiple Strata.....	9
2.2. Biodegradation of Perchlorate.....	12
2.2.1 Perchlorate Reducing Bacteria (PRB).....	17
2.2.2 Enzymes Involved in Perchlorate Reduction.....	19
2.2.3 Molecular Tools for Identification of PRB.....	23
2.3 Thermodynamics, Biochemical Reactions, and Microbial Kinetics of Perchlorate Degradation Pathway.....	31
2.3.1 Thermodynamics of Perchlorate Reduction Pathway.....	31
2.3.2 Microbial Kinetics of the Reduction Pathway.....	34
2.3.3 Biochemical Reactions and Stoichiometry Involved in the Reduction Process	38
2.4 Denitrification.....	40
2.5 Factors Affecting Perchlorate Reduction Pathway.....	42
2.5.1 Effect of Electron Donor.....	42
2.5.2 Effect of Competition of Other Electron Acceptors.....	43
2.5.3 Salinity.....	48
2.5.4 Temperature and pH.....	50
2.6 Ex-situ Treatment with Fixed Film Biological Reactors.....	51
2.6.1 Fixed Film Reactors for Perchlorate Reduction.....	51
2.6.2 Backwashing in a FBR.....	54
2.7 Biofilm Modeling for a FBR.....	56

2.7.1 Biofilm Detachment.....	62
2.7.2 Biofilm Density and Thickness.....	65
2.7.3 Substrate Transport Mechanism in Biofilm.....	68
2.7.4 Components of Biofilm Model.....	68
2.7.5 Test of the Model.....	71
2.8 Available Technology to Measure Particles in Water.....	72
2.8.1 Image Processing Technique in Drinking Water.....	75
2.8.2 Image Processing Software, ImageJ.....	75
2.9 Electron Donor for In-situ and Ex-situ Bioremediation.....	76
2.9.1 Biodegradation of Vegetable Oils.....	77
2.9.2 Emulsified Oil Substrate as Slow Release Electron Donor.....	80
CHAPTER 3 METHODOLOGY.....	83
3.1 Enrichment of Perchlorate-Reducing Culture.....	83
3.1.1 Identification of Perchlorate-Reducing Bacteria.....	85
3.1.2 Comparison of High and Low Concentration Kinetics of Culture.....	86
3.2 Ex-situ Perchlorate Bioremediation with a FBR.....	87
3.2.1 PBR Inoculation in the FBR.....	87
3.2.2 FBRs Operation.....	88
3.2.3 Image Processing as Tool for Determination of Backwashing Period.....	89
3.2.4 Biomass Measurement.....	90
3.2.5 Microbial Analysis.....	90
3.3 In-situ Perchlorate Bioremediation Approach.....	91
3.3.1 Preliminary Tests.....	93
3.3.2 Microcosm Testing of Perchlorate Degradation by Indigenous Microbes in Soil from the Contaminated Site.....	95
3.3.3 Operation of Soil and Plastic Bioreactor Columns.....	96
3.3.4 Sampling.....	98
3.3.5 Microbial Analysis.....	99
3.4 Analytical Methods.....	99
3.4.1 Total Suspended Solids, Turbidity, and Optical Density.....	100
3.4.2 pH.....	100
3.4.3 Nitrate Concentration.....	100
3.4.4 Perchlorate Concentrations.....	101
3.5 Quality Assurance/Quality Control.....	101
CHAPTER 4 BIOLOGICAL REDUCTION OF PERCHLORATE AND CO- CONTAMINANTS USING EMULSIFIED OIL AS AN ELECTRON DONOR.....	105
4.1 Introduction.....	105
4.2 Methodology.....	109

4.2.1 Source of Soil Samples and Characterization.....	109
4.2.2 Contaminant Concentration in Soil Samples.....	110
4.2.3 Preliminary Column Bioreactors Testing Using Soils and Groundwater from the Site.....	112
4.2.4 Microcosm Testing of Perchlorate Degradation by Indigenous Microbes in Soil from the Contaminated Site.....	113
4.2.5 Operation of Column Bioreactors Using Soil and Plastic Media.....	114
4.2.6 Effect of Nitrate on Perchlorate Biodegradation in the Column Bioreactors....	117
4.2.7 Sampling.....	117
4.2.8 Microbial analysis.....	118
4.3 Results.....	119
4.3.1 Microcosm Testing for Perchlorate and Nitrate Using Emulsified Oil.....	119
4.3.2 Emulsified Oil Release from Column Bioreactor Packed with Contaminated Soils.....	121
4.3.3 Biodegradation of Nitrate and Perchlorate in Soil Column Bioreactors	126
4.3.4 Biodegradation of Nitrate and Perchlorate in Plastic Columns Bioreactors.....	130
4.4 Conclusions.....	137

CHAPTER 5 EVALUATION OF IMAGE PROCESSING AS A TOOL TO FORECAST BACKWASHING FREQUENCY IN FLUIDIZED BED REACTORS (FBR) TREATING PERCHLORATE CONTAMINATED WATER.....	140
5.1 Introduction.....	140
5.2 Methodology.....	143
5.2.1 Enrichment of Perchlorate-Reducing Culture.....	144
5.2.2 Identification of Perchlorate-Reducing Bacteria.....	146
5.2.3 Comparison of High and Low Concentration Kinetics of Culture.....	147
5.2.4 Biofilm Thickness Measurement Using Biomass.....	147
5.2.5 FBR Operation and Digital Imaging for Backwashing Forecast.....	148
5.2.6 Microbial Analysis.....	151
5.2.7 Analytical Methods.....	152
5.2.8 Quality Assurance/Quality Control.....	154
5.3 Results.....	157
5.3.1 Characterization of Bacterial Community.....	157
5.3.2 Perchlorate Reduction at High (ppm) and Low (ppb) Concentrations by the Enrichment Culture in Batch Reactors.....	163
5.3.3 Test of Biofilm Model to Determine Backwashing of FBR Based on Biofilm Kinetics.....	165
5.3.4 Preliminary Test to Estimate Biofilm Thickness Using Biomass Growth in Bioreactors.....	167

5.3.5 Perchlorate Removal in FBR: Use of Image Processing for Determining Backwash Time Coupled with Biofilm Model.....	169
5.3.6 FBR Backwashing Frequency and Media Loss Evaluation Using Image Processing Technique.....	174
5.3.7 Test of Biofilm Model to Determine Backwashing of FBR based on Image Analysis of Media Flootation in FBR.....	176
5.4 Conclusions.....	178
6. CONCLUSIONS AND RECOMMENDATIONS.....	180
6.1 Conclusions.....	180
6.2 Recommendations for Future Research.....	183
REFERENCES.....	184
APPENDIX A CALCULATION OF STOICHIOMETRIC EQUATION.....	208
APPENDIX B CULTURE DEVELOPMENT.....	210
APPENDIX C OPTICAL DENSITY VS TOTAL SUSPENDED SOLIDS.....	211
APPENDIX D GAC TESTS.....	212
APPENDIX E FBR REACTOR DESIGN.....	216
APPENDIX F COLUMN BIOREACTOR DESIGN FOR TESTING SLOW RELEASE ELECTRON DONOR (EMULSIFIED OIL).....	224
APPENDIX G BATCH TESTS.....	227
APPENDIX H IDENTIFIED LIST OF BACTERIA.....	228
APPENDIX I REPORTED KINETICS AND EFFECT OF ELECTRON ACCEPTORS ON THE PERCHLORATE REDUCING BACTERIA, AND TYPES OF REACTORS USED IN PERCHLORATE BIOREMEDIATION FROM LITERATURE.....	242
APPENDIX J CHECKING THICKNESS OF THE BIOFILM.....	249
CURRICULUM VITAE.....	251

LIST OF TABLES

Table 2.1: Typical Values of Hydraulic Conductivities for Different Soil Type.....	11
Table 2.2: Hydraulic Conductivities Corresponding to the Flow Rates of the Experimental Column.....	12
Table 2.3: Sources Used for Isolating Perchlorate Reducing Microorganisms.....	14
Table 2.4: Molecular Tools.....	28
Table 2.5: Reported Gibbs' Free Energy (ΔG°) for Various Electron Acceptors (oxygen, chlorate, nitrate, perchlorate, and sulfate), Coupled with Electron Donors (acetate, hydrogen and sulfur).....	32
Table 2.6: Kinetic Parameters of Pure/Mixed Cultures Used for Perchlorate Reduction from Literature.....	36
Table 2.7: Stoichiometric Reactions Reported for Acetate (Electron Donor) with Various Electron Acceptors (Oxygen, Nitrate, Perchlorate, and Chlorate).....	39
Table 2.8: Effects of Other Electron Acceptor on Perchlorate Degradation.....	44
Table 2.9: Reported Effects of Salinity on Perchlorate Degradation.....	49
Table 2.10: Effect of Temperature and pH on Perchlorate Reduction.....	50
Table 2.11: Configuration of Reported Reactors Used for Perchlorate Removal.....	53
Table 2.12: Characteristic Lengths Delineating a Biofilm.....	65
Table 2.13: Reported Variation of Biofilm Thickness and Biofilm Density.....	66
Table 2.14: Reported Biofilm Thickness and Biofilm Density.....	66
Table 2.15: Estimation of Biofilm Parameters Used for Biofilm Model.....	69
Table 2.16: Input Parameters for Biofilm Modeling.....	70
Table 2.17: Suspended Solid Sensors and Probes Used to Detect Particles in Water.....	73
Table 2.18: Hydrogen Release by Biodegradation of Oils and Other Substrate.....	79
Table 2.19: Hydrogen and Oil Demand for the Electron Acceptors.....	80
Table 2.20: COD Concentrations for Electron Donors Used in Bioremediation Tests Measure.....	82
Table 3.1: Chemicals Used for Enriching the Perchlorate Reducing Culture.....	84
Table 3.2: Amount of Enrichment Solution, Washed Culture, and DI Water for Batch Test.....	86
Table 3.3: Permeability Test with Soil Mixed at Different Percent.....	95
Table 3.4: Parameters Analyzed and Analysis Frequency.....	98
Table 3.5: Analytical Methods and Equipment Used for Analyzing Samples.....	99

Table 3.6: Standards and Conditions for IC.....	101
Table 3.7: Accuracy, Precision, Detection Limit and R^2 of the Methods Opted for Various Parameters.....	104
Table 4.1: Composition of Soil Extracts from the Contaminated Site.....	111
Table 4.2: Parameters Analyzed and Analysis Frequency.....	118
Table 4.3: Percent Removals of Nitrate and Perchlorate in Soil Columns During Different Operation Periods.....	127
Table 4.4: Percent Removals of Nitrate and Perchlorate in Plastic Columns During Different Operation Periods.....	131
Table 5.1: Analytical Methods and Equipment Used for Analyzing Samples.....	152
Table 5.2: Standards and Conditions for IC.....	154
Table 5.3: Accuracy, Precision, Detecting Limit, and R^2 of the Methods Opted for Various Parameters.....	157
Table 5.4: Bacterial Community in PRB Culture Enriched in UNLV Environmental and Water Quality Laboratory.....	158
Table 5.5: Bacterial Community on the FBR Media.....	162

LIST OF FIGURES

Figure 1.1: Hydraulic and microbial expansion of media in ex-situ bioremediation using a FBR.....	3
Figure 2.1: The ground water contamination site (BMI) at Henderson, NV.....	6
Figure 2.2: The groundwater contamination site in Texas.....	8
Figure 2.3: Equivalent hydraulic conductivity in a multiple layer area.....	10
Figure 2.4: Microbial perchlorate degradation pathway indicating complete perchlorate reduction into chloride and oxygen in presence of acetate as energy and carbon source.....	16
Figure 2.5: Periplasmic enzymes, perchlorate reductase, and chloride dismutase involved in perchlorate reduction.....	19
Figure 2.6: Proposed perchlorate reduction model by the periplasmic perchlorate reductase and chlorite dismutase in gram negative perchlorate reducing bacteria.....	22
Figure 2.7: Molecular tools commonly used to identify microbes present in an environmental sample.....	25
Figure 2.8: Graph obtained from qPCR of a sample containing three microbial DNA.....	29
Figure 2.9: E. coli plasmid vector showing an insert that terminates the lacZ expression....	30
Figure 2.10: The biological nitrogen cycle pathway.....	40
Figure 2.11: Schematic representation of biomass growth in media.....	57
Figure 2.12: Conceptual biofilm model showing substrate diffusion into biofilm.....	58
Figure 2.13: GAC with a biofilm of thickness t	71
Figure 2.14: Biofilm thickness estimated using experimental biomass growth in batch bioreactors and the model developed for perchlorate as the sole electron acceptor.....	72
Figure 2.15: Biological degradation of vegetable oil	78
Figure 3.1: Perchlorate-reducing culture (master culture) enriched from returned activated sludge (a) and Sub-culture enriched from the master culture (b).....	83
Figure 3.2: Flowchart of molecular tools to identify bacteria present in the enriched culture and check the phylogenic closeness to the known PRB (KJ).....	85
Figure 3.3: Experimental set-up for batch test sampled at 2, 4, 6, 8, 10, 17, 24, 30, and 45 hours	87
Figure 3.4: Schematic diagram of inoculation of the culture for a week (a), and operation of the reactor (Ex-situ treatment) (b).....	88

Figure 3.5: Snap shots from the phase contrast microscopy, showing bacteria, extracellular polymerase, and eukaryotic organisms.....	91
Figure 3.6: Schematic diagram of the column set-up for (In-situ treatment) (a), Groundwater quality (b), Properties of EOS-PRO measured at the Environmental laboratory, UNLV (c), and Plastic media used in the column (d).....	92
Figure 3.7: Soil profile with soil particle size and characteristics (a), and Physical properties and Chemical constituents of soil extract at 25-30 feet and 35-40 feet depths (Soil Laboratory, UNLV, 2015) (b).....	94
Figure 3.8: Soil and plastic samples collected for microbial analysis.....	99
Figure 4.1: The ground water contamination site at the BMI, Henderson, NV.....	107
Figure 4.2: Soil profile with soil particle size and (a), Physical properties and Chemical constituents of soil extract at 25-30 feet and 35-40 feet depths (Soil Laboratory, UNLV, 2015) (b), and Results of permeability test (Soil Laboratory, UNLV, 2015) (c).....	110
Figure 4.3: Schematic diagram of the set-up (a), Groundwater quality (b), Properties of EOS-PRO measured at the Environmental laboratory, UNLV (c), and Plastic media used in the column (d).....	115
Figure 4.4: Nitrate and perchlorate removal in microcosms tested with EO and glycerol as electron donors.....	119
Figure 4.5: Percent removals of perchlorate and nitrate in the microcosms with (i) EO, (ii) EO and Phosphorus, and (iii) EO, Glycerol, and Phosphorus within the ten-day study period.....	121
Figure 4.6: Effluent nitrate (a) and perchlorate (b) concentrations throughout the study period (130 days).....	123
Figure 4.7: Effluent nitrate and COD concentrations over time for the first EO addition with 7 mg/L average influent nitrate concentration (a) and second EO addition with 27 mg/L average influent nitrate concentration (b).....	125
Figure 4.8: Ratio of effluent COD measured (mg) to mass of COD in the feed water.....	126
Figure 4.9: Nitrate removals as mg-N/d in soil columns for the first EO addition (a) and second EO addition (b).....	129
Figure 4.10: Perchlorate removals as mg/d in soil columns for the first EO addition (a) and second EO addition (b).....	130
Figure 4.11: Effluent nitrate concentration (a) and perchlorate concentration (b) in the plastic column bioreactors.....	132
Figure 4.12: Mass removals of nitrate (a) and perchlorate (b) in the plastic columns 1 and 2 during operation days 24 to 91.....	134

Figure 4.13: Effluent nitrate concentration (a) and perchlorate concentration (b) in the plastic columns 1 and 2 during addition of nitrate period.....	136
Figure 5.1: Hydraulic and microbial expansion of media in ex-situ bioremediation using a FBR.....	143
Figure 5.2: Experimental set-up for operating two FBRs with camera mounted to take pictures.....	144
Figure 5.3 Perchlorate-Reducing Culture (master culture) enriched from returned activated sludge (a) and Sub-Culture enriched from the master culture (b).....	145
Figure 5.4: Flowchart of molecular tools to identify the bacteria present in the enriched culture and check the phylogenic closeness to the known PRB (KJ).....	146
Figure 5.5: Schematic diagram of inoculation of the culture for a week (a) and operation of the reactor (Ex-situ treatment) (b).....	149
Figure 5.6: Snap shots from the phase contrast microscopy showing bacteria, extracellular polymerase, and eukaryotic organisms.....	152
Figure 5.7: Bacteria under proteobacteria phylum identified in the culture enriched at the UNLV-Environmental Engineering and Water Quality Laboratory.....	159
Figure 5.8: Electrophoresis gel ran for PCR products to identify presence of perchlorate reductase.....	160
Figure 5.9: Bacteria at species level in the GAC FBR media fed with varying perchlorate concentrations.....	163
Figure 5.10: Residual perchlorate concentration for 100 ppm and 100 ppb batches with time.....	164
Figure 5.11: Biofilm thickness computed by the model for perchlorate, as the sole electron acceptor, at concentrations 100 ppm, 100 ppb, and 10 ppm.....	166
Figure 5.12: Biofilm thickness estimated from biomass growth on GAC media due to perchlorate degradation (100 mg/L).....	169
Figure 5.13: Average percent perchlorate removal in both FBRs for 100 ppm, 100 ppb, and 10 ppm for overall period	172
Figure 5.14: Average perchlorate effluent concentration (bars) in the FBRs operated at 100 ppm (a), 100 ppb (b), and 10 ppm (c) with average influent (horizontal line), pump head failures (arrows), and backwash (lines).....	173
Figure 5.15: Final analyzed pictures of the operating zone using ImageJ.....	174
Figure 5.16: Percent area available for media expansion in the operating depth against time for FBRs operated at 100 ppm (a), 100 ppb (b), and 10 ppm (c).....	176
Figure 5.17: Biofilm thickness (cm) estimated using model, and actual biofilm thickness computed from biomass to obtain the appropriate backwash time.....	177

LISTS OF ACRONYMS

Acronym	Description
ADCP	Acoustic Doppler Current Profiler
ADV	Acoustic Doppler Velocimetry
BMI	Basic Management Industrial
BOD	Biological Oxygen Demand
COD	Chemical Oxygen Demand
DO	Dissolved Oxygen
EBCT	Empty Bed Contact Time
EO	Emulsified Oil
EPA	Environmental Protection Agency
FBR	Fluidized Bed Reactor
GAC	Granular Activated Carbon
HRT	Hydraulic Residence Time
IX	Ion-Exchange
LCFA	Long-Chain Fatty Acids
OD	Optical Density
PCR	Polymerase chain reaction
ppb	Parts-Per-Billion
ppm	Parts-Per-Million
PRB	Perchlorate Reducing Bacteria
qPCR	Quantitative Polymerase Chain Reaction
TDS	Total Dissolved Solids
TOC	Total Organic Carbon
TSS	Total Suspended Solid
UNLV	University of Nevada, Las Vegas

CHAPTER 1

PROBLEM STATEMENT

1.1 Background

Perchlorate (ClO_4^-) is a contaminant of concern for drinking water and has been widely detected in the United States (US), particularly in the Southwest region. Ground and surface water are contaminated with perchlorate due to anthropogenic production of perchlorate salts used in pyrotechnics and rocket fuel as a solid propellant (Batista et al., 2003; Kesterson et al., 2007). Naturally formed perchlorate also has been found in nitrate deposits in arid area, such as Chile and Antarctic Dry Valleys, and the southern high plains of the US, where perchlorate has never been used (Ericksen, 1981; Kounaves et al., 2010; Dasgupta et al., 2005).

Perchlorate interferes with production of thyroid hormone, which is important for human metabolism and child's brain development (Ginsberg et al., 2007). Therefore, the US Environmental Protection Agency (EPA) has listed perchlorate on the contaminant list as well as in the Unregulated Contaminant Monitoring Rule. Even though several states, such as California and Massachusetts, have regulated perchlorate levels in drinking water, no federal standard for perchlorate exists (Sellers, 2007).

Ion-exchange (IX) and biological reduction are the most commonly used technologies for perchlorate removal from water. IX is generally adopted for treating drinking water with perchlorate concentrations at parts-per-billion (ppb) levels due to its simplicity for implementation and operation. Biological reduction is preferred for treating water which is not intended for drinking and contains perchlorate and other co-contaminants at concentrations of parts-per-million (ppm). However, the State of California has recently approved conditional use

of biological reduction for perchlorate removal from drinking water (WVWD, 2012). A large Fluidized Bed Reactor (FBR) plant is now under construction in Rialto, CA (Envirogen, 2011). In biological reduction, bacteria use perchlorate as an electron acceptor in presence of an electron donor and convert it to innocuous chloride (Cl^-) without any residual waste (Kijung and Logan, 2000).

The largest perchlorate-contaminated site in the US is in the Basic Management Industrial (BMI) area in Henderson, Nevada. Perchlorate used for various purposes was produced at this site for the entire nation since the 1940s by the Kerr-McGee Corporation and the Pacific Engineering and Production Company of Nevada. Perchlorate-laden industrial wastes disposed into unlined ponds contaminated the groundwater (Batista et al., 2003). In 1997, perchlorate was discovered in the Lower Colorado River and also traced back to the Las Vegas Wash (NDEP, 2011). Since its discovery, various measures have been taken to confine and treat the perchlorate plumes as well as to avoid contamination of Lake Mead and the Colorado River (NDEP, 2011). In the beginning, a temporary IX treatment system was installed, which was replaced by a FBR with granular activated carbon (GAC) as media and ethanol as an electron donor. Despite being highly biodegradable, the perchlorate persisted to date in the BMI groundwater because of the lack of electron donors (Batista et al., 2003).

In FBR, bacteria – which grow on the media as a thick film – reduce perchlorate to chloride. The growth of the bacteria increases the buoyancy of the media resulting in the media expansion and loss in the effluent (Figure 1.1). The media loss can be prevented by frequent backwashing, which is a common method of cleaning the media. However, excessive backwashing decreases efficiency of a bioreactor and also changes the dominant microbial community in a reactor (Choi et al., 2007; Li et al., 2011).

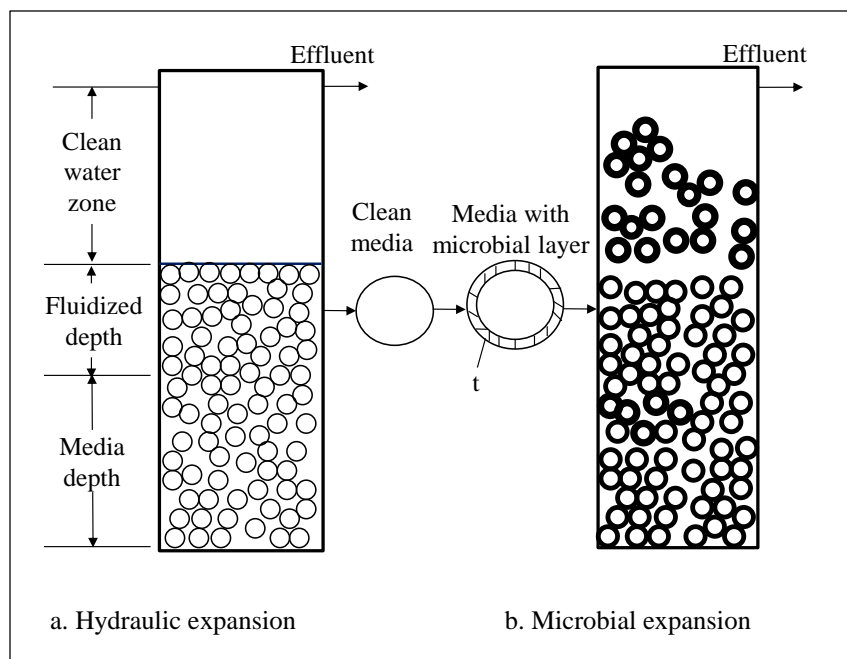


Figure 1.1: Hydraulic and microbial expansion of media in ex-situ bioremediation using a FBR. (Modified from Webster et al.,2009).

A biofilm model developed by McCarty and Meyer (2005) indicated that biofilm thickness governs the mass transfer limitations for electron donors and acceptors in perchlorate degradation. Currently, the timing and frequency of backwashing are determined by visual inspection and experience of an operator (Li et al., 2012). A systematic approach for backwashing FBRs used for perchlorate treatment, which takes into consideration the interaction between the biomass and the media assuring FBR performance, is needed and is addressed by this research.

Generally, ex-situ treatment of perchlorate contaminated water is expensive because of the cost associated with pumping and achieving desired fluidization (Webster and Togna, 2009). Ex-situ perchlorate treatment also involves high labor cost associated with operation and maintenance of the plant.

In-situ treatment could be an alternative for an existing ex-situ treatment. In-situ treatment of perchlorate involves injecting an electron donor into groundwater to support growth of indigenous perchlorate-reducing bacteria (Batista et al., 2003). In-situ perchlorate bioremediation using electron donors, such as acetate and ethanol, indicated perchlorate removal (ITRC, 2008). However, soluble substrates migrate with flowing groundwater and most of them are lost before biodegradation occurs. Consequently, soluble substrates must be added frequently to the groundwater, and often the groundwater is recirculated to recover the lost substrate.

For in-situ bioremediation at sites with high hydraulic conductivity, such as at the BMI site, a slow releasing electron donor would be beneficial. In this study, a slow-release electron donor, emulsified oil (EO), was investigated as a potential electron donor to support in-situ bioremediation of perchlorate-contaminated groundwater. EOs are organic oils that are relatively soluble in water, adsorb to soil, and slowly release electron donors and nutrients over time (Borden, 2007). EOs are commercially available and have been used in the past to support bioremediation of various contaminants as electron donors and carbon sources (Borden, 2007; Watson et al., 2013).

1.2 Objectives and Hypotheses

This dissertation focuses on two important but not completely researched issues related to in-situ and ex-situ perchlorate biodegradation and has two specific objectives:

Issue One- Loss of Media in Bioreactor Treating Perchlorate in FBR.

The objective of this research to address Issue One is to evaluate the use of electronic images as a tool to determine an appropriate backwashing time to avoid media loss and optimize

performance in FBRs treating perchlorate. An addition goal is to couple the image processing tool with a biofilm model to determine the suitability of image processing tool as an operation tool.

Hypothesis: It is hypothesized that media expansion in the reactor can be identified using an image processing technique to decide backwashing time. In addition, a model developed using biomass growth on the granulated active carbon GAC can be coupled with the results of the image processing technique and used as a suitable tool for identifying an appropriate time for backwashing FBRs treating perchlorate.

Issue Two- Loss of Soluble Substrates Used to Promote Perchlorate and Co-contaminants in In-situ Bioremediation.

The objective of Issue Two of the research is to evaluate the feasibility of using emulsified oils, a slow release electron donor, as a suitable donor for in-situ perchlorate bioremediation.

Hypothesis: It is hypothesized that relatively immobile and slow release donors can be a better option for in-situ bioremediation of perchlorate and co-contaminants. Such donors can minimize the cost associated with excessive loss of electron donors and/or recirculation of water to recover the donor. It is also expected that the emulsified oil could be a better electron donor for in-situ bioremediation because of its slow release characteristic.

CHAPTER 2

STATE OF KNOWLEDGE

2.1 Perchlorate Contamination Sites - Case Studies

2.1.1 Basic Management Industrial Complex, Nevada

In Nevada, two industries, Kerr-McGee and PEPCON, located in the Basic Management Industrial (BMI) complex, produced and handled perchlorate based rocket fuels and pyrotechnics from the early 1940s until 1988 (Batista et al., 2003). The BMI complex is located in Henderson, Nevada, approximately 13 miles southeast of Las Vegas. The soil condition and geology of the BMI complex facilitates spreading of contaminants from the complex area into the Las Vegas Wash and Lake Mead (Batista et al., 2003). The past practice of waste disposal in the facility to achieve “zero discharge” status as mandated by the Clean Water Act, and the storage of the industries’ wastewater in unlined ponds, resulted in contamination of the underlying soil and ground water (Batista et al., 2003). Figure 2.1 shows the contaminated industrial complex and perchlorate contaminated plume concentrations at the ppm level.

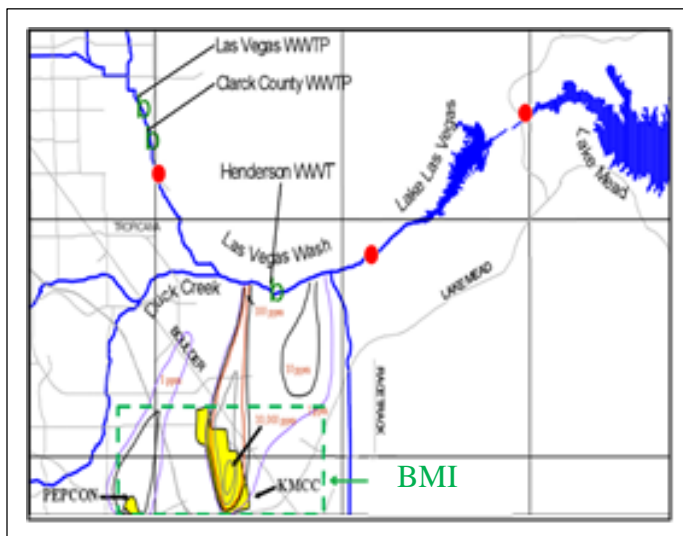


Figure 2.1: The ground water contamination site (BMI) at Henderson, NV. (Source: Boralessa and Batista, 2000).

The geological study of the industrial facilities indicated that the site has alluvial fan deposits, highly permeable, poorly sorted, gravels, cobbles, and sands, with a small fraction of silt and clay, and the Muddy Creek Formation underneath the alluvial fan (Batista et al., 2003). The alluvial deposits have uniform sand and gravel channels which increase the hydraulic conductivity. The upper part of the Muddy Creek Formation also has sand and silt deposits which increase the ground water velocity (Batista et al., 2003). The reported ground water velocity ranges from 5.64×10^{-5} m/s (1778.6m/year) to 1.76×10^{-6} m/s (55.5m/year) in the alluvial fan deposits and 1.87×10^{-6} m/s (59 m/year) in the Muddy Creek Formation (Batista et al., 2003).

The contaminated ground water flows north towards the Las Vegas Wash, located approximately 6,000 feet from the site and seeps into the Wash. The seepage has impacted the water quality of the Lake Mead, the major source of drinking water for the Vegas Valley and also the Colorado River, which is a source of drinking water and agriculture in California (Batista et al., 2003).

Currently, the ground water at the site is treated with an ex-situ treatment unit (pump and treat, using a Fluidized Bed Reactor). In-situ treatment bioremediation could be a possible option for the site.

2.1.2 Naval Weapons Industrial Reserve Plant, McGregor, Texas

The US Army Ordinance Corps established weapon industry, which manufactured perchlorate from 1942 to 1992. The industry manufactured, and stored ammonium perchlorate for weapons and solid-fuel rocket propulsion systems and disposed wastes containing ammonium perchlorate without treatment (ITRC, 2008). The contaminated industrial site (Figure 2.2) was investigated by Texas Commission for Environmental Quality (TCEQ), EPA, and City of McGregor in 1996 to treat the perchlorate laden groundwater. The average

groundwater concentrations typically ranged 3000–8000 ppb of perchlorate, but at main plumes the concentrations were about 27 ppm. Currently, the site is being treated by both ex-situ (for ppm level contamination) and in-situ (for ppb level contamination) bioremediation of groundwater, and ex-situ bioremediation of contaminated soil. The hydrogeology of the site shows that the site consists of four major types of soil formation- Crawford silty clay, Purves gravelly silty clay, Denton silty clay, and Slidell silty clay – with high gradient (1 to 3%).



Figure 2.2: The groundwater contamination site in Texas (ITRC, 2008).

For in-situ treatment, a permeable reactive barrier was created using granular activated carbon (GAC), cotton seed meal and compost at one site, and combination of soybean oil and woodchips in another site. ITRC (2008) reported that in the first site with GAC-combination barrier, the perchlorate concentrations decreased from 27 ppm to below detection limit (around 4 ppb) within three weeks. However, due to large volume of groundwater and limitation with supply of electron donor remediation was switched to a fluidized bed reactor (FBR) system after a year. Another in-situ treatment site with soybean oil barrier with various combinations of wood chips had option for re-addition of the electron donor is in operation. The perchlorate concentration in the groundwater decreased from more than 900 ppb to below detection limits

(20 ppb). The electron donor was added for the second time after operating for 20 months, when the perchlorate concentration increased and the TOC concentrations declined in the effluent.

The ex-situ bioremediation using FBR was established in 2001 with a capacity of 400 gallons per minute. ITRC (2008) stated that the FBR was chosen for the contaminated site because it was the best technology compared to ion-exchange (IX) and fixed bed reactor for the expected groundwater flowrates, extent of contamination, and the operating cost. The FBR treated groundwater pumped at 125 gallons per minute (maximum of 286 gallons per minute) with an average influent perchlorate concentration of 2.4 ppm (maximum of 4.7 ppm) to an effluent concentration below 4 ppb (ITRC, 2008)

2.1.3 Equivalent Hydraulic Conductivity at Sites with Multiple Strata

Hydraulic conductivity is an important parameter for in-situ perchlorate bioremediation because it determines the retention time of electron donor within the aquifer and therefore it influences perchlorate biodegradation. Depending on the site, the contaminated saturated zone may contain strata with varying hydraulic conductivities. Groundwater flowrate is proportional to the change in hydraulic head and the cross-sectional area of flow, and inversely proportional to the length of flow. Darcy's law is used to estimate the flowrate of the groundwater:

$$V = -K \Delta H;$$

where,

V = flowrate of groundwater,

K = hydraulic conductivity of groundwater (also known as permeability) varies with type of soil, variability in strata, and gradient, and

ΔH = hydraulic gradient

The hydraulic head is the force that drives the water from one point to the other. The hydraulic gradient is the change in water head as it flows through the horizontal distance in the soil i.e. $\Delta H = \frac{dh}{dx}$;

where,

ΔH = hydraulic head,

dh = change in water head, and

dx = change in horizontal distance

Strata that houses groundwater conditions may constitute a homogeneous layer, isotropic in nature. However, such conditions may not always be the case. In case of multiple strata, the hydraulic conductivity varies in each stratum, so an equivalent hydraulic conductivity must be calculated. Figure 2.3 shows the two directions of flow in the ground – (i) parallel to the strata (i.e. groundwater flowing horizontally in the stratified soil; horizontal arrows in Figure 2.3) and (ii) perpendicular to the strata (i.e. water infiltrating through the stratified soil; vertical arrow in Figure 2.3). A list of typical hydraulic conductivities in different homogeneous and isotropic natured soil is presented in Table 2.1.

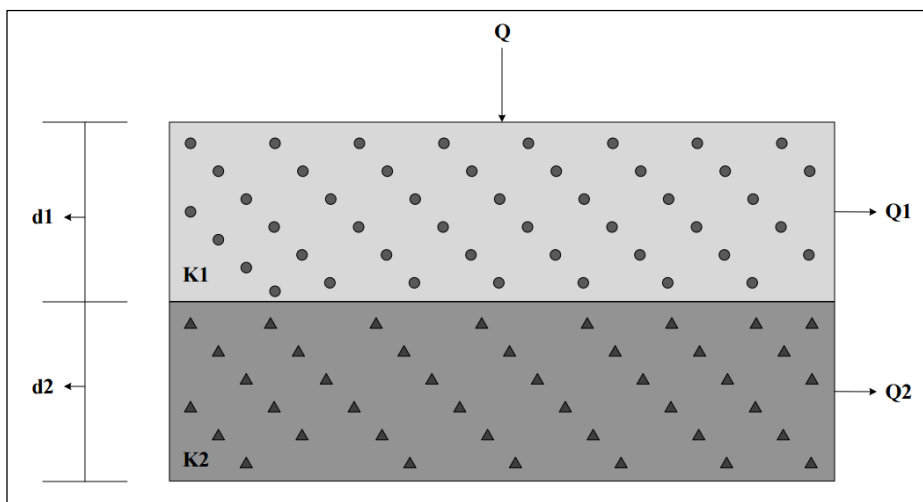


Figure 2.3: Equivalent hydraulic conductivity in a multiple layer area.

Table 2.1: Typical Values of Hydraulic Conductivities for Different Soil Type

Soil Type	K m/sec
Clean Gravel	$3*10^{-4}$ to $3*10^{-2}$
Coarse Sand	$9*10^{-7}$ to $6*10^{-3}$
Fine Sand	$2*10^{-7}$ to $2*10^{-4}$
Silty Clay	$1*10^{-9}$ to $2*10^{-6}$
Clay	$1*10^{-11}$ to $4.7*10^{-9}$

In case of groundwater flowing parallel to the strata, the hydraulic conductivity is given by:

$K = \sum \frac{K_i d_i}{d_i}$; where, $i = 1$ to n ($n = 2$ for Figure 2.3), K is hydraulic conductivity, and d is the depth of the stratum layer.

In case of groundwater flowing perpendicular to the strata, the hydraulic conductivity is given by: $K = \frac{\sum d_i}{\sum \frac{d_i}{K_i}}$; where, $i = 1$ to n ($n = 2$ for Figure 2.3).

The experimental columns used in this study represented horizontal groundwater flow through a homogenous and isotropic soil layer. To provide constant water head on the columns, the columns were fed with a step-feed arrangement that included two 2-gallon buckets at a foot elevation difference. The feed bucket was placed two feet above the column. The groundwater was pumped into the top bucket, from which water flows in to the lower bucket by gravity. The lower bucket was fitted with a floating valve to control the flow from top bucket and maintain water depth of 1 foot in the lower bucket.

The columns experienced total the water head of 3 foot, media height (5.5 feet) and diameter of the columns (2.5 inches), the groundwater flowrate in soil column 1 and soil column 2 can be converted into hydraulic conductivity of the soil media using Darcy's law.

$$V = -K * \frac{dh}{dx} \quad \text{Or, } K = \frac{V}{\frac{dh}{dx}}$$

The hydraulic conductivity of flowrate of 6 mL/minute, K value would be 5×10^{-5} m/second.

Table 2.2 shows the hydraulic conductivities corresponding to the flowrates measured in the experimental column bioreactors for this study. The reported average hydraulic conductivity in the alluvial layer in the contamination site, Henderson, Nevada ranged from 2.37×10^{-5} to 4.63×10^{-4} m/second and for Muddy creek formation ranged from 3.06×10^{-6} to 2.57×10^{-5} m/second.

Table 2.2: Hydraulic Conductivities Corresponding to the Flow Rates of the Experimental Column

Flowrate in the Experimental Column (mL/min)	K (m/s)
1	2.32E-05
6	6.95E-05
0.1	1.51E-04
0.6	6.95E-06

2.2 Biodegradation of Perchlorate

Biological perchlorate degradation is well studied and documented for groundwater, ion-exchange brines, and domestic and industrial wastewater laden with perchlorate (Korenkov et al., 1976; Attaway and Smith, 1993; Gingras and Batista, 2002; Venkatesan et al., 2010; Logan et al., 2001; Gullick et al., 2001; Rikken et al., 1996; Wallace et al., 1996). Perchlorate salts are highly soluble in water (Urbansky, 1998; Liu, 2000), and requires a low redox potential ($E_h < -0.2$ V) for natural abiotic reduction (Bardiya and Bae, 2008). Perchlorate is highly oxidized compound, with a high Gibbs' free energy (ΔG°) -1073.79 KJ/mole, but the rate of chemical reduction is very slow because of the large activation energy barrier (oxidation state of +7) (Gurol and Kim, 1999; van Ginkel et al., 1995; Gingras and Batista 2002). All chemical reactions of perchlorate in water are kinetically controlled exhibiting chemical stability (Urbansky, 1998; Wallace et al., 1998). Liu (2000) suggested that the chemical structure and high bond strength between chlorine and oxygen atoms of perchlorate as a factor inhibiting the

reactivity of perchlorate. A perchlorate molecule has a chlorine atom surrounded by four oxygen atoms. Such tetrahedral orientation provides a larger surface area for distribution of the charges evenly, fulfilling the eight electrons required for the outer shell. More than 70 years ago, biodegradation of chlorate, an oxyanion closely related to perchlorate, used as a herbicide, by soil microorganism was reported (Sharbatmaleki, 2010). Since then, various studies have indicated that the microbial enzymes act as catalysts which overcome the high activation energy needed for perchlorate reduction (Attaway, 1994; Gingras and Batista, 2002; Wallace et al., 1996; Liu, 2000; Logan, 2000).

Recent perchlorate biodegradation studies focus on contamination in drinking water sources with perchlorate at low concentrations (Frankenberger and Herman, 2000). The reported perchlorate concentration in drinking water sources ranges between 18 to 75 ppb (Gingras and Batista, 2002). Treatment technologies currently opted for perchlorate removal, such as ion exchange (IX), involve high cost and waste disposal issues, and have made biological perchlorate reduction a low cost option and a better solution (Achenbach et al., 2001; Bardiya and Bae, 2008; Webster and Togna, 2009). Webster and Togna (2009) observed lower capital cost and operating cost at 50 ppb perchlorate concentration in an IX system (\$17-\$546/kg of perchlorate treated) than a FBR unit (\$103-\$2,069/kg of perchlorate treated). However, the study observed a lower operating cost for perchlorate removal FBR compared to IX at perchlorate concentrations of 1000 ppb (\$226/kg of perchlorate treated, while the IX system is \$369/kg of perchlorate treated, and 250 ppb (FBR: \$450/kg of perchlorate treated and IX: \$767/kg of perchlorate treated).

In a biological reactor, Miller and Logan (2000) cited that the abiotic perchlorate degradation was not significant enough as compared to biodegradation. Brown et al. (2002) concluded that

any reduction in perchlorate in reactors with the virgin GAC as the media would be because of ion-exchange, rather than abiotic degradation (Brown et al., 2002).

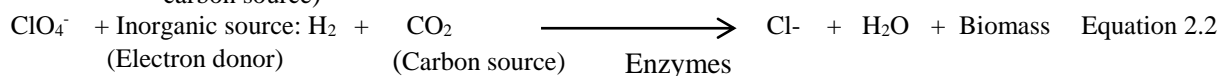
Many studies in the past decade have enriched and isolated pure cultures of perchlorate reducing microbes from various environments, indicating ubiquity of these organisms in the environment (Kim and Logan, 2000, Logan, 1998, Logan et al., 2001; Rikken et al., 1996; Wu et al., 2001; AWWaRF, 2004; Kesterson, 2005). Perchlorate reducing microorganisms isolated from different sources are listed in Table 2.3.

Table 2.3: Sources Used for Isolating Perchlorate Reducing Microorganisms

Culture	Source	Reference
<i>Vibrio dechloratans</i>	Municipal sludge	Korenkov et al. 1976
Mixed culture	Anaerobic digester sludge	Attaway and Smith, 1993
GR-1	Activated sludge	Rikken et al. 1996
<i>Wolinella succinogenes</i> HAP-1	Anaerobic sewage	Wallace et al. 1996 and 1998
Perlace	Biosolids from wastewater plant	Herman and Frankenberger 1998
CKB	Paper mill waste	Bruce et al., 1999
Mixed culture (BALI)	Municipal wastewater sludge	Liu, 2000
KJ	Municipal wastewater	Logan et al., 2001
PDX	Municipal wastewater	Logan et al., 2001
<i>Acinetobacter thermotoleranticus</i>	Match factory wastewater	Gingras and Batista, 2002
IsoA, IsoB and IsoC	Sediments from Cargill salt evaporation facility	Okeke et al., 2002
SN1A, ABL1, INS, RC1		Waller et al., 2004
W3330A, W3413A, W4716A, W1716B, W4413C, W4330A and W2921A	Lake Mead water	Kesterson, 2005
S429A, S429B, S2128C, S41013A, S51220B, S1128A, S51013A, S429C, and S2128D	Las Vegas Wash soils	Kesterson, 2005
PC1		Nerenber et al. 2006
HCAP-C	Municipal activated sludge	Dudley et al., 2008
Mixed culture	Anaerobic sludge	Wang et al., 2008
Mixed culture	Wastewater treatment plant	Ricardo et al., 2012
<i>Archaeoglobus fulgidus</i> strain VC-16	Hot vent close to Vulcano island	Liebensteiner et al., 2013
<i>P4B1 Marinobacter vinifirmus</i>	Wastewater	Xiao and Roberts, 2013

The perchlorate reducing microbes occur in a wide range of natural and engineered environments. Most perchlorate reducing microorganisms identified today were isolated from nearly all environments such as hot vents in volcanic island, industrial (paper and pulp) and municipal wastewater and sludge, pristine water sources (lake samples from Antarctica) and contaminated soil and aquatic sediments (Batista et al., 2005; Coates et al., 1999; Liu 2000; Achenbach et al., 2001; Liebensteiner et al., 2013).

Most of the perchlorate reducing microorganisms studied today belong to the bacterial domain except *A. fulgidus* strain VC-16, which belongs to the archaeal domain (Liebensteiner et al., 2013; Webster et al., 2009). Recently, Liebensteiner et al. (2013) found perchlorate reduction by *Archaeoglobus fulgidus* strain VC-16, a hyperthermophile, isolated from hot vent close to Vulcano Island in Italy. Archaea were present in the early age of the earth. Liebensteiner et al. (2013) hypothesized that if perchlorate was present in the earth naturally then the reduction by those archaeal strains might have occurred for oxygen generation, even before photosynthetic oxygen generation began. Equation 2.1 and Equation 2.2 show the general pathways for biological perchlorate degradation.



The perchlorate reducing microbes have shown a diversified metabolism in terms of capability to use energy and carbon sources (Kesterson, 2005). In the biological reduction process, organic compounds (such as acetate, lactate, ethanol and yeast extracts) or inorganic substances (such as hydrogen gas and elementary sulfur) have been used as source of energy (Attaway and Smith, 1993, Wallace et al., 1996; Sahu et al., 2005, Liebensteiner et al., 2013).

The organic compounds also fulfill the carbon required for cell synthesis, and for autotrophic growth, carbon dioxide (CO_2) serves as source of carbon. Many studies have demonstrated various bacterial strains were capable to reduce perchlorate and chlorate into chloride under anaerobic conditions and in the presence of a carbon source, but their reduction pathways were not specified (Korenkov et al., 1976; Attaway and Smith, 1993; Malmqvist et al., 1994). Rikken et al. (1996) proposed the perchlorate degradation pathway as shown in Figure 2.4.

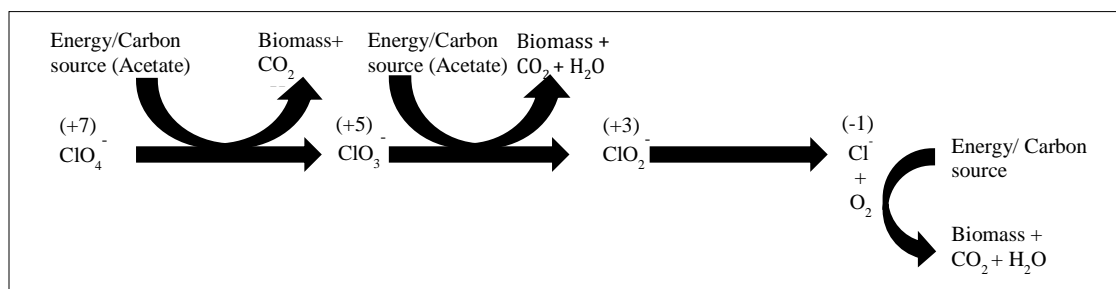


Figure 2.4: Microbial perchlorate degradation pathway indicating complete perchlorate reduction into chloride and oxygen in presence of acetate as energy and carbon source. (Modified from Rikken et al., 1996).

Rikken et al. (1996) hypothesized that perchlorate reduction involved three steps; at first, perchlorate is reduced to chlorate, then to chlorite and finally, yields chloride via unstable intermediates hypochlorite or dichlorooxide (Figure 2.4). The first two processes involve energy yielding enzymatic activity, but the final step, conversion of chlorite to chloride, is non-energy yielding process (Rikken et al., 1996). The authors hypothesized that chlorite disproportionate to chloride and oxygen, independent of electron transfer and that is occurred under both aerobic and anaerobic conditions. Liebensteiner et al. (2013) hypothesized that in archaeal strains the reduction of perchlorate and chlorate to chlorite is an enzymatic activity, and chlorite further undergoes abiotic reduction to chloride with sulfur.

2.2.1 Perchlorate Reducing Bacteria (PRB)

Biological perchlorate removal is practiced and had been most studied with pure or mixed bacterial culture (Herman and Frankenberg, 1998; Logan, 1998; Liu, 2000; Gingras and Batista, 2002; Webster et al., 2009). More than 50 species of pure strains capable to reduce perchlorate have been identified, isolated from different sources, such as soil and sediments and wastewater, enriched as pure culture, and studied (Batista et al., 2005; Bardiya and Bae, 2011; Coates and Achenbach, 2004). PRB are characterized by diverse metabolic pathways and ubiquity in the environment. These bacteria are present even in soil and water without perchlorate or chlorate contamination (Coates and Achenbach, 2004).

PRB are the members of *Proteobacteria*. This group constitutes the majority of the bacteria known today, including *E. coli*, *Pseudomonas* and other well-known pathogens such as *Salmonella*, and *Neisseria* (Madigan et al., 2009). *Proteobacteria* exhibit diverse morphology, metabolic pathways and physiological characteristics. The perchlorate reducers have diverse morphology (rod shaped or spiral) and are flagellated suggesting their motile characteristic (AwwaRF, 2004; Coates and Achenbach, 2004; Malmqvist et al., 1991; Malmqvist et al., 1994; Wallace et al., 1996). Most commonly known PRB are gram-negative, except for *M. perchloratireducens* which is gram positive (Bardiya and Bae, 2011). These perchlorate respiring bacteria are non-fermenting, catalase negative (except *I. dechloratons* which is weakly positive), and cytochrome-c oxidase positive (Malmqvist et al., 1994). Most of the PRB are non-spore forming, except *M. perchloratireducens* and *Sporomusa* sp. strain An4 (Bardiya and Bae, 2011). PRB can be categorized as heterotrophs (uses organic carbon such as acetate), autotrophs (uses inorganic carbon, CO₂) and mixotrophs (use both organic and inorganic carbon).

Physiologically, PRB is diversified as facultative anaerobes and microaerophilic bacteria indicating that these bacteria can utilize oxygen as electron acceptors (Wallace, 1996; AwwaRF, 2004; Madigan et al., 2009). This is supported by immediate consumption of oxygen generated as transient intermediate of perchlorate reduction pathway (van Ginkel et al., 1996 and Logan et al., 1999). So far, all known PRB can utilize chlorate, but not all chlorate or nitrate respiring bacteria can utilize and grow in perchlorate (Achenbach et al., 2001; AwwaRF, 2004; Xu et al., 2004).

Phylogenetically, based on 16S rRNA, *Proteobacteria* are classified as α , β , γ , δ , and ϵ sub-classes. PRB isolates known today are phylogenetically diverse and fall under four sub-classes (α , β , γ , and ϵ), but the majority of PRB (>70%) known are β - *Proteobacteria* belonging to genera such as *Dechloromonas* or *Dechlorosoma*, *Dechlorospirillum*, *Wollinella succinogenes*, *Vibrio dechloraticans*, and *Azospira* (Bardiya and Bae 2008; Chaudhuri et al., 2002; Li et al., 2012; Min et al., 2003 and Xu et al., 2003). Bardiya and Bae (2003) observed perchlorate respiration in two strains of *Citrobacter* spp., JB 101 and JB 109, belonging to γ - *Proteobacteria* group. These PRB have similar phylogenic similarities and are related to each other. Strains *Dechloromonas* (β - *Proteobacteria*) and *Azospira* (α - *Proteobacteria*) are dominant groups of PRB.

For identification of strains responsible for perchlorate reduction, phylogenetic similarity alone does not confirm perchlorate reducing capability of a bacteria (Coates and Achenbach, 2004; Bardiya and Bae, 2005). *R. tenuis* and *F. limneticum* (β - *Proteobacteria*) are closely related to PRB, with 99% similarity in 16S rDNA sequence, have distinct physiologies and characteristics. *R. tenuis*, a phototrophic purple nonsulfur bacteria, is found in shallow waters and soils exposed to sun, and *F. limneticum*, an obligate anaerobe, non-fermenting, dissimilatory

iron (Fe III) reducer. These strains cannot grow in perchlorate despite closeness in the phylogeny tree (Coates and Achenbach, 2004). Perchlorate reducing strain PK (γ -*Proteobacteria*) can respire perchlorate, but has 99.8% similar phenotypic and genotypic attributes to *Pseudomonas stutzeri*, a non-PRB (Bardiya and Bae, 2008). On the other hand, distantly related *W. succinogenes* strain HAP-1 (ϵ -*Proteobacteria*), and *Dechloromarinus* strain NSS, *Pseudomonas* strain PK, strains PDA and strain PDB (γ - *Proteobacteria*) were capable to respire perchlorate (Bardiya and Bae, 2011; Coates et al., 2002).

2.2.2 Enzymes Involved in Perchlorate Reduction

Figure 2.5 depicts the most commonly accepted enzymatic model for biological perchlorate reduction. Perchlorate reduction occurs in three steps with help of specialized enzymes, perchlorate reductase and chlorite dismutase, under anaerobic conditions and in presence of an electron donor (Rikken et al., 1996; Logan et al., 2000; Nerenberg et al., 2002 and 2006; Bardiya and Bae, 2011).

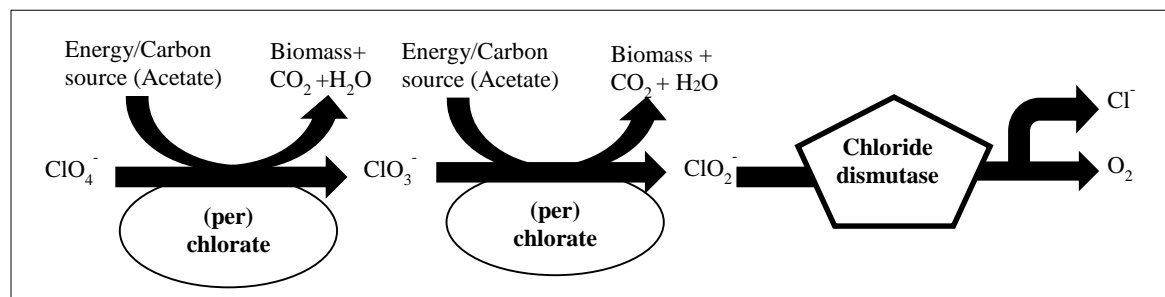


Figure 2.5: Periplasmic enzymes, perchlorate reductase, and chloride dismutase involved in perchlorate reduction. (Modified from Nerenberg et al., 2002).

Both enzymes (perchlorate reductase and chlorite dismutase) are soluble proteins, located at the periplasmic layer of cell. The perchlorate reductase reduces perchlorate (ClO_4^-) to chlorate (ClO_3^-) and further to chlorite (ClO_2^-) involving transfer of two-electron in each step. The

second specialized enzyme, chlorite dismutase, disproportionates chlorite to chloride (Cl⁻) and oxygen, without any external electron transfer.

Kengen et al. (1999) performed a chromatographic study of purified perchlorate reductase, and concluded the enzymatic reduction pathway for reducing perchlorate to chlorate and chlorate to chlorite occurred within the same enzyme, perchlorate reductase. However, all species that can reduce chlorate cannot grow with perchlorate as the sole electron acceptor. For example, species of *Proteus* and *Pseudomonas* can reduce chlorate, but cannot utilize perchlorate as an electron acceptor (AWWaRF, 2004). Further, Dudley et al. (2008) developed a competitive pathway for perchlorate and chlorate in a perchlorate reducing strain *Dechlorosoma* sp. HCAP-C. The model indicated that the strain reduced perchlorate, but accumulated chlorate about 20% of the initial perchlorate on weight basis. The authors concluded that different behavior may be due to a modified or distinct perchlorate reductase enzyme present in the strain. Nerenberg et al. (2006) also observed inhibition in perchlorate reduction when chlorate was added. The PC1 culture utilized chlorate first, and the biomass growth in the presence of chlorate was faster than in case with perchlorate as sole electron acceptor (Nerenberg et al., 2006).

Initially, perchlorate reduction was related to denitrifying bacteria, and it was hypothesized that nitrate reductase was responsible for perchlorate and chlorate reduction (van Ginkel et al., 1995; Xu et al., 2004). The enzyme, nitrate reductase, supported perchlorate and chlorate reduction activities (Okeke et al., 2002). However, nitrate reducers' lack of chlorite dismutase, needed to remove the harmful intermediates, hinders the growth of denitrifiers in media with perchlorate as electron acceptor (Wolterink, 2004). Further, cultures enriched in nitrate cannot support perchlorate reduction, suggesting perchlorate reduction is not supported by enzymes used for nitrate reduction (Xu et al., 2004). It is widely accepted now that perchlorate and nitrate

reduction follow two independent pathways (Logan 2001, 1998; Bruce et al., 1999; Xu et al., 2004). However, Xu et al. (2004) further reported that PRB has potential to use the same enzyme for nitrate and perchlorate reduction depending upon the enrichment medium. PRB enriched with nitrate only prevented perchlorate/chlorate reduction, and PRB cultured in perchlorate showed a minimum denitrification, suggesting that the enzymes are stimulated while enriching the culture (Xu et al 2003). Chaudhuri et al. (2002) also observed effects of enrichment solution; strain *D. suillum* enriched in perchlorate solution reduced nitrate and perchlorate immediately, but the same strain when enriched in nitrate solution showed a lag of 40 hours before reducing nitrate and perchlorate.

The assimilatory nitrate reduction involve membrane bound enzyme (nitrate reductase), but dissimilatory perchlorate reduction utilizes periplasmic enzyme (Einsle and Kroneck, 2004; Bardiya and Bae, 2011). Xu et al. (2004) implied that though the pathways for perchlorate and nitrate reduction are different, some PRB can utilize both perchlorate and nitrate, indicating possible relation between those enzyme activities. PRB strains such as GR-1 and isolate *Ideonella dechloratans* reduced nitrate to nitrogen gas completely (Rikken et al., 1996; Malmqvist et al., 1994), and incomplete reduction of nitrate to nitrite was observed in PRB *Wolinalla succinogenes* HAP-1 strain (Wallace et al., 1996). On the contrary, strain CKB could not reduce nitrate supporting the independent activities of perchlorate and nitrate reductase (Bruce et al., 1999).

Chlorite dismutase is a key enzyme for perchlorate removal in eliminating chlorite accumulation, by proportional dismutation of chlorite into chloride and oxygen. The molecular oxygen is produced outside the cell, and is used up by the membrane bound oxidase rapidly, preventing accumulation of oxygen in the PRB (Riken et al., 1996; Backlund et al., 2009,

Bender, 2004). Chlorite dismutase is a hexameric crystal structured protein with iron at the center (de Geus et al., 2009). The iron present in the enzyme gives the red color to the enrichment (van Ginkel et al., 1996). The heme based enzyme reduces toxic intermediates of perchlorate reduction (chlorite) (Logan, 2001; AwwaRF 2004; deGeus et al., 2009). Attaway and Smith (1993) reported that perchlorate reduction was inhibited by nitrite and chlorite even at low concentrations. Chlorite dismutase is not sensitive to oxygen, but under aerobic condition the enzyme is not expressed (Chaudhuri et al. 2002; Xu et al. 2004). Further, Chaudhuri et al. (2002) observed that maintaining *D. suillum* under anaerobic conditions could not initiate chlorite dismutase, thus suggesting that oxygen is required to induce chlorite dismutase activity, but making the culture anaerobic during log phase growth enhanced both perchlorate reduction and chlorite dismutase activities. Figure 2.6 shows the predicted model of perchlorate reduction using periplasmic enzymes.

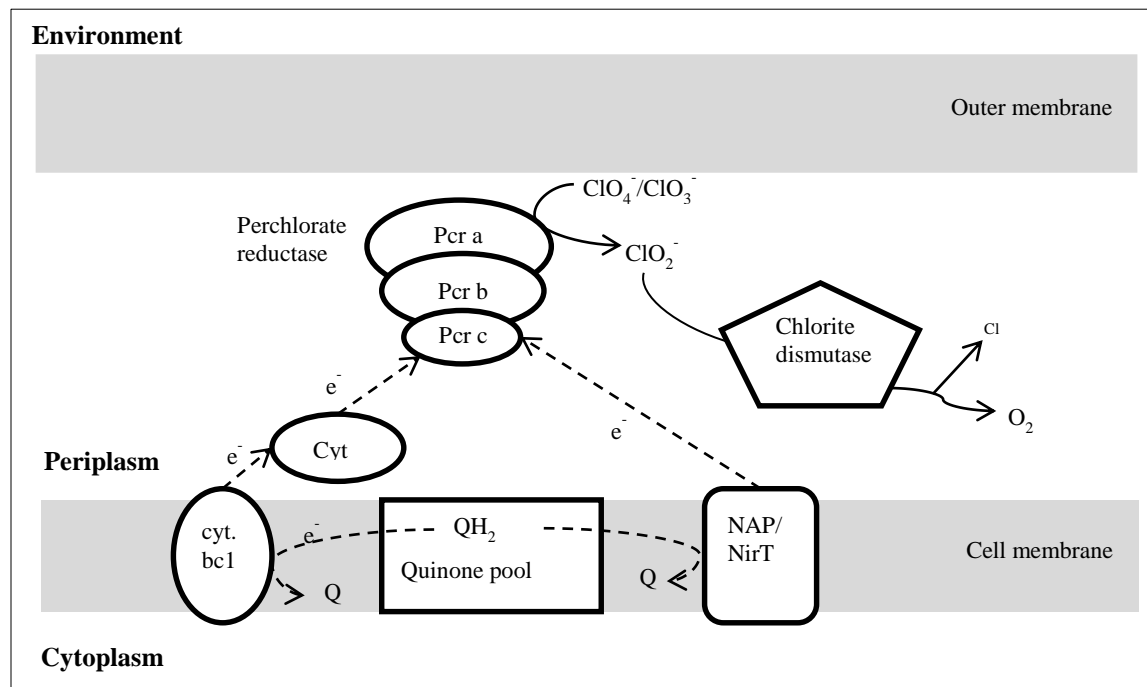


Figure 2.6: Proposed perchlorate reduction model by the periplasmic perchlorate reductase and chlorite dismutase in gram negative perchlorate reducing bacteria. (Modified from Bender et al., 2005 and Backlund et al., 2009).

Figure 2.6 shows the electron transfer for perchlorate reduction. Studies have shown that type c cytochrome shuttles electrons from bc1 complex in perchlorate reduction pathway (Bruce et al., 1999 and Coates et al., 1999). Another suggested pathway involves NAP/NirT type cytochrome for electron transfer from the membrane bound quinone pool to the perchlorate reductase (Bender et al., 2005).

Thrash et al. (2007) demonstrated that perchlorate reduction involves electron transport mediated by enzymes. The study includes an electrochemical cell with PRB (*Dechloromonas agitata*, in cathodic chamber connected to a close circuit, open circuit and chamber with acetate. The perchlorate reduction in closed circuit was comparable to reduction when acetate was present in the system, though bacterial growth was observed only when acetate was added. Further, perchlorate reduction was not observed in an open circuit condition initially, but perchlorate reduction was established after addition of acetate as electron donor.

Factors that control enzyme expression and activity during perchlorate reduction include enzyme induction, oxygen concentration, nitrate and nitrite concentrations, (per) chlorate intermediates, temperature, electron donor, and pH (Adham et al., 2004).

2.2.3 Molecular Tools for Identification of PRB

Identification of microbial community using molecular tools has gained attention because these tools simplify the complexity of the microbial community. Earlier, microbial studies were limited to plate culture technique, but new molecular tools have helped to manipulate DNA in a test tube and transfer the genes among original or other bacteria, and provided a rapid and successful tool to analyze bacterial communities (Madigan et al., 2009; Kesterson, 2005). Marsh et al. (2000) hypothesized that standard plate culture technique, isolation of strains in agar plates, might restrict the total analysis of the microbial community, because some bacteria are viable but

did not grow in plates (Kesterson, 2005). Bramucci and Nagarajan (2006) supported the hypothesis as they observed that most of bacteria detected by modern molecular approach were β -Proteobacteria, but bacteria cultured from the same sludge were γ -Proteobacteria. The difference might be because the culture based approach detected a small population of bacteria that could be cultured, but the modern tools identify the dominant members of the microbial community.

Culture dependent techniques are classic approach involving physiological and biochemical tests to enumerate bacteria. Theron and Cloete (2000) questioned the reliability of those methods to obtain the actual structure of the community because the result from plating might be biased due to selectivity of media. Bramucci and Nagarajan (2006) concluded that integration of culture and non-culture based approach can provide a better characterization of the microbial community present in a sample.

Over the past decades, several molecular techniques have been developed to cut DNA of interest in fragments, purify them and insert the genetic material into living bacteria to study the characteristics of the microbes (Madigan et al., 2009). These tools are based on sequencing 16S ribosomal RNA (rRNA), a phylogenetic marker (Marsh et al., 2000). The analyses of 16S rRNA sequence have been used to investigate the microbial community structure, diversity and phylogeny under various environmental conditions (Theron and Cloete, 2000; Coats and Alebach, 2004; Kesterson, 2005; Krauter et al., 2005). The molecular approach has also been used to prepare inventory of microbes in many wastewater treatment plants (Bramucci and Nagarajan, 2006). Theron and Cloete (2000) summarized the most common culture independent methods used for analyzing microbial community (Figure 2.7). In brief, culture independent molecular approach, with the development of robust polymerase chain reaction (PCR) and PCR

related techniques, electrophoresis, DNA cloning, and sequencing procedures, and facilitates analyses of complex environment as well as individual or group of specific bacteria.

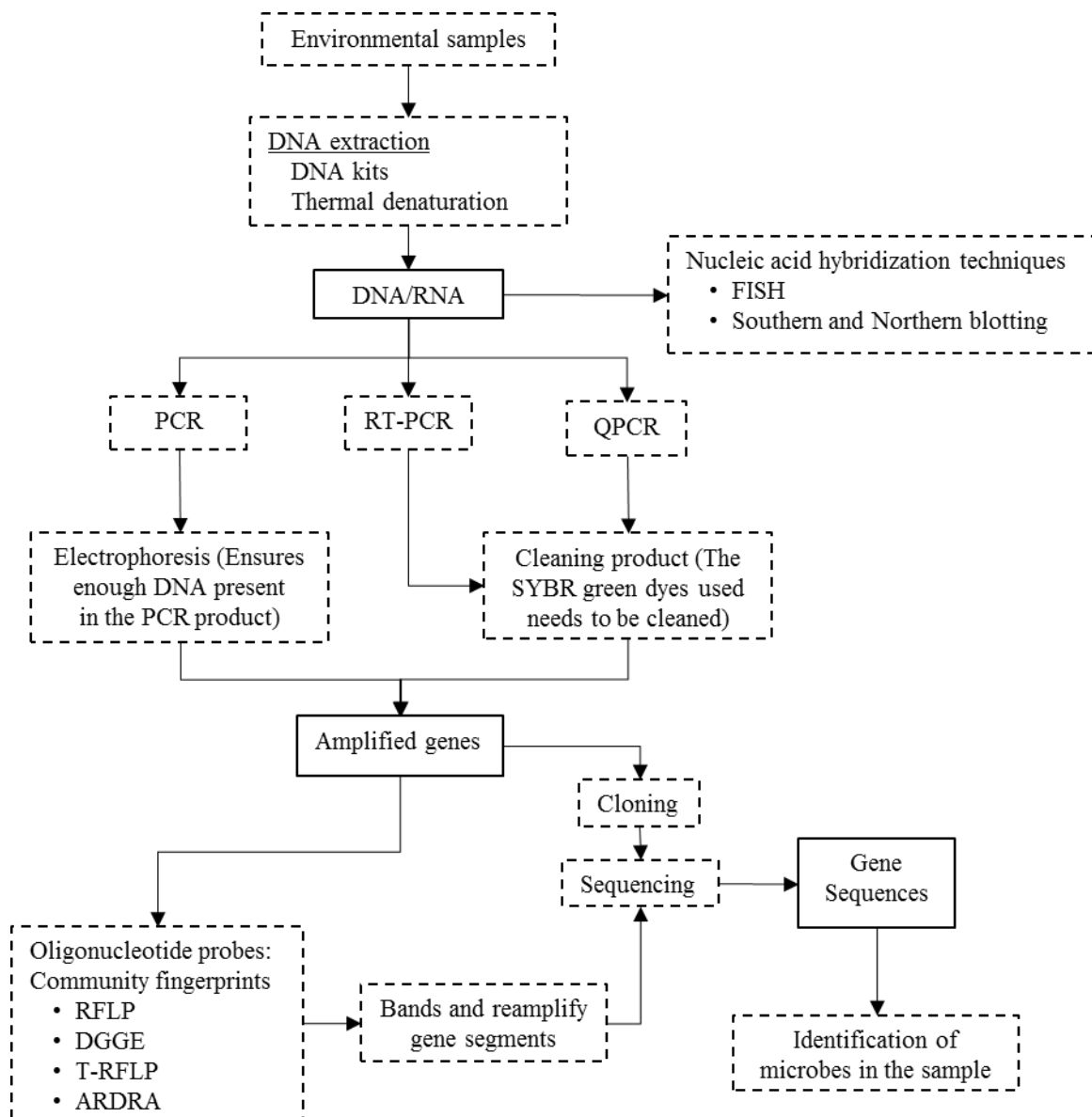


Figure 2.7: Molecular tools commonly used to identify microbes present in an environmental sample. (Modified from Theron and Cloete, 2000).

PCR amplifies DNA sequence of interest using a thermostable DNA polymerase, often *Taq* enzyme from *Thermus aquaticus*, in presence of a forward and a backward primer (Theoron and

Cloete, 2000). The amplified DNA is used to identify bacteria with additional processes. Polymorphism based procedures coupled with PCR or/and electrophoresis such as Restriction Fragment Length Polymorphism (RFLP), Amplified rDNA Restriction Analysis (ARDRA), Denaturing Gradient Gel Electrophoresis (DGGE), and Terminal Restriction Fragment Length Polymorphisms (T-RFLP) generate a “fingerprint” representing banding pattern of nucleic acid fragments in gel electrophoresis which provides the structure and diversity of a community (Liu et al., 1997; Gich et al., 2000; Lapara et al., 2000). However, these techniques cannot identify the type of individual microbes present in the community (Theron and Cloete, 2000; Gich et al., 2000). RFLP includes digestion of DNA samples into fragments containing fluorescent dyes and DNA is analyzed by the electrophoresis process; no PCR is required for this procedure. ARDRA creates patterns of restriction fragments formed by digesting amplified 16S rDNA of the community by the restriction endonuclease and can be used for quick assessment of genotypic changes in community (Theron and Cloete, 2000; Gich et al., 2000; Kesterson, 2005). DGGE utilizes the electrophoretic mobility of DNA fragments of same size but with different nucleic acid sequences in polyacrylamide gel, and analysis of band pattern indicates biodiversity in the sample. T-RFLP incorporates amplification of microbial DNA using fluorescently labeled primers (either both forward and backward or only forward) to identify the microbes in the environment (Abdo et al., 2006). To classify the microbes based on these techniques require a clone library of 16S rRNA genes to create genetic distance matrix (Abdo et al., 2006).

Other technique includes nucleic acid hybridization process which uses hybridization of nucleic acid (oligonucleotide) probes targeting microbial nucleic acid extracts (complementary DNA or RNA). The process using fluorescent nucleic acid probes is known as fluorescence in situ hybridization (FISH). Other hybridization technique includes Southern or Northern blotting

probes for hybridization of known sequence to the fragments of DNA or RNA in electrophoresis gel (Madigan et al., 2009). These hybridization probes are faster, but to use them sufficient knowledge of the community is needed to target appropriate sequences (Gich et al., 2000).

PCR related technique has been widely used in analysis of microbial communities in various bioreactors used to treat water and wastewater (Wallace et al., 1998; Lapara et al. 2000; Song et al., 2010; Li et al., 2012). PCR, real time PCR and qPCR amplifies the DNA segments of interest. First, the DNA strands are denatured by applying heat (90°C), then as the mixture is allowed to anneal allowing the two oligonucleotide- forward and backward primers to yield a copy of the DNA in presence of DNA polymerase (Madigan et al., 2009). The most commonly used primers to identify PRB are listed in Table 2.4.

Table 2.4: Molecular Tools

Method	Primer	Primer/ Probe Sequence	Final Process	Identification	Reference
Pooled PCR	Universal primer	8F 5'-AGAGTTTGATCCTGGCTCAG-3' 1492 R 5'GG(C/T)TACCTTGTTACGACTT-3'	Cloning with <i>E. Coli</i>	Ribosomal Database Project II (RDP)	Choi et al., 2008
PCR	Universal primer	16S 341F CGC CCG CCG CGC CCC CGC CCC 16S 907F CCG CCG CCG CCC CCG CCT ACG 341F GGA GGC AGC AG	Polyacrylamide gel using a denaturant gradient of denaturant gel Electrophoresis	BLAST software package	
FISH		CG TCA ATT CMT TTG AGT TT ATGCTTAGGAATCTGCCCAGTAG TG CTTTCAGTGGGGAAGAAAGCCTT CGAGTCTTGACTTGACGTTAACT TAG GCTGCGTTACTCAGAAAG AGTTTCCTCTCCGAACAA			
Probebase		GTCAGTATCGAGCCAGTGAG GACGGGCGGTGTGTACAA GTGCTCCCCCGCCAATTCCT			Xiao et al., 2010
PCR	Universal primer	f 968 r1401	Denaturing gradient gel electrophoresis (DGGE)	ClustalV, GeneDoc and GenBank BLAST software package	Krauter et al., 2005
PCR		27F 5'-AGAGTTTGATC(AC)TGGCTCAG-3'	cloning vector using TOPO TA cloning kit and insertion into <i>E. Coli</i> , use LB medium to isolate the colonies	CLUSTAL-W, MEGA4 program, Database Project II and BLAST from GenBank software	Ahn et al., 2009
PCR		1492R 5-GGTTACCTTGTTACGACTT-3'			
PCR		8F 5'-AGAGTTTGATCCTGGCTCAG-3'	cloning vector using TOPO TA cloning kit and insertion into <i>E. Coli</i> , incubated at 37°C on LB medium to isolate the colonies	RDP Clustal-W and LIBSHUFF for similarity	
		1429R 5'GG(C/T)TACCTTGTTACGACTT-3' TTGACATGTCCAGAAGCCCGAAG A F TGTCACCGGCAGTCTCGTTAAAG R T			
QPCR				GenBank	Li et al., 2012

In case of samples containing RNA instead of DNA, first a complementary DNA (cDNA) is made using a reverse transcriptase enzyme, and cDNA is then amplified. The electrophoresis gel is used to ensure proper DNA amplification by PCR. In case of a real time PCR and qPCR, electrophoresis is not required because these techniques include fluorescent dyes that allows rapid detection and absolute quantification of 16S rRNA gene (Song et al., 2010). The primers contain dyes such as SYBR green, or TaqMan Probe with reporter and quencher which fluoresces as the gene gets amplified, and the fluorescent detector plots the amplified DNA segment as shown in Figure 2.8.

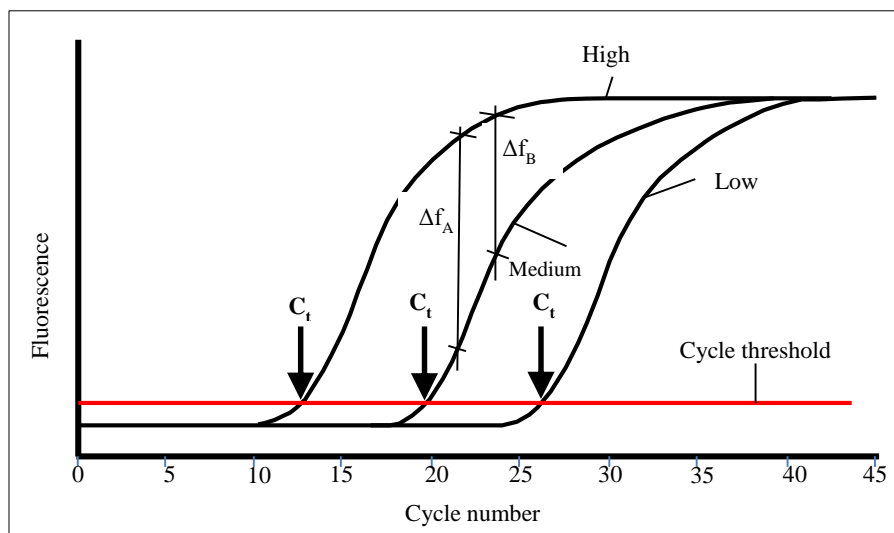


Figure 2.8: Graph obtained from qPCR of a sample containing three microbial DNA. (Modified from: Bhattacharjee, 2013).

Both real time PCR and qPCR produces graphs as shown in Figure 2.8, but the main difference between real time PCR and qPCR is that the qPCR can be used to quantify the initial concentration of genes of different microorganism present in a sample. The curve labeled as high in Figure 2.8 represents the most abundant DNA in the sample whereas low represents the least DNA present in the sample. The ratio of fluorescence between two genes at any time in qPCR graph represents the ratio of two DNAs in the original sample, but graph obtained from

real time PCR cannot be used to quantify the initial composition of bacteria. The exponential phase of the product is analyzed based on cycle threshold to quantitate the initial concentration. The product of both real time PCR and qPCR needs to be cleaned before proceeding to the next step.

PCR or real time PCR or qPCR product is then inserted into a vector such as plasmid and then cloned to a competent cell such as *E. coli* (Figure 2.9). The cloned *E. coli* is plated on Lysogeny Broth (LB) plates with ampicillin and incubated overnight. The insert suppresses the lacZ gene needed for hydrolysis of beta-galactosidase in the *E. coli* resulting in white colonies, and those cells without the insert can express lacZ gene and grow as blue colonies on the LB plates (Madigan et al., 2009). The white colonies are transferred into well plate for sequencing.

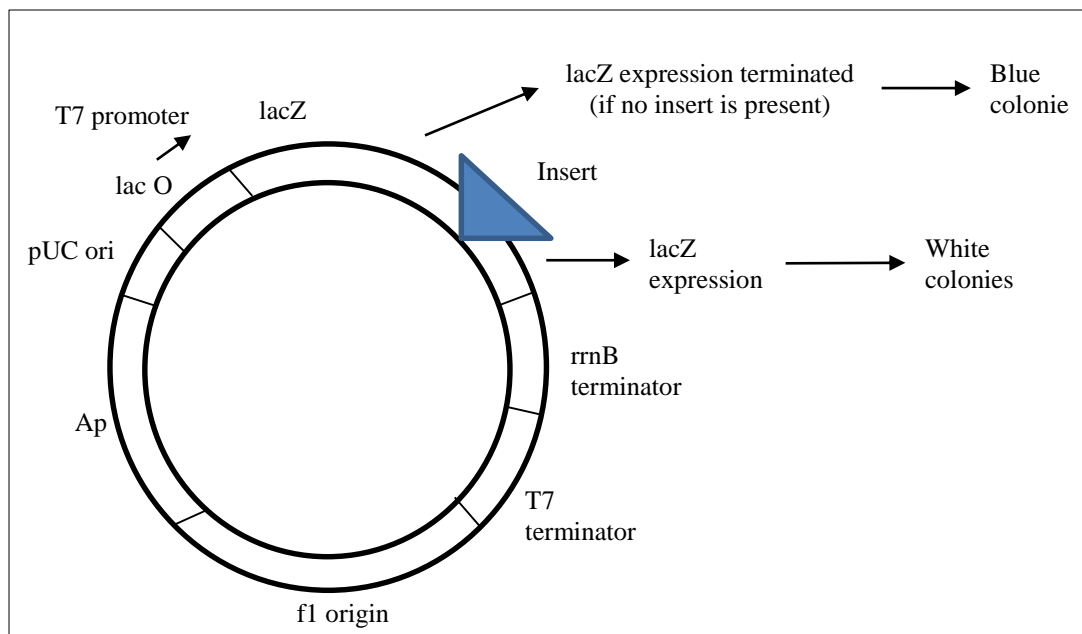


Figure 2.9: *E. coli* plasmid vector showing an insert that terminates the lacZ expression. (Modified from: Madigan et al., 2009).

The process to determine order of nucleotides of genomic DNA or RNA molecule is termed sequencing. Just like in the PCR process, sequencing also requires a primer, typically 10-20

nucleotides. Most commonly used process is the Sanger sequencing in which DNA fragments of different lengths are generated ending at the four bases labeled with radioactivity or a fluorescent dye (Madigan et al., 2009). The fragments are separated by electrophoresis process, and X-ray film or fluorescence is used to obtain the sequence of the fragments. An automated gel electrophoresis with fluorescent detecting lasers, and the sequence for the gene is read based on the spectrum generated (Shendure and Ji, 2008; Madigan et al., 2009). Second-generation DNA sequencing, also known as ultra-throughput sequencing, generates can produce large sequence data. This method uses pyrosequencing, polymerase based sequencing by synthesis, and ligation based sequencing technique (Mardis, 2008). Commercially available products such as 454 sequencing, Solexa, SOLiD platform, and HeloScope Single Molecule Sequencer technology rely on bridge PCR and emulsion PCR instead of chain termination of dideoxynucleotide method in Sanger's sequencing method (Shendure and Ji, 2008).

The final step in the molecular tools is the identification of microbe based on gene database. Various computer programs such as BLAST, clustal-W, and LIBSHUFF are used to obtain the similarities between various genes recorded in database such as GenBank (Choi et al., 2008; Xiao et al., 2010; Ahn et al., 2009). The comparison can be used to identify microbes based on the percentage similarity in sequence and protein structure for the microbe.

2.3 Thermodynamics, Biochemical Reactions, and Microbial Kinetics of Perchlorate Degradation Pathway

2.3.1 Thermodynamics of Perchlorate Reduction Pathway

Thermodynamically, biological perchlorate reduction is an energetically favorable electron acceptor (Herman and Frankberger, 1998; Coates and Achenbach, 2004). Under anaerobic conditions, bacteria utilize perchlorate as electron acceptor and organic compounds (e.g. acetate,

ethanol and methanol) or inorganic compound (e.g. hydrogen and sulfur) as electron donor, and reduce perchlorate (oxidation state of +7) to chloride (oxidation state of -1). The stoichiometric Gibbs' free energy at pH 7 ($\Delta G^{\circ'}$) for perchlorate reduction and other electron acceptors under anaerobic conditions with various electron donors are presented in Table 2.5.

Table 2.5: Reported Gibbs' Free Energy ($\Delta G^{\circ'}$) for Various Electron Acceptors (oxygen, chlorate, nitrate, perchlorate, and sulfate), Coupled with Electron Donors (acetate, hydrogen and sulfur)

<u>Electron Donor:</u> Electron Acceptor	$\Delta G^{\circ'}$ (KJ/mol)	Reference
<u>Acetate: $\text{CH}_3\text{COO}^- / \text{HCO}_3^-$</u>		
$\text{O}_2/\text{H}_2\text{O}$	-844 to -948	Rikken et al., 1996; Malmqvist et al., 1991; van Ginkel et al., 1995
$\text{ClO}_3^- / \text{Cl}^-$	-746 to -1056	van Ginkel et al., 1995; Rikken et al., 1996; Bardiya and Bae, 2011; Malmqvist et al., 1991
$\text{ClO}_4^- / \text{Cl}^-$	- 822 to -988	Rikken et al., 1996; Bardiya and Bae, 2011
$\text{ClO}_4^- / \text{ClO}_3^-$	-752 to -918	Shrout and Parkin, 2006; Gurol and Kim, 1999;
$\text{ClO}_3^- / \text{ClO}_2^-$	-787	Rikken et al., 1996
$\text{ClO}_4^- / \text{ClO}_2^-$	-801	Rikken et al., 1996
$\text{ClO}_2^- / \text{Cl}^-$	0	Rikken et al., 1996
$\text{NO}_3^- / \text{N}_2$	-792 to -1030	Rikken et al., 1996, Malmqvist et al., 1991; Bardiya and Bae, 2011; van Ginkel et al., 1995
$\text{S O}_4^{2-} / \text{HS}^-$	-48	Malmqvist et al. 1991
<u>Hydrogen H_2/H^+</u>		
$\text{O}_2/\text{H}_2\text{O}$	-948.8	Nerenberg et al., 2002
$\text{NO}_3^- / \text{N}_2$	-897.6	Nerenberg et al., 2002
$\text{ClO}_4^- / \text{Cl}^-$	-896.8	Nerenberg et al., 2002
$\text{Mn}^{3+} / \text{Mn}^{2+}$	-225.47*	Madigan et al., 2009
$\text{Fe}^{3+} / \text{Fe}^{2+}$	-154*	Madigan et al., 2009
$\text{S O}_4^{2-} / \text{HS}^-$	-153.6	Nerenberg et al., 2002
<u>Elementary sulfur $\text{S}^0/\text{SO}_4^{2-}$</u>		
$\text{ClO}_4^- / \text{Cl}^-$	-904	Sahu et al., 2009
$\text{NO}_3^- / \text{N}_2$	728	Sahu et al., 2009

* Calculated using Free energies of formation ($\text{Fe}^{3+} = -4.6$ KJ/mol, $\text{Fe}^{2+} = -78.87$ KJ/mol, $\text{Mn}^{3+} = -82.12$ KJ/mol and $\text{Mn}^{2+} = -227.93$ KJ/mol)

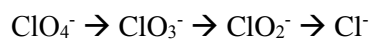
$E = (0.059 \text{ V}) \cdot \text{pe}$ for temperature maintained at 25°C,

$\Delta G^{\circ'} = -nFE$ where, n= no of electrons, F= Faraday's constant (96.48 KJ/V e⁻eq.)

The energy generated during reduction of perchlorate and other electron acceptors in presence of electron donors (acetate, hydrogen and sulfur) is shown in Table 2.5. The reported energies (highest values) shows that energy yielded by chlorate reduction to chloride (-1056 KJ/mol) and perchlorate to chloride (-988 KJ/mol) are comparable to that of oxygen (-948

KJ/mol). Malmaqvist et al. (1994) hypothesized that evolution of enzymes in the PRB might be affected by the preference for electron acceptor. Perchlorate/chlorate being an anthropogenic pollutant, microbes have had short time for bacterial evolution to develop the enzymes required, and hence, oxygen is preferred over the oxyanions (Malmaqvist et al., 1994). However, naturally formed perchlorate was found in arid area such as nitrate deposits in Chile and Antarctic Dry Valleys (Ericksen, 1981; Kounaves et al., 2010). Ericksen (1983) and Kounaves et al. (2010) observed perchlorate in nitrate mineral ore and soil respectively at higher elevations (>1000 m) with limited rainfall. Kounaves et al. (2010) found 31-620 ug perchlorate/kg soil at higher elevation (1000-2000m), and below 62 ug perchlorate/kg soil at coastal and inland areas in Antarctic Dry Valleys. The chemical process involved in perchlorate formation requires high temperature and pressure which cannot occur naturally on the earth's surface (Ericksen, 1983). Kounaves et al. (2010) suggested possible atmospheric perchlorate formation and deposition on land at higher elevation with extreme arid conditions. Further, Bender et al. (2004) isolated and identified two genera of bacteria capable of perchlorate reduction from lakes in lower Antarctic Dry Valleys, suggesting presence of perchlorate-reducing strains in nature. Additionally, a recent study involving four chlorate reducers reported genetic regulation of perchlorate reductase through plasmid involving composite transposon capable of horizontal insertion and suggested the chlorate reducing bacteria evolved from microbes capable of reducing chlorate (Clark et al., 2013).

The energies ($\Delta G_o'$) listed in Table 2.5 are the energy generated from complete perchlorate and chlorate reduction shown by Equation 2.3. The first two reactions yielded the energy, but the final step, disproportionation of chlorite to chloride and oxygen does not yield any energy (Kengen et al., 1999; Rikken et al., 1996).



Equation 2.3

The $\text{ClO}_4^-/\text{Cl}^-$ and NO_3^-/N_2 in Table 2.5 have similar $\Delta G_o'$, which indicates nitrate outcompetes perchlorate. The higher reduction potential for perchlorate over sulfate, manganese and iron indicate that perchlorate is comparatively preferred over the latter electron acceptors. Other studies have indicated that these electron acceptors (sulfate, manganese and iron) have no effect on perchlorate reduction (Malmqvist et al., 1991; Brown et al. 2003; Sellers 2007).

Table 2.5 shows that the same electron donor/acceptor pair has different energies. For example, $\Delta G^{o'}$ for $\text{ClO}_4^-/\text{Cl}^-$ (for acetate as electron donor) has -822 to -988 KJ/mol. This variation is due to different stoichiometric equation used by the studies, and the assumptions used for the conversion of Eh and pe to $\Delta G^{o'}$.

2.3.2 Microbial Kinetics of the Reduction Pathway

Microbial kinetics is important in a biological treatment unit to model and design the systems, as well as to predict and evaluate their results. During perchlorate reduction, PRB utilizes a carbon source as an electron donor, and perchlorate as an electron acceptor. The energy generated from the reduction process is used for biomass growth and cell synthesis (Rittman and McCarty, 2001).

The kinetics of perchlorate degradation is most commonly expressed by Monod's equation (Dudely et al., 2008; Logan et al. 2001; Nerenberg et al., 2006; Wang et al.; 2008). The utilization of electron donor/acceptor is governed by the concentration of microbes, and their biomass growth is proportional to the electron donor/acceptor available for energy generation. Many studies have investigated and reported kinetic parameters for pure and mixed cultures used for perchlorate reduction (Table 2.6). Kinetic parameters shown in Table 2.6 are maximum

substrate utilization rate (q_{\max}), half saturation constants (K_s), biomass yield (Y), and maximum growth rates (μ_{\max}) for various PRB (pure and mixed).

Table 2.6: Kinetic Parameters of Pure/Mixed Cultures Used for Perchlorate Reduction from Literature

Culture	Electron Donor	Electron Acceptor	q _{max} (mg ClO ₄ ⁻ /mg DW-d)	μ _{max} h ⁻¹	K _p (mg ClO ₄ ⁻ /L)	Y (g VSS/ g Acetate)	Decay Constant d ⁻¹	Reference
Mixed		Perchlorate	2.57					Attaway and Smith, 1993
GR-1	Acetate	Perchlorate	5.65	0.1		0.24		Rikken et al., 1996
		Chlorate	7.48					
Mixed	Acetate	Perchlorate		0.2	20	0.5	0.01	Urbansky, 2000
PDX	Acetate	Perchlorate	0.41*	0.24 (0.21) ^a	12±4			Logan et al., 2001
	Lactate	Chlorate		0.15				
<i>C. amalonaticus</i> JB101	Acetate	Perchlorate				0.09 ^b		Bardiya and Bae, 2004
INS	Acetate	Perchlorate	4.35	0.067	18	0.37		Waller et al., 2004
Mixed heterotrophic	Acetate	Perchlorate		0.1				Bardiya and Bae, 2004
Mixed	Ethanol	Perchlorate	0.002	0.13				Matos et al., 2006
PC1	Hydrogen	Perchlorate	3.1		0.14	0.23	0.055	Nerenberg et al., 2006
		Chlorate	6.3		<0.014	0.22		
Dechloromonas sp. HZ	Hydrogen	Perchlorate	0.22		8.9			Yu et al., 200
HCAP-C	Hydrogen	Perchlorate	4.39		76.6 ^c	0.36		Dudley et al., 2008
		Chlorate	8.3		58.3 ^c	0.30		
Mixed	Acetate	Perchlorate	0.49	0.004 ^e	<0.1	0.2	0.05	Wang et al. 2008
JB116	Acetate	Perchlorate				0.08 ^b		Bardiya and Bae, 2008
Mixed	Hydrogen	Perchlorate	0.043		0.03			London et al., 2011
Mixed	Ethanol	Perchlorate	0.3	0.082	4.97	3.64		Ricardo et al., 2012
		Nitrate	10.79	60	1.05	0.18		
P4B1	Acetate	Perchlorate	1.176	0.005	18	0.1		Xiao and Robers, 2013

^a Specific growth μ^b Values expressed as mg protein/mg Ac^c Y from fs assuming NH₄⁺ as source of nutrient (20 e- eq) (Rittman and McCarty, 2001)^d Calculated using: u=q*Y^e Higher kinetics were observed due to presence of another chlorate reducing strain in addition to pure culture of HCAP-C* values expressed as mg ClO₄⁻/ mg protein-hr

The q_{\max} indicated in Table 2.6 signifies the amount of perchlorate uptake by every gram of dried biomass per day. For pure culture of PRB, q_{\max} value found by previous researchers is between 0.41 to 6 mg $\text{ClO}_4^-/\text{mg DW-d}$ for acetate as electron donor and perchlorate as sole electron acceptor, and 0.22 to 4.39 mg $\text{ClO}_4^-/\text{mg DW-d}$ for hydrogen as electron donor and perchlorate as electron acceptor. The reported q_{\max} values for chlorate as sole electron acceptor are 7.48 and 8.3 for acetate and hydrogen as electron donors, respectively. This indicates that the q_{\max} for chlorate is higher than perchlorate for both electron acceptors. The higher q_{\max} value for chlorate suggests that for the same amount of biomass formation, microbes reduce larger amount of chlorate than perchlorate. The q_{\max} values are lower than following q_{\max} values calculated for denitrifiers: 24.87 g $\text{ClO}_4^-/\text{g VSS-d}$ (16 g BOD/g VSS-d) for BOD, 15.5 g $\text{ClO}_4^-/\text{g VSS-d}$ (1.25 g $\text{H}_2/\text{g VSS-d}$) for hydrogen and 7.81 g $\text{ClO}_4^-/\text{g VSS-d}$ (6.7 g S/g VSS-d) for sulfur as electron donor (Rittmann and McCarty, 2005).

The reported maximum growth rate (μ_{\max}) for these pure cultures with perchlorate as electron acceptor and acetate as electron donor ranges from 0.067 to 0.24/h. Rittmann and McCarty (2001) listed μ_{\max} values 0.04 (for denitrifiers utilizing hydrogen or sulfur), and 0.16 (for heterotrophic denitrifiers). These listed values are comparable to the reported μ_{\max} values in Table 2.6.

The electrons needed for complete reduction of perchlorate is 8 and for chlorate is 6, suggesting that a less acetate is required for chlorate than perchlorate. Biomass yield is defined as gram of biomass produced per gram of acetate utilized. Table 2.6 shows the reported biomass yield (Y_{\max}) ranging between 0.2 to 0.69 for all electron acceptors and donors. The minimum reported yield is comparable to the yield for heterotrophic denitrifiers (0.25), but maximum reported yield is more than the yield for aerobic heterotrophs (0.42) (Rittmann and McCarty,

2005). The low yields of *C. amalonaticus*, *C. farmer* and JB116 might be because of different biomass analysis (mg protein/mg acetate).

The reported half saturation constant (K_p) for perchlorate is low when acetate was used as sole electron donor (2.2 to 18 mg ClO_4^-/L) compared to hydrogen as electron donor (0.14-76.6 mg ClO_4^-/L). Further, half saturation constant for chlorate (electron donor) is 710 mg ClO_4^-/L for acetate and 58.3 mg ClO_4^-/L for hydrogen as electron acceptor. As compared to the kinetics of chlorate, perchlorate will have faster kinetics at low concentrations of perchlorate. However, the large K_p values might be of concern for biological treatment of perchlorate in drinking water due to the slow microbial kinetics.

For mixed culture, reported q_{\max} values are 0.49 mg $\text{ClO}_4^-/\text{mgDW-d}$ for acetate, and a range of 0.043 to 2.92 for hydrogen as electron donor. K_p values range between 0.1 to 20 mg ClO_4^-/L for acetate and 0.01 to 567.3 mg ClO_4^-/L for hydrogen as electron acceptor. However, μ_{\max} and biomass yield were within the range as the pure culture. Appendix I (Table I.1) lists other reported kinetics.

2.3.3 Biochemical Reactions and Stoichiometry Involved in the Reduction Process

The knowledge of reaction energetic can be used to calculate theoretical molar ratio between electron donor, acceptor, and biomass generated from the donor. The stoichiometry of overall reaction of perchlorate utilization in presence of other electron can be estimated using biochemical reactions for each electron acceptor, and their stoichiometry as moles of electron donor required per mole of electron acceptor.

For electron donor, acetate, electron acceptors were oxygen, nitrate and perchlorate, and nitrate as the nutrient for cell synthesis, f_s and f_e can be obtained as 0.47 and 0.53 (Appendix A). Further assumptions: b_{det} was 0.23d^{-1} , and the transfer efficiency of electron from carrier to the

synthesis (ϵ) was 0.4 (McCarty and Meyer, 2005). McCarty and Meyer (2005) observed similar f_s for perchlorate (0.48), but the carbon source used for the study was ethanol. For aerobic oxidation of ethanol, with same assumptions for f_d and b , f_s was obtained to be 0.5. This difference may be caused by difference in nutrient source (ammonia or nitrate) assumption which affected the calculation for energy needed for converting pyruvate to cellular carbon. For this study, the overall stoichiometry can be obtained by replacing f_s and f_e for perchlorate in presence of oxygen and nitrate in Equation A1 (Appendix A). The stoichiometric reactions reported for acetate with various electron acceptors are shown in Table 2.7.

Table 2.7: Stoichiometric Reactions Reported for Acetate (Electron Donor) with Various Electron Acceptors (Oxygen, Nitrate, Perchlorate and Chlorate)

Stoichiometric Reactions	Reference
$1.7 \text{ CH}_3\text{COO}^- + \text{ClO}_4^- + 0.28\text{NH}_4^+ + 0.28\text{HCO}_3^- \rightarrow 0.28 \text{ C}_5\text{H}_7\text{O}_2\text{N} + \text{Cl}^- + 1.7 \text{ HCO}_3^- + 0.58\text{CO}_2 + 1.42 \text{ H}_2\text{O}$ Equation 2.4	Waller et al., 2004
$2.44 \text{ CH}_3\text{COO}^- + \text{ClO}_4^- + \text{NH}_4^+ \rightarrow 0.58 \text{ C}_5\text{H}_7\text{O}_2\text{N} + \text{Cl}^- + 1.87 \text{ CO}_2 + 0.096 \text{ HCO}_3^- + 1.87 \text{ H}_2\text{O}$ Equation 2.5	Kesterson, 2005
$\text{CH}_3\text{COO}^- + 0.522 \text{ O}_2 + 0.494 \text{ NO}_3^- + 0.245 \text{ ClO}_4^- + 0.494 \text{ H}^+ \rightarrow 0.064 \text{ C}_5\text{H}_7\text{O}_2\text{N} + 0.215 \text{ Cl}^- + \text{HCO}_3^- + 0.678 \text{ CO}_2 + 1.021 \text{ H}_2\text{O} + 0.215 \text{ N}_2$ Equation 2.6	This study
$\text{H}_2 + 0.105 \text{ O}_2 + 0.114 \text{ NO}_3^- + 0.049 \text{ ClO}_4^- + 0.115 \text{ H}^+ + 0.134 \text{ CO}_2 \rightarrow 0.027 \text{ C}_5\text{H}_7\text{O}_2\text{N} + 0.049 \text{ Cl}^- + 0.963 \text{ H}_2\text{O} + 0.044 \text{ N}_2$ Equation 2.7	This study
$\text{C}_3\text{H}_8\text{O}_3 + 0.751 \text{ O}_2 + 0.804 \text{ NO}_3^- + 0.349 \text{ ClO}_4^- + 0.803 \text{ H}^+ \rightarrow 0.182 \text{ C}_5\text{H}_7\text{O}_2\text{N} + 0.349 \text{ Cl}^- + 2.090 \text{ CO}_2 + 3.764 \text{ H}_2\text{O} + 0.311 \text{ N}_2$ Equation 2.8	This study

* No consumption of acetate during disproportionation of chlorite

Equations 2.6 indicates that 1 mole of acetate is needed to reduce 1.42 mole of oxygen, 1.13 mole of nitrate and 0.71 mole of perchlorate (Table 2.7). Studies have been shown that approximate ratio of carbon source to perchlorate ratio is between 1.65 to 1.72 mole acetate/mole perchlorate. The optimum ratio of electron donor to perchlorate reported is about 1.2 g COD/g ClO_4^- (Chaudhuri et al., 2002; Waller et al., 2004; Shrout and Parkin, 2006).

2.4 Denitrification

Denitrification is a microbial-facilitate process in which nitrate is reduced to nitrogen gas in four steps (Figure 2.10). Several species of bacteria are involved in the complete reduction of nitrate to molecular nitrogen, and more than one enzymatic pathway have been identified in the reduction process. Figure 2.10 shows the four enzymes nitrate reductase, nitrite reductase, nitric oxide reductase and nitrous oxide reductase involved in complete denitrification process for dissimilatory nitrate reduction. In an anaerobic environment, denitrification occurs as a dissimilatory nitrate reduction, but in a comparatively insignificant amount assimilatory nitrate reduction may also occur (Tiaje, 1988).

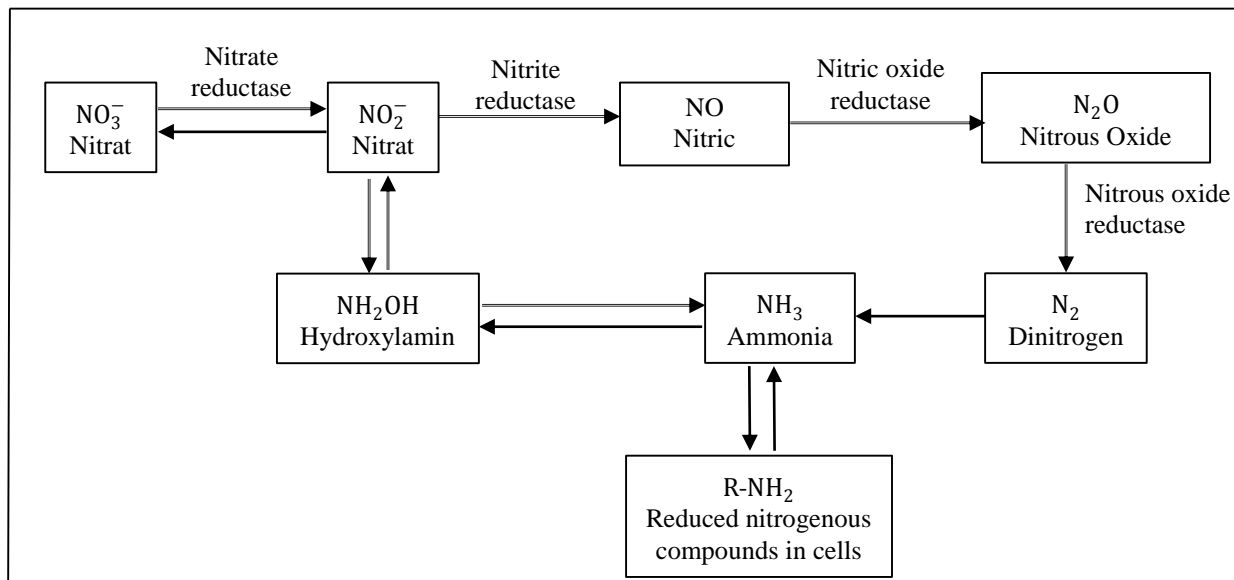


Figure 2.10: The biological nitrogen cycle pathway (Modified from: Shapleigh, 2016).

Denitrifying bacteria belong to different physiological and taxonomic groups. Most of the bacteria belong to *Proteobacteria* group and the nitrate reduction pathway can be found in organotrophs (such as *Pseudomonas*, *Alcaligenes* and *Acinetobacter*), lithotrophs (*Alcaligenes*, *Pseudomonas* and *Paracoccus*) and phototrophs (*Rhodospseudomonas*) (Tiaje, 1988). These

bacteria are facultative gram negative bacteria, but some gram positive strains have shown possibility to denitrify (such as *Bacillus*) (Suharti et al., 2001). Some halophilic bacteria, such as *Paracoccus* and archaeal strain *Halobacterium* have capability to reduce nitrate (Tiaje, 1988; Rittman and McCarty, 2001).

Denitrifying bacteria can utilize other electron acceptors including oxygen, perchlorate and sulfate. The Presence of perchlorate and sulfate does not affect nitrate reduction due to their lower redox potential, but oxygen can inhibit nitrate reduction completely. Nitrate-reducing enzyme is relatively insensitive to oxygen, but in the presence of oxygen, nitrate reduction by *Mycobacterium tuberculosis* ceased due to interference of nitrate transport in the bacterial cell (Sohaskey, 2005). Another study with *Pseudomonas aeruginosa* also showed oxygen inhibition in nitrate reduction, specifically by nitrate uptake (Hernandez and Rowe, 1987). The study indicated that the degree of inhibition was dependent on the oxygen concentration and increasing nitrate concentrations did not overcome the inhibition (Hernandez and Rowe, 1987). Two strains *A. magnetotacticum* and *N. europaea*, which are microaerophilies have shown possibility to denitrify in presence of oxygen (Tiaje, 1988).

The diversity of microorganism in a biological system is also affected by type of carbon source. Osaka et al. (2006) observed that in reactors with methanol as carbon source, the dominating *Proteobacteria* belonged to family *Methylophilaceae* and *Hyphomicrobiaceae*. In acetate fed reactors, bacteria belonging to *Comamonadaceae* and *Rhodocyclaceae* were dominant. Shah and Coulman (1978) reported that denitrification is a first-order reaction. The study reported that for complete nitrate removal, the organic carbon should be three times the stoichiometric requirement for nitrate as nitrogen. The kinetics parameters for denitrification are shown in Table 2.6.

The reported half saturation constant (K) for nitrate varies with type of electron donor; the lowest K value was reported as 0.25 mg/L for biological oxygen demand (BOD) present in wastewater as electron donor, 0.85 to 2 mg/L when acetate was used as sole electron donor, and 1 mg/L for ethanol as electron donor. When compared to the kinetics of perchlorate, nitrate has faster kinetics at low concentrations levels.

2.5 Factors Affecting Perchlorate Reduction Pathway

2.5.1 Effect of Electron Donor

Perchlorate-reducing bacteria can utilize various electron donors, either organic or inorganic compounds, as source of energy. Most commonly used organic electron donors are acetate, lactate, methanol and ethanol, and these compounds act as both carbon source and electron donor (Wallace et al., 1998; Urbansky 2000; Xu et al., 2003). Attaway and Smith (1993) observed growth of perchlorate reducing mixed culture enriched with simple sugars, alcohol and organic acids, though these carbon sources did not support perchlorate reduction. However, the culture degraded perchlorate when enriched in rich protein-based carbon sources. Other studies also observed perchlorate reduction in enrichment of *Wollinella succinogenes* (HAP1) with proteins, and peptides as electron donor (Logan, 2001; Wallace et al., 1998). van Ginkel et al. (1995) observed that glucose act as both electron donor and acceptor for chlorate reducers; growth of these organisms did not yield chloride in the solution. Glucose was fermented, producing acetic acid, formic acid, ethanol and traces of lactic acid, and the byproducts were later used as electron donors for chlorate reduction.

van Ginkel et al. (1995) and Bruce et al. (1999) observed chlorate reduction with hydrogen sulfide, but oxidation of hydrogen sulfide did not support biomass growth in strain CKB and

demonstrated limited growth with addition of acetate (Bruce et al., 1999). The strain, CKB, did not support growth with fermentation or autotrophically with hydrogen gas.

Perchlorate reduction with autotrophic perchlorate-reducing bacteria has been reported and documented for membrane bioreactors (van Ginkel et al., 1995; Logan and LaPoint, 2001; AwwaRF 2004; Wolterink 2004; Nerenberg et al., 2003, 2004 and 2006; Dudely et al., 2008; London et al, 2011; Ontiveros-Valencia et al., 2013; Sahu et al., 2009). These autotrophic bacteria utilize inorganic sources such as hydrogen gas, and elementary sulfur as electron donor (Nerenberg et al., 2003; Nerenberg et al., 2006; Nerenberg and Rittmann 2004; Sahu et al., 2009), and require a carbon source for microbial cell synthesis and growth. These autotrophic PRB utilize CO₂ as carbon source (Logan and LaPoint, 2001; Nerenberg et al., 2006; Dudley et al., 2008; London et al, 2011; Ontiveros-Valencia et al., 2013; Sahu et al., 2009), but some strains increased perchlorate reduction in the presence of other organic carbon sources (AWWaRF, 2004; Shrout et al., 2005). Shrout et al. (2005) suggested chlorite dismutase activity can be improved by switching from inorganic to organic electron donor in autotrophic PRB (hydrogen gas as electron donor and CO₂ as carbon source).

Studies have indicated that lack of electron donor decreases the perchlorate reduction (Liu, 2000). The ratios of electron donor to perchlorate affected the reduction potential maintained in an oxidized condition in the reactor (Shrout and Parkin, 2006). The ratio of chlorate to acetate in batch culture was 1:1, but 25 to 30% of acetate was used for anabolic reactions or cell synthesis (van Ginkel et al., 1995).

2.5.2 Effect of Competition of Other Electron Acceptors

Oxygen and Nitrate are the most common competitive electron acceptors coexisting in groundwater contaminated with perchlorate, and are usually present in one to three orders of

magnitude concentration compared to perchlorate (Xu et al. 2003; Batista et al., 2002; Batista et al., 2005; Gu and Coates, 2006). Other commonly found contaminants in groundwater include sulfate, iron, and manganese oxides.

Gingras (2003) listed the chemical characteristics of groundwater of perchlorate contaminated sites (such as Kerr McGee Seepage, Nevada), and drinking water sources (such as Lake Mead, Nevada); typical concentrations in drinking water sources, for perchlorate range between 8 to 200 ug/L, for oxygen between 0 to 4 mg/L and for sulfate and nitrate concentrations below the drinking water standards (250 mg/L as SO_4^{2-} and 44.3 mg/L as NO_3^-). Iron and manganese concentrations were very low in groundwater contaminated with perchlorate (Herman and Frankenberger, 1997). van Ginkel et al. (1995) observed no effect on biological perchlorate reduction due to high concentrations of sulfate, manganese and iron. The low potential energy compared to perchlorate also suggests that these electron acceptors (manganese iron, and sulfate) do not compete with perchlorate reduction (Table 2.5; van Ginkel et al., 1995; Herman and Frankenberger, 1997). Table 2.8 shows the effect of oxygen and nitrate on perchlorate reduction (Details in Table I.2).

Table 2.8: Effects of Other Electron Acceptor on Perchlorate Degradation

Electron Acceptors	Perchlorate Degradation in Presence of Other Electron Acceptors	Reference
Oxygen	2 mg/L inhibited chlorite dismutase	Chaudhuri et al., 2002; Song and Logan, 2003
	4 mg/L no perchlorate degradation	Choi et al., 2007
	Simultaneous degradation observed	Attaway and Smith, 1993; Ricardo et al., 2012
Nitrate	No perchlorate reduction	Chaudhuri et al., 2002; Xiao et al., 2010
	Perchlorate removal not affected with culture enriched in perchlorate	Okeke et al., 2002; Bardia and Bae, 2004

All the past studies have indicated that the presence of oxygen prohibits the perchlorate reduction process (Attaway and Smith, 1993; Kengen et al., 1999; Chaudhuri et al., 2002; Xu et al., 2003; Song and Logan, 2004; McCarty and Meyer, 2005; Choi et al., 2007). The bacteria gain more energy and biomass yield from oxygen than from utilizing nitrate or perchlorate, making oxygen a preferred electron acceptor over the other two (van Ginkel et al., 1995; Coates et al., 1999; Choi et al., 2007).

Attaway and Smith (1993) and van Ginkel et al. (1995) observed inhibition of perchlorate reduction under aerobic condition; exposure to oxygen for more than 12 hours completely terminated the ability of *W. succinogenes* HAP1 to reduce perchlorate (Attaway and Smith, 1993). van Ginkel et al. (1995) detected no chloride production in solution with chlorate-reducing inocula enriched from activated sludge in the presence of acetate and chlorate when molecular oxygen was introduced. Song and Logan (2004) observed that *Dechlorosoma* sp. KJ in a chemostat (suspended growth) ceased the biodegradation process with exposure to dissolved oxygen (DO) at 6-7 mg/L for more than 12 hours, and for DO exposure for less than 12 hours, perchlorate degradation was observed. However, the time required for regaining perchlorate degradation was not mentioned. Similarly, Choi et al. (2007) observed no perchlorate degradation at elevated DO, but regained complete perchlorate degradation within 30 min after decreasing the DO to 1 mg/L in a FBR with mixed culture. Choi et al. (2007) observed that the DO within the biofilm approximates 1 mg/L when influent DO was 4 mg/L. The biofilm has the advantage of mass transfer limitation over suspended growth, and was expected to have reduced the impact of oxygen on perchlorate degradation. However, surprisingly the oxygen concentration to inhibit perchlorate degradation was 4mg/L, which is lower than the threshold DO concentration (6-7 mg/L) for the suspended culture experiment by Song and Logan (2004).

The difference in threshold oxygen concentration reported by the two studies might be because of two different enrichments: pure strain (Song and Logan, 2004) and mixed culture (Choi et al., 2007).

The effect of oxygen in water might also be due to the oxygen sensitive enzymes of perchlorate reductase and chlorite dismutase, which are not expressed under aerobic conditions, inhibiting perchlorate reduction (Chaudhuri et al., 2002; Xu et al., 2004). Chaudhuri et al. (2002) indicated a significant role of genetic regulation in perchlorate reduction; even a low concentration of oxygen (<2 mg/L) can inhibit chlorite dismutase expression. Chaudhuri et al. (2002) further demonstrated that anaerobic condition alone cannot support enzymatic activities. van Ginkel et al. (1995) observed slow chlorate reduction in enrichment from anaerobic sludge compared to activated sludge. Switching the aerobic reactor into anaerobic at the beginning of a log growth phase can enhance enzymatic activity in the PRB (Chaudhuri et al., 2002).

Nitrate also reduced the enzymatic activity of perchlorate, but the effect of nitrate on perchlorate reduction is debatable (Table 2.8; Table I.2; Chaudhuri et al., 2002; Attaway and Smith 1993). Many PRB can denitrify completely or partially, but not all perchlorate respiring bacteria (e.g. strain CKB) could use nitrate for growth (Kengen et al., 1999; Chaudhuri et al., 2002; AWWaRF, 2004). Xu et al. (2004) and Chaudhuri et al. (2002) observed that enrichment medium affects the development of the enzymes needed for perchlorate and nitrate. The studies also demonstrated that PRB prefer nitrate over perchlorate. PRB cultures acclimatized to nitrate or perchlorate alone utilized perchlorate only after complete nitrate reduction (Chaudhuri et al., 2002). This result supports the thermodynamics of nitrate and perchlorate reduction. A PRB strain, CKB, reduced perchlorate rapidly in perchlorate solution, but the rate and extent of perchlorate reduction in solution was decreased in presence of both nitrate and perchlorate,

suggesting the nitrate competitively inhibited perchlorate reduction (Chaudhuri et al., 2002). The study also observed a simultaneous reduction of perchlorate and partial denitrification; despite the strain, CKB, cannot grow by nitrate reduction (Chaudhuri et al., 2002; Bruce et al., 1999). This suggests possible and nitrate by perchlorate reductase (Chaudhuri et al., 2002). Herman and Frankenberger (1998) observed a relatively small difference in perchlorate reduction by strain perlace in presence of nitrate, and complete denitrification was observed simultaneously. Interestingly, in presence of both nitrate and perchlorate in solution, nitrate reduction was completed in 48 hours, whereas perchlorate was reduced within 36 hours.

Attaway and Smith (1993) indicated no effect on perchlorate reduction in presence of nitrate under anaerobic conditions. Bardiya and Bae (2004) also observed a higher amount of perchlorate reduction compared to nitrate for PRB strains JB 101 and JB 109 (similar to *Citrobacter* spp.). Recently, Xiao and Roberts (2013) also observed no effect of nitrate on perchlorate reduction by the *Marinobacter vinifirmus* P4B1 strain; instead simultaneous degradation of nitrate and perchlorate was observed. The culture was acclimatized in solutions of nitrate, perchlorate, and a mixture of both nitrate and perchlorate. The culture enriched in solution with both nitrate and perchlorate surprisingly degraded perchlorate rapidly, but nitrate degradation was not significant. Nitrate degradation started only when perchlorate was reduced by half. Biodegradation in presence of multiple electron acceptors such as oxygen and nitrate will require more electron donor (Gu and Coates, 2006). Brown et al. (2003) observed that in the presence of oxygen and nitrate, the carbon source requirement for perchlorate removal was twice that of the amount.

2.5.3 Salinity

The effect of salinity in microbial growth and biological degradation of perchlorate is well documented (Logan et al., 2001; Batista et al., 2002; Kesterson, 2005; Ahn et al., 2009; Sharbatmalekhi, 2010; Xiao et al., 2010; Venkatesan et al., 2011; Xiao and Roberts, 2013). Studies have shown possibility of biodegradation of high concentration perchlorate in brines and high salinity regenerant wastes from ion exchange (Logan et al., 2001; Batista et al., 2002; Kesterson, 2005; Sharbatmalekhi, 2010; Venkatesan et al., 2011). However, high salinity inhibits microbial growth and may change the microbial community in the reactor (Ahn et al., 2009). Except for halophilic bacteria, most bacteria cannot grow in environments with high salinity due to the osmotic pressure on the microbes (Madigan et al., 2009). Some halophiles can accumulate organic (such as amino acids, and glycerol), or inorganic (such as Mg^{2+} and K^{+}) solutes and balance the ionic strength of their cytoplasm with the saline environment, but the process consumes energy (Oren, 1999). Logan et al. (2001) observed decrease in microbial growth with increase in salinity in the pure enrichment. The growth rate decreased to 0.06/d at 5% salt concentration, while at salt concentrations > 9%, the growth rate was limited to 0.039/d (Logan et al., 2001). Further increase in salt concentration to 11% reduced growth rate by 38%, and no growth was observed at salinity >13% (Logan et al., 2001). Ahn et al. (2009) observed change in microbial community at 3% salinity in a membrane biofilm reactor treating synthetic ion exchange brine. Perchlorate reduction yields chloride at 1:1 ratio and accumulates in the system; culture enrichment requires frequent wasting to prevent chloride accumulation exceeding 1% (AWWaRF, 2004).

Salinity also affects the removal efficiency of bioreactors; salinity as low as 1% hindered perchlorate degradation (Liu, 2000; Logan et al. b, 2001). However, some studies indicated that

a stepwise acclimatization of PRB collected from marine sources exhibited salt tolerance characteristics (Bardiya and Bae, 2011). Table 2.9 lists the previous studies of salinity effect on perchlorate degradation.

Gingras and Batista (2002) observed a decrease in perchlorate reduction by half when salinity was 0.5% and further decreased by more than 90% at salinity level of 1 to 1.5%. Salt concentrations exceeding 4% may inhibit perchlorate reduction completely (Bardiya and Bae, 2011). Okeke et al. (2002) and Lehman et al. (2008) demonstrated PRB sustained at 7.5% and degradation of perchlorate in stepwise acclimatized culture (Table 2.9).

Table 2.9: Reported Effects of Salinity on Perchlorate Degradation

Reference	Culture	Salinity (%)	Initial	Removal mg/L-h
Gingras and Batista, 2002	BALI	0	100	0.29
		0.5	100	0.14
		0.5	100	0.13
		1	100	0.03
		1	100	0.03
		1.5	100	0.01
		1.5	100	0.02
Okeke et al., 2002	Citrobacter (IsoCock1)/perclase	7.5	100	0.61
	Citrobacter (IsoCock1)/perclase	7.5	100	0.28
	Citrobacter (IsoCock1)	7.5	100	0.26
	Citrobacter (IsoCock1)	7.5	100	0.39
	Perclase	7.5	100	0.38
	Perclase	7.5	100	0.17
	Citrobacter(IsoCock1)/perclase	0	500	2.48
	Citrobacter(IsoCock1)/perclase	2.5	500	2.35
	Citrobacter(IsoCock1)/perclase	5	500	2.45
	mixed (step acclimatization to 3-6% salinity)	6	65	6.49
Xiao and Roberts, 2013	P4B1 (derived from previously enriched culture)	3	450	3.75

2.5.4 Temperature and pH

The effect of temperature is well known in wastewater treatment, because the microbial metabolic activity is reduced at low temperature (Metcalf and Eddy, 2003). pH affects the enzymatic activities in PRB by altering the acidic and basic groups of the substrate molecules or the ionic forms of the active site of the enzyme (Wang et al., 2008). The effect of temperature and pH on perchlorate reduction is shown in Table 2.10.

Table 2.10 shows that the maximum perchlorate reduction was observed at temperature 30 °C and pH of 7.5. The most reported temperature range for perchlorate degradation is 10 to 40°C with an optimum range of 28 to 37°C (Min et al., 2004; Brown et al., 2005; Bruce et al., 1999; Chaudhuri et al., 2002; Okeke et al., 2002). In general, for bacterial, the optimum temperature is 30 to 35°C (Madigan et al., 2009). Bardiya and Bae (2011) observed 10°C as the critical threshold temperature for effective perchlorate reduction (Bardiya and Bae, 2011).

Table 2.10: Effect of Temperature and pH on Perchlorate Reduction

Culture	Temperature (°C)	Perchlorate Removal (%)	pH	Perchlorate Removal (%)	Reference
Citrobacter sp.	20	60	6	38	Okeke et al., 2002
	25	95	7	40	
	30	98	7.5	98	
	35	95	8	38	
	40	8	9	30	
			10	0	

Many studies have reported a pH range of 6.5 to 8.5 (Attaway and Smith, 1993, Bruce et al., 1999, Okeke et al., 2002), and an optimum pH of 7 to 7.2 for most PRB (Herman and Frankenberger, 1998). Herman and Frankenberger (1998) observed an optimum pH of 7.5 for perlace, and Okeke et al. (2002) also observed pH of 7.5 as the optimum pH for perchlorate

reduction by *Citrobacter sp.* The perchlorate degradation decreased to half as pH was changed by half log units (Table 2.10), indicating the sensitivity of pure culture perchlorate degradation on pH. In order to keep the pH within the optimum range, most of the laboratory studies have used either phosphate buffer or bicarbonate buffer in the system (Xu et al., 2003).

2.6 Ex-situ Treatment with Fixed Film Biological Reactors

Fixed film reactors are widely used for biological perchlorate reduction, either as fixed bed or FBR. Contaminated water flows in the downward direction in a fixed bed reactor and upwards in a FBR. These reactors contain media such as sand and/or GAC, which provides surface area for microbial growth. The microbes grow on the media, forming a biofilm which increases their retention time in the reactor, and hence reduces the reactor size as compared to suspended growth reactors. Biofilms formed in the media also provide protection against perturbations in temperature, pH, desiccation, and other environmental factors (Wallace et al., 1998). Nutrients and a supplemental carbon source, such as acetate, ethanol and glucose, are injected into the reactor to foster the growth of the bacteria.

2.6.1 Fixed Film Reactors for Perchlorate Reduction

Perchlorate concentration in drinking water is in the parts per billion (ppb) range (Batista et al., 2002). Based on the microbial kinetics for perchlorate reduction, fixed film reactors are preferred over suspended growth (Urbansky, 2000). Table 2.11 lists the configuration of reported reactors (FBR, fixed bed and membrane reactors) used for biological perchlorate removal (Details in Table I.2). Most of the studies are focused on high concentration of perchlorate due to the slow microbial kinetics at lower perchlorate concentration.

In a FBR, media is maintained in suspension by the upward stream of water which maintains the pressure gradient across the media which equals the total weight of the media (Characklis 1990; Rittmann and McCarty, 2001). The fluidization of media in FBR increases the media surface area available for microbial growth by 15 to 20%. FBR maintains a high biomass density even when the influent loading rate is very high (Hatzinger, 2005). The ability to maintain very high biomass concentrations in the FBR results in less time for complete perchlorate reduction (Min et al., 2004).

The design and operation of a FBR used for perchlorate reduction is influenced by factors such as ambient temperature and pH, electron donor selected, concentration of oxygen, nitrate and perchlorate in the feed, design flow rate, and concentrations of nutrient, electron donor and acceptor (Adham et al., 2004; Brown et al., 2003).

Table 2.11: Configuration of Reported Reactors Used for Perchlorate Removal

Reactor Configuration	Media Bed Depth (m)	Microbes	Flow (mL/min)	HRT (h)	Electron Donor	Electron Acceptor	Influent Conc.	Perchlorate Removal (mg/min)	Reference
Upflow bioreactor									
1.17 m length and 7.6 m diameter with diatomaceous earth pellet (1.17 m depth)	Waste stream from rocket motor wash	W. succinogenes HAP1	0.5	1.17	Brewers yeast extract (BYF-100)	ClO ₄ ⁻	1500	0.6	Wallace et al., 1998
			0.5	0.46			500	0.2	
Sand (32% expansion)	Ground water from Nevada	Mixed, dentirifying	11.5	2.1	Ethanol	ClO ₄ ⁻	400	4.595	Hatzinger et al., 2000
						NO ₃ ⁻	20	0.219	
						ClO ₃ ⁻	480	5.474	
GAC (full scale plant)	Ground water from California		2574	ClO ₄ ⁻		8	20.582		
				NO ₃ ⁻		1.5	3.861		
				ClO ₃ ⁻		20	51.480		
0.7 m long and 0.15 m internal diameter with plastic media (0.63 m depth)	Synthetic water	Mixed	26	8	Acetate	ClO ₄ ⁻ only (ug/L)	1000	25.896	Choi and Silverstein, 2008
						ClO ₄ ⁻ (ug/L)	1000	25.636	
						NO ₃ ⁻	10 to 16	0.416	
Fixed bed reactor									
0.125 m and 0.025 m internal diameter glass beads (0.1 m depth)	0.1	Mixed	2.3	0.018-0.022	Hydrogen		740	1.055	Miller and Logan, 2000
28 cm long 2.5 cm dia with sand (0.28 m depth)	0.28	Pure (MS2)	50	0.035	Acetate	ClO ₄ ⁻	25.6	1.280	Kim and Logan, 2001
14 cm long, 2.5 cm dia with sandy soil (0.14 m depth)	0.14	Mixed	2.2	0.5	Acetate	ClO ₄ ⁻	20	0.044	
Membrane bioreactor									
Membrane	mixed				Lactate	ClO ₄	100,000	0	Liu, 2000
						NO ₃ ⁻	60	0	

2.6.1.1 Tracer Test in a FBR

Reactors are designed based on ideal plug flow or complete mix assumption, but may not fulfill those assumptions (Wolf and Resnick, 1963). Actual hydraulic condition of the reactors is important to evaluate the design and actual operation conditions. Tracer test is used to characterize the hydraulic regime of a reactor (Teefy and Singer, 1990). The tracer test is performed with a conservative tracer, such as sodium chloride salts and dyes, injected into the reactor at a known concentration, and measuring the effluent tracer concentration with time. The FBR is assumed to be a completely mixed reactor, unlike typical fixed bed reactors which are designed to achieve a plug flow configuration. The results of a tracer test provide of mean hydraulic residence time, dispersion number, and allows for analysis of the breakthrough model (Levenspiel, 1972). Furthermore, the data can be analyzed using an analytical approach to produce a function curve, $F(t)$ curve, as described in Wolf and Resnick (1963). The $F(t)$ curve represents the fraction of total tracer that arrived at the sampling point during the test. For perfect mixing, $F(t)$ is given as:

$$F(t) = 1 - e^{-t/\theta}$$

2.6.2 Backwashing in a FBR

Backwashing of FBR to remove accumulated biomass plays an important role in proper operation of the reactor and controlling microbial activities. However, backwashing of FBR reactors to treat perchlorate has not yet been characterized properly and lacks in-depth studies (Li et al. 2011). In fixed bed reactors, media get clogged due to excessive microbial growth (biomass), resulting in increased head loss and short circuiting in the reactor (Min et al., 2004), whereas in FBR, excessive biomass results in media buoyancy and loss in the effluent, and limits mass transfer of electron donors in the biofilm (Laurent et al., 2003). A bioreactor is periodically

backwashed to clean the media, maintain the hydraulic capacity and desired filter runs times, and prevent undesired breakthrough (Eleuterio, 2007). Backwashing involves rapid mixing of the media impregnated with biomass using water only or mixture of water and air; the abrasion between the media particles scours the biomass and cleans the media

Laurent et al. (2003) observed a 3% improve in ammonia removal after backwash of FBR, which might be due to improved oxygen availability to the microbes after backwash. However, backwashing can impair biological development on the media (Bouwer and Crowe 1988; Laurent et al., 2003; Emelco et al. 2006). Urfer (1998) emphasized the importance of careful monitoring of biomass in filtration cycles, and effective control of biomass losses for the success of a biofilter. Some studies observed no biomass loss in fixed bed reactors after backwashing (Servais, 1991; Miltner et al., 1995; Laurent et al., 2003). Servais (1991) observed removal of 4-8% of microbes attached to the media due to backwashing and concluded that majority of biomass removal was due to mortality. Miltner et al. (1995) further stated that backwashing removes the suspended cells only, and the abrasion of the media does not change the biomass. Laurent et al. (2003) indicated possible vertical redistribution of media and biomass after backwashing, but observed no significant difference in the potential nitrifying activity before and after backwash in the reactor. However, Laurent et al. (2003) reported a faster ammonia removal before backwashing at EBCT of 2.3 minutes whereas after backwash the filter required EBCT of 4.5 minute to achieve 89% removal

Choi et al. (2007) observed a lag of 12-hour after backwashing for perchlorate removal in a fixed bed reactor depending upon oxygen concentration in backwash water and intensity of backwashing. The backwashing was replicated by stirring the entire reactor content in a beaker with a magnetic stirrer, and speed (rpm) of the stirrer indicated different intensities of

backwashing. The intensities were categorized as weak (75 rpm) and strong (150 rpm). A negative effect of backwashing was observed on perchlorate removal at both backwash intensities, with or without air (Choi et al. 2007). Another study, with the same backwash intensities as Choi et al. (2007), by Li et al. (2012), also observed negative impact of backwashing intensity on perchlorate removal. The study showed that after a high intensity backwashing, the dominant population of microbes was aerobic microbial strains instead of PRB strain, the facultative bacteria capable of perchlorate removal (Li et al., 2012).

2.7 Biofilm Modeling for a FBR

A fixed film reactor such as FBR has microbes growing in layers on the media, known as biofilm which immobilizes the microbes, providing a large solid retention time, and maintaining a high biomass content in the system at any given time. Biofilm is defined as an aggregation of bacteria on a solid surface forming a slime layer (Characklis and Marshall, 1990). Figure 2.11 shows a schematic representation of biofilm growth in a media. Biofilms require electron donor, electron acceptor and nutrient for biofilm growth; these will be termed substrate hereafter. Most engineering processes are focused on bacterial community in a biofilm, but the biofilm may also contain higher organisms, other than bacteria. This dissertation focuses on bacterial growth on biofilm.

Biofilms in Fixed-growth systems provide a stable biomass within the system and do not require recycling after a solid-liquid separation process. For design and optimization of a fixed-film reactor, it is necessary to understand biofilm kinetics for growth and substrate utilization.

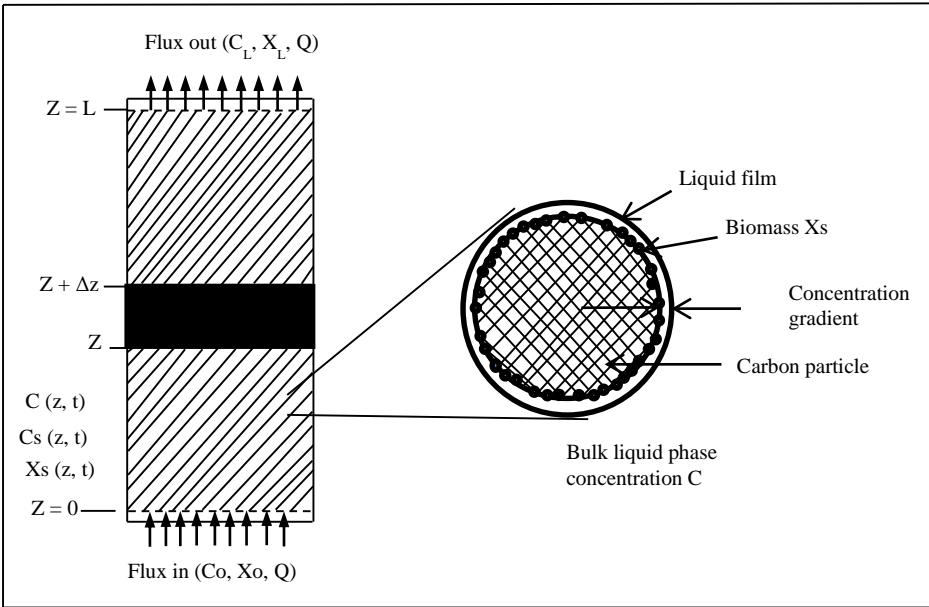


Figure 2.11: Schematic representation of biomass growth in media (Modified from Ying and Weber, 1979).

In fixed film system, the microbes are not uniformly exposed to the substrate present in the water. A biofilm creates a significant gradient in substrate concentration depending upon the available substrate concentration within the biofilm. Characklis and Marshall (1990) developed a conceptual double layered biofilm model which showed that with increase in biofilm thickness, the bacteria attached to the surface (i.e. base of the biofilm) become inactive because of limited substrate availability. The biofilm exposed to the bulk liquid has more access to the substrate and the microbes close to the media may be deprived of the substrate depending upon the thickness of the biofilm. Figure 2.12 shows an idealized double layer biofilm showing the simultaneous diffusion of substrate from the bulk liquid to the biofilm and bacterial community utilized the substrate for growth and cell maintenance, followed by diffusion of waste from biofilm to bulk liquid. McCarty and Meyer (2005) and Zhu et al. (2010) further showed the theoretical biofilm configuration with simultaneous substrate diffusion and biological reaction at steady state. Based on biofilm thickness, the system is characterized as fully penetrated (very

thin biofilm), shallow (thick biofilm but substrate is available at the media) and deep (no substrate available at the media). The diffusion coefficient of the substrate and mass transport of substrate in water and through the biofilm controls the rate of substrate utilization and bacterial cell growth. When biofilms become too thick and no substrate can diffuse to the biofilm base, the microbes immediate to the media may die off and detach from the media; this is known as biofilm sloughing.

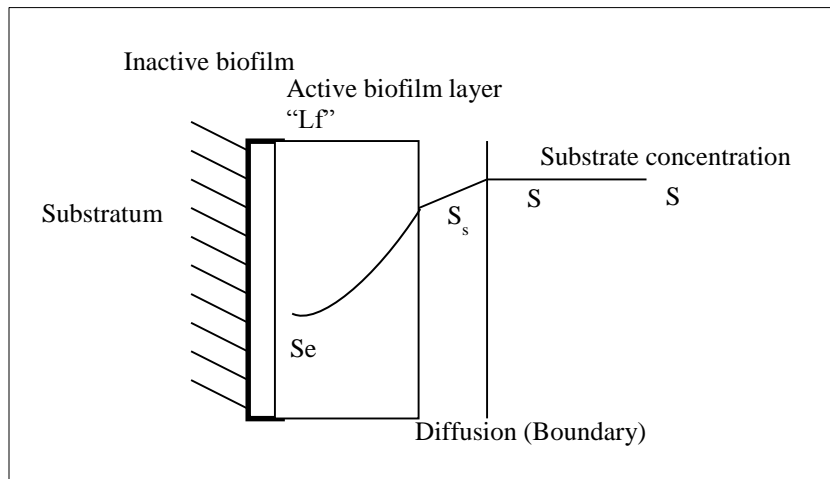


Figure 2.12: Conceptual biofilm model showing substrate diffusion into biofilm (Modified from Rittmann and McCarty, 2001).

Figure 2.12 depicts the concentration gradient of substrate from bulk liquid to the surface and to the base of the biofilm. The substrate concentration at the surface of the biofilm (S_s) is less than the concentration in the bulk liquid (S) because of the external mass transport resistance posed by the boundary (diffusion) layer (Figure 2.12; Rittman and McCarty, 2001; McCarty and Meyer, 2005; Zhu et al., 2010). Figure 2.12 shows the dual layer formed in a biofilm with increase in biofilm thickness; inactive layer, attached to the substratum is deprived of the substrate, and active layer, exposed to the substrate (S_s) and the concentration diminishes across the active biofilm layer (S_e) (Characklis and Marshall, 1990). Biofilm process is suitable for

drinking water system with low concentration of substrate (perchlorate) because of the large amount of bacteria accumulated within the system (Eleuterio, 2007; Zhu et al., 2010). Zhu et al. (2010) explained the use of biofilm-based systems in various drinking water treatment applications including riverbank filtration, slow sand filters, biological active filter, GAC and denitrification filters.

In biofilms, the microbes within the effective depth are actively utilizing the substrate. The flux per unit surface area of the biofilm increases with increase in biofilm thickness up to critical depth beyond which there is no increase in flux with increase in depth (Williamson and McCarty, 1976). The conceptual biofilm model (Figure 2.12) is based on assumption that the biofilm develops on the filter media with uniform thickness (L_f), biomass density (X_f) and mass transport in the system is governed by molecular diffusion of the substrate. The bulk liquid substrate concentration (S) diffuses through the diffusion layer to a concentration of substrate (S_s) at the surface of biofilm according to Fick's first law of diffusion.

$$J = \frac{D}{L} (S - S_s) \quad \text{Equation 2.9}$$

Where,

J = Substrate flux into the biofilm

D = Molecular diffusion coefficient of the substrate of interest

S = Substrate concentration in the bulk liquid

S_s = Substrate concentration at the interface of biofilm and the liquid

The mass transport resistance in the biofilm further reduces the concentration of substrate in the biofilm (S_f). Substrate utilization at any point in the biofilm can be represented by the Monod's Equation:

$$r_{ut} = \left(\frac{dS}{dt} \right)_{ut} = - \frac{\hat{q} X_f S_f}{K_s + S_f} \quad \text{Equation 2.10}$$

Where,

\hat{q} = maximum specific rate of substrate utilization, mg/mg VS-day

X_f = Concentration of biomass in the biofilm, mg VS/cm³

S_f =Substrate concentration at the base of biofilm, mg/L

K_s =Half maximum rate concentration or half saturation constant, mg/L

The molecular diffusivity of the substrate in biofilm follows the Fick's second law of diffusion (Rittmann and McCarty, 2001).

$$\left(\frac{dS_f}{dt} \right)_{Diff} = D_f \frac{d^2 S_f}{dz^2} \quad \text{Equation 2.11}$$

Where,

D_f = Molecular diffusion coefficient of the substrate in the biofilm = 80% of diffusion of substrate in water (Rittmann and McCarty, 2001)

Z = depth of biofilm from the biofilm surface

The overall mass balance on substrate can be obtained by combining equations 2.10 and 2.11. Since the substrate utilization and diffusion occur simultaneously and are equal, the substrate mass balance is:

$$D_f \frac{d^2 S}{dz^2} - \frac{\hat{q} X_f S_f}{K_s + S_f} = 0 \quad \text{Equation 2.12}$$

To solve the biofilm equation, a first boundary condition for the biofilm is that there is no flux at the attachment surface. $\frac{dS_f}{dz} = 0$ at $Z = L_f$ Equation 2.13

The second boundary condition is that the external mass transport at the surface of the biofilm follows the Fick's first law of diffusion as explained by Equation 2.14 and is expressed as below:

$$J = D_f \left(\frac{dS_f}{dz} \right)_{z=0} \quad \text{Equation 2.14}$$

Integration of Equation 2.14 times diffusion coefficient yields the flux of substrate. The substrate flux is defined as the substrate utilization per unit surface area of biofilm. Further, the second integration yields the substrate profile as a function of biofilm depth (z). The solution of Equation 2.14 requires knowledge of all the kinetics (\hat{q} , K, and L), mass transport parameters (D and D_f) and biofilm properties (X_f and L_f).

When substrate concentration is much smaller than K_s , the Equation 2.14 can be expressed as:

$$D_f \frac{d^2 S}{dz^2} - k_1 X_f S_f = 0 \quad \text{Equation 2.15}$$

$$\text{Where, } k_1 = \text{first order rate coefficient} = \frac{q}{K_s} = \frac{\mu_{max}}{Y * K}$$

Further, integrating Equation 2.15, the solution for the flux and S_f is:

$$J_1 = \frac{D_f * S_s * \tanh \frac{L_f}{\tau_1}}{\tau_1} \quad \text{Equation 2.16}$$

$$S_f = \frac{S_s * \cosh \frac{(L_f - z)}{\tau_1}}{\cosh \frac{L_f}{\tau_1}} \quad \text{Equation 2.17}$$

$$\text{Where, } \tau = \text{First order standard biofilm thickness} = \sqrt{\frac{D_f}{X_f * k_1}} \quad \text{Equation 2.18}$$

2.7.1 Biofilm Detachment

Biofilm detachment may occur due to combination of biological, chemical, and physical processes (Horn and Lackner, 2014). The detachment occurs when external forces (e.g., through shear during backwash) are larger than the internal strength of the biofilm matrix. Decrease in internal strength due to hydrolysis of polymeric biofilm matrix may also result in biofilm detachment (Horn and Lackner, 2014).

Biofilm detachment rate in a biofilter is generally expressed by the biomass lost in the effluent to the total biomass growth on the media before detachment.

$$bs = \frac{\text{total biomass rate in effluent}}{\text{total biomass on the media}} = \frac{QXe}{W_m * X_m} \quad \text{Equation 2.19}$$

Rittmann (1981) modified the effect of shear stress on biofilm obtained by Trulear and Characklis (1980) on a biofilm which had a mass per unit area of 0.078 mg/cm² is expressed by Equation 2.20.

$$Rs = -2.66 * 10^{-4} * W^{1.16} * \left(\frac{X_f * L_f}{0.078} \right) \quad \text{Equation 2.20}$$

The diffusion coefficient in water at 20°C, D, can be estimated using Wilke-Chang equation for each substrate of interest.

$$D = 5.06 * 10^{-7} \frac{T}{v * V^{0.6}} \quad \text{Equation 2.21}$$

Where,

T= Temperature (K)

v = Viscosity of water (centipoise)

V= Molal volume of the substrate. LeBas Method can be used to estimate the molal volume of the chemical.

The thickness of effective diffusion layer, L, for a spherical media can be estimated as:

$$L = \frac{D * Re^{0.75} * Sc^{0.67}}{5.7 * u} \quad \text{Equation 2.22}$$

Where,

$$Re = \text{Modified Reynold's number} = \frac{2 * \rho w * dp * u}{(1 - \varepsilon) * \nu}$$

dp= diameter of solid medium

$$Sc = \text{Schmidt number} = \frac{\nu}{\rho w * D}$$

$$u = \text{Superficial flow velocity} = \frac{Q}{A}$$

ε = porosity of the media

ν = absolute viscosity

$$\text{Biofilm depth, } L_f = \frac{J * Y}{X_f * b'} \quad \text{Equation 2.23}$$

Biofilm has the capability to regain steady-state quickly. However, substrate loadings, variation in temperature, backwashing intensity, and biomass detachment due to shear result in non-steady state condition in FBRs. Rittmann and McCarty (2001) developed a pseudo-analytical solution for such non-steady-state biofilm (Equation 2.21).

$$J = \eta * \hat{q} * X_f * L_f * \frac{S_s}{K_s + S_s} \quad \text{Equation 2.24}$$

Where,

η = the effectiveness factor, which is the ratio of actual flux to flux that would occur if the biofilm were fully penetrated at concentration S_s . The value expresses the effects of internal mass-transport resistance.

The pseudo-analytical solution is carried out in a dimensionless domain and requires intermediate estimation of η and dimensionless substrate concentration at the biofilm's outer

surface (S_s^*). For non-dimensionalization and solution includes following dimensionless parameters.

$$S^* = \frac{S}{K} \quad \text{Equation 2.25}$$

$$L^* = \frac{L}{\tau} \quad \text{Equation 2.26}$$

$$L_f^* = \frac{L_f}{\tau} \quad \text{Equation 2.27}$$

$$D_f^* = \frac{D_f}{D} \quad \text{Equation 2.28}$$

The value of effectiveness factor, η , ranges from 0 to 1. The start value is given by Equation 2.29. The value is suitable to represent first-order kinetics within the biofilm. For a shallow biofilm, η approaches 1, and for deep biofilm, η approaches Equation 2.30. The solution of Equation 2.31 can be used to estimate S_s^* from S^* . The S_s^* can be used to compute a dimensionless flux (J^*) using Equation 2.31 and J^* using Equation 2.32. Finally, flux can be estimated using the dimensionless parameters (Equation 2.33).

$$\eta = \frac{\tanh L_f^*}{L_f^*} \quad \text{Equation 2.29}$$

$$\eta = \frac{\sqrt{\frac{D_f(K_S + 2S_s^*)}{\hat{q}^* X_f}}}{L_f} = \frac{\sqrt{1 + 2S_s^*}}{L_f^*} \quad \text{Equation 2.30}$$

$$S_s^* = \frac{1}{2} \left[(S^* - 1 - L^* L_f^* D_f^* \eta) + \sqrt{(S^* - 1 - L^* L_f^* D_f^* \eta)^2 + 4S^*} \right] \quad \text{Equation 2.31}$$

$$J^* = D_f^* L_f^* \eta \frac{S_s^*}{1 + S_s^*} \quad \text{Equation 2.32}$$

$$J = J^* \left(\frac{KS^*D}{\tau} \right) \quad \text{Equation 2.33}$$

2.7.2 Biofilm Density and Thickness

Biofilm density commonly indicates the volumetric mass density and is the amount of biomass (dry weight) in a given volume of biofilm. Peyton (1994) calculated areal density which is the amount of dry biomass attached to unit area of media in addition to volumetric density to obtain biofilm density. Areal density is highly affected by environmental conditions, such as shear stress, and is not commonly reported (Peyton, 1994).

Biofilm thickness, the perpendicular distance from the media surface to the biofilm-bulk liquid interface, is important parameter in the operation of a fixed film reactor. However, accurate measurement of biofilm thickness is difficult because the biofilm thickness has spatial variation over the media (Characklis and Marshall, 1990). The most common methods for measuring biofilm thickness are optical microscope, volumetric displacement, and electrical conductance (Characklis and Marshall, 1990). The biofilm thickness in case of a pure culture exhibits considerably uniform thickness in the media as compared to mixed culture (Characklis and Marshall, 1990). Characklis and Marshall (1990) listed the characteristic lengths in a biofilm system (Table 2.12).

Table 2.12: Characteristic Lengths Delineating a Biofilm

Component of Biofilm	Thickness or Size (um)
Cell	1-10
Mass transfer boundary layer	10-100
Diffusion layer	10-1000
Biofilm	10-1000
Media	1000-100,000

Volumetric mass density decreases with distance from the substratum (Characklis and Marshall, 1990). Table 2.13 shows the variation of biofilm density with biofilm thickness.

Table 2.13: Reported Variation of Biofilm Thickness and Biofilm Density (Updated from Characklis and Marshall, 1990)

Biofilm Layer	Biofilm Thickness (um)	Depth from Water-Biofilm Interface (um)	Density (kg/m ³)
Surface film	400	0-400	37
Intermediate	200	400-600	98
Base film	130	600-730	102

Peyton (1994) developed an equation assuming a negative one-half order expression to fit the volumetric mass density with biofilm thickness. The equation predicted a high volumetric density values for thin biofilm and low density values for thick film supporting the decreasing trend of biofilm density with increase in biofilm thickness (Table 2.14). However, many biofilm models are based on monolayer volumetric density (Rittmann and McCarty, 2001). Table 2.14 lists the reported biofilm thickness and volumetric density.

Table 2.14 Reported Biofilm Thickness and Density

Biofilm Thickness (um)	Density (kg/m ³)	Type of Biofilm	Reference
160-210	66-130	Mixed, heterotrophic, and steady state	Kornegay and Andrews, 1967
30-1300	20-105	Mixed, heterotrophic	Hoehn and Ray, 1973
150-580	42-109	Mixed, heterotrophic, nitrifying, and steady state	Williamson and McCarty, 1976
100	50 ^a	Mixed, heterotrophic, and steady state	Rittman and McCarty, 1978
119-126	5 ^b	Mixed, heterotrophic	Rittman and McCarty, 1980
0-125	5 ^b	Mixed, heterotrophic	Rittman and McCarty, 1981
10-124	10-65	Mixed, heterotrophic	Trulear and Characklis, 1982
36-47	17-47 ^c	Pure (<i>Pseudomonas aeruginosa</i>),	Trulear, 1983
0-60	27	Pure (<i>Pseudomonas aeruginosa</i>),	Bakke, 1986
0-1	199±41	Pure (<i>Pseudomonas aeruginosa</i>), and steady state	Peyton, 1994
29		Pure (<i>P. aeruginosa</i>)	Murga et al., 1995
100		Pure (<i>K. pneumonia</i>)	
400		<i>P. aeruginosa</i> and <i>K. pneumonia</i> combined	
32-109	10 ^d	Mixed	McCarty and Meyer, 2005
75-220		Mixed	Wood et al., 2000

^a Calculated assuming biofilm is 80% volatile solids

^b Calculated assuming biofilm is 50% carbon

^c Calculated from measured thickness corrected for refractive index of biofilm

^d Assumed value

Peyton (1994) observed that biofilm thickness, measured using an optical microscope, increased with substrate loading rate. At each loading rate, the biofilm increased with time, but formed a plateau after reaching a maximum thickness. At steady state, shear stress had no significant effect on the biofilm thickness. Further, the study observed no significant effect of shear stress had on the volumetric mass density (Peyton, 1994). One previous study at low substrate loading rates observed an increase in biofilm density with increasing shear stress contradicting Peyton's work. However, Peyton (1994) cited another study that observed no effect of shear stress was observed at high substrate loading rates.

Confocal microscopy is a non-invasive technique used to measure biofilm thickness. Murga et al., (1995) measured the biofilm thickness by embedding on to an agent, sectioning, and applying image analysis to construct thickness profiles (up to 1 cm in length) across the substratum. The technique can measure biofilm with a thickness profiles up to 1 cm in length across the substratum (Murga et al., 1995). Wood et al., (2000) measured biofilm depth ranging between 75-220 μm using reflected-light confocal microscopy. The images indicated that the biofilm was a heterogeneous structure with channels and void filled with water. Despite of the benefit of the confocal microscopy in retaining the microbial characteristic while measuring the biofilm thickness, confocal microscopy has limitation to dense biofilm and microbes with pigmentation (Pawley, 2006). The autofluorescence microbe, such as cyanobacteria, produces a weak signal, and the microbe cannot be seen under confocal microscopy. Secondly, in case of dense biofilm, the image obtained from the microscopy gets overlapped that require further image processing (Pawley, 2006).

2.7.3 Substrate Transport Mechanism in Biofilm

The biofilm thickness affects the penetration of substrate and nutrient into the biofilm (Peyton, 1996). Based on one dimensional biofilm data, including slow diffusion rates in a biofilm, Peyton (1996) suspected convection could be the dominant mass transport mechanism in a heterogeneous biofilm. However, many studies have designed biofilm model considering diffusion as the dominant mechanism of mass transport (Charkalis and Marshall, 1990; Rittmann and McCarty, 2001).

2.7.4 Components of Biofilm Model

Biofilm model was developed based on the biofilm growth model described by McCarty and Meyers (2005) considering kinetics of substrate utilization, molecular diffusion of electron acceptors, and biomass loss due to shear (Rittmann and McCarty, 2001). The molecular diffusion for perchlorate, oxygen and nitrate were calculated based on Wilke and Chang's correlation (McCarty and Meyers, 2005). Table 2.15 shows the parameters used for estimating biofilm thickness and Table 2.16 shows the input variables for the model.

Table 2.15: Estimation of Biofilm Parameters Used for Biofilm Model

Parameter	Equations
Diffusion coefficient using Wilke-Chang equation	$D = 5.06 \cdot 10^{-7} \frac{T}{v \cdot v^{0.6}}$
Diffusion coefficient in biofilm	$D_f = 0.8 \cdot D$
The thickness of effective diffusion layer	$L = \frac{D \cdot Re^{0.75} \cdot Sc^{0.67}}{5.7 \cdot u}$ <p>Where,</p> <p>Re= Modified Reynold's number = $\frac{2 \cdot \rho w \cdot dp \cdot u}{(1-\varepsilon) \cdot v}$</p> <p>dp= diameter of solid medium</p> <p>Sc=Schmidt number = $\frac{v}{\rho w \cdot D}$</p> <p>u= Superficial flow velocity = $\frac{Q}{A}$</p> <p>ε = porosity of the media</p> <p>v = absolute viscosity</p>
Biofilm-loss coefficient	$b' = b + b_{det}$ <p>Where,</p> <p>b= First order decay coefficient</p> <p>b_{det}= Specific biofilm-detachment loss coefficient</p>
Dimensionless substrate concentration, normalized to K	$S^* = \frac{S}{K}$
Dimensionless transport indicator	$K^* = \frac{D}{L} \left[\frac{K}{\hat{q} \cdot X_f \cdot D_f} \right]^{1/2}$ (value < 1 means that external mass transport is slow and exerts significant control on flux)
Ratio expressing the actual flux reduction	$f = \tanh \left[\alpha \left(\frac{S_s^*}{S_{min}^*} - 1 \right)^\beta \right]$
Coefficients that depend on S_{min}^*	$\alpha = 1.557 - 0.4117 \tanh[\log_{10} \cdot S_{min}^*]$ $\beta = 0.5035 - 0.0257 \tanh[\log_{10} \cdot S_{min}^*]$
Effectiveness factor	η approaches 1 (for shallow biofilm) $\eta = \frac{\sqrt{\frac{D_f(K_s + 2 \cdot S_s)}{\hat{q} \cdot X_f}}}{L_f} = \frac{\sqrt{1 + 2 \cdot S_s}}{L_f^*} \text{ (for thick biofilm)}$
Dimensionless substrate concentration at the biofilm/liquid boundary	$S_s^* = \frac{1}{2} \left[(S^* - 1 - L^* L_f^* D_f^* \eta) + \sqrt{(S^* - 1 - L^* L_f^* D_f^* \eta)^2 + 4 S^*} \right]$
Dimensionless steady-state flux	$J^* = K^* (S^* - S_{min}^*)$
Actual steady-state flux	$J = J^* \cdot \left(\frac{K_s \cdot D}{\tau} \right)$
Biofilm depth	$L_f = \frac{J \cdot Y}{X_f \cdot b'}$

Table 2.16: Input Parameters for Biofilm Modeling

Variable	Definition	Units	Value	Reference
GAC characteristics				
ds	diameter of GAC	cm	0.05	Retained on sieve with 500 μm opening
e	porosity		0.6	
ρ_{GAC}	Density	g/cm ³	1.42	measured
$\rho_{biofilm}$	Density	g/cm ³	0.8 (0.38 to 1.4)	van Veen and Paul,
Biofilm parameters				
Xf	Amount of biomass per unit volume of the media	mgVS/cm ³ surface area	38	
Y	Yield		0.2	
b	Endogenous decay	per day	0.15	McCarty and Meyers, 2005
$K_{perchlorate}$	Half saturation constant for microbial growth	mg/L	10	
\hat{q}	Maximum specific substrate utilization rate	mg/mg VS-day	10	
$\hat{\mu}$	Maximum specific growth rate	per day	0.1	Bardiya and Bae, 2004
$\frac{D_f}{D}$	Ratio of diffusion of perchlorate in biofilm to diffusion of perchlorate in bulk water		0.8	Rittmann and McCarty, 2001
$\rho_{biofilm}$	Density	g/cm ³	0.8	
t	thickness	cm	variable	Calculated
Reactor condition for this study				
S_p	Perchlorate concentration	mg/L	100	
S_o	Oxygen	mg/L	<0.5 to 1.5	
Q	Influent flow to maintain hydraulic expansion	mL/s	1.6	
v	N-s/m ² at oC	N-s/m ²	0.001002	
d	Diameter of reactor	cm	2.5	
H_F	GAC fixed depth	cm	110	
H_E	GAC expanded depth (Fluidized depth)			
Stoichiometric requirement				
Electron acceptor		Oxygen	Nitrate	Perchlorate
Biomass per mole as equivalent to perchlorate		0.326	0.261	0.163

Biofilm thickness was also estimated using the weighted average density (Equation 34) for the GAC and biofilm growing on it with a thickness of t as shown in Figure 2.13.

$$\text{The weighted average density } (\rho_{avg}) = \frac{\rho_{GAC} * d^3 + \rho_{biofilm} * ((d+2*t)^3 - d^3)}{((d+2*t)^3)} \quad \text{Equation 2.34}$$

The ρ_{avg} was calculated varying values of t . The threshold thickness (t') for floating the GAC was at which ρ_{avg} approaches 1. For this study, the threshold thickness (t') is 0.018 μm .

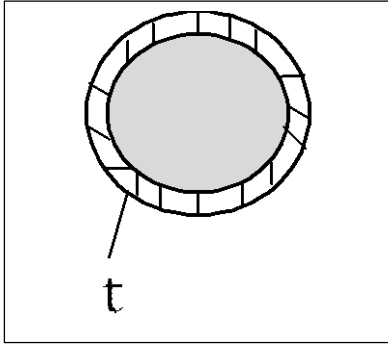


Figure 2.13: GAC with a biofilm of thickness t .

2.7.5 Test of the Model

In this dissertation, the reactor and batches for biomass growth were operated using perchlorate only. The model was developed incorporating biomass growth due to oxygen, nitrate and perchlorate so that it can be used for water consisting of all or any of these three electron acceptors. Figure 2.14 shows the model tested for water containing perchlorate only as electron acceptor. The model estimates biomass growth at each time.

The threshold biomass thickness calculated based on weighted average density is shown by the horizontal red line in Figure 2.14. The backwash time according to the model is the time corresponding to the time at which the biomass thickness exceeds the horizontal red line. The backwash time obtained from the model was on day 5, 16 and 38 for perchlorate concentrations

100 mg/L, 10 mg/L and 100 ppb respectively. In the batches with 100 mg/L, the first backwash required was on 9th day in batches and 10th day in the actual reactor.

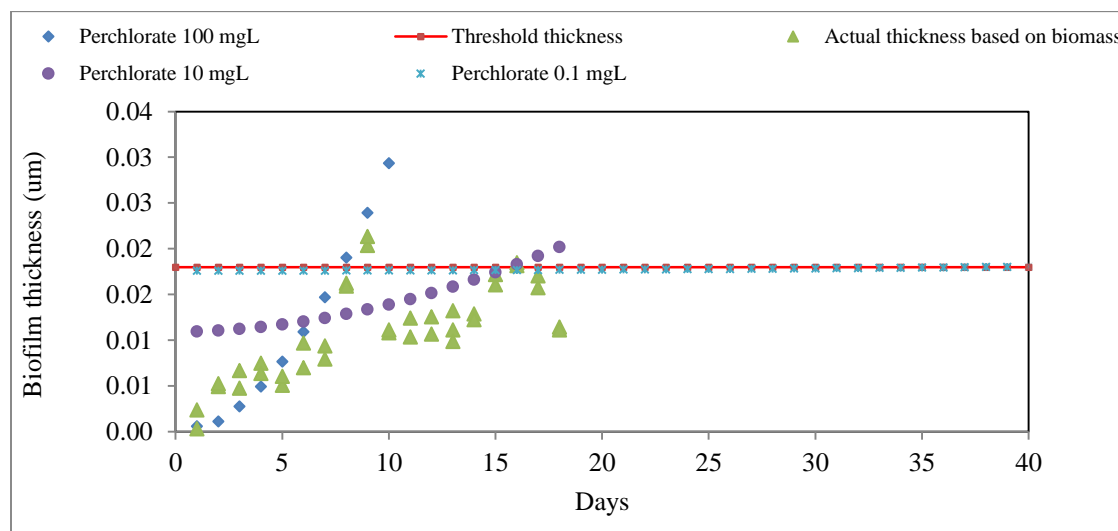


Figure 2.14: Biofilm thickness estimated using experimental biomass growth in batch bioreactors and the model developed for perchlorate as the sole electron acceptor. The red line is the threshold thickness. The time for backwash corresponds to the time when the biofilm thickness exceeds the threshold thickness.

2.8 Available Technology to Measure Particles in Water

Various types of total suspended solid probes and sensors have been developed and used to measure amount of particles floating in water. These probes and sensors are designed to quantify the particles based on reflection of light or sound. Table 2.17 lists some of the most commonly used probes and sensors.

Since several decades, mixed liquor suspended solid probes have been used to operate activated sludge systems. These probes measure the concentration of solids in an aeration tank as well as in the recycled activated sludge to determine whether to increase or decrease the sludge wasting from the system (Royce, 2015). In drinking water treatment plants, the presence of particles requires more coagulants and can also hinder capacity of disinfectant. Therefore,

drinking water treatment plants have suspended solid sensors, particle counters, and turbidity meters as an online and/or offline technique to measure suspended and colloidal particles.

Table 2.17: Suspended Solid Sensors and Probes Used to Detect Particles in Water

Suspended Solid Probe/Sensor				Measurement	Range	Reference
Paab probe				90o Scattering/Light absorption	0-30,000 mg/L	
Phototransistors detector				Infrared LED detection with 64 detectors vertically stacked		Markland, 2016
Galvanic probe	Monitek	Acoustic		Ultrasonic reflection	0-10 and 0-30,000 mg/L	Chemtronic, 2015
Hach sensor				Modified absorption measurement	1-500,000 mg/L	Hach, 2015
Insite IG analyzer				Single gap optical	0-30,000 mg/L	
Royce Analyzer and Sensor (online or portable)				Single gap optical	10-80,000 mg/L	Royce, 2015
Hach Counter	2200	PCX	Particle	Laser-diode-based particle counting sensors	25,000 cells/minute (particle size: 2 to 750 μ m)	EPA, 2009
FlowCAM ®				Laser diffraction, and light obscuration	1000 cells/ minute (particle size: 2 to 3 mm)	FlowCAM, 2011; EPA, 2009
Sonar Acoustic technology				Acoustic waves reflected by the sludge blanket		White, 2013
Acoustic profilers (ADCP)	Doppler	current		Backscattering a single frequency acoustic signal		Kim et al., 2004
Acoustic sensor	backscatter	intensity		Backscattering a single frequency acoustic signal		Hanes et al., 1988
Acoustic Doppler Velocimetry				Backscattering a single frequency acoustic signal	3500 mg/L (fine particles)	Marttila et al., 2010)

Acoustic Doppler Current Profiler (ADCP) and Acoustic Doppler Velocimetry (ADV) have been adopted to estimate and regulate turbidity in estuaries and bays, shallow rivers, headworks and drainage networks (Kim et al., 2004; Marttila et al., 2010). Acoustic Doppler technique measures turbidity based on the strength of scattered sound pulses from the particles in the fluid. ADCP has been widely used to monitor increase sediment loads after a flooding event and siltation in estuaries (Kim et al., 2004). ADCP uses large sound producing unit and is mostly used in large water bodies (Marttila et al., 2010). Conversely, ADV sensor uses smaller unit and

is suitable for small drainage networks or small water bodies. ADV can measure particulate concentrations up to 3500 mg/L. The ADV sensor is reliable with fine particles only and the result varies with particle size, shape, concentration and sediment type (Marttila et al., 2010).

Sensors, with phototransistor or infrared acoustic detectors, have been developed for measuring sludge depth in anaerobic ponds, septic tanks and clarifiers (Markland, 2016; White, 2013). In County Sanitation Districts of Los Angeles County, CA, infrared sensors (Miltronics IQ160) were used to measure the depth of liquid surface or foam above the sludge layer in anaerobic digesters (Achman and Le, 2006). The infrared detectors emit an audible sound when the sludge layer approaches the maximum level (Westerman et al., 2008). The use of the infrared detector in the anaerobic digester resulted in rapid fluctuation of the sludge depth in small time period indicating false echoes and excessive signal noise in echo profiles. In addition, the infrared detector was sensitive and produced false echoes in water with high solids (Achman and Le, 2006).

In biofilters, excessive biomass growth on the media reduces the density of the media, and the media begins to float above the operational depth and gets lost in the effluent. Various measures, such as mechanical scrubbing and backwash, are used to control excessive biofilm formation in the biofilters. Infrared sensors are the only one that has indicated possibility to measure particles floating in water. However, the infrared detector technique might not be useful because of the issue with false signal might. To the best of the author's knowledge, no other probe or sensors have been used to date to measure particles floating or lost due to biomass growth in FBRs. Therefore, in this dissertation, image processing technique was selected as a tool for measuring particle floating due to biomass growth.

2.8.1 Image Processing Technique in Drinking Water

Image processing tool is a relatively new technology and is gaining attention in water treatment sectors. Recent study showed that using imaging tools in differential interface contrast and fluorescence microscopy with fluorescence provided a reliable detection of oocyst in drinking water (Fernandez-Canque et al., 2008). EPA investigated FlowCAM®, a laser-diode based particle counter and image based identification unit, as a suitable online particle monitoring technology for drink water distribution system (EPA, 2009). The result indicated that FlowCAM® could be a real time contamination warning indicator in detecting contamination in drinking water. FlowCAM® is based on flow cytometry system with online particle imaging and analysis (FlowCAM, 2011). FlowCAM® has the ability to detect biological agents and growth media on water distribution system. FlowCAM® takes high-resolution digital images of particles and cells in the water. The images are analyzed by a proprietary software program to count, identify size and shape, and other properties such as intensity, transparency, color, bio-volume, compactness, roughness, and elongations of the particles. A study in China used image processing and pattern recognition technique to control the flocculant addition in drinking water by monitoring turbidity in water after flocculation. The study used images of alum, which was added as flocculant agent, and analyzed the images by a computer program developed for the study (En et al., 2013).

2.8.2 Image Processing Software, ImageJ

ImageJ is a java based software package developed by the Research Services Branch of the US National Institutes of Health (Schneider et al., 2012). The software is a flexible, open-source biological image analysis package (Bizukojc, 2005). It is used to analyze individual images

rather than high-throughput work, but programs can be written for high-throughput work by the user (Schneider et al., 2012).

The ImageJ has various tools to treat digital images and program modules that can be used as needed. A study using the ImageJ as tool for counting laboratory grown microorganisms tested the number of images needed for reliability of the program. The results indicated that taking four images ensured the reliability of the measurement (Mallard et al., 2013). Moreover, the reliability of the program was depended on the quality of the still background of the picture (Mallard et al., 2013).

For this study, obtained pictures were cropped in such way that only the operation depth of the FBR is selected. The pictures were converted into monochromatic colors to obtain a grey scale image. Next, a threshold was set for the pictures, such that it measures the area of the bright section (empty space above the GAC and the effluent of the FBR) and converts the bright section into red color. The final step was to calculate the percentage area of bright section. When using the image processing to decide on backwashing, as the area tends to zero, then backwashing should commence.

2.9 Electron Donor for In-situ and Ex-situ Bioremediation

Ex-situ treatment of contaminated groundwater, also known as Pump & Treat (P&T), has been widely used for groundwater remediation. However, according to EPA reports for years 2005-2008, in-situ remediation has exceeded P&T (Careghini et al., 2013) in the US in remediation applications. In-situ remediation generally does not require bioaugmentation because native microflora is stimulated through addition of needed electron donors (Bardiya and

Bae, 2011). In in-situ bioremediation, required substrates are injected into the ground to create biologically active treatment zones in the aquifer where treatment takes place.

For perchlorate remediation, the addition of an electron donor is needed to support growth of indigenous perchlorate-reducing bacteria (Batista et al., 2003). Electron donor, such as acetate, ethanol, and lactate are most commonly used sources (Attaway and Smith, 1993; Gingras and Batista, 2002). The Interstate Technology & Regulatory Council (ITRC) recommended perchlorate removal with in-situ bioremediation using soluble electron donors (ITRC, 2008). However, soluble substrates migrate in flowing groundwater and most of them are lost before biodegradation occurs. Consequently, soluble substrates must be added frequently to the groundwater, and often the groundwater is recirculated to recover the lost substrate, which increases the capital and operation & maintenance costs (Borden, 2008).

2.9.1 Biodegradation of Vegetable Oils

Anaerobic biodegradation of oils has been proposed as a clean-up technology for vegetable oil spills (Li et al. 2005). Conversely, vegetable oils can be used as electron donor to promote the degradation of target contaminants that may serve as electron acceptors (e.g. nitrate, perchlorate, TCE, etc.). Initially vegetable oils were directly injected into contaminated aquifers to serve as electron donors. Because of the hydrophobic nature of vegetable oil and its tendency to fill large voids in the aquifer, significant loss in hydraulic conductivity was observed (Lindow, 2003, Coulibay and Borden, 2004). To overcome this limitation, emulsified oils were developed by mixing oil with non- ionic surfactants. Emulsified oil injection result in moderate loss in hydraulic conductivity because physical straining of oil droplets is minimized - the main oil retention mechanic in soils is oil capture by the surface of the sediments of the aquifer (Borden, 2007). In an experiment to determine the amount of oil adsorbed to a mixture of sand with 10%

clay, Borden (2007) found that as much as 3.5 g oil/Kg sediment can be retained. He also concluded that the distribution of oil in an aquifer is independent on injection flowrate or the dilution of the injected oil.

Aerobic biodegradation of oil occurs by enzymatic hydrolysis of ester linkage between glycerol and long-chain fatty acids (LCFAs) (ESTCP, 2006). Glycerol is soluble and readily available electron donor/carbon source for microbial growth. Glycerol or Glycerin ($C_3H_8O_3$) is a highly biodegradation compound that is usually fermented to volatile fatty acids and alcohols, such as propionate, and 1,3-propandiol, which further degrades to acetate (Li et al., 2005). However, the specific glycerol degradation pathway and end products will depend on the type of bacteria present and environmental conditions (ESTPC, 2006). Figure 2.15 shows a schematic diagram for the biodegradation of vegetable oil.

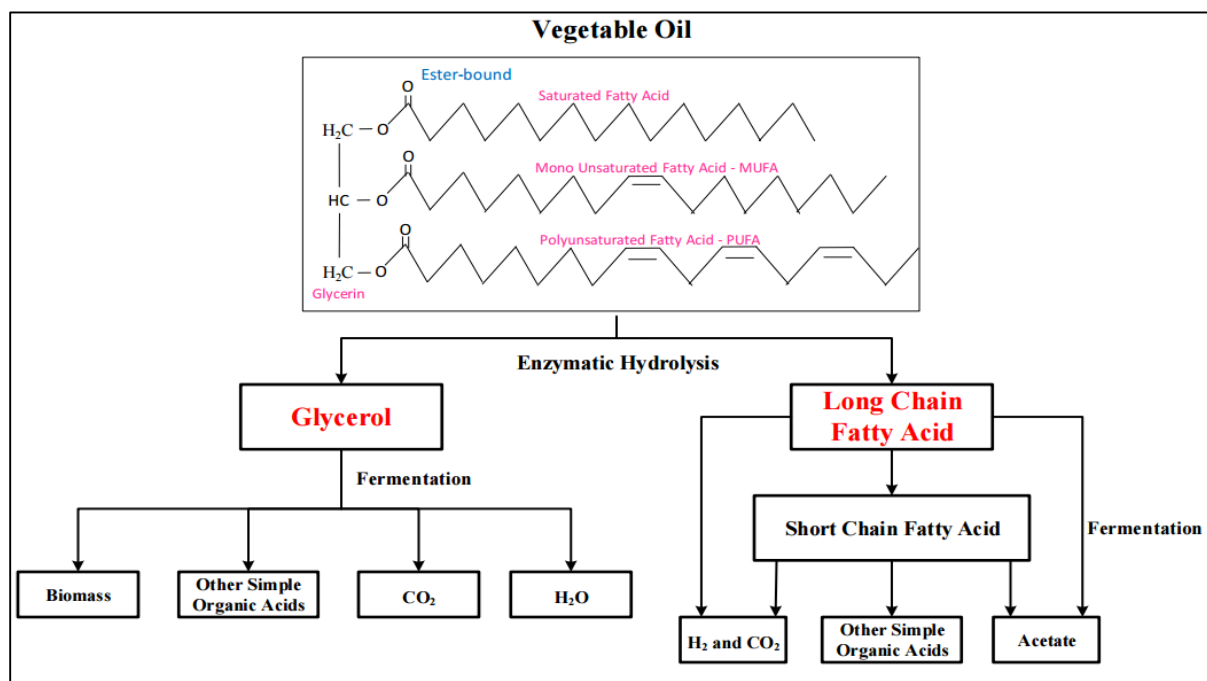


Figure 2.15 Generalized biodegradation of vegetable oil.

Produced LCFAs are degraded farther by hydrogen-producing acetogenic bacteria, generating acetate, hydrogen and short-chain fatty acids. The short-chain fatty acid further undergoes biodegradation generating hydrogen and acetate and other simple organic acids. One mole of acetate and four moles of hydrogen are generated from one mole of saturated LCFA and two moles of hydrogen and one mole of acetate from unsaturated LCFA (ESCTP, 2006). Equation 35 shows a generalized equation for degradation of LCFA. Table 2.18 shows the gram hydrogen release per gram of substrate.

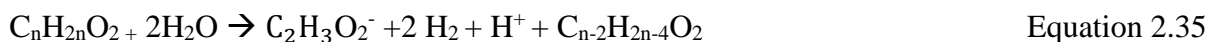


Table 2.18: Hydrogen Release by Biodegradation of Oils and Other Substrate

Substrate	Molecular Weight	H ₂ Released Per Mole of Substrate	Gram H ₂ Released per Gram of Substrate
Glycerol (C ₃ H ₈ O ₃)	180.2	7	0.0766
Acetate (C ₂ H ₃ O ₂ ⁻)	60.1	4	0.0666
Soybean oil (C ₅₆ H ₁₀₀ O ₆)*	868	156.5	0.359
Emulsified Oil*			0.4
Emulsified Oil (EOS-PRO)*			0.25

* ESTCP, 2010

† 59.8% soybean oil, 10% surfactant, and 4% of slow release substrate (assumed glycerol)

Indigenous microorganisms ferment the oil over time into dissolved organic molecules and hydrogen (H₂) gas as illustrated by Equation 36 (Solutions-IES, 2010). The soybean oil produces 156.5 moles of hydrogen per mole of oil such that every gram of soybean oil produces 0.359 g H₂ (Equation 36). As shown in Table 2.18, a mole of acetate would produce only 4 moles of hydrogen (or 0.066 gram H₂ per gram acetate). The comparison indicates that soybean oil can generate 5 times more H₂ than acetate and glycerol, commonly used electron donors for perchlorate and nitrate biodegradation. The emulsified oil from EOS-PRO selected for this study is composed of 59.8% soybean oil, 10% surfactant and 4% rapidly biodegradable soluble

substrate (assumed glycerol) (EOS, 2016). Thus, the total theoretical grams of H₂ generated by EOS-PRO was obtained as the fraction of soybean and glycerol, which was 0.25 gram H₂/gram EOS-PRO. Table 2.19 shows the hydrogen and EOS-PRO demand for the electron acceptors-oxygen, nitrate and perchlorate. Notice that the highest demand is for perchlorate, followed by nitrate. On mass basis, it takes about the same amount of oil to remove perchlorate or nitrate. The demand for oxygen is roughly 36% less.

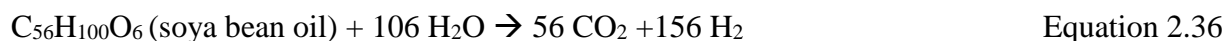


Table 2.19: Hydrogen and Oil Demand for the Electron Acceptors

Electron Acceptor	Reduction Equation	Moles H ₂ /moles Acceptor	wt/wt H ₂	Pounds/ Pounds EOS-PRO
Oxygen	$\text{O}_2 + 2 \text{ H}_2 \rightarrow 2 \text{ H}_2\text{O}$	2.0	7.94	3.176
Nitrate	$2 \text{ NO}_3^- + 2 \text{ H}^+ + 5 \text{ H}_2 \rightarrow \text{N}_2 + 6 \text{ H}_2\text{O}$	2.5	12.40	4.960
Perchlorate	$\text{ClO}_4^- + 4 \text{ H}_2 \rightarrow \text{Cl}^- + 4 \text{ H}_2\text{O}$	4.0	12.38	4.952

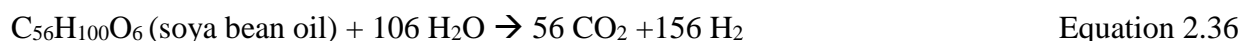
2.9.2 Emulsified Oil Substrate as Slow Release Electron Donor

Emulsified edible oils have been studied as a cost-effective alternative to soluble electron donors for removal of various contaminants. These oils have soil retention ability and slowly release the substrate over time into aquifer (EOS, 2015). The injection of emulsified oil in the contaminated site can provide required electron donor for many years. Emulsified oil injected into the ground creates a permeable zone within the aquifer without need of surface amendments, and supports anaerobic biodegradation of the target contaminants over an extended time period (Borden 2008; Borden and Lieberman, 2009).

ESTPC demonstrated successful use of emulsified oil as a primary source of organic carbon in two pilot studies ESTPC (2010). A single application of the oil in that pilot study was effective for almost three years without replenishment.

Borden (2007) reports that both liquid soybean oil and semi-solid hydrogenated soybean oil could support complete biological dehalogenation of TCE to Ethene. Hunter (2001 and 2002) demonstrated that soybean oil could be used to stimulate anaerobic degradation of other problem contaminants including nitrate and perchlorate in microcosms. Use of oil resulted in complete and rapid perchlorate biodegradation in all lab and pilot scale in-situ treatment (Borden, 2006 and 2007). Schaefer et al. (2007) observed immediate nitrate reduction and perchlorate reduction below detection limit within twenty days of microcosm experimenting a bioaugmentation study for PCE treatment it was found that the use of the oils required longer contact time for degradation, which might be because of slow release of the hydrogen.

Various types of emulsified oils are available, such as EOS-PRO (supplemented with nutrients to support biological growth) and EOS-100 (for better adsorption in aquifer with high flow velocity) (EOS b, 2015). These EOS are pre emulsified oil, typically contains soybean oil, and generates emulsion droplets of 1 μm when mixed with groundwater, whereas mixing soybean oil may not result in similar emulsion (Borden, 2008). Indigenous microorganisms ferment the oil over time into dissolved organic molecules and hydrogen (H_2) gas as illustrated by Equation 36 (Solutions-IES, 2010).



There are advantages in using emulsified oil as an electron donor for in situ bioremediation; it generates more H_2 equivalents per mole of substrate resulting in less amount of substrate. In addition, slow release substrates require fewer re-injections, thereby decreasing operating costs. One issue with use of oils is the potential formation of methane from unused hydrogen or acetate. Fermentation is irreversible and therefore acetate or hydrogen is not available for reduction of any contaminant once methane is formed. Thus, the addition of oil should account

for possible methane generation because methane production is inevitable (ESTCP, 2006).

Another issue with oil use is potential toxicity of bacteria with LCFAs. Lalman and Bagley (2002) observed that a culture not acclimatized to LCFA presented self-inhibition of butyrate degradation. However, no effects on degradation of hydrogen and glucose, by the products of LCFA biodegradation, were observed. Conversely, Li et al. (2005) reports that self-inhibition of bacteria due to some LCFAs has caused instability in anaerobic treatment of lipid-rich wastes.

The COD values measured at UNLV- Environmental Engineering and Water Quality Laboratory (EWL) for the emulsified oil, EOS-PRO, and Glycerol are given in Table 2.20.

Table 2.20: Measured COD Concentrations for Electron Donors (UNLV-EWL)

Electron Donor	Average COD Value (mg/L)
EOS-PRO	2,070,000
Glycerol	1,210,000

CHAPTER 3

METHODOLOGY

3.1 Enrichment of Perchlorate-Reducing Culture

The perchlorate-reducing culture was developed from the returned activated sludge obtained from the Clark County Water Reclamation District, Las Vegas, Nevada. The culture was enriched with acetate (carbon source/electron donor) and perchlorate (nutrient, buffer, and electron acceptor) under anaerobic condition in a two-liter serum bottle (Figure 3.1). The entire culture was stirred using a magnetic stirrer to ensure the bacteria remained in suspension. The enrichment media used for the culture was modified from the composition devised by van Ginkel et al. (1995) (Liu, 2000; Gingras, 2003). Table 3.1 shows the composition of chemicals required to prepare stocks of buffer, nutrient, and electron donor and acceptor. In this study, the adopted molar ratio of electron donor to acceptor was 3:1.

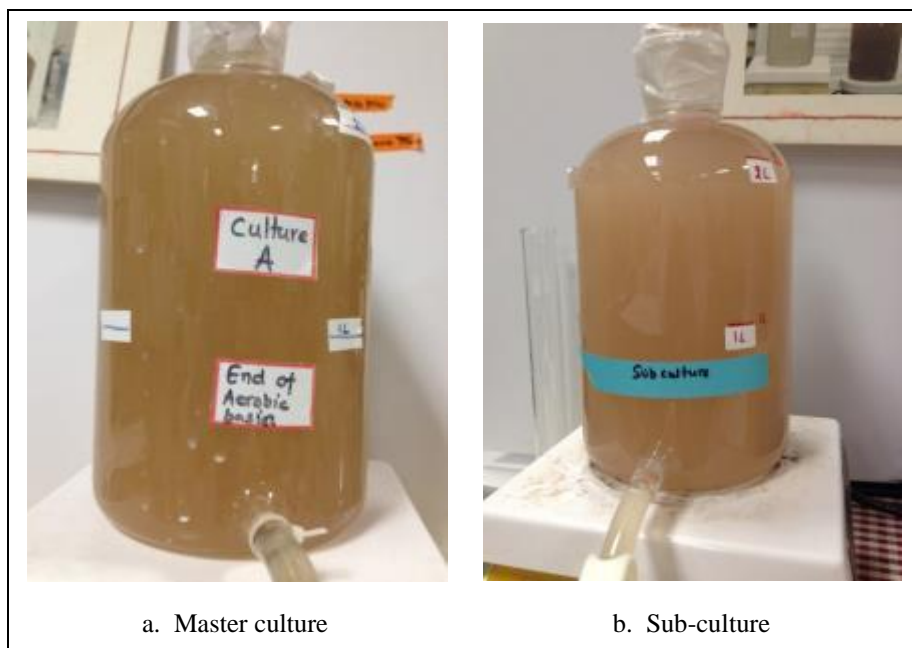


Figure 3.1: Perchlorate-reducing culture (master culture) enriched from returned activated sludge (a) and Sub-culture enriched from the master culture (b).

Table 3.1: Chemicals Used for Enriching the Perchlorate Reducing Culture

Nutrient (X100)		Buffer (X10)	
Component	Wt (g) for 1 L	Component	Wt (g) for 1 L
MgSO ₄ · 7H ₂ O	10.000	K ₂ HPO ₄	155.000
EDTA	0.300	NaH ₂ PO ₄ · H ₂ O	97.783
ZnSO ₄ · 7H ₂ O	0.200	NH ₄ H ₂ PO ₄	50.000
CaCl ₂ · 2H ₂ O	0.100	Electron donor	
FeSO ₄ · 7H ₂ O	0.400	Component	Wt (g) for 1 L
Na ₂ MoO ₄ · 2H ₂ O	0.040	Acetate	120
CuSO ₄ · 5H ₂ O	0.020	Electron acceptor	
CoCl ₂ · 6H ₂ O	0.040	Component	Wt (g) for 1 L
MnCl ₂ · 4H ₂ O	0.100	Perchlorate	40
NiCl ₂ · 6H ₂ O	0.010		
NaSeO ₃	0.010		
H ₃ BO ₃	0.060		

In the beginning, the perchlorate and acetate were added into the culture without wasting. After ten days, the culture turned red and the perchlorate concentration started to decline. Then, the culture was fed at a waste-feed mode (wasting 200 mL culture and adding enrichment media and DI water purged with nitrogen every alternate day). The culture reduced 1000 mg/L of perchlorate up to 97% within a week. Appendix B shows the amounts of buffer, nutrient, acetate, and perchlorate added to the activated sludge to start up and sustain the culture.

After three months of feeding, the percent perchlorate degradation and the optical density of the culture started to decline. Chloride accumulation resulted from perchlorate degradation was suspected for the declination. Therefore, 500 mL of the culture was wasted every two weeks. The wasted 500 mL of culture was used to start up a sub-culture, which was fed in the same pattern as the master culture. As compared to the master culture, the sub-culture was easy to maintain; so all the experiments were conducted using the sub-culture (Figure 3.1 b). Sub-culture is termed as “culture” hereafter.

3.1.1 Identification of Perchlorate-Reducing Bacteria

The culture was analyzed to identify the perchlorate-reducing bacteria (PRB) in it. DNA was extracted and cleaned using the Mo Bio Ultra Clean Soil DNA Extraction Kit, following instructions provided by the manufacturer. The purity and concentration of the extracted DNA were quantified using a NanoDrop 1000. Electrophoresis gel was run for a part of the extracted DNA with *Dechloromonas agitata* as positive controls, while *Pseudomonas aeruginosa* (PA) and water as negative controls. The remaining extracted DNA was shipped to the Research and Testing Laboratory, Texas for identification of the bacterial community in the culture. The laboratory performed DNA amplification and sequencing using the universal 16S rRNA primer, 8F and 1492R and identified the bacteria up to the species level. The sequences obtained from the laboratory were used to prepare a phylogenetic tree using a multiple sequence alignment program, Mafft, (Mafft, 2015). Figure 3.2 shows the procedure for phylogenetic analysis using molecular tools.

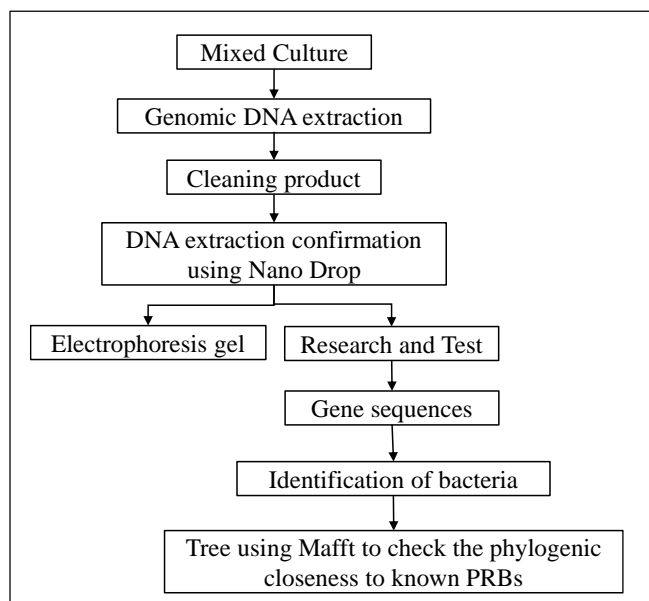


Figure 3.2: Flowchart of molecular tools to identify bacteria present in the enriched culture and check the phylogenetic closeness to the known PRB (KJ).

3.1.2 Comparison of High and Low Concentration Kinetics of Culture

For comparison between high and low concentration kinetics, 100 µg/L and 100 mg/L perchlorate concentrations were selected. For each perchlorate concentration, nine 25 mL-bioreactors and a duplicate for each were prepared (Figure 3.3). The bioreactors were filled with the enrichment solution (acetate, perchlorate, buffer and nutrient), DI water, and washed culture; their amount required for each bioreactor is shown in Table 3.2.

Table 3.2: Amount of Enrichment Solution, Washed Culture, and DI Water for Batch Test

	BATCH 1 (100 µg/L)	BATCH 2 (100 mg/L)
Reactor size (mL)	25	25
Buffer 10X (mL)	2.5	2.5
Nutrient 100X (mL)	0.25	0.25
Volume of perchlorate (mL)	0.50	3.13
Volume of electron donor (mL)	0.21	2.09
Culture (mL)	10.42	10.42
DI water (mL)	10.79	6.62

The enrichment media and DI water were purged using nitrogen gas for approximately two hours. The culture was washed to prevent possible contribution of perchlorate and acetate from the culture. At first, the culture was centrifuged for 10 minutes at 3500 rpm (Legend RT Sorvall centrifuge, Kendro, Thermo Fisher Scientific, Inc., Waltham, MA), and the supernatant was discarded carefully. DI water with buffer was added in to the settled culture to replenish the initial volume, vortexed for 10 to 20 seconds, and centrifuged for 10 minutes. Again, the supernatant was discarded. This process was repeated twice so that the culture did not contribute additional perchlorate and acetate to the bioreactors. DI water was added to the washed culture to achieve a suspended solid concentration of 1000 mg/L. The total suspended solid (TSS) determination was based on correlation between TSS and the optical density (OD) for the culture (Appendix C). The bioreactors were sealed using butyl rubber stopper crimped with aluminum

caps (Wheaton Industries, Inc., Millville, NJ) to maintain anaerobic condition and stirred at 300 rpm on an Orbital Shaker (Cole Parmer, Series 51704) to keep the bacteria in suspension. Figure 3.3 shows the experimental set-up for the batch test. In each sampling period, a bioreactor and its duplicate were sacrificed and analyzed for perchlorate, total organic carbon (TOC), and bacterial growth.

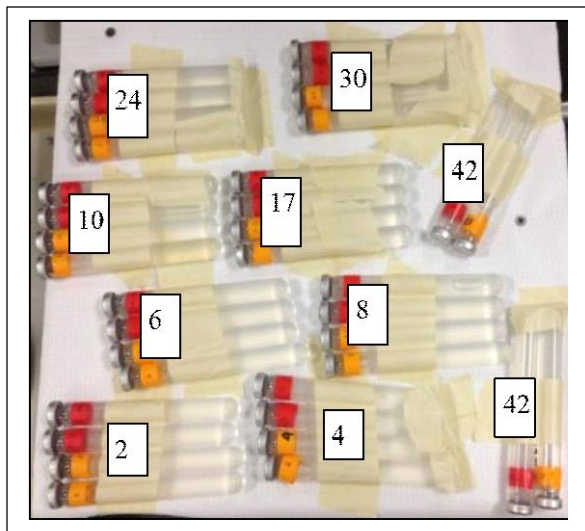


Figure 3.3: Experimental set-up for batch test sampled at 2, 4, 6, 8, 10, 17, 24, 30, and 45 hours.

3.2 Ex-situ Perchlorate Bioremediation with a FBR

Two laboratory- scale FBR were designed and operated at 25% fluidization (Figure 3.4). The reactors were filled with clean granular activated carbon (GAC) media with nominal size greater than 0.5 mm sieve and a density (using the water displacement method) of 1419 kg/m^3 (Appendix D). The hydraulic equations used for the calculation of fluidized bed depth and porosity, tracer test results, and design is included in Appendix E.

3.2.1 PRB Inoculation in the FBR

The mixed enrichment culture was recirculated in the reactors for 48 hours to inoculate the FBRs (Choi and Silverstein, 2008; Miller and Logan, 2000; Logan and LaPoint, 2002) (Figure

3.4 a). Lui et al. (2011) observed that a high flow of feed water during the inoculation of bacteria in a reactor improved the bacterial cell-media bonding. So, the culture was pumped at 1.6 mL/second (Table 3.3) to ensure the biofilm formed on the media was capable of withstanding shear due to hydraulic pressure under normal operation.

3.2.2 FBRs Operation

After 48 hours of inoculation, the FBRs were operated in continuous mode to meet the design flow (1.6 mL/s) by pumping DI water with buffer and nutrient, stock perchlorate, and stock acetate simultaneously into the reactor using a peristaltic pump (Figure 3.4 b).

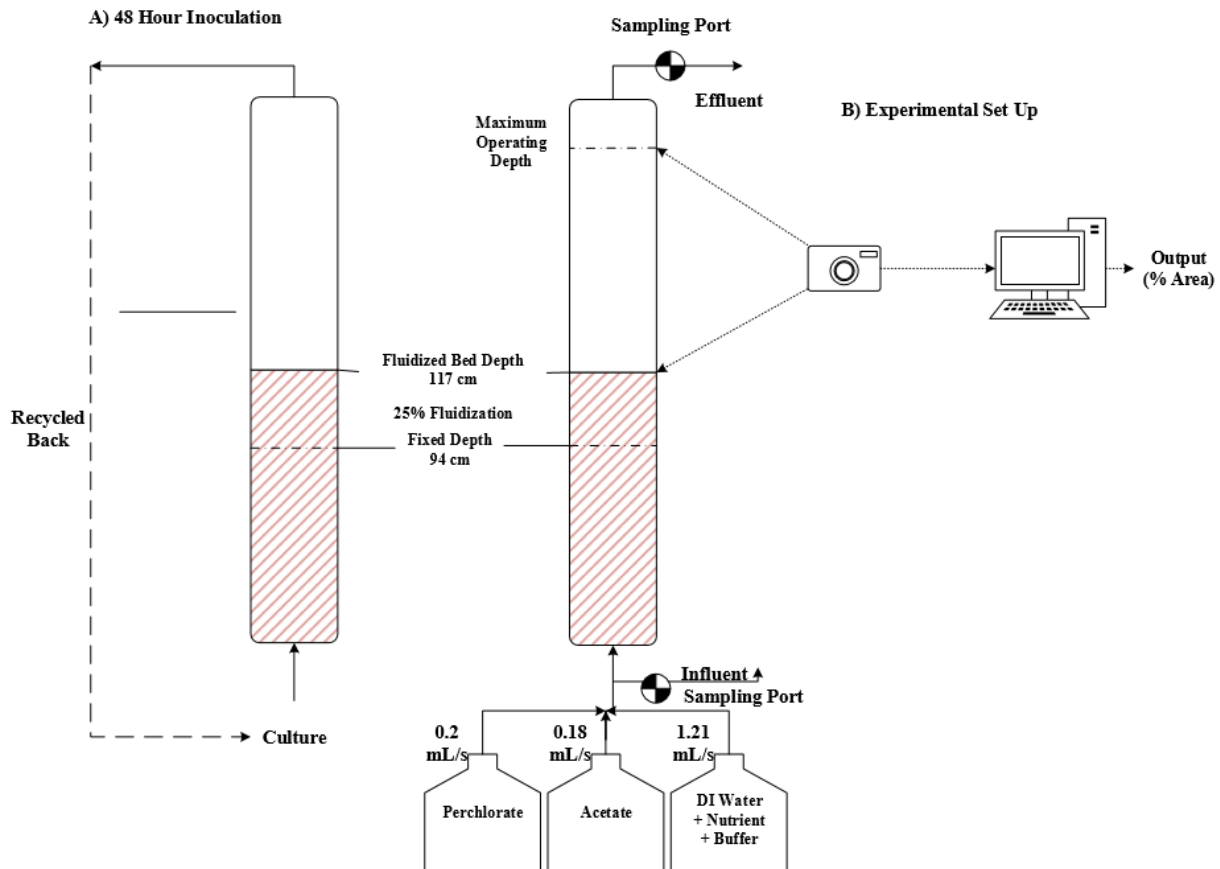


Figure 3.4: Schematic diagram of inoculation of the culture for a week (a), and operation of the reactor (Ex-situ treatment) (b).

The perchlorate concentration was maintained at 100 ppm, 100 ppb, and 10 ppm for the various cycles runs. The concentration of the acetate was maintained three times the stoichiometric requirement for perchlorate removal. The stock concentrations of perchlorate and acetate were based on the result of the hydraulic test for the pumps (Appendix F). The stocks of perchlorate and acetate were prepared once every three days and added to the feed tanks after purging with nitrogen gas for 30 minutes to remove oxygen from the feed solutions. In addition, the mixture of DI water, buffer, and nutrient was added to the feed tank every day after purging with nitrogen gas. The influent and effluent were collected daily, and analyzed for the concentrations of perchlorate and TOC, which was an indirect measure to the acetate concentration added. When needed, the pumps were shut down to change the tubing in the pump heads.

3.2.3 Image Processing as Tool for Determination of Backwash Period

A preliminary trial of the FBR operation with the same perchlorate-reducing culture indicated that the GAC moves as a block rather than discrete particles for 500 μm GAC. Results of the preliminary FBR is shown in Appendix E.

A camera (Canon EOS Rebel 3Ti with Canon EF 50mm f2.5 compact macro lens) was mounted on a metal brace and pointed towards the FBR operating depth. The camera was selected in consultation with UNLV professional photographer R. Marsh Starks. The camera was programmed to take five pictures every time. A remote control timer (Timer Remote Control, APTR1C, Aperture) was connected to the camera to take pictures every one and half hours in the beginning and 15 minutes as the GAC began to move up in the reactor. The lights in the laboratory where the FBR were installed were left on at all times to assure high quality

pictures. The pictures were transferred from the camera to a computer and processed using image-processing software, ImageJ. The camera was shut down only to change the battery.

3.2.4 Biomass Measurement

Biomass growth evaluations were conducted in 125 mL bioreactors with 20 grams of 500 μ m GAC, enrichment solution (perchlorate, acetate, buffer and nutrient), DI water and washed culture. Two bioreactors were sacrificed each day to measure the biomass growth, and one additional bioreactor (totaling to three bioreactors) was sacrificed on 5, 10, 15, 20, 25 days. Perchlorate concentration in the bioreactors was maintained at 100 mg/L and acetate at 300 mg/L. Each day, 10 mL solution was wasted and replaced with fresh enrichment solution and DI water.

3.2.5 Microbial Analysis

The media from FBR 1 was collected at the end of the operation with 100 mg/L perchlorate, and the media with biofilm was observed under phase contrast microscopy. The visual inspection of the samples under the microscope indicated presence of Eukaryotic microorganisms, such as amoeba, in addition to rod-shaped bacteria and thick extracellular polymeric substance (Figure 3.5). The GAC media with biofilm was also shipped to a commercial microbiology laboratory (Research and Testing Laboratory, Lubbock, Texas) for bacterial and eukaryotic community analysis. The primer selected for the bacterial community analysis was 8F [59-AGAGTTTGATCCTGGCTCAG-39] and 1525R [59-AAGGAGGTGATCCAGCC-39]), and eukaryotic community analysis was EukA7F [AACCTGGTTGATCCTGCCAGT] and Euk570R [GCTATTGGAGCTGGAATTAC] (Al-

Ihani et al., 2014). The laboratory provided the percentages of each organism identified (considering 90% or more similarity).

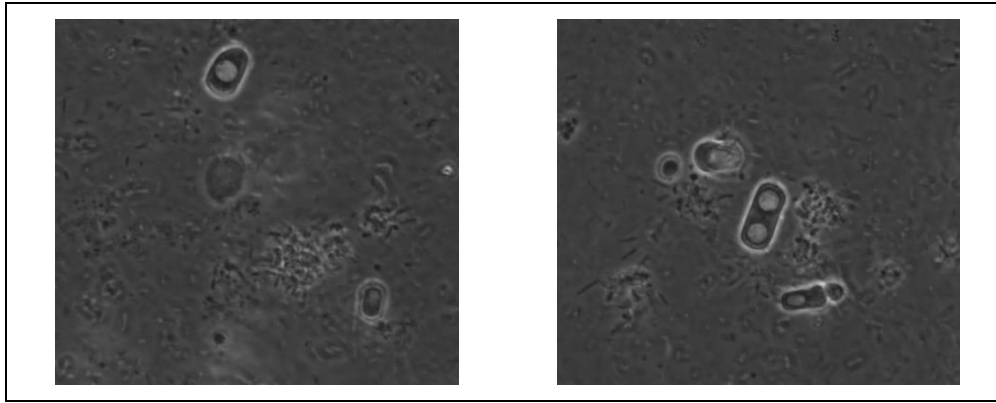


Figure 3.5: Snap shots from the phase contrast microscopy, showing bacteria, extracellular polymerase, and eukaryotic organisms.

3.3 In-situ Perchlorate Bioremediation Approach

The feasibility of using the slow releasing electron donor, emulsified oil for in-situ perchlorate bioremediation was evaluated using four laboratory column bioreactors (Figure 3.6). The bioreactor columns were designed to treat perchlorate-contaminated groundwater obtained from the contaminated site in Henderson, NV. The flowrate tested in the reactors simulated varying hydraulic conductivities at the BMI site. The reported velocities of the groundwater at the BMI site range from 5.64×10^{-5} m/s (1778.6m/year) in alluvial fan deposits to 1.87×10^{-6} m/s (59 m/year) in Muddy Creek Formation (Batista et al., 2003).

The bottom six inches of the columns were filled with pebbles (approximately 1 cm diameter) and glass beads to create a base for the media. Two of the columns were filled with soil obtained from bore holes drilled at the BMI site from depths of 25 to 40 feet (named as Soil 1 and Soil 2); and other two columns were filled with 1.5 cm long Jaeger (Pall) rings as plastic media (RASCHIG USA Inc., 2015) (named as Plastic 1 and Plastic 2). The plastic media was selected to mimic the high hydraulic conductivities found in some areas of the site. The

bioreactor columns filled with soil simulated the areas of low hydraulic conductivity. The dimension and operational parameters of the columns are shown in Figure 3.6.

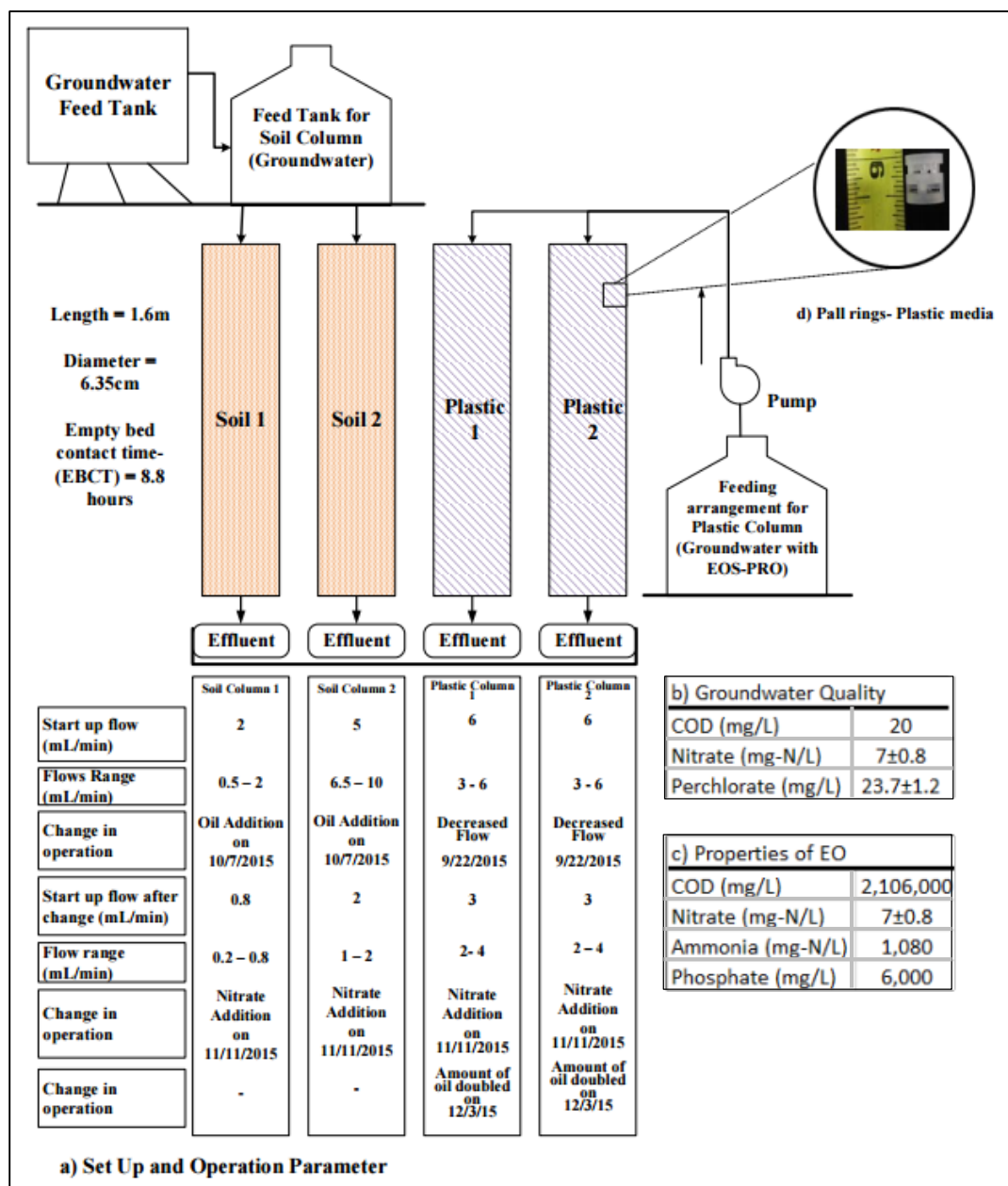


Figure 3.6: Schematic diagram of the column set-up for (In-situ treatment) (a), Groundwater quality (b), Properties of EOS-PRO measured at the Environmental laboratory, UNLV (c) and Plastic media used in the column (d) (The surface area available for bacteria to grow on the plastic rings is 350 m²/m³ and the relative density of the ring is 110 kg/m³).

EOS-PRO emulsified oil was added to the columns as the electron donor/carbon source to support bioremediation. No bioaugmentation was necessary because a several PRB have been isolated from the BMI site and they are ubiquitous in the area (Batista et al. 2003). The characteristics of EOS-PRO emulsified oil are shown in Appendix G. The amount of EOS-PRO to be used was calculated using the amounts of nitrate and perchlorate present in the groundwater. It was also assumed that one pound of EOS-PRO generates 0.4 pounds of hydrogen (Appendix G).

3.3.1 Preliminary Tests

3.3.1.1 Soil Characterization

Soil used in this study was obtained from five bore holes drilled at the BMI site. Soil core samples were collected at four-foot depth intervals between 25 and 40 feet below ground surface. The physical characteristics, moisture content, porosity, and bulk densities, of the soil samples measured at the Soil Laboratory, UNLV are presented in Figure 3.7. The soil samples obtained from the site were mixed, sundried at 104 to 108°F, sieved through sieves #10, 40, 100, and 200 according to ASTM D-422 and the soils retained on the sieves were washed. Soils retained on the sieve # 10, 200, and the pan was termed coarse soil, fine soil, and superfine soil, respectively.

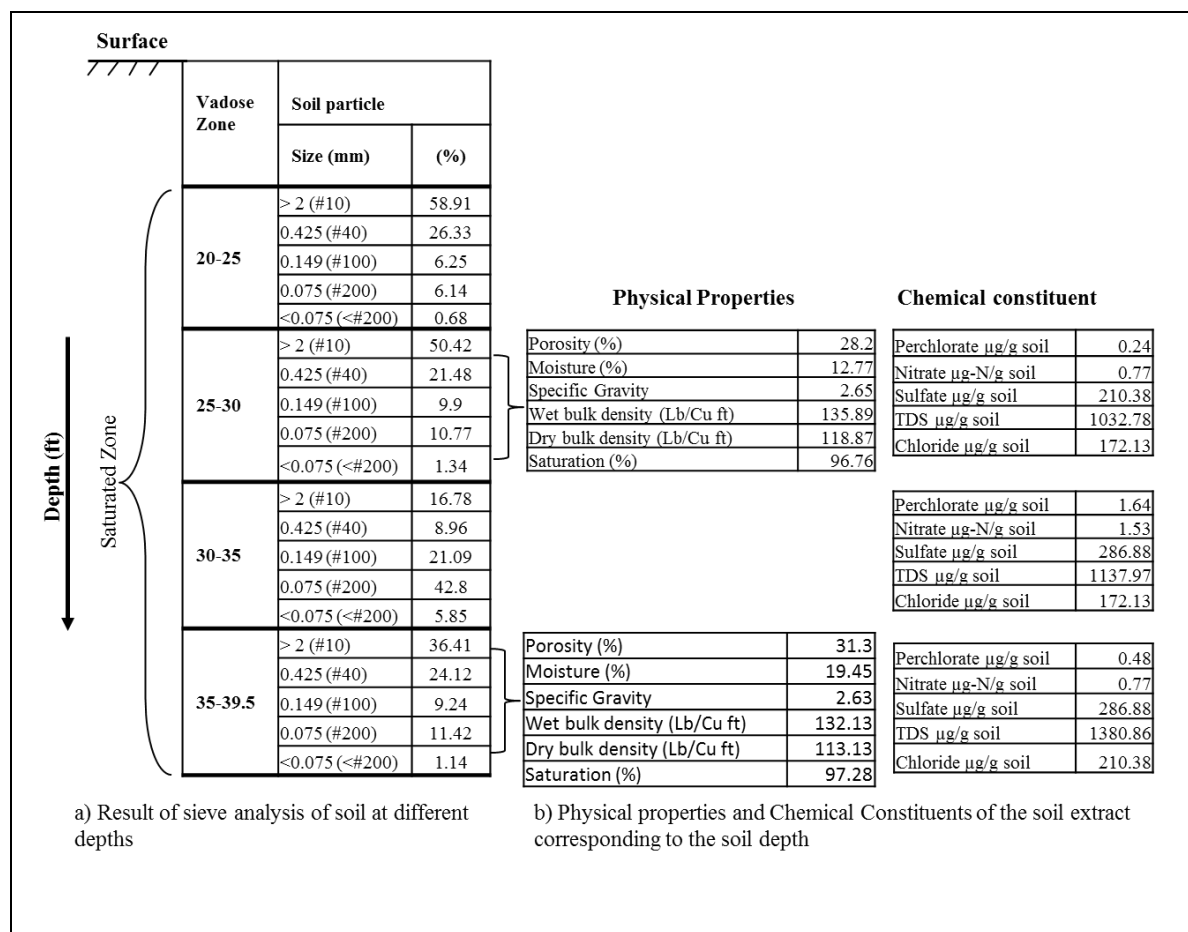


Figure 3.7: Soil profile with soil particle size and characteristics (a), and Physical properties and Chemical constituents of soil extract at 25-30 feet and 35-40 feet depths (Soil Laboratory, UNLV, 2015) (b).

The percentages corresponding to the particle size is the result of sieve analysis using <0.075mm (< 200 mesh), 0.075 mm (retained on 200 mesh), 0.149 mm (retained on sieve No 100), 0.425 mm (retained on sieve No 40) and greater than 2 mm (retained on sieve No 10) sieves.

3.3.1.2 Beta Testing of Bioremediation Using a Bioreactor Column

Using the raw soil as collected from the site in the bioreactor columns was unfeasible because of the large amount of fines present. Therefore, permeability tests were performed with various soil mixtures prepared at different proportions of the coarse, fine and superfine soils to determine a good mix to be used (Table 3.3). Flow rate of each soil mixture was measured and the best soil mixture with that provided a flow rate greater than 6 mL/min was selected for a Beta column test.

Table 3.3: Permeability test with soil mixed at different percent

Trials	Coarse (%)	Fine (%)	Superfine (%)	Flow (mL/min)
1	100	0	0	28.6
2	97	0	3	Saturation was not achieved in 24 hour
3	99	0	1	6.75
4	98	2	0	18.4
5	96	4	0	5.02

Based on the permeability, a combination of coarse and 2% fine soil was selected as the media for a preliminary study with the Beta-column. EOS-PRO, which was selected as the electron donor for the study, was added to the mixture of coarse and fine soil (15 grams of oil per kg soil). A small amount of soil was added to the column and the column was tapped with a rubber hammer to assure soil was well packed and to avoid short-circuiting. The process was repeated until the column was full. The column was gravity fed with groundwater from the contaminated site. The Beta column could not achieve 18.4 mL/min flow as achieved in the permeability test and got clogged within a month of operation. Thus, for soil bioreactor column testing, the amount of fine soil was reduced to 0.5%. The result of Beta-column testing is presented in Appendix F.

3.3.2 Microcosm Testing of Perchlorate Degradation by Indigenous Microbes in Soil from the Contaminated Site.

This experiment was carried out using twenty 125 mL anaerobic bottles filled with forty grams of soil and 100 mL groundwater obtained from the site contaminated with perchlorate and nitrate. In ten bottles, 0.2 mL EOS-PRO was added and in other ten bottles glycerol was added. Bottles were crimped close using butyl rubber caps and aluminum rings. The bottles were then

mixed using a rotary shaker at 30 rpm. Two bottles were sacrificed at days 2, 6, 8, 12, and 16 to take samples on the designated day. The sacrificed bottles were open and their contents centrifuged to separate the solids from the liquid phase. The liquid portion was filtered and analyzed for the constituents of interest for that designated day.

In addition, a comparative study was made to test the effectiveness of EOS-PRO alone as electron donor, EOS-PRO with glycerol, and EOS-PRO with glycerol and phosphorus. Six 125 mL anaerobic bottles were filled with forty grams of soil, 100 mL groundwater obtained from the site contaminated with perchlorate and nitrate, and 0.2 mL EOS-PRO (as obtained from the manufacturer) was added. In two of the bottles glycerol was added, and in other two bottles Glycerol and Phosphorus were added. The last two bottles had EOS-PRO alone as electron donor. All six bottles were crimped close using butyl rubber caps and aluminum rings and were mixed using a rotary shaker at 30 rpm for ten days. After ten days, the bottles were open and their contents centrifuged to separate the solids from the liquid phase. The liquid portion was filtered and analyzed for the constituents of interest.

3.3.3 Operation of Soil and Plastic Bioreactor Columns

3.3.3.1 Soil Bioreactor columns

The soil bioreactor columns were well packed with 5 kg of soil mixed with EOS-PRO (15 grams of oil/ kg soil). The soil packed into the columns contained only 0.5% of fines to allow for higher hydraulic conductivity. At the top of the media, glass beads and a thin layer of cheese cloth were added to prevent suspension of media while feeding the columns. The well-packed columns were fed with groundwater collected from the contaminated site in down-flow mode from the top of the soil columns. Groundwater samples were collected 1-2 times a week and

kept refrigerated. The saturated soil depth was notated on the outer wall of the column for every 30 minutes until the water started to flow out of the column.

In the beginning, all columns were gravity fed with two 5 gallon bottles on the top, one for soil columns and another for plastic columns. Ball valves were used to control the flows in all columns. Soil column 1 did not have any issue with feeding arrangement, but the water head and the flow rate in the Soil column 2 could not be maintained. Thus, to provide constant water head on the columns, the feed tank was replaced with a step-feed arrangement that included two 2-gallon buckets at a foot elevation difference (Figure 3.6). The groundwater was pumped into the top bucket, from which water flows in to the lower bucket by gravity. The lower bucket was fitted with a floating valve to control the flow from top bucket and provide a constant head in the columns.

3.3.3.2 Plastic Bioreactor Column

The plastic columns were packed with 1.5 cm long Jaeger (Pall) rings as media (RASCHIG USA Inc.). The surface area available for bacteria to grow on the plastic rings is $350 \text{ m}^2/\text{m}^3$, and the relative density of the ring is $110 \text{ kg}/\text{m}^3$ (RASCHIG, 2015).

The feed for plastic columns was a mixture of four grams of EOS-PRO in five gallons of contaminated groundwater. The gravity flow feeding arrangement in the plastic columns could not maintain 6 mL/sec because the scum (calcium and oil precipitate) clogged the effluent ball valves frequently. To avoid the clogging issue, a peristaltic pump was used after two weeks of operation.

Initially, the plastic columns were operated in recirculation mode to allow indigenous bacteria present in the groundwater to grow on the plastic media. Fresh feed was prepared based on the COD value of the effluents. After three weeks, the columns stabilized and were switched

to continuous mode maintained at 6 mL/min. Fresh feed water was prepared every two days. The feed tank was changed and washed with soap after each feed to prevent possible biodegradation within the tank. The flow in the plastic columns was reduced from 6 to 3 mL/minute to observe the effect of flow on the nitrate and perchlorate removal.

To observe the effect of high nitrate on perchlorate reduction, 7 mL nitrate was added to 5 gallons groundwater, so that 25-30 mg-N/L concentration was achieved in the feed for both soil and plastic columns. Later, the amount of oil in the feed for the plastic column was doubled to support perchlorate degradation.

3.3.4 Sampling

The effluent from each column was collected in two gallon bottles surrounded by ice packs, which were changed twice a day, to prevent biodegradation in the bottles. Each day, a composite sample was taken from each effluent bottle, and the samples were analyzed for various parameters (Table 3.4). After sampling, the bottles were switched with clean bottles, and were washed with soap and Clorox. The amount of effluent collected in the bottle was measured and recorded every day. Along with the effluent samples, the ground water (feed to soil columns) and plastic feed were also analyzed.

Table 3.4: Parameters Analyzed and Analysis Frequency

Frequency	Daily		Twice in a Week
Parameters analyzed/measured	Throughput volume	pH	Iron
	COD	DO	Hexavalent Chromium
	Nitrate	TDS	Phosphate
	Perchlorate	ORP	Sulfate
			Total Nitrogen

3.3.5 Microbial Analysis

The media from the soil and plastic bioreactor were collected at the end of the study (Figure 3.8) and were shipped to a commercial laboratory (Research and Company, City, Texas) for bacterial community analysis. The primer selected for the study was 8F [59-AGAGTTTGATCCTGGCTCAG-39] and 1525R [59-AAGGAGGTGATCCAGCC-39]). The company provided the percentages for each organism identified (using their database considering 90% or more similarity) up to species level.

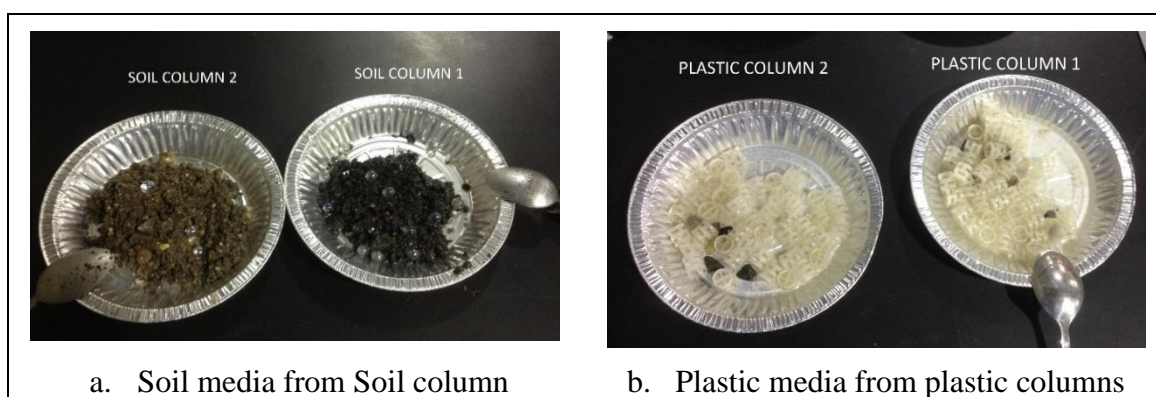


Figure 3.8: Soil and plastic samples collected for microbial analysis.

3.4 Analytical Methods

Analytical methods and equipment used to analyze the samples from the culture, FBR, and the columns are presented in Table 3.5. The analytical methods are discussed further in the following paragraphs.

Table 3.5: Analytical Methods and Equipment Used for Analyzing Samples

Parameter	Method	Equipment
COD	Hach 8000	Spectrophotometer DR 5000
Nitrate	Hach 10020	Spectrophotometer DR 5000
Perchlorate	EPA 314	Dionex ICS 2000
Turbidity		2100 N Turbidimeter
Optical Density		Spectrophotometer DR 5000
pH	EPA 9045 D	
DO		DO Meter

3.4.1 Total Suspended Solids, Turbidity, and Optical Density

Total suspended solids (TSS) was used as a measure to observe bacterial growth in the enriched culture. TSS was conducted once for the culture and was correlated with the Optical Density ($R^2 = 0.99$). Data are shown in Appendix C. Every week before feeding 20 mL sample was filtered using a Whatmann glass-fiber microfilter (GF-C). The GFC was weighed before filtration. After filtration, the filter was, first, dried at 103-105°C for 1 hour before and was weighed. The difference in the weight of the filter before and after filtration gives the total suspended solids per 20 mL.

Optical density was measured using a Spectrophotometer (HACH DR 5000) at 600 nm, and turbidity was measured using HACH 2100 N Turbidimeter (Standard Methods 2130 B). The correlation between turbidity and TSS is also presented in Appendix C. The turbidimeter was calibrated using five formazin polymer standard factory referred solutions of <0.1, 20, 200, 1000, and 4000 NTU.

3.4.2 pH

pH was measured to ensure the neutral pH in the enrichment. The pH meter was calibrated using a two-point calibration with pH 4 and 9 buffers.

3.4.3 Nitrate Concentration

A Hach DR-5000 spectrophotometer was used for determining nitrate concentration. In a Hach test and tube vial, 1 mL sample or DI water (for blank) was added, and Hach nitrate pillows were added. The content in the test and tube vials were mixed well and were kept undisturbed for reaction for 5 minutes. The concentration of the nitrate was measured in the spectrophotometer as mg-N/L at 410 nm.

3.4.4 Perchlorate Concentrations

Perchlorate and chloride concentrations were measured using a Dionex- 2000 ion chromatograph (IC) that consists of an Ion Suppressor ASRS-ULTRA (4 mm), IonPac AS16 column and guard (4 mm), and AS 40 autosampler. The IC was controlled and operated using a program interface, Chromeleon 6.0. Table 3.6 shows the standards and conditions opted for using IC for perchlorate and chloride.

Table 3.6: Standards and Conditions for IC

Compound	Standard Concentration	Column/ Guard	Current (mA)	Eluent Conc. (mM)
Sodium perchlorate (ClO ₄ ⁻) High(mg/L)	1, 2, 3, 4, 5, 6, 7 (1, 5, 10, 20, 50, 100)*	AS 16	100	35

* Perchlorate standard used for evaluation of master and sub-cultures.

Interferences in IC may be realized in presence of chloride, sulfate, carbonate, and high TDS (Motzer 2000).

3.5 Quality Assurance/Quality Control

The goal of quality assurance/quality control (QA/QC) is to ensure the quality of the data collected and analyzed. The QA/AC plan included minimizing personal and systematic errors associated with the procedure and instrument, check detection limits of the method opted, and accuracy and precision of the experiment. The following precautions were taken to ensure quality of the research:

1. Sampling and storage

For evaluation of the perchlorate and acetate concentrations in master and sub-cultures, 10mL of culture were wasted before collecting samples to prevent collection of settled culture at the sampling port, whereas for all the batch tests, the vials were well mixed before collecting

samples. Turbidity, pH, OD, and TSS of samples were immediately measured after sampling. The samples were filtered through 0.2 μm , kept in 10 mL glass vials, and stored in refrigerator (4°C). All vials used for sampling and storage were labeled, dated, and capped to prevent contamination. The concentrations of perchlorate and acetate were measured within 48 hours of storage. IC standards were prepared every two weeks and stored in well labeled and capped glass vials.

2. TSS test

Aluminum dishes used for TSS test were pre-ignited at 550°C for about an hour to avoid weight loss during the test, and were stored in desiccator to prevent moisture interference. All glass micro-fiber filter papers used in the test were also stored in desiccator prior use to prevent moisture interference.

3. Calibration

The IC, pH meter, turbidity meter, and spectrophotometer were calibrated with known standards every time before measurement. In addition, analytical balance, micropipette, and conductivity meter were calibrated every week.

- a) For perchlorate and chloride, the IC was calibrated with at least five standards.
- b) pH meter was calibrated based on two-point method with 4.1 and 10.01 pH buffer standards prior each sample measurement. If the slope was above 90%, the pH meter was considered calibrated.
- c) Turbidity meter was calibrated before every use using Formazin solutions.

Spectrophotometer was calibrated with a blank sample as required by the methodology, before measuring the samples.

- d) The analytical balance was calibrated weekly with 5 g and 50 g standard weights. Every year, the balances were also calibrated by Precise Weighing Systems (Santa Clarita, CA).
- e) Micropipettes were calibrated every week. The volume of water transferred by the micropipettes was measured on the analytical balance, if the weight of water was same as transferred volume, then the micropipette was considered calibrated.
- f) Conductivity meter was used to check DI water quality. Conductivity meter was calibrated every week as mentioned in the manual.

4. Precaution for IC

The standards for calibration were measured from low to high concentration to prevent carry over effect in IC measurement. Further, two blanks (DI water) were introduced after the standards, and a blank was introduced between samples to prevent contamination.

5. Temperature of oven

A thermometer placed on the oven was monitored every week to ensure consistent temperature at 103°C.

6. DI water quality

Tap water was treated with a carbon filter, Reverse Osmosis and nanofilter is termed as DI water, and is free from ionized impurities, organics, microorganisms, and particulate matter larger than 0.2 μm . The DI water was used to prepare standards. The quality of DI water was measured using a conductivity meter to ensure specific resistance below 18 Mohm-cm and monitored every week.

7. Sterilization

The vials used for collecting samples and storage were soaked in Clorax[®] and soap for 6 to 12 hours, rinsed with tap water, and triple rinsed with deionized water. The vials were air dried

prior use. All glassware and glass beads, pipette tips and solutions were autoclaved to ensure no microbial contamination.

8. Safety precautions and waste handling

Online trainings provided by the UNLV Environmental Health and Safety on Biosafety, Chemical Hygiene, and Personal safety were taken at the very beginning before starting experiments. Personal protection and exposure control measures were taken for handling microbial samples. Transfers of microbial samples to the agar plates and to the batch reactors were done under the biological UV hood. The batch reactors with ethanol were prepared under the chemical hood. Lab coats and gloves were worn all the times in the laboratory.

9. Quality control

Table 3.7 lists the quality controls for all the experiment, based on accuracy, precision, detection limit, and coefficient of determination (R^2) of the methodology. The accuracy of the data was determined by calibration of the instrument using the known standard solutions and obtaining R^2 value in each run, and the precision was determined by the duplicates for each sample. Detection limits for perchlorate and chloride were obtained based on the best fit of a wide range of standards.

Table 3.7: Accuracy, Precision, Detection Limit, and R^2 of the Methods Opted for Various Parameters

Parameter	Method	R^2	Precision (Confidence Limit)	Detection Limit	Calibration Range
Perchlorate	IC	0.9997	95 %	4 $\mu\text{g/L}$	1, 2, 3, 4, 5, 6, 7
Nitrate	HACH		95 %		
COD (Low and ultra-low ranges)	HACH	N/A	95 %	N/A	0-1500 ppm and 0- 40 ppm

CHAPTER 4

BIOLOGICAL REDUCTION OF PERCHLORATE AND CO-CONTAMINANTS USING EMULSIFIED OIL AS AN ELECTRON DONOR

4.1 Introduction

Perchlorate is a highly soluble contaminant and it has been detected in groundwater throughout the US. The effect of perchlorate on the human thyroid gland, which plays an important role in human metabolism and a child's brain and organ development, has posed concerns of perchlorate exposure from drinking water (Ginsberg et al., 2007). The US Environmental Protection Agency (EPA) has listed perchlorate as a candidate drinking water contaminant in the Unregulated Contaminant Monitoring Rule. Several states such as California and Massachusetts have regulated perchlorate levels in their drinking water. However, there is no federal standard for perchlorate (Sellers, 2007).

Currently, ion-exchange and biological reduction are the technologies of choice to treat perchlorate. Various studies have confirmed perchlorate biodegradation promoted by microbial enzymes that overcome the high activation energy needed for perchlorate reduction (Gingras and Batista, 2002; Logan, 2000). Perchlorate reducing bacteria (PRB) are ubiquitous and have been identified in pristine water sources and in perchlorate contaminated water (Coates et al., 1999). The kinetics of perchlorate degradation in pure and mixed cultures has been found to be first order in relation to perchlorate concentration (Logan, 2001). The reported half saturation constant for perchlorate (K_s), the concentration at which perchlorate reduction proceeds at half its maximum rate, has been reported to average 9-14 mg/L for heterotrophic reduction (Logan et al., 2001; Urbansky, 2000) to 6-149 mg/L for autotrophic degradation (Miller and Logan, 2000; Nerenberg et al., 2006; Dudley et al., 2008; Cheong et al., 2010; London et al., 2011; Ricardo et

al.) Therefore, perchlorate degradation kinetics are faster at higher concentrations, typically found in contaminated industrial sites (i.e. in parts-per-million levels, ppm), and slower in groundwater contaminated with low perchlorate concentrations (i.e. parts-per-billion levels, ppb).

In the United States, two industries, Pacific Engineering and Production Company of Nevada (PEPCON) and Kerr-McKee, located in Basic Management Industrial (BMI), Henderson, Nevada, were the sole producers of ammonium perchlorate and other perchlorate salts for the entire nation from the early 1940s until 1988. Before the establishment of the Resource Conservation and Recovery Act of (RCRA) in 1976, which provided a framework for management of hazardous and solid wastes in the US, industry unknowingly of the consequences, discharged wastes into soil, water, and air. In Henderson, the wastes from perchlorate manufacturing were disposed into unlined ponds and ditches resulting in massive contamination of the groundwater with perchlorate (Batista et al., 2003). In 1997, perchlorate was discovered in the lower Colorado River and traced back to the Las Vegas Wash and seepage of contaminated groundwater from the perchlorate manufacturing sites in Henderson (NDEP, 2011) (Figure 4.1). A groundwater contamination model developed in 2003 estimated that about 8 million gallons of groundwater have been contaminated with a total load of perchlorate of over 21 million pounds. (Batista et al., 2003). In 1997, perchlorate concentrations at the Las Vegas Wash (LVW) were 10-800 ppb and Lake Mead was 25 -120 ppb (Kesterson et al., 2005). Since their discovery, various measures have been taken to confine the perchlorate plumes to the site, including the installation of a seep water collection system, a temporary ion exchange (IX) treatment system, and creation of a slurry wall to confine the contaminated plume. In 2004, the IX system was replaced with a biological treatment unit, using fluidized bed reactors (FBRs),

with granular activated carbon as media. Currently perchlorate bioremediation includes eight fluidized bed reactors (FBRs) operated at 1000 gallons per minute treating ppm level perchlorate. The FBRs use 300 gallons of ethanol per day as the electron donor to support the degradation of perchlorate and its co-contaminants (Hatzinger, 2010). The groundwater extracted and treated in the FBR is discharged back to the Las Vegas Wash.

Figure 4.1: The ground water contamination site at the BMI, Henderson, NV (Source: Boralessa and Batista, 2000).

Bacteria prefer electron acceptors which provide more energy and biomass yield over perchlorate (Choi et al., 2007). In the presence of multiple electron acceptors, reduction occurs in the preference order - oxygen, nitrate, chlorate, selenate and perchlorate (Envirogen, 2011). All the past studies have indicated that oxygen is preferentially utilized by bacteria than perchlorate (Choi et al., 2007). The sensitivity of perchlorate reductase and chlorite dismutase enzymes to oxygen results in inhibition of perchlorate reduction (Chaudhuri et al., 2002). Nitrate is also reported to reduce the enzymatic activity of perchlorate degrading bacteria. However, some studies have reported no effect of nitrate on perchlorate degradation as well as simultaneous nitrate and perchlorate degradation (Ricardo et al., 2012; Bardiya and Bae, 2004).

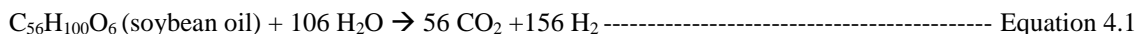
Selenate is another co-contaminant and electron acceptor that is thermodynamically preferred over perchlorate. Even though, no PRB have been identified that can degrade selenate (Xu et al., 2003), Chung et al. (2006) speculated that PRB may have functional diversity for reducing selenate. Similarly, many perchlorate reducers have been identified that can reduce chlorate, a thermodynamically preferred electron acceptor (Bardiya, 2011).

At a perchlorate contaminated site, such as BMI, competitive electron acceptors that are preferable to bacteria, such as oxygen, nitrate and chlorate, coexist in the groundwater and usually present at concentrations two to three times that of perchlorate depending on the location (Batista et al., 2005). This fact makes perchlorate removal at the site more complex and costly because sufficient electron donor must be provided to reduce all the preferred electron acceptors before perchlorate can be removed.

The persistence of perchlorate since 1940s at the BMI area, despite the ubiquity of PRB, is due to the lack of electron donors to support perchlorate reduction. Given the magnitude of contamination at the BMI site and the cost associated with pumping and ethanol consumption, in-situ bioremediation needs to be explored as an alternative to clean-up the site. The BMI site has alluvial channels with high hydraulic conductivities (Batista et al., 2003), which causes migration of soluble electron donors with groundwater. Therefore, frequent addition or recirculation of the groundwater is required to sustain bioremediation. In-situ bioremediation was explored in the PEPCON area at BMI using ethanol. The results indicated that recirculation of groundwater resulted in biofouling and clogging of pipes and pumps (EPA, 2006).

In an aquifer with very high groundwater velocities, such as at the BMI site, an electron donor with a higher soil-retention capacity and slow release over time is desirable for bioremediation. Emulsified oils (EO) are organic oils that are relatively soluble in water.

Emulsified soybean oils are commercially available and have been used in the past to support bioremediation as electron donors and carbon sources (Bordon, 2007; Watson et al., 2013). EO has high soil retention ability and are slowly released over time (EOS, 2015). Indigenous microorganism ferment EOs over time into soluble organic carbons, such as acetate and glycerol, carbon dioxide, and hydrogen (H₂) gas as shown by Equation 4.1 (Solutions-IES, 2010).

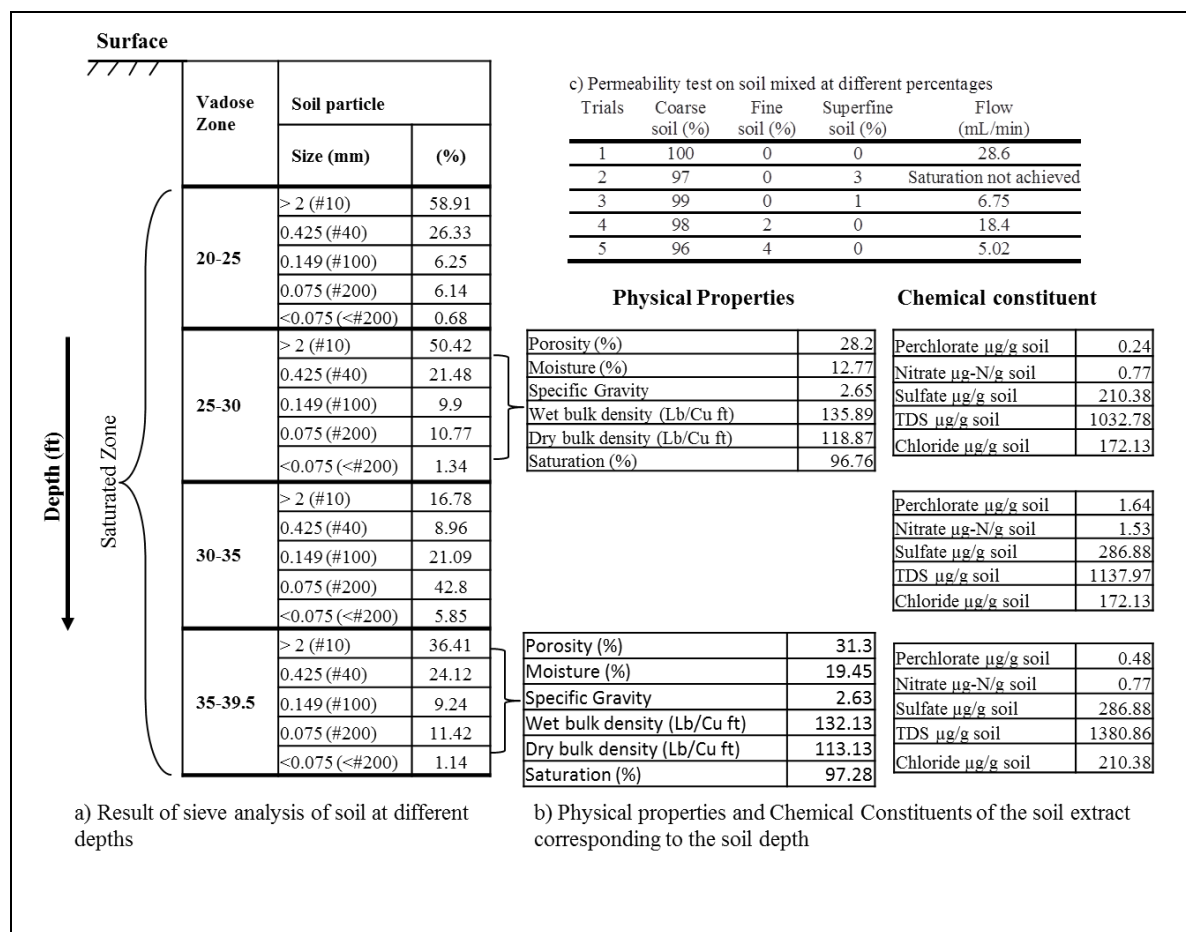


This research explores the potential of in-situ bioremediation of the perchlorate using emulsified oil. Specifically, the capacity of EO to support biological reduction of perchlorate and nitrate, under high and low groundwater velocities, and using the indigenous bacteria present in the soil and groundwater, was investigated.

4.2 Methodology

4.2.1 Source of Soil Samples and Characterization

Soil used in this study was obtained from five borings drilled through the saturated zone of a perchlorate-contaminated site. Soil samples were collected by auger drilling at four -foot depth intervals from 20 feet to 40 feet. Approximately 3 gallons of soil were aseptically collected from each interval. Sterilized metal hand shovels and plastic buckets and pans were used to collect the soils samples at the site. Samples were transferred to the laboratory on ice and stored in a large refrigerator. The physical characteristics, moisture content, porosity, and bulk densities of the soil samples were measured at the UNLV Soils Laboratory (Figure 4.2 a, and Figure 4.2 b). The soil samples obtained from different depths were mixed at equal weight proportions, sundried at 107°F, sieved with sieves #10, 40, 100, and 200 according to ASTM D-422. Soil retained on the sieve # 10 was termed “coarse soil”; in sieve #200, “fine”; and that collected on the pan, “super fine”.



a) Result of sieve analysis of soil at different depths

b) Physical properties and Chemical Constituents of the soil extract corresponding to the soil depth

Figure 4.2: Soil profile with soil particle size and (a), Physical properties and Chemical constituents of soil extract at 25-30 feet and 35-40 feet depths (Soil Laboratory, UNLV, 2015) (b), and Results of permeability test (Soil Laboratory, UNLV, 2015) (c)..

The percentages corresponding to the particle size is the result of sieve analysis using <0.075mm (< 200 mesh), 0.075 mm (retained on 200 mesh), 0.149 mm (retained on sieve No 100), 0.425 mm (retained on sieve No 40) and greater than 2 mm (retained on sieve No 10) sieves.

4.2.2 Contaminant Concentration in Soil Samples

The contribution of perchlorate and nitrate was assessed by extracting soil samples with deionized (DI) water using a centrifuge. Forty gram soil samples from different depths –25-30 feet and 35-40 feet were centrifuged with 100 mL DI water for 30 minutes at 3500 rpm (Legend RT Sorvall centrifuge, Thermo Fisher Scientific, Inc., Waltham, MA). Next, the supernatant was carefully transferred from the centrifuged tubes to labeled sterile-tubes. Next, 20 mL DI water

was added to the settled soil, vortexed for a few seconds, and centrifuged again. The supernatant was added to the original extract and the extract was analyzed for the contaminants of interest. Figure 4.2 b shows the chemical constituents of the soil samples obtained from 25-30 and 30-40 feet depth. The procedure of extraction and analysis were repeated for sieved soils (coarse, fine and superfine). Table 4.1 lists the chemical constituent in the coarse, fine and superfine soil extract.

Table 4.1: Composition of Soil Extracts from the Contaminated Site

Soil Fraction	Perchlorate $\mu\text{g/g Dry Soil}$	Nitrate $\mu\text{g-N /g Dry Soil}$	Sulfate $\mu\text{g/g Dry Soil}$	COD $\mu\text{g/g Dry Soil}$	TDS $\mu\text{g/g Dry Soil}$	Hardness $\mu\text{g/g Dry Soil as CaCO}_3$
Coarse	2.03 \pm 0.22	1.09 \pm 0.17	20 \pm 3	15.48 \pm 0.61	389.36 \pm 15.41	132.7 \pm 5.2
Fine	5.32 \pm 0.05	2.32 \pm 0.01	54.91 \pm 1.8	21.15 \pm 4.35	1394.98 \pm 35	337.9 \pm 1.9
Super-fine	5.97 \pm 2.62	1.57 \pm 1.02	55.5 \pm 12.9	55.5 \pm 12.94	1367.84 \pm 337	369.9 \pm 147.9

The fraction extract results indicate that the super-fine and fine fractions of the soil contain the majority of the contaminants of concern compared to the coarse fraction. In general, the soil contains twice as much perchlorate than nitrate. However, the fine and superfine fractions contain about twice as much perchlorate and nitrate than the coarse fraction. A similar trend was found for sulfate and COD measurements. However, for TDS, the fine and superfine fractions have values 3.5 times greater than that of the coarse fraction. The TDS of the fines and superfine fractions averaged 1380 $\mu\text{g/g}$ soil. The average values for perchlorate, nitrate, and sulfate combined is about 63 $\mu\text{g/g}$ soil. Therefore, the majority of TDS in the soil samples is associated with salts other than nitrate, sulfate, and perchlorate; it is likely to be due to sodium chloride, the raw material used to make perchlorate salts.

4.2.3 Preliminary Column Bioreactor Testing Using Soils and Groundwater from the Site

Using the raw soil as collected from the site in the bioreactor columns was unfeasible because of the large amount of fines present. Therefore, permeability tests were performed with various soil mixtures prepared at different proportions of the coarse, fine and superfine soils to determine a good mix to be used (Figure 4.2.c). Water flowrates through each soil mixture was measured, and the best soil mixture that provided a flow rate greater than 6 mL/min was selected. Based on the permeability test, a combination of 98% coarse and 2% fine soil was selected as the media for a preliminary bioreactor study.

A two-inch-diameter, 6-feet clear acrylic columns was fitted with an effluent valve to serve as the bioreactor. The first 4 inches of the column was filled with gravel and glass beads so to form a drainage system for the column. Emulsified oil (EO) was added to the soil, mixed well (15 mL per kg of dry soil), and packed into the column. The EO added to the soil was used as the electron donor and carbon source to promote degradation. The amount of oil added to the soil was computed using overall biological growth reactions for estimated amounts of perchlorate, chlorate, and nitrate present in the soil and in the groundwater.

The column bioreactor was gravity fed with groundwater obtained from the contaminated site. The groundwater from the contaminated site was collected in five 5-gallons sterile bottles weekly and were stored in a refrigerator maintained at 32°F. The effluent from the test column was collected using two-gallons containers placed on ice to minimize degradation outside the column. Samples were then centrifuged for 10 minutes at 3500 rpm (Legend RT Sorvall centrifuge, Thermo Fisher Scientific, Inc., Waltham, MA) and analyzed for COD, nitrate, and perchlorate.

4.2.4 Microcosm Testing of Perchlorate Degradation by Indigenous Microbes in Soil from the Contaminated Site.

This experiment was carried out using twenty 125 mL anaerobic bottles filled with forty grams of soil and 100 mL groundwater obtained from the site contaminated with perchlorate and nitrate. In ten bottles, 0.2 mL EO was added and in other ten bottles glycerol was added. Bottles were crimped close using butyl rubber caps and aluminum rings. The bottles were then mixed using a rotary shaker at 30 rpm. Two bottles were sacrificed at days 2, 6, 8, 12, and 16 to take samples on the designated day. The sacrificed bottles were open and their contents centrifuged to separate the solids from the liquid phase. The liquid portion was filtered and analyzed for the constituents of interest for that designated day.

In addition, a comparative study was made to test the effectiveness of EO alone as electron donor, EO with phosphate, and EO with glycerol and phosphate. Six 125 mL anaerobic bottles were filled with forty grams of soil, and 100 mL groundwater obtained from the site contaminated with perchlorate and nitrate. In two of the bottles, 0.2 mL EO was added, other two of the bottles EO and phosphate was added, and in last two bottles Glycerol and Phosphate were added. All six bottles were crimped close using butyl rubber caps and aluminum rings and were mixed using a rotary shaker at 30 rpm for ten days. After ten days, the bottles were open and their contents centrifuged to separate the solids from the liquid phase. The liquid portion was filtered and analyzed for the constituents of interest.

4.2.5 Operation of Column Bioreactors Using Soil and Plastic Media

The feasibility of using a slow release electron donor, emulsified oil (EO), for in-situ perchlorate bioremediation was evaluated using four laboratory column bioreactors (Figure 4.3). The bioreactor columns were designed to treat perchlorate-contaminated groundwater obtained

from a contaminated a contaminated site. The target is the saturated zone portion of the aquifer and therefore both soils and groundwater from the site were used. Many perchlorate reducing bacteria have been isolated from this site (Batista et al., 2003), but biodegradation has not occurred because of the absence of an electron donor and carbon source. Therefore, it was assumed that both, soil and groundwater from the site contain sufficient amount of naturally occurring bacteria capable of degrading perchlorate and nitrate. The flowrate tested in the reactors simulated varying hydraulic conductivities present in the site. The reported velocities of the groundwater at the site range from 5.64×10^{-5} m/s (1778.6m/year) in alluvial fan deposits to 1.87×10^{-6} m/s (59 m/year) in Muddy Creek Formation (Batista et al., 2003). Two of the columns were packed with soil obtained from the contaminated site to create a low conductivity scenario and the other two columns were filled with 1.5 cm long Jaeger (Pall) plastic rings (RASCHIG USA Inc.) as media to create a higher conductivity scenario.

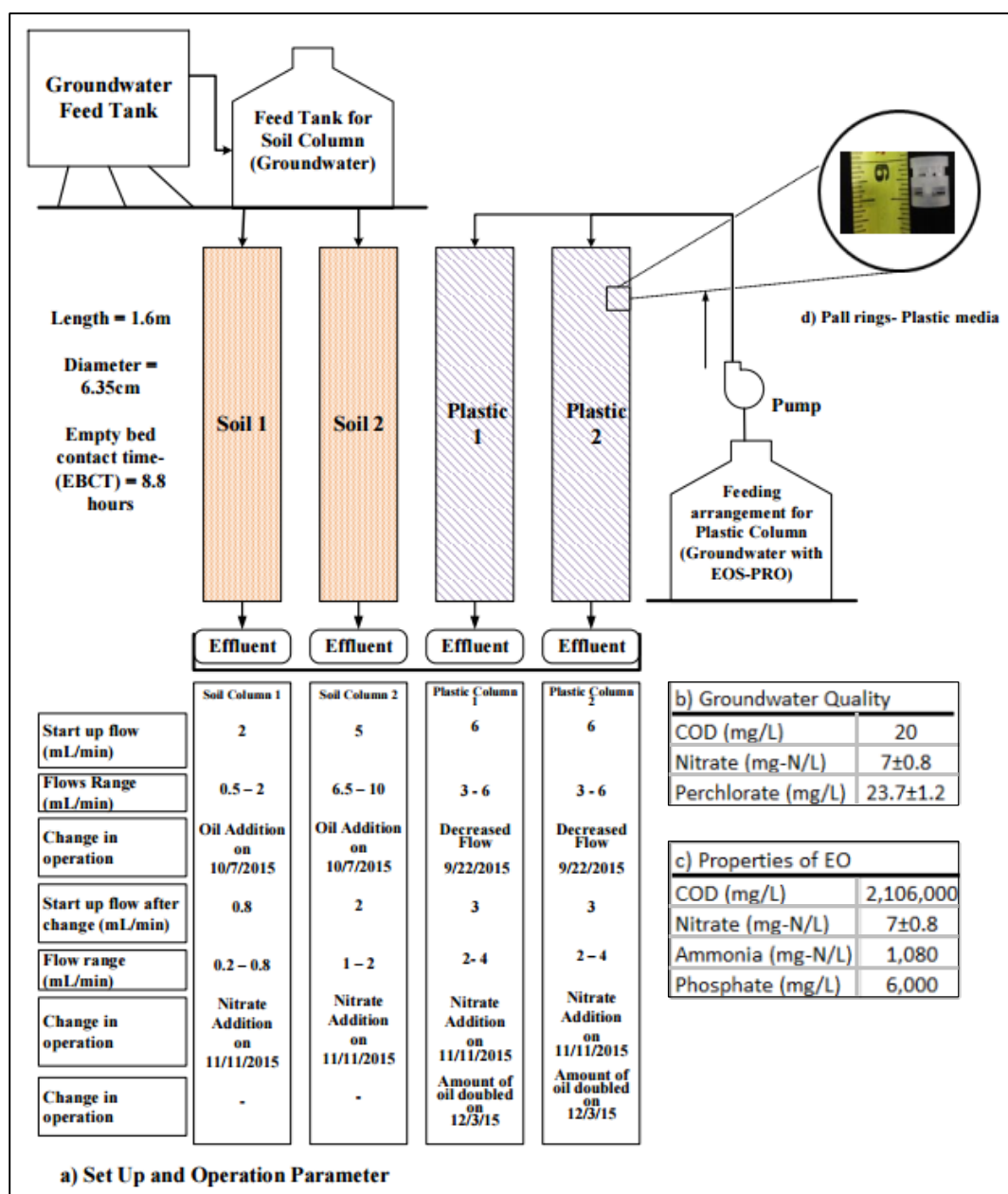


Figure 4.3: Schematic diagram of the set-up (a), Groundwater quality (b), Properties of EOS-PRO measured at the Environmental laboratory, UNLV (c), and Plastic media used in the column (d). (The surface area available for bacteria to grow on the plastic rings is 350 m²/m³ and the relative density of the ring is 110 kg/m³).

4.2.5.1 Soil Column Bioreactors

The soil column bioreactors were well packed with 5 kg of soil mixed with emulsified oil (15 g oil/ kg soil). The amount of oil to be added was computed using the manufacturers' estimation (0.4 lbs hydrogen gas per pound substrate). The soil packed into the columns contained only

0.5% of fines to allow for higher hydraulic conductivity. At the top of the media, glass beads and a thin layer of cheesecloth were added to prevent suspension of media while feeding the columns. The well-packed columns were fed with groundwater collected from the contaminated site in a down-flow mode. Groundwater samples from the site were collected 1-2 times a week in sterile five-gallons bottles and refrigerated at 32°F. As the soil became saturated, the saturated soil depth was noted on the outer wall of the column for every 30 minutes until the water started to flow out of the column.

In the beginning, all columns were gravity fed with two five-gallons bottles on the top, one for soil columns and another for plastic columns. Ball valves were used to control the flows in all columns. Soil column 1 did not have any issue with feeding arrangement, but the water head and the flow rate in the Soil column 2 could not be maintained. Thus, to provide constant water head on the columns, the feed tank was replaced with a step-feed arrangement that included two 2-gallon buckets at a foot elevation difference (Figure 4.3). The groundwater was pumped into the top bucket, from which water flows in to the lower bucket by gravity. The lower bucket was fitted with a floating valve to control the flow from top bucket and provide a constant head in the columns.

4.2.5.2 Plastic Column Bioreactor

The plastic column bioreactors were packed with 1.5 cm long Jaeger (Pall) rings as media (RASCHIG USA Inc.). The surface area available for bacteria to grow on the plastic rings is 350 m²/m³, and the relative density of the ring is 110 kg/m³ (RASCHIG, 2015).

The feed for the plastic columns was a mixture of four grams of EO in five gallons of contaminated groundwater. The gravity flow feeding arrangement in the plastic columns could not maintain 6 mL/second because the scum (calcium and oil precipitate) clogged the effluent

ball valves frequently. To avoid the clogging issue, a peristaltic pump was used for feeding after two weeks of operation.

Initially, the plastic columns were operated in recirculation mode to allow indigenous bacteria present in the groundwater to grow on the plastic media. Fresh feed was prepared based on the COD value of the effluents. After three weeks, the columns stabilized and were switched to continuous mode maintained at 6 mL/min. Fresh feed water was prepared every two days. The feed tank was changed and washed with soap and bleach after each feed to prevent possible biodegradation within the tank. The flow in the plastic columns was reduced from 6 to 3 mL/minute to observe the effect of flow on the nitrate and perchlorate removal.

4.2.6 Effect of Nitrate on Perchlorate Biodegradation in the Column Bioreactors

To observe the effect of high nitrate on perchlorate reduction, 7 mL of 300 mg/L stock nitrate solution was added to 5-gallon groundwater, so that 25-30 mg-N/L concentration was achieved in the feed for both soil and plastic columns. Later, the amount of oil in the feed for the plastic column was doubled to support perchlorate degradation.

4.2.7 Sampling

The effluent from each column was collected in two-gallon bottles surrounded by ice packs, which were changed twice a day, to prevent biodegradation in the bottles. Each day, a composite sample was taken from each effluent bottle, and the samples were analyzed for various parameters (Table 4.2). After sampling, the bottles were switched with clean bottles, and were washed with soap and bleach. The amount of effluent collected in the bottle was measured and recorded every day. Along with the effluent samples, the ground water (feed to soil columns) and

plastic feed were also analyzed. All samples were filtered through 2 μm filters. The contaminated groundwater collected twice a week and were refrigerated at 32°C.

Table 4.2: Parameters Analyzed and Analysis Frequency

Frequency	Daily	Twice in a Week
Parameters analyzed/measured	Throughput volume	Phosphate(EPA 365.1)
	COD(Hach 8000)	Sulfate IC and Hach EPA 8051
	Nitrate Hach EPA 10206 and EPA 352.1	Ph
	Perchlorate IC (EPA 314)	TDS(SM 2540, EPA 160.1)

4.2.8 Microbial Analysis

The media from the soil and plastic bioreactor were collected at the end of the study and shipped to a commercial laboratory (Research and Testing Laboratories, Lubbock, Texas) for bacterial community analysis. The primer selected for the study was 8F [59-AGAGTTTGATCCTGGCTCAG-39] and 1525R [59-AAGGAGGTGATCCAGCC-39] (Coates et al., 1999).

The laboratory uses Illumina next-generation sequencing technology that uses clonal amplification and sequencing by synthesis. Once the sequences were generated, the data undergo detection and removal of short, singleton, noisy and bad read sequences. The quality checked sequences were clustered at a 4% divergence using USEARCH clustering algorithm. The sequences were identified using in-house-maintained database of that is derived from NCBI. The final result obtained from the laboratory included the percentages for each organism identified up to species level.

4.3. Results

4.3.1 Microcosm Testing for Perchlorate and Nitrate Using Emulsified Oil

Preliminary microcosm testing was performed to determine the impact of electron donor type and addition of the nutrient phosphate on the biological reduction of nitrate and perchlorate present in groundwater and soil samples. Emulsified oil (EO) and glycerol were used as electron donors. The impact of electron type and phosphate on nitrate and perchlorate removal is shown in Figures 4.4 and 4.5. The initial concentration of nitrate was 27.72 mg-N/L and that of perchlorate was 59.53 mg/L.

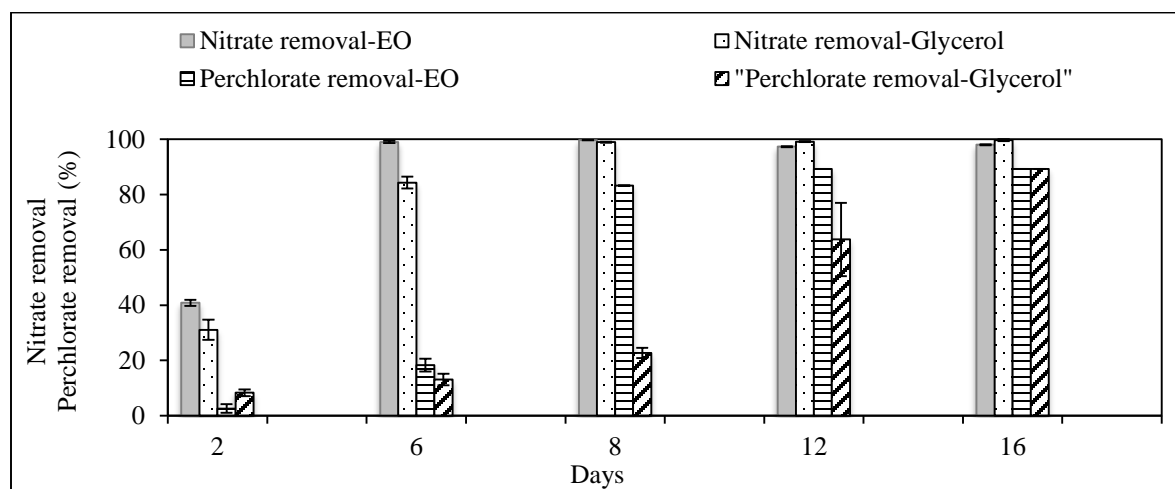


Figure 4.4: Nitrate and perchlorate removal in microcosms tested with EO and glycerol as electron donors. Initial nitrate and perchlorate concentrations were 27.72 mg N/L and 59.53 mg/L, respectively.

In microcosms with EO, 40% nitrate and 2% perchlorate removals were observed within 2 days. Microcosm fed glycerol performed somewhat better removal of nitrate (30%) and perchlorate (8%) during the same period. Nitrate removal exceeded 99% within 6 days in EO microcosms, but for glycerol fed microcosms, 8 days were required to achieve the same percent removal. The results indicate that emulsified oil (EO) promoted faster perchlorate and nitrate removal than glycerol. Despite of initial greater perchlorate removal observed with glycerol

within 2 days (8%) compared to (2%) with EOS, perchlorate removal with EO achieved more than 80% within 6 days; glycerol microcosm required 16 days to achieve the same percent removal. The reason might be because glycerol is more soluble and readily available for biological reduction of perchlorate than EO. As bacteria fermented EO into soluble products, the perchlorate removal excelled in the EO microcosms. Nonetheless, the average nitrate and perchlorate removal were not significantly different ($p > 0.05$) in the microcosms with the two electron donors.

Figure 4.4 shows decrease in nitrate removal on days 12 and 16 in the EO microcosms. The nitrate concentration on those days increased which might be associated with the change in analytical method. It is important to note that the EO used contains nutrients. The concentration of nitrate and ammonia measured in the raw EO as purchased, was 7 mg-N/L nitrate and 1000 mg/L ammonia. The manufacturer reports the nutrient content of the EO is 1% (EOS, 2015).

A negative impact of nitrate on perchlorate degradation was clearly observed. Although perchlorate degradation was observed in days 2 and 6 in EO microcosms, the percent removal increased above 80% on day 8 when the nitrate concentrations were less than 0.5 mg-N/L. Similarly, in glycerol microcosm, percent removal increased above 60% on day 12 after nitrate concentration decreased below 0.5 mg-N/L. The percent perchlorate removal in both microcosms before and after nitrate removal were statistically significantly different ($p < 0.05$).

It is worth to note that the EO oil used in this experiment has 6000 mg P/L. Therefore, based on the amount of EO added, all microcosms contained about 3 mg P/L from EO itself. Additional 6 mg P/L was added to some microcosms, for a total of 9 mg P/L. The addition of extra phosphate to microcosms had no effect on nitrate removal, which was 100% within the 10 days period. However, perchlorate removal was impacted by addition of extra phosphate.

Perchlorate removal in the EO only fed microcosms was more than 96% within 10 days, whereas in microcosms EO and phosphate was 50%, and microcosm fed with EO, Glycerol, and phosphate was 77% (Figure 4.5). The reason for such decreased in perchlorate removal might be due to presence of higher phosphate concentration in the microcosm. It might be that higher phosphate concentrations stimulate the growth of other bacteria that do not degrade perchlorate. Nonetheless, the results point to the importance of carefully considering phosphate addition in perchlorate removing bioreactors. Perchlorate removal was higher in microcosm fed with a mixture of EO and glycerol. Being readily available, glycerol can be more quickly utilized than EO improving perchlorate removal.

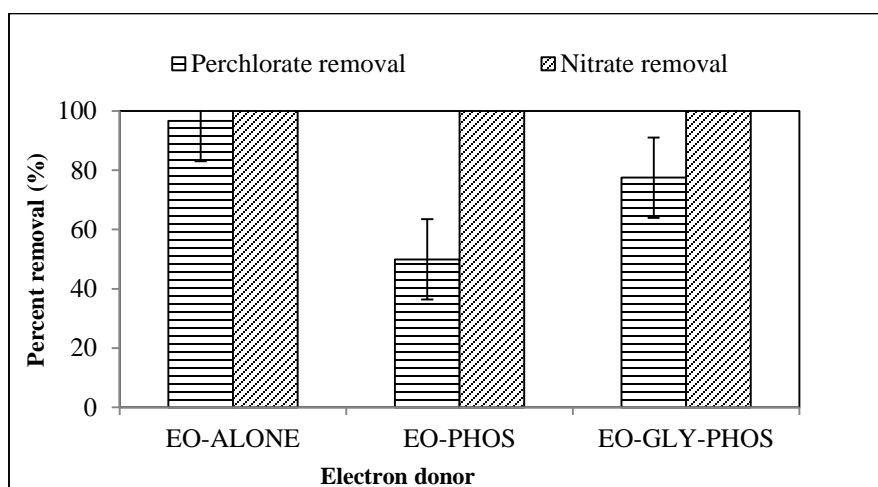


Figure 4.5: Percent removals of perchlorate and nitrate in the microcosms with (i) EO, (ii) EO and Phosphorus, and (iii) EO, Glycerol, and Phosphorus within the ten-day study period.

4.3.2 Emulsified Oil Release from Column Bioreactor Packed with Contaminated Soils

Emulsified oil has been reported to adsorb to soils and slowly release to support biodegradation (Borden, 2007; Jung et al., 2006). In this research chemical oxygen demand (COD) measurements were used as a surrogate for the presence of EO. For the first 56 days of operation of the soil bioreactors, EO was mixed directly into the soil prior to packing (15 grams

per kg soil). For the remaining 74 days of operation, EO was added directly to the groundwater fed to bioreactor column. In the bioreactors containing plastic media EO was also added directly to the groundwater feed (four grams per five gallons).

COD values measurements in the effluent of the bioreactor columns revealed that EO adsorbs to soil and is slowly released as water percolates through the soil. EO was also shown in this study to promote biodegradation of nitrate (Figure 4.6 a) and perchlorate (Figure 4.6 b). In preliminary microcosm test, the nitrate degraded immediately within two days, but the perchlorate removal was observed only when the most of the nitrate degraded (Figure 4.4). Thus, it was expected the same in the columns, so the decision of second addition of EO to the soil columns was made when the effluent COD concentration was low enough to decline the nitrate removal (i.e. increase in nitrate concentration in the effluent) in the columns.

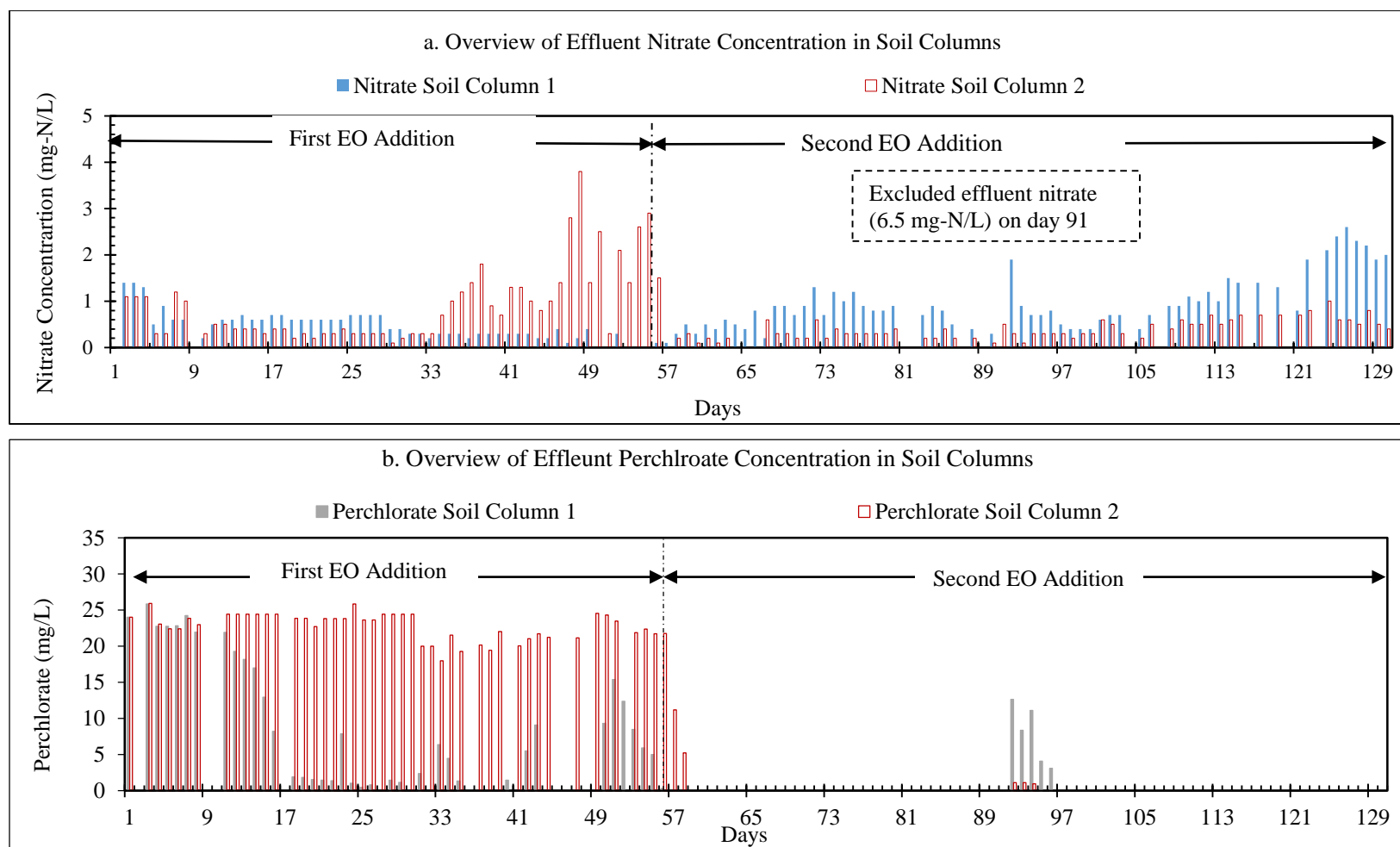


Figure 4.6 b: Effluent nitrate (a) and perchlorate (b) concentrations throughout the study period (130 days). The vertical dotted line shows the second EO addition on Day 56.

For the first two days of operation, a high COD values $> 1,000$ mg/L was observed in the effluent of the soil columns. This high initial COD value is indicative of the washing of excess oil that was not adsorbed to the soil. After two days, the COD in the effluent of the column stabilized around 100 mg/L and slowly decreased to about 30 mg/L after 35 days of operation for soil column 2 (Figure 4.7a). For soil bioreactor 1, which was operated at about half the flowrate of bioreactor 2, the COD concentrations were higher during the run and above 30 mg/L even after 35 days of operation (Figure 4.7a). The stable decrease in COD in the effluent of the bioreactors indicate that EO is slowly released from the soil. Furthermore, the results show that EO release is proportional to the amount of water processed through the column. On the 56th day, the COD concentration in the soil bioreactors decreased to < 30 mg/L, EO was added to both columns. ESTPC (2010) reported that for pilot in-situ bioremediation treating perchlorate (3.1 to 20 mg/L) and other co-contaminants (such as trichloroethane at a concentration of 5.7 to 17 mg/L), the effectiveness of the first EO reduced by eighteen months. However, EO was not injected for the second time. Post injection of EO, approximately 61 pounds of perchlorate was removed from the contaminated groundwater over the entire 42-month study period (ESTPC, 2010). The hydraulic conductivity of the contaminated site reported in the ESTPC (2010) was 80 to 400 feet per year, which is almost 3 times lower than the lowest hydraulic conductivity measured among the column bioreactors in this study (i.e. 2000 feet per year). The same study reported that in a laboratory scale column test (80 cm long and 2.5 cm diameter), almost 97% of the EO injected was adsorbed in the column media; total organic carbon (TOC) was used as surrogate to EO measurement.

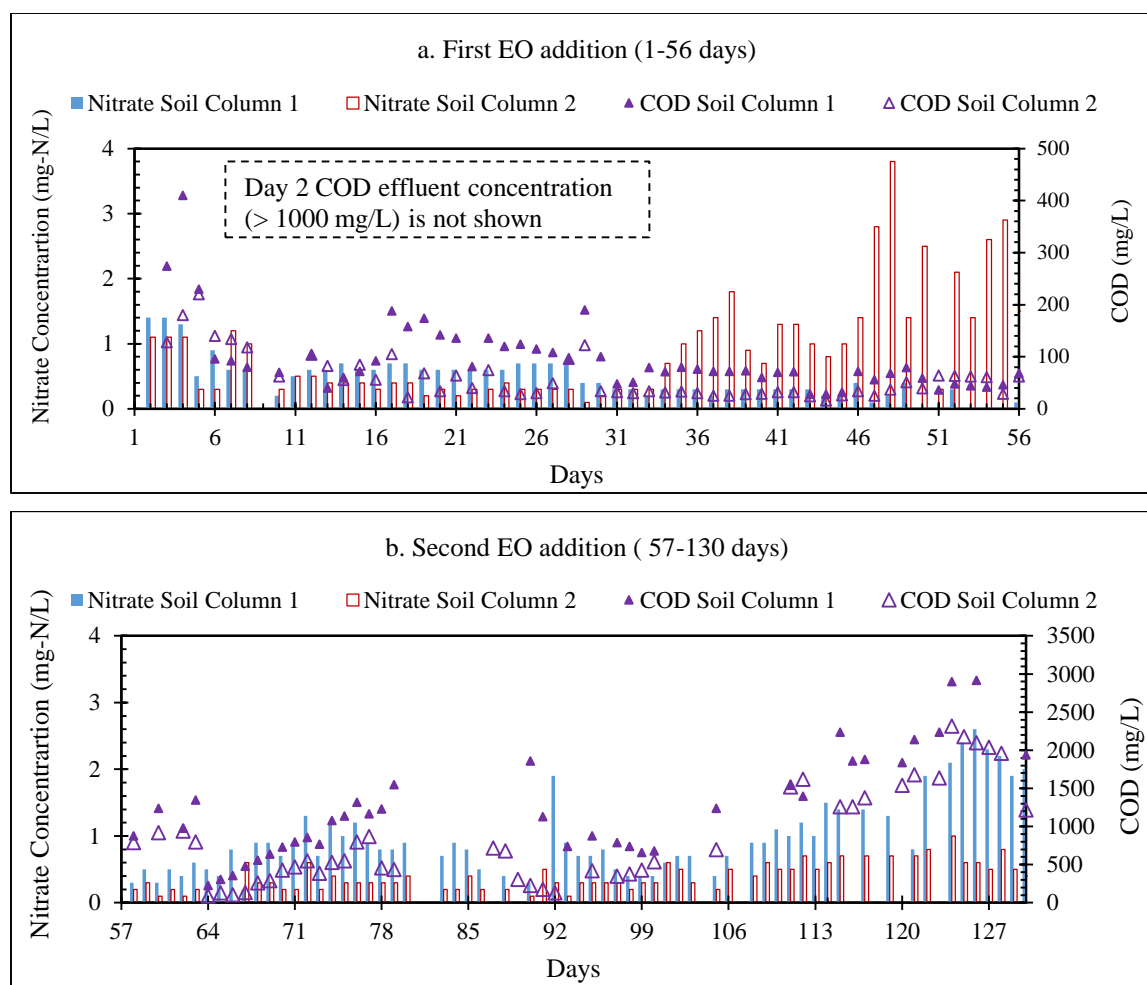


Figure 4.7: Effluent nitrate and COD concentrations over time for the first EO addition with 7 mg/L average influent nitrate concentration (a) and second EO addition with 27 mg/L average influent nitrate concentration (b).

For second injection, EO was added directly to the groundwater fed to the columns (15 mL per kg dry soil). After the oil addition, the effluent COD increased above 1000 mg/L immediately, but decreased below 200 mg/L within a week in both columns. However, the effluent COD concentration increased above 1000 mg/L again during the last 56 days in soil column bioreactor 1 and for the last 25 days in the soil column bioreactor 2. Such increase in COD effluent may suggest that the soil did not adsorb in the same manner as in the first addition. However, ratio of the mass of EO (in terms of CODs, mg) in the effluent to the total mass of EO added to the column shows that almost 70% of the oil were adsorbed to the soil (Figure 4.8).

This might suggest that the microbes responsible for biodegradation of EO into its soluble organic acids were in large amount that in the first injection period. Further, the second addition reduced the hydraulic conductivities greatly in both soil column bioreactors, possibly due to the high biomass growth. The hydraulic conductivities were computed using flowrate through the column that were measured every day and using water head of 2.5 feet (measured from the top of soil columns to the water level in the lower feed tank). The effective hydraulic conductivity by 66% was observed by Coulibaly and Borden (2004), however, in that study the reduced hydraulic conductivity contributed by the high viscous emulsified oil.

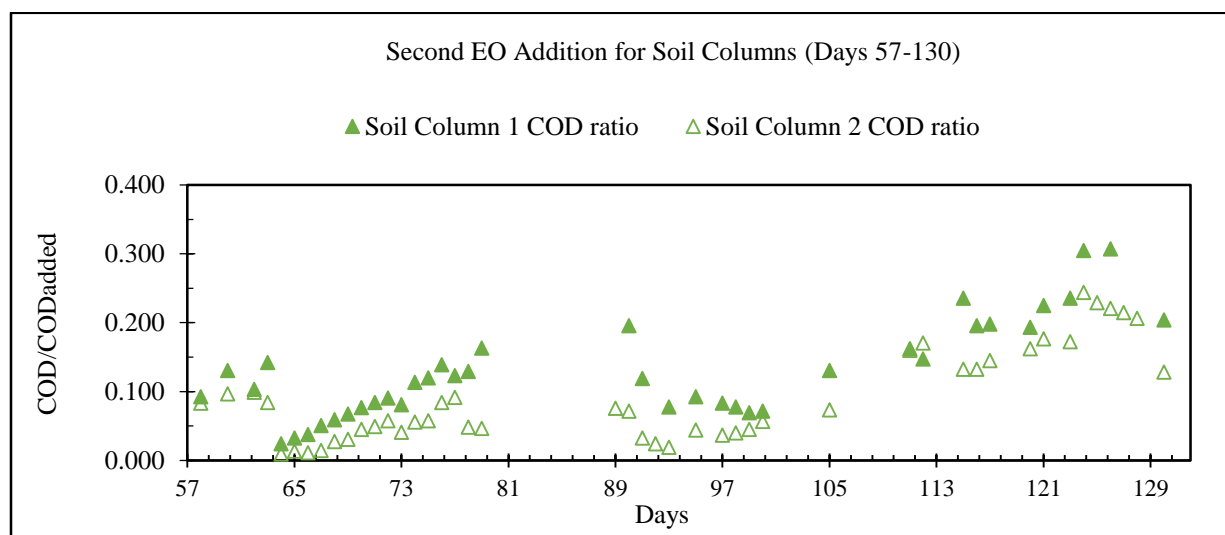


Figure 4.8: Ratio of effluent COD measured (mg) to mass of COD in the feed water.

4.3.3 Biodegradation of Nitrate and Perchlorate in Soil Column Bioreactors

The soil column bioreactor data were analyzed for the entire period of 130 days, and classifying the data into first and second oil injection period. After the second addition of EO in the soil, nitrate concentration was increased to 27 to 30 mg/L on day 92. So, data for the second EO addition was analyzed further as low and high nitrate concentrations. Tables 4.3 list the percent removals of nitrate and perchlorate during the study period.

Table 4.3: Percent Removals of Nitrate and Perchlorate in Soil Columns During Different Operation Periods

Operation Period		Nitrate Removal (%)		Perchlorate Removal (%)		p
		Soil 1	Soil 2	Soil 1	Soil 2	
Day 1 to 130	(Entire study period)	89 \pm 3.3	91 \pm 3.6	87 \pm 26	75 \pm 40	
Day 1 to 56	(First EO Addition)	91.10 \pm 4	93.3 \pm 4	71.1 \pm 39	7.7 \pm 8	< 0.05
Day 57 to 130	(Second addition of EO)	87.1 \pm 11	95.1 \pm 3	100	98 \pm 8	
Day 57 to 93	(Low Nitrate)	91.1 \pm 4	97.1 \pm 2	100	98 \pm 8	< 0.05
Day 94 to 130	(High Nitrate)	84.7 \pm 17	92.8 \pm 13	96 \pm 12	99.7 \pm 1	

The nitrate removal over the entire operation period indicated that average nitrate removal was approximately 90% and perchlorate removal varied from 75% to 87% in the soil columns.

The effluent concentration of nitrate (Figure 4.6 a) indicated that the nitrate removal was observed immediately in both columns suggest (i) the columns were under anaerobic condition, and (ii) indigenous PRB were present in the soil and groundwater to reduce nitrate in presence of the EO as an electron donor and carbon source. However, perchlorate concentration (Figure 4.6 b) did not reduce for two weeks in soil column bioreactor 1 and a month in soil column bioreactor 2, probably due to preferential electron acceptor use by bacteria (as proven by the preliminary microcosm test result in which the nitrate degraded immediately within two days, but the perchlorate removal was observed only when nitrate concentration reduced below 0.5 mg-N/L (Figure 4.4). The delay in the perchlorate reduction might also be because of the acclimation time required for the perchlorate to have sufficient biomass capable to reduce perchlorate. The limited perchlorate removal in soil bioreactor 2 might be due to the higher hydraulic conductivity in the bioreactor that reduced the residence time for reduction or due to faster decline of electron donor as indicated by effluent COD concentrations (Section 4.3.2). The rapid decrease in the perchlorate effluent concentrations after second EO addition probably supports the latter reasoning. These results point to the fact that nitrate is preferentially reduced

and that longer retention time period is needed to degrade perchlorate. Figure 4.9 a, and Figure 4.9 b shows the mass removals for nitrate. The mass removals show that the soil column 2 removed about 40 mg-N/d nitrate whereas soil column 1 removed only about 20 mg-N/d during the first EO addition. Figure 4.10 a, and Figure 4.10 b for mass removals of perchlorate for the first EO addition and second EO addition respectively.

Denitrification is dependent on hydraulic residence time of a reactor, so the removal efficiency was expected to be high in the bioreactor 1. Willems et al. (1997) showed that denitrification of groundwater containing 14 to 36 mg-N/L in wetlands system reduced when the hydraulic conductivity was increased by nine-fold. In case of in-situ bioremediation using sub-surface wood chips as electron donor, King et al. (2012) cited that the groundwater flowrate had inverse relation with nitrate removals. However, the soil column bioreactor 1 has low removal than soil column bioreactor 2, despite of a high residence time in the bioreactor 1. The reason of low nitrate reduction in soil column 1 was not understood.

After second EO addition, the nitrate removals in both columns were impacted. It might be because of excessive growth of oil fermenting bacteria that hindered growth of nitrate reducers. The microbial composition of soil 1 showed presence of bacteria belonging to *Clostridiales* order – which are known as fermenters of long chained hydrocarbon (Omoregie et al., 2013) – were at a higher percent (19%) than in other columns. Further, the higher COD concentrations in the effluent might also suggest more fermentation in the column. Increasing the nitrate concentration improved the removals in bioreactor 2, but could not meet the removals as before.

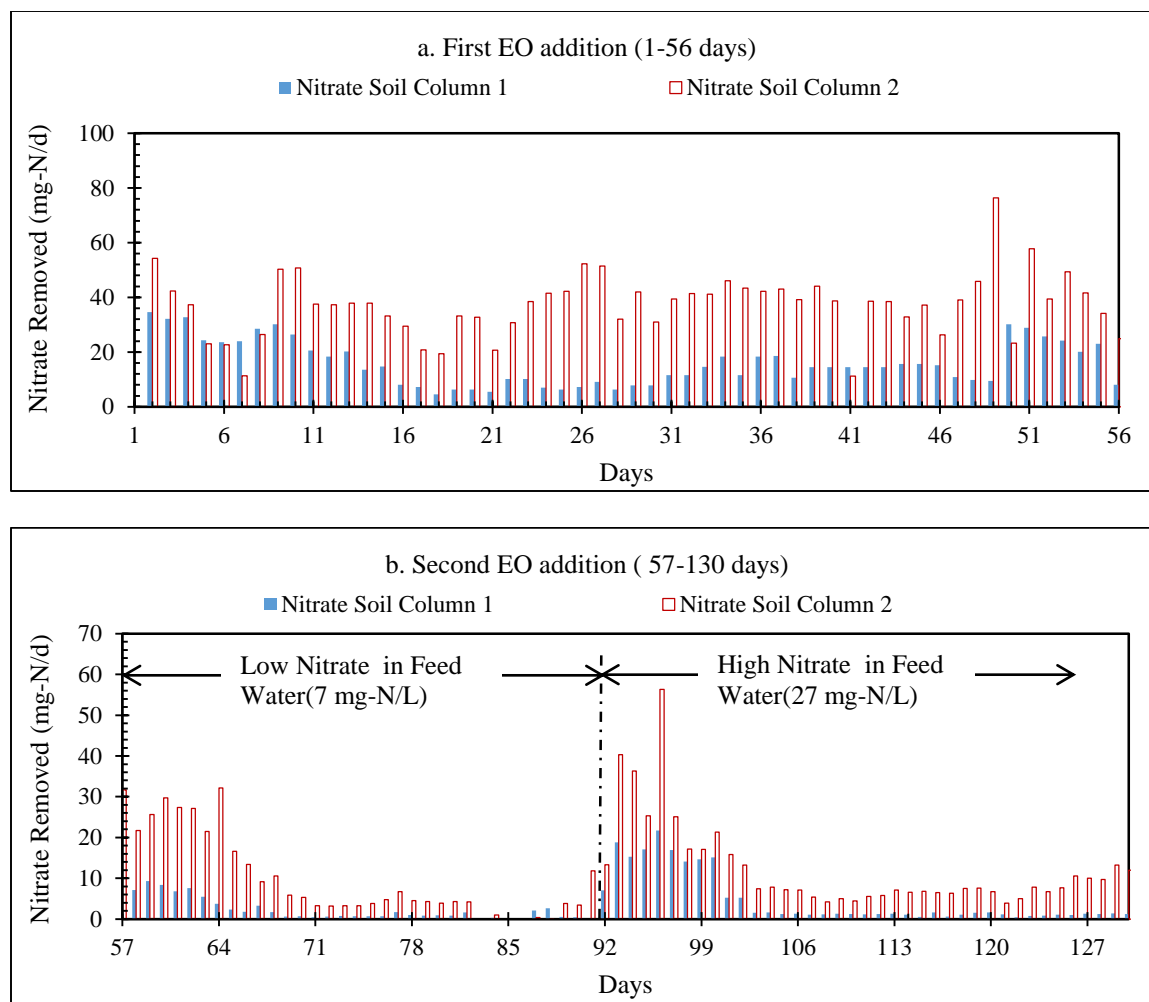


Figure 4.9: Nitrate removals as mg-N/d in soil columns for the first EO addition (a) and second EO addition (b).

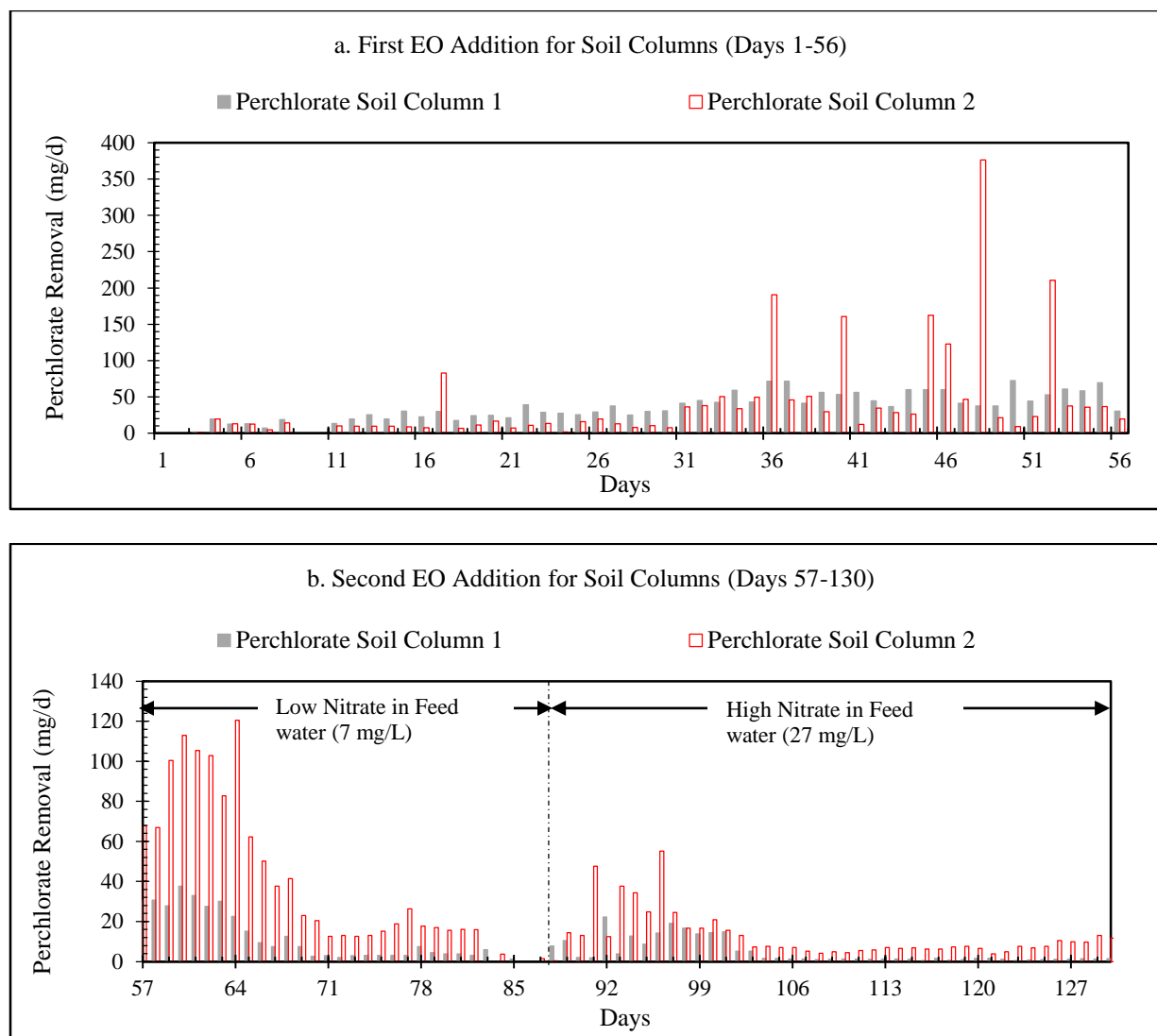


Figure 4.10: Perchlorate removals as mg/d in soil columns for the first EO addition (a) and second EO addition (b).

4.3.4 Biodegradation of Nitrate and Perchlorate in Plastic Column Bioreactors

The groundwater with EO (4 grams per 5 gallons) was recirculated for three weeks to allow indigenous microbes to grow on the plastic media. Once the perchlorate degradation was observed, the column bioreactors were switched to continuous flow at a rate of 6 mL/minute, which simulated the aquifers with a high hydraulic conductivity value (1.16×10^{-4} m/second). The hydraulic residence time at the flowrate was 0.4 day or 9.6 hours. The flowrate was reduced

to 3 mL/minute (i.e. 5.8×10^{-5} m/second), which corresponds to the hydraulic residence time of 0.81 day or 19.5 hours, to improve the perchlorate biodegradation in the plastic column bioreactors. Tables 4.3 list the percent removals of nitrate and perchlorate during the study period.

Table 4.4: Percent Removals of Nitrate and Perchlorate in Plastic Columns During Different Operation Periods

Operation Period		Nitrate Removal (%)		Perchlorate Removal (%)		p
Sampling Dates		Plastic 1	Plastic 2	Plastic 1	Plastic 2	
24 to 130 days Entire period (excluding recirculation)		93.2 \pm 15	93.6 \pm 14	68.9 \pm 33	67.6 \pm 36	
Day 24 to 41	High Flow (i.e. Residence time of 0.4 day)	94.8 \pm 2	95.1 \pm 2	51.4 \pm 30	41.7 \pm 36	<0.05
Day 42 to 130	Low Flow (i.e. Residence time of 0.81 day)	97.7 \pm 3	97.8 \pm 2	86.8 \pm 23	90.7 \pm 19	
Day 42 to 91	Low Nitrate	97.7 \pm 3	97.8 \pm 2	86.8 \pm 23	90.7 \pm 19	<0.05
Day 92 to 112	High Nitrate	77.7 \pm 28	79.4 \pm 26	20.8 \pm 27	19.3 \pm 26	
Day 113 to 130	(Doubled EO)	98.2 \pm 1	98.0 \pm 2	68.1 \pm 25	58.0 \pm 28	<0.05

The average nitrate and perchlorate removals were approximately 93% and 68% in both columns, respectively (Table 4.4). Table 4.4 suggests that change in flowrate did not improve much nitrate removal, but perchlorate percent removal was increased to about 90% in both bioreactors. The effluent nitrate and perchlorate in the plastic columns over the entire study period (excluding recirculation period) are presented in Figure 4.11 (a) and Figure 4.11 (b), respectively.

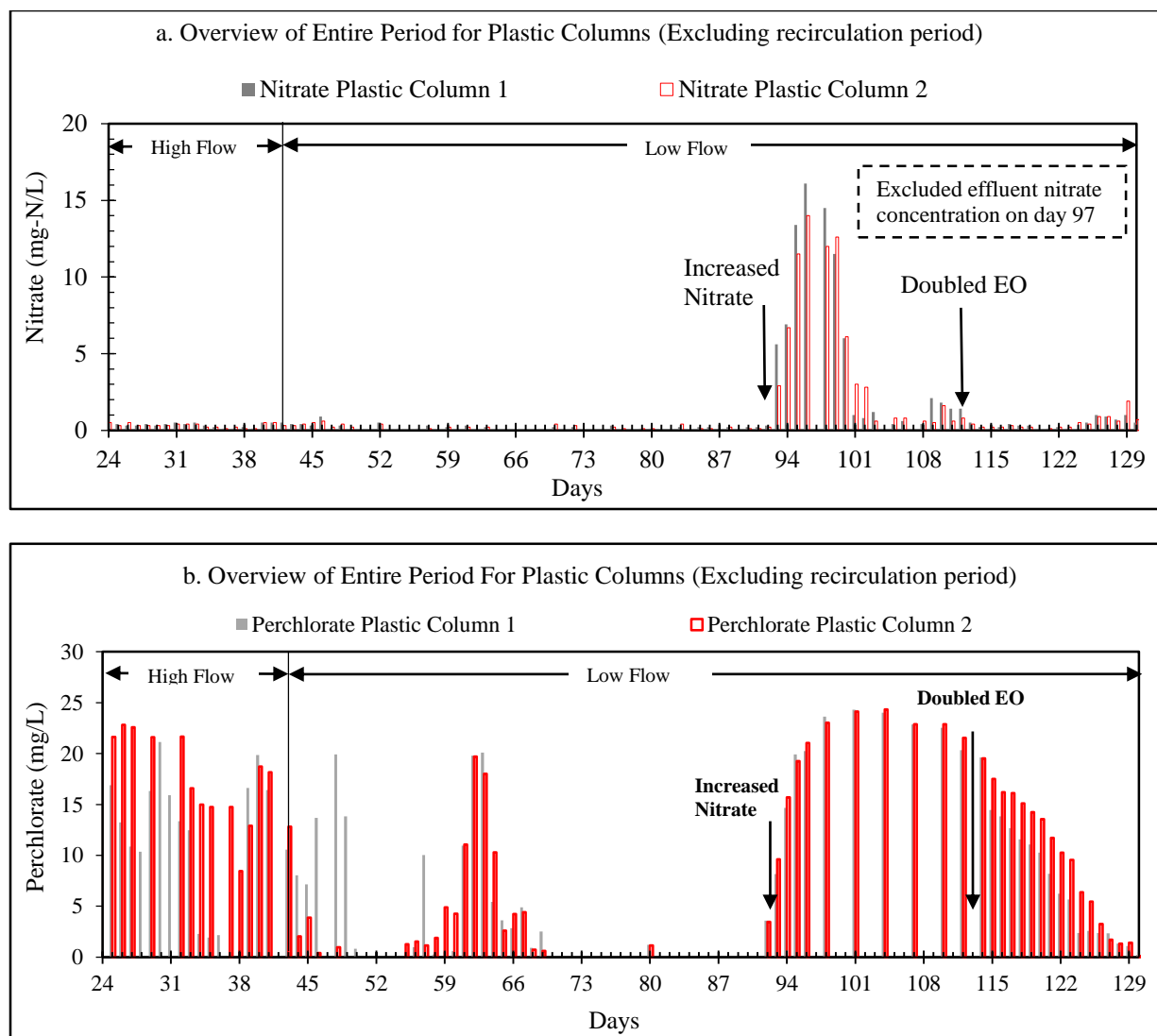


Figure 4.11: Effluent nitrate concentration (a) and perchlorate concentration (b) in the plastic column bioreactors. The feed groundwater consists of about 7 mg-N/L nitrate and 24 mg/L perchlorate. Arrows indicate days when nitrate solution was added to achieve influent nitrate concentration of 27 mg/L, and EO was doubled in the feed.

Figure 4.11 (a) shows that the nitrate was removed immediately below 1 mg-N/L with an overall removal of 93% (Table 4.4). Despite of almost three weeks of recirculation, perchlorate degradation, however, was observed only in one of the reactors (bioreactor 1) immediately. Bioreactor 2 required ten more days before the perchlorate degradation was observed. Increasing nitrate concentration in the feed impacted degradation of nitrate as well as perchlorate.

4.3.4.1 Effect of flowrate (residence time) on perchlorate and nitrate degradation

The hydraulic residence time (HRT) at high flowrate (6 mL/minute) was 0.4 day and during low flowrate (3 mL/minute) was 0.81 day. The nitrate percent removal during high flowrate was approximately 95% in both plastic column bioreactors whereas the perchlorate removal was 51% in plastic column 1 and 41% in column bioreactor 2.

The mass of average nitrate entering the bioreactors were 60 and 30 mg-N/L at residence time of 0.4 day and 0.81 day, respectively. Similarly, mass of perchlorate entering the bioreactor were approximately 207 mg/L and 103 mg/L at residence time of 0.4 day and 0.81 day, respectively. The mass nitrogen removed during low residence time is almost double the mass removed during high residence period. Therefore, it was not clear whether the improved removal was due to reduced nitrate loadings or due to the increased residence time. Even though, the mass perchlorate removal improved with increasing residence time and remained consistent throughout the remaining study period. However, it was not clear that the improvement was due to the reduced loading or the increased residence time. Figures 4.12 a and 4.12 b show the mass nitrate and perchlorate removal in the plastic column bioreactors during days 24 to 91.

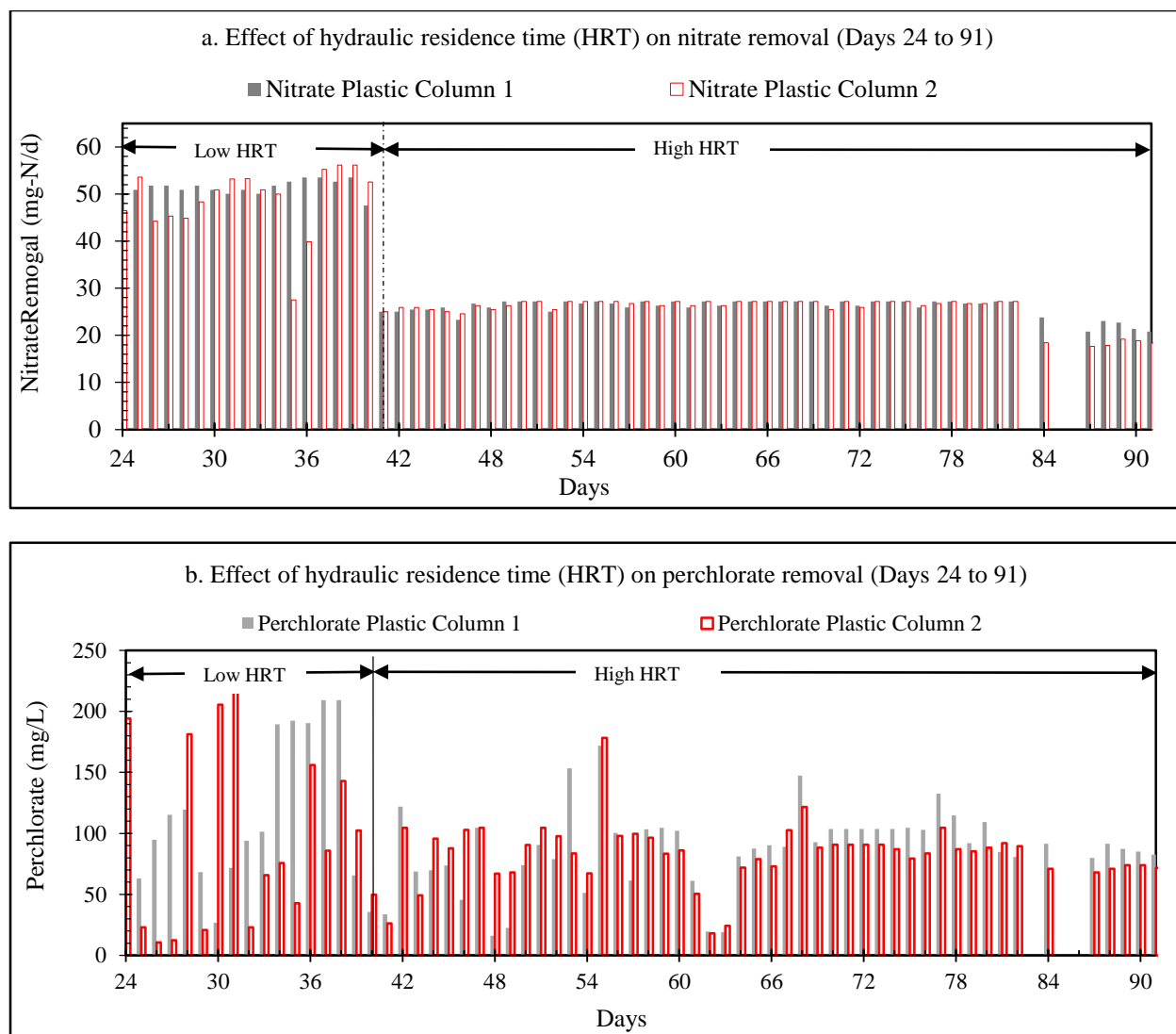


Figure 4.12: Mass removals of nitrate (a) and perchlorate (b) in the plastic columns 1 and 2 during operation days 24 to 91.

4.3.4.2 Effect of nitrate on perchlorate degradation

Increasing nitrate concentration in the feed water decreased the percent removal of nitrate and perchlorate significantly (Table 4.4). Figure 4.13 a, and Figure 4.13 b show the mass nitrate and perchlorate removal in plastic columns during days 42 to 130, respectively. The increase in nitrate concentration in the feed water increased the mass entering the bioreactors. The nitrate removal was reduced by 20% after adding the nitrate. The nitrate removal slowly improved after

a week, and the doubling of EO did not impart much improvement (Figure 4.13 a). The effluent concentrations for the bioreactors (Figure 4.11) a shows that the effluent nitrate concentration was below 1 mg/L without doubling the EO. The duration (one week) when the nitrate removal decreases is likely the time required for acclimation of bacteria to high nitrate condition.

In contrast to the soil columns, where perchlorate degradation was observed despite of nitrate in the effluent, perchlorate degradation in plastic columns reduced to approximately 20% in presence of higher nitrate concentration in the feed water (Table 4.4). However, it is important to keep in mind that the plastic columns are operated at higher flowrates than the soil bioreactors. The percent removal of perchlorate in the plastic columns improved after doubling the EO in feed water (Table 4.4). Figure 4.13 b also shows that for perchlorate degradation improved after doubling EO. This might indicate that once the perchlorate biodegradation begins, sudden increase in co-contaminant concentration will not affect perchlorate removal as long as sufficient electron donor is available.

The decline of perchlorate removal after addition of nitrate shows a negative impact of nitrate on perchlorate degradation. Similar result was observed by Chaudhuri et al. (2002); nitrate competitively inhibited perchlorate reduction and perchlorate reduction started only after complete reduction of nitrate. The concentrations of both perchlorate and nitrate used by Chaudhuri were 310 mg/L which is at least ten-fold higher concentrations of the contaminants than used in this column bioreactor study. Interestingly, Herman and Frankenberger (1998) observed simultaneous nitrate and perchlorate reduction in solutions containing 120 mg/L of each. At high concentrations of nitrate (62 mg/L) and low concentration (0.08 mg/L) of perchlorate), they found that perchlorate reduction by strain perlace required more than 48 hours to reduce perchlorate in presence of nitrate compared to 36 hours when nitrate was not present.

Studies by Attaway and Smith (1993), Bardiya and Bae (2004) and Xiao et al. (2010) observed no effect on perchlorate reduction in presence of nitrate under anaerobic conditions by a culture enriched in perchlorate solution. The concentrations of perchlorate used in those studies were twice the amount used in the column bioreactors and the nitrate concentrations were more than 50 times the concentration used in this study. Therefore, the relative amounts of perchlorate and nitrate present in the contaminated water will have impacts on the degradation kinetics.

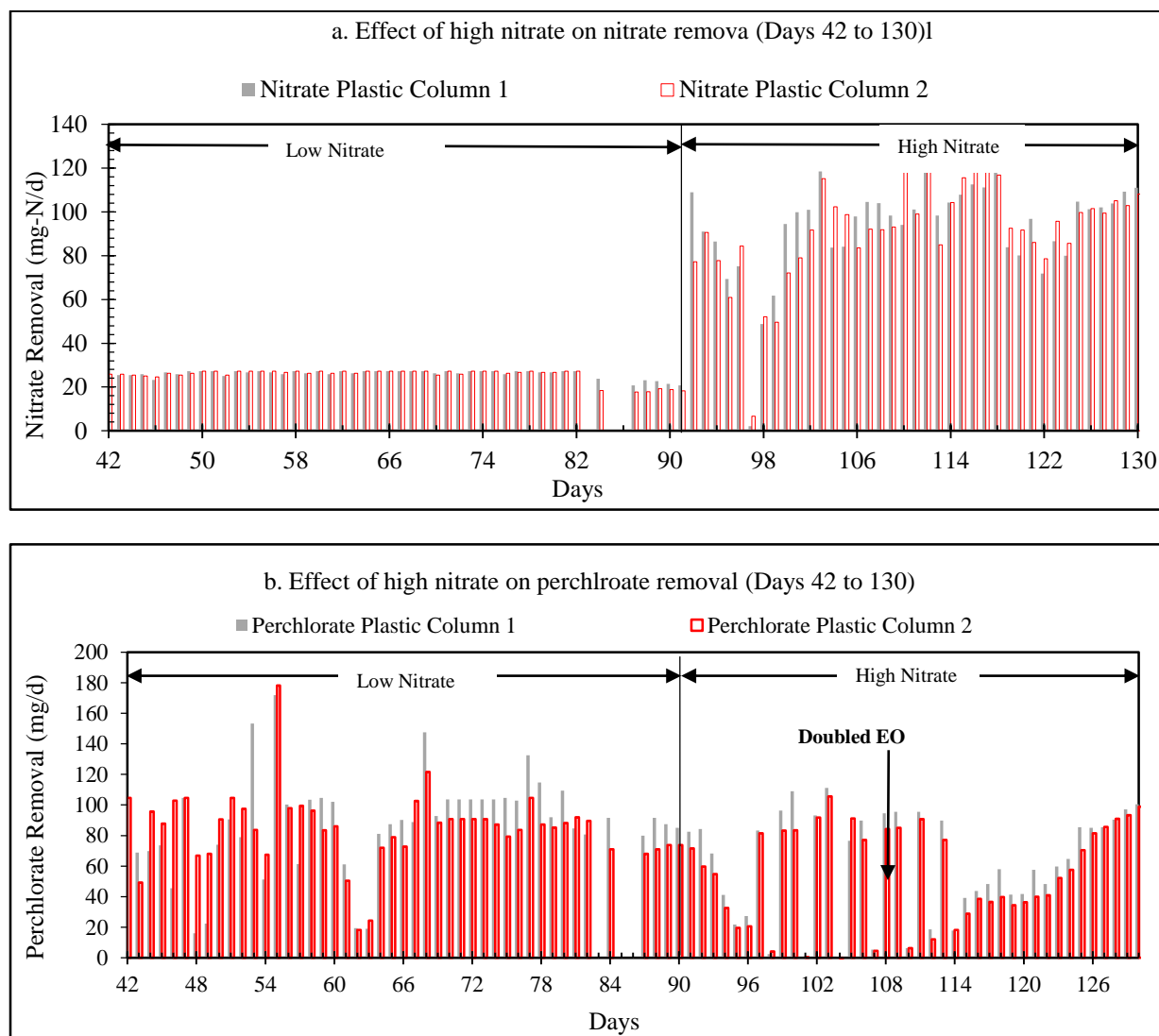


Figure 4.13: Effluent nitrate concentration (a) and perchlorate concentration (b) in the plastic columns 1 and 2 during days 42 to 130 (addition of nitrate period).

4.4 Conclusions

This research explored the use of a slow releasing electron donor, emulsified oil, to serve as electron donor for in-situ bioremediation of high concentrations of perchlorate and nitrate. Both retention time in the column and the presence of sufficient electron donor were found to be the key for sustaining the degradation of both, nitrate and perchlorate. The following can be concluded from the data obtained in this research.

- 1) EO was proven to be an effective electron donor to degrade nitrate and perchlorate under the investigated conditions. Perchlorate degradation in this research required more than 10 days to in soil columns and three weeks in plastic column bioreactors. While both soil and groundwater from the site contained perchlorate reducing bacteria, in the plastic column bioreactor, the source of bacteria was the groundwater only. The oil was mixed directly to the soil to represent the first oil injection and the second addition was by mixing the same amount of oil to five gallons of water. It is not clear how much EO desorbed and remained in the soil after the first injection.
- 2) A negative impact of nitrate on perchlorate degradation was clearly observed in this study. In the presence of nitrate, perchlorate removal in the EO microcosms was only 18%, but when the nitrate concentration reduced below 0.5 mg-N/L, perchlorate reduction increased up to 80% was observed. Similar result was observed in column bioreactors. Perchlorate reduction was observed after an acclimatization period of 30 days. After the acclimation period, perchlorate removal recovered back to 98% within 5 days after increasing nitrate concentration in the groundwater by four folds. Despite of incomplete removal of nitrate in the column bioreactors, perchlorate reduction was observed after the acclimation period. This result may suggest that in terms of full-scale application, an acclimation

period is need to develop sufficient biomass that promote the degradation of perchlorate and the other co-contaminants.

- 3) The EO desorption values, measured as COD, and suggested that EO attached to the soil leached out in the effluent over a period of 30 days. After a month, when the COD levels reduced to 30 mg/L, the nitrate removal ceased. After addition of EO to the soil columns for the second time, nitrate as well as perchlorate removal was observed immediately. Although it was observed that the EO was reduced in the effluent with time, this research did not investigate if residual EO remains in the soil that is not desorbed for use by bacteria. This is also an area where research is still lacking.
- 4) The results of this study indicated that perchlorate removal was observed only when the hydraulic residence time was increased twice the initial design. However, mass removal comparison suggested that the improvement in the perchlorate removal might be because of reduced perchlorate mass entering the system. Therefore, it might suggest that at sites with high hydraulic conductivity and containing high nitrate concentrations, perchlorate removal might not occur due to insufficient hydraulic residence time.
- 5) EO has the potential to reduce the flow rate in the soil column bioreactor with low hydraulic conductivities. Such tendency may be detrimental to the bioremediation at low hydraulic conductivity areas. On the other hand, areas of high hydraulic conductivities may benefit from a slowdown in flowrates. Coulibaly and Borden (2004) observed permeability loss by 66% after injection of oil and concluded that the permeability loss increased with increase in clay content in the media and with the ratio of oil-emulsion droplet size to pore size. Borden (2007) observed 77% reduction in permeability due to oil after injection in the ground. However, in large scale implementation, the groundwater

flow velocity was reduced by 31% and did not result in bypassing the permeable bio-barrier (Borden, 2007).

CHAPTER 5

EVALUATION OF IMAGE PROCESSING AS A TOOL TO FORECAST BACKWASHING FREQUENCY IN FLUIDIZED BED REACTORS TREATING PERCHLORATE CONTAMINATED WATER

5.1 Introduction

The high concentrations (i.e. parts per million levels) of perchlorate are found in the groundwater where perchlorate were manufactured, and low level concentrations is observed in places where perchlorate is used for various purposes. The use of perchlorate in various applications has also resulted in low level contamination (i.e. parts per billion level) (Frankenberger and Herman, 2000). In 2005, the US Environmental Protection Agency (EPA) detected perchlorate in drinking water samples obtained from 26 different states, with levels from 4 to 420 ug/L (Yu et al., 2006). The majority of perchlorate contamination is due to production and use of perchlorate salts, but naturally formed perchlorate measuring above 20 ug/L was reported in groundwater in southern high plains of Texas (Dasgupta et al., 2005). It is widely accepted that perchlorate competitively prevents iodide uptake in thyroid gland and reduces thyroid hormone production (Blount et al., 2006). Therefore, the presence of perchlorate in drinking water has posed concerns on human health due to its exposure from drinking water (Ginsberg et al., 2007). Several states, such as California and Massachusetts, have regulated perchlorate levels in drinking water, but no federal standard for perchlorate exists (Sellers, 2007). EPA has listed perchlorate as a drinking water contaminant and recently included it in the Unregulated Contaminant Monitoring Rule.

Biological reduction and Ion-exchange (IX) are the most commonly used technologies for perchlorate removal from water. In biological reduction, bacteria use perchlorate as an electron

acceptor in the presence of an electron donor, and reduce perchlorate to innocuous chloride (Cl^-) (Kijung and Logan, 2000). IX is generally adopted for treating drinking water with perchlorate concentration at ppb level because of simplicity of implementation and operation. In the presence of high concentration of perchlorate and other co-contaminants, the exchange capacity of perchlorate in the resins reduces substantially (Ricardo et al., 2012).

While IX is preferred in drinking water treatment with ppb levels perchlorate concentration, biological reduction is more preferred for treating contaminated waters with parts-per-million (ppm) level of perchlorate that are not intended for drinking. The kinetics of perchlorate reduction favors high concentrations of perchlorate. Biological reduction of parts-per-billion (ppb) level perchlorate concentrations is very slow. At the old industrial site, Basic Management Industrial (BMI) in Henderson, biological reduction is currently used to treat ppm level perchlorate using eight fluidized bed reactors (FBRs), with granular activated carbon as media. The FBRs are operated at 1000 gallons per minute and are supplied with 300 gallons of ethanol per day as the electron donor to support the degradation of perchlorate and its co-contaminants (Hatzinger, 2010). In recent years, the State of California has approved conditional use of biological treatment for perchlorate removal from drinking water (WVWD, 2012). A large FBR treatment plant is now under construction in Rialto, CA for biological perchlorate removal from drinking water (Envirogen, 2011). Given the slow kinetics associated with the biological reduction of low level perchlorate, the reactors being designed are expected to be large.

Based on the microbial kinetics for perchlorate reduction, fixed film reactors are preferred over suspended growth for drinking water contaminated with ppb level of perchlorate because of a large value of half-saturation constant for perchlorate (K_s), the concentration at which perchlorate reduction proceeds at half its maximum rate (Urbansky, 2000). The reported K_s

values for perchlorate reduction are 9-14 mg/L for heterotrophic reduction (Logan et al., 2001; Urbansky, 2000) and 6-149 mg/L for autotrophic reduction (Miller and Logan, 2000; Ricardo et al., 2012). Therefore fluidized bed and other fixed film reactors have been investigated for biological perchlorate removal (Webster et al., 2008; Choi et al., 2007; Nerenberg et al., 2002).

In FBR, the water is pumped upwards so that the media expands (hydraulic expansion) and remains in suspension. The hydraulic expansion (typically 25 to 30% of original depth of media) increases the surface area available for microbial growth by 15 to 20% (Webster et al., 2009). FBRs maintain a high biomass density – which reduces the hydraulic retention time needed for complete perchlorate reduction (Min et al., 2004) – even when the influent rate is very high (Hatzinger, 2005).

In FBRs, bacteria – which grow on the media as a thick film – reduce perchlorate to chloride. The growth of the bacteria increases the buoyancy of the media resulting in the media expansion and loss to the effluent (Figure 5.1). The media loss can be prevented by adequate backwashing, which is a common method of cleaning the media. Excessive backwashing decreases efficiency of a bioreactor and changes the dominant microbial community in a reactor (Choi et al., 2007; Li et al., 2011). Delay in backwashing may result in undesirable media loss, as mentioned earlier.

A biofilm model developed by McCarty and Meyer (2005) indicated that biofilm thickness governs the mass transfer limitations for electron donor and acceptor in perchlorate degradation. Currently, the timing and frequency of backwashing are determined by visual inspection and experience of an operator (Li et al., 2012). A systematic approach to determine the time for FBR backwashing used for perchlorate treatment, which accounts the interaction between the biomass and the media assuring FBR performance, is needed.

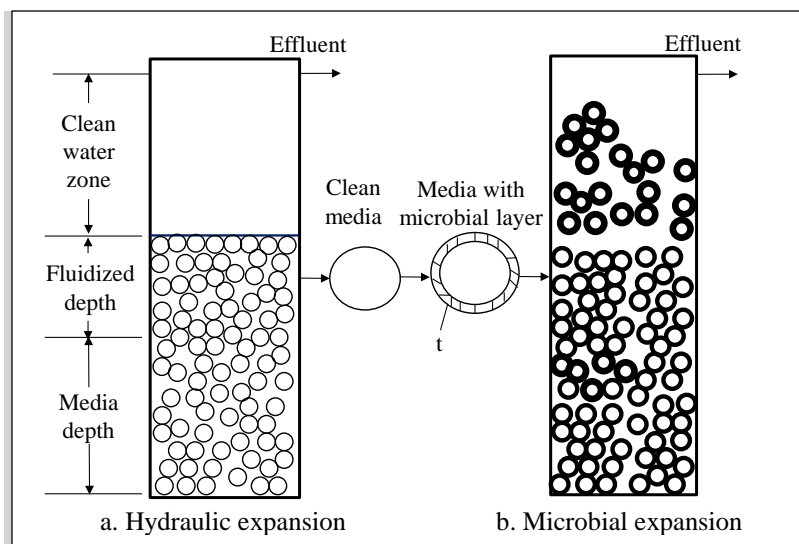


Figure 5.1: Hydraulic and microbial expansion of media in ex-situ bioremediation using a FBR (Modified from Webster et al., 2009).

This research explores the potential use of digital images and imaging processing as a tool to forecast appropriate backwashing time for FBRs treating perchlorate contaminated water. An additional goal is to couple the image processing tool with a biofilm model to determine the suitability of image processing as an operation tool for FBRs treating perchlorate.

5.2 Methodology

To test the suitability of image processing as a tool to forecast backwashing frequency in FBRs, two laboratory-scale FBRs were constructed (Figure 5.2). The FBRs were operated for more than 80 days to remove perchlorate from water contaminated with ppm and ppb level perchlorate. The zone above the hydraulic bed expansion was targeted with a high resolution digital camera mounted on the side of the columns as show in Figure 5.2

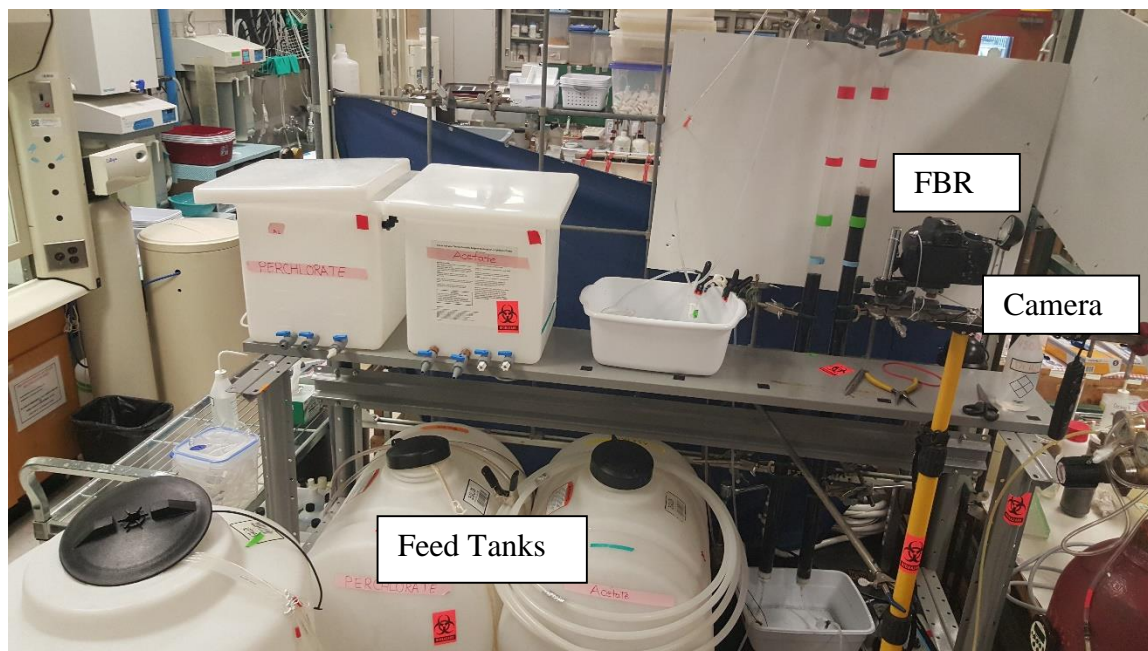


Figure 5.2: Experimental set up for operating two FBRs with camera mounted to take pictures.

5.2.1 Enrichment of Perchlorate-Reducing Culture

The perchlorate-reducing culture used to seed the FBRs was developed from the returned activated sludge obtained from the Clark County Water Reclamation District, Las Vegas, Nevada. The culture was enriched with acetate (carbon source/electron donor) and perchlorate (nutrient, buffer, and electron acceptor) under anaerobic condition in a two-liter serum bottle (Figure 5.3). The entire culture was stirred using a magnetic stirrer to ensure the bacteria remained in suspension. The enrichment media used for the culture was modified from the composition devised by van Ginkel et al. (1995) (Liu, 2000; Gingras, 2003). In this study, the adopted molar ratio of electron donor to acceptor was 3:1.

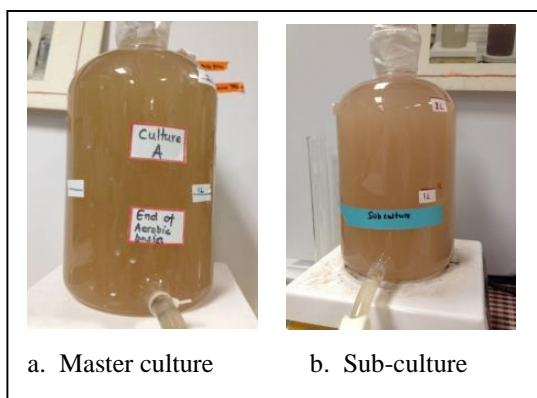


Figure 5.3: Perchlorate-reducing culture (master culture) enriched from returned activated sludge (a) and Sub-culture enriched from the master culture (b).

In the beginning, perchlorate and acetate were added into the culture without wasting. After ten days, the culture turned reddish and perchlorate concentration started to decline. Then, the culture was fed at a waste-feed mode (wasting 200 mL culture and adding enrichment media and DI water purged with nitrogen every alternate day). The culture reduced 1000 mg/L of perchlorate up to 97% within a week. Appendix B shows the amounts of buffer, nutrient, acetate, and perchlorate added to the activated sludge to start up and sustain the culture.

After three months of feeding, the percent perchlorate degradation and the optical density of the culture started to decline. It is believed this decline was caused by toxicity of chloride accumulated as a result of perchlorate degradation. It is known that salt concentrations as low as 0.5% can negatively impact perchlorate degradation (Gingras and Batista, 2001). Therefore, 500 mL of the culture was wasted every two weeks. The wasted 500 mL of culture was used to start up a sub-culture, which was fed in the same pattern as the master culture. As compared to the master culture, the sub-culture was easy to maintain; so all the experiments were conducted using the sub-culture (Figure 5.3 b). Sub-culture is termed as “culture” hereafter.

5.2.2 Identification of Perchlorate-Reducing Bacteria

The culture was analyzed to identify the perchlorate-reducing bacteria (PRB) present. DNA was extracted and cleaned using the Mo Bio Ultra Clean Soil DNA Extraction Kit, following instructions provided by the manufacturer. The purity and concentration of the extracted DNA were quantified using a NanoDrop 1000. Electrophoresis gel was run for a part of the extracted DNA with *Dechloromonas agitata* as positive controls, while *Pseudomonas aeruginosa* (PA) and water as negative controls. The remaining extracted DNA was shipped to a commercial laboratory (Research and Testing Laboratory, Lubbock, Texas) for identification of the bacterial community in the culture. The laboratory performed DNA amplification and sequencing using the universal 16S rRNA primer, 8F [59-AGAGTTTGATCCTGGCTCAG-39] and 1525R [59-AAGGAGGTGATCCAGCC-39]), and identified the bacteria up to the species level. The sequences obtained from the laboratory were used to prepare a phylogenetic tree using a multiple sequence alignment program, Mafft, (Mafft, 2015). The molecular tools used in this test is summarized in Figure 5.4.

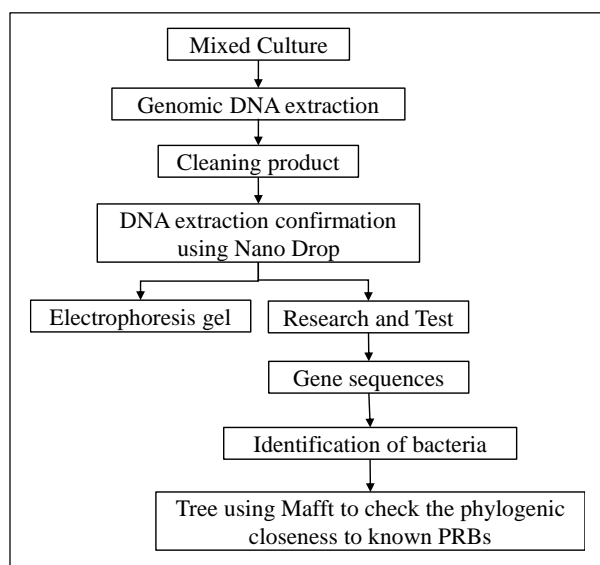


Figure 5.4: Flowchart of molecular tools to identify the bacteria present in the enriched culture and check the phylogenetic closeness to the known PRB (KJ).

5.2.3 Comparison of High and Low Concentration Kinetics of Culture

For comparison between high and low concentration kinetics, 100 µg/L and 100 mg/L perchlorate concentrations were selected. For each perchlorate concentration, nine 25 mL-bioreactors and a duplicate for each were prepared. The bioreactors were filled with the enrichment solution (acetate, perchlorate, buffer and nutrient), DI water, and washed culture. The enrichment media and DI water were purged using nitrogen gas for approximately two hours. The culture was washed to prevent possible contribution of perchlorate and acetate from the culture. At first, the culture was centrifuged for 10 minutes at 3500 rpm (Legend RT Sorvall centrifuge, Kendro, Thermo Fisher Scientific, Inc., Waltham, MA), and the supernatant was discarded carefully. DI water with buffer was added in to the settled culture to replenish the initial volume, vortexed for 10 to 20 seconds, and centrifuged for 10 minutes. Again, the supernatant was discarded. This process was repeated twice so that the culture did not contribute additional perchlorate and acetate to the bioreactors. DI water was added to the washed culture to achieve a suspended solid concentration of 1000 mg/L. The total suspended solid (TSS) determination was based on correlation between TSS and the optical density (OD) for the culture (Appendix C). The bioreactors were sealed using butyl rubber stopper crimped with aluminum caps (Wheaton Industries, Inc., Millville, NJ) to maintain anaerobic condition and stirred at 300 rpm on an Orbital Shaker (Cole Parmer, Series 51704) to keep the bacteria in suspension. In each sampling period, a bioreactor and its duplicate were sacrificed and analyzed for perchlorate, total organic carbon (TOC), and bacterial growth.

5.2.4 Biofilm Thickness Measurement Using Biomass

A preliminary trial to measure biofilm thickness using a phase contrast microscopy was not successful. A 125 mL anaerobic bioreactor was prepared with was prepared with 20 grams of

500 μm GAC, enrichment solution (perchlorate, acetate, buffer and nutrient), DI water and washed culture. After five days, ten slides were prepared with at least three GAC from the bioreactors fixed in 1% Agarose gel to observe biofilm on the GAC under the phase contrast microscopy. Some of the GAC from the bioreactor were treated with a nucleic acid stain SYTO 10 dye, rinsed with buffer to clear up the excess dye, and fixed on to five slides with 1% Agarose gel. Other five were fixed on the slide without dying. Biofilm was transported to slides using sterile tweezers. Transferring the biofilm to the slide was a great challenge because the biofilm came off very easily. The microscopy slides with dyed GAC showed very few colonies of bacteria. The GAC without dying showed much more colonies of bacteria, but not enough to measure the biofilm thickness with the microscopy. Thus, the biofilm was estimated using biomass only.

Biomass growth evaluations were conducted in 125 mL bioreactors with 20 grams of 500 μm GAC, enrichment solution (perchlorate, acetate, buffer and nutrient), DI water and washed culture. Two bioreactors were sacrificed each day to measure the biomass growth, and one additional bioreactor (totaling to three bioreactors) was sacrificed on 5, 10, 15, 20, and 25 days. These additional bioreactors were previously planned for phase contrast microscopy. Perchlorate concentration in the bioreactors was maintained at 100 mg/L and acetate at 300 mg/L. Each day, 10 mL solution was wasted and replaced with fresh enrichment solution and DI water.

5.2.5 FBR Operation and Digital Imaging for Backwashing Forecast

Two laboratory- scale FBR were designed and operated at 25% fluidization (Figure 5.5). The reactors were built with 2.5 cm diameter and 172 cm long clear plexiglass columns with screens attached to the bottom adaptor. A sample port, 5 cm below the effluent, was drilled in the columns. The reactors were filled with clean GAC media (Calgon carbon, Brand, Pittsburgh,

PA) with nominal size greater than 500 μm mm sieve and a density (using the water displacement method) of 1419 kg/m^3 .

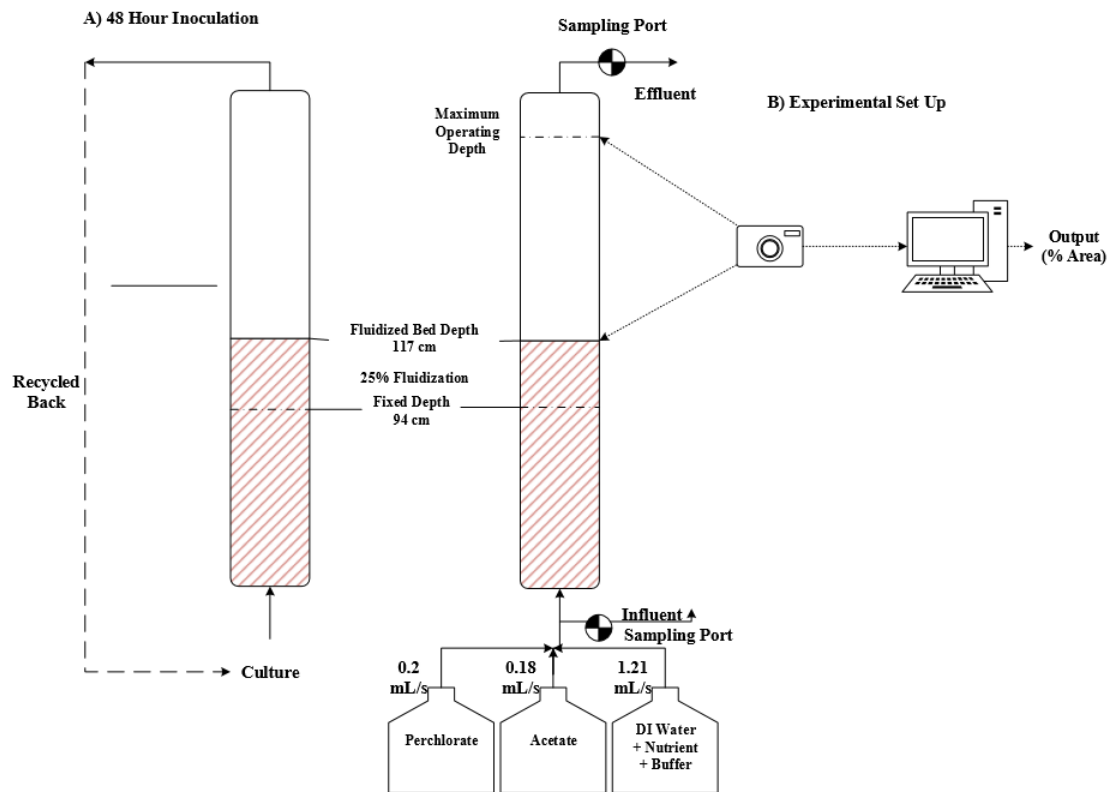


Figure 5.5: Schematic diagram of inoculation of the culture for a week (a) and operation of the reactor (Ex-situ treatment) (b).

5.2.5.1 PRB Inoculation in FBR

Two liters of mixed enrichment culture, with TSS of 2000 mg/L, was recirculated in the reactors for 48 hours to inoculate the FBRs (Choi and Silverstein, 2008; Miller and Logan, 2000; Logan and LaPoint, 2002) (Figure 5.5 a). Li et al. (2011) observed that a high flow of feed water during the inoculation of bacteria in a reactor improved the bacterial cell-media bonding. Therefore, the culture was pumped at 1.6 mL/second (Figure 5.5) to ensure the biofilm formed on the media was capable of withstanding shear due to hydraulic pressure under normal operation. The culture was previously enriched at 1000 ppm perchlorate environment.

5.2.5.2 FBRs Operation

After 48 hours of inoculation, the FBRs were operated in continuous mode to meet the design flow (1.6 mL/s) by pumping DI water with buffer and nutrient, stock perchlorate, and stock acetate simultaneously into the reactor using a peristaltic pump (Figure 5.5 b). The reactors were started up with 100 ppm concentration in the feed water.

The perchlorate concentration was maintained at 100 mg/L, 100 µg/L, and 10 mg/L for the various cycles run respectively. The concentration of the acetate was maintained three times the stoichiometric requirement for perchlorate removal. The stock concentrations of perchlorate and acetate were based on the result of hydraulic testing and capability of the available pumps. The stocks of perchlorate and acetate were prepared once every three days and added to the feed tanks after purging with nitrogen gas for 30 minutes to remove oxygen from the feed solutions. In addition, the mixture of DI water, buffer, and nutrient was added to the feed tank every day after purging with nitrogen gas. The influent and effluent were collected daily, and analyzed for the concentrations of perchlorate and TOC, which was an indirect measure to the acetate concentration added. When needed, the pumps were shut down to change the tubing in the pump heads. The columns were backwashed as the GAC exceeded the operating limit.

5.2.5.3 Image Processing as Tool for Determining Backwashing Frequency

A preliminary trial of the FBR operation with the same perchlorate-reducing culture indicated that the GAC moves as a block rather than discrete particles for 500 µm GAC. Results of the preliminary FBR is shown in Appendix E.

A camera (Canon EOS Rebel 3Ti with Canon EF 50mm f 2.5 compact macro lens) was mounted on a metal brace and pointed towards the FBR operating depth. The camera was selected in consultation with UNLV professional photographer R. Marsh Starks. The camera was

programmed to take five pictures every time. A remote control timer (Timer Remote Control, APTR1C, Aputur) was connected to the camera to take pictures every one and half hours in the beginning and 15 minutes as the GAC began to move up in the reactor. The lights in the laboratory, where the FBR were installed were left on at all times to assure high quality pictures. The pictures were transferred from the camera to a computer and processed using image-processing software, ImageJ (NIH, 2015). The camera was shut down only to change the battery.

5.2.6 Microbial Analysis

The media from FBR 1 was collected at the end of the operation with 100 mg/L perchlorate, and the media with biofilm was observed under phase contrast microscopy without any dye. In preliminary trials, a nucleic acid stain SYTO 10 dye was used, but bacteria were lost while performing the rinses after using the dye. The visual inspection, GAC with biofilm under the microscope indicated the presence of Eukaryotic microorganisms, such as amoeba, in addition to rod-shaped bacteria and thick extracellular polymeric substance (Figure 5.6). The GAC media with biofilm was also shipped to a commercial microbiology laboratory (Research and Testing Laboratories, Lubbock, Texas) for bacterial and eukaryotic community analysis. The primer selected for the bacterial community analysis was 8F [59-AGAGTTTGATCCTGGCTCAG-39] and 1525R [59-AAGGAGGTGATCCAGCC-39]), and eukaryotic community analysis was EukA7F [AACCTGGTTGATCCTGCCAGT] and EUK570R [GCTATTGGAGCTGGAATTAC] (Al-Ihani et al., 2014).

The laboratory uses Illumina next-generation sequencing technology that uses clonal amplification and sequencing by synthesis. Once the sequences are generated, the data undergo detection and removal of short, singleton, noisy and bad read sequences. The quality checked

sequences are clustered at a 4% divergence using USEARCH clustering algorithm. The sequences are identified using an in-house-maintained database of that is derived from NCBI (Research and testing laboratory, 2015). The final result obtained from the laboratory included the percentages for each organism identified up to species level.

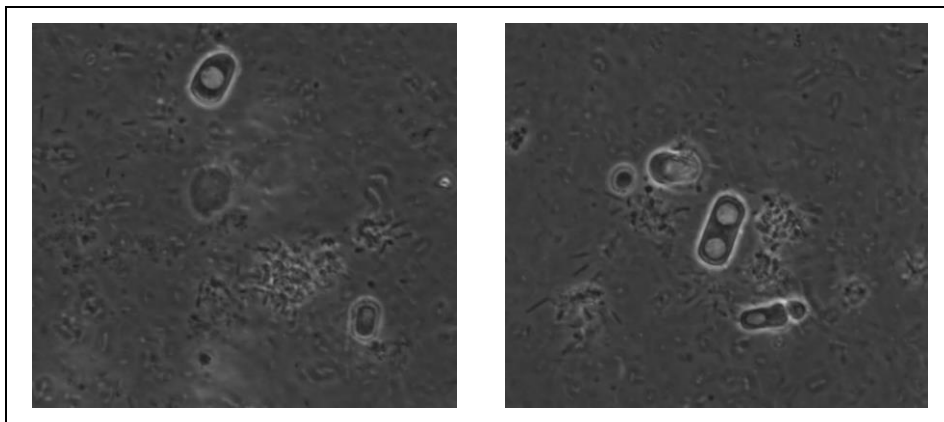


Figure 5.6: Snap shots from the phase contrast microscopy showing bacteria, extracellular polymerase, and eukaryotic organisms.

5.2.7 Analytical Methods

Analytical methods and equipment used to analyze the samples from the culture, FBR, and the columns are presented in Table 5.1. The analytical methods are discussed further in the following paragraphs.

Table 5.1: Analytical Methods and Equipment Used for Analyzing Samples

Parameter	Method	Equipment
COD	Hach 8000	Spectrophotometer DR 5000
Perchlorate	EPA 314	Dionex ICS 2000
Turbidity		2100 N Turbidimeter
Optical Density		Spectrophotometer DR 5000
DO		DO Meter

5.2.7.1 Total Suspended Solids, Turbidity, and Optical Density

Total suspended solids (TSS) was used as a measure to observe bacterial growth in the enriched culture. TSS was conducted once for the culture and was correlated with the Optical Density ($R^2 = 0.99$). Data are shown in Appendix C. Every week before feeding 20 mL sample was filtered using a Whatmann glass-fiber microfilter (GF-C). The GF-C was weighed before filtration. After filtration, the filter was, first, dried at 103-105°C for 1 hour before and was weighed. The difference in the weight of the filter before and after filtration gives the total suspended solids per 20 mL.

Optical density was measured using a Spectrophotometer (Hach DR 5000) at 600 nm, and turbidity was measured using HAC 2100 N Turbidimeter (Standard Methods 2130 B). The correlation between turbidity and TSS is also presented in Appendix C. The turbidimeter was calibrated using five formazin polymer standard factory referred solutions of <0.1, 20, 200, 1000, and 4000 NTU.

5.2.7.2 pH

pH was measured to ensure the neutral pH in the enrichment. The pH meter (Acumet –AR-10) was calibrated using a two-point calibration with pH 4 and 9 buffers.

5.2.7.3 Perchlorate Concentrations

Perchlorate and chloride concentrations were measured using a Dionex- 2000 ion chromatograph (IC) fitted with an Ion Suppressor ASRS-ULTRA (4 mm), IonPac AS16 column and guard (4 mm), and AS 40 autosampler. The IC was controlled and operated using a program interface, Chromeleon 6.0. Table 5.2 shows the standards and conditions opted for using IC for perchlorate and chloride.

Table 5.2: Standards and Conditions for IC

Compound	Standard Concentration	Column/ Guard	Current (mA)	Eluent Conc. (mM)
Sodium perchlorate (ClO ₄ ⁻)				
High(mg/L)	1, 2, 3, 4, 5, 6, 7 (1, 5, 10, 20, 50, 100)*	AS 16	100	35

* Perchlorate standard used for evaluation of master and sub-cultures.

Interferences in IC may be realized in presence of chloride, sulfate, carbonate, and high TDS (Motzer, 2000).

5.2.8 Quality Assurance/Quality Control

The goal of quality assurance/quality control (QA/QC) is to ensure the quality of the data collected and analyzed. The QA/QC plan included minimizing personal and systematic errors associated with the procedure and instrument, check detection limits of the method opted, and accuracy and precision of the experiment. The following precautions were taken to ensure quality of the research.

1. Sampling and Storage

For evaluation of the perchlorate and acetate concentrations in master and sub-cultures, 10mL of culture were wasted before collecting samples to prevent collection of settled culture at the sampling port, whereas for all the batch tests, the vials were well mixed before collecting samples. Turbidity, OD, and TSS of samples were immediately measured after sampling. The samples were filtered through 0.2 µm, kept in 10 mL glass vials, and stored in refrigerator (4°C). All vials used for sampling and storage were labeled, dated, and capped to prevent contamination. The concentrations of perchlorate and acetate were measured within 48 hours of storage. IC standards were prepared every two weeks and stored in well labeled and capped glass vials in refrigerator.

2. SS Test

Aluminum dishes used for TSS test were pre-ignited at 550°C for about an hour to avoid weight loss during the test, and were stored in desiccator to prevent moisture interference. All glass micro-fiber filter papers used in the test were also stored in desiccator prior use to prevent moisture interference.

3. Calibration

The IC, pH meter, turbidity meter, and spectrophotometer were calibrated with known standards every time before measurement. In addition, analytical balance, micropipette, and conductivity meter were calibrated every week.

- a) For perchlorate and chloride, the IC was calibrated with at least five standards.
- b) pH meter was calibrated based on two-point method with 4.1 and 10.01 pH buffer standards prior each sample measurement. If the slope was above 90%, the pH meter was considered calibrated.
- c) Turbidity meter was calibrated before every use using Formazin solutions.

Spectrophotometer was calibrated with a blank sample as required by the methodology, before measuring the samples.
- d) The analytical balance was calibrated weekly with 5 g and 50 g standard weights. Every year, the balances were also calibrated by Precise Weighing Systems (Santa Clarita, CA).
- e) Micropipettes were calibrated every week. The volume of water transferred by the micropipettes was measured on the analytical balance, if the weight of water was same as transferred volume, then the micropipette was considered calibrated.
- f) Conductivity meter was used to check DI water quality. Conductivity meter was calibrated every week as mentioned in the manual.

4. Precaution for IC

The standards for calibration were measured from low to high concentration to prevent carry over effect in IC measurement. Further, two blanks (DI water) were introduced after the standards and a blank was introduced between samples to prevent the effect.

5. Temperature of Oven

A thermometer placed on the oven was monitored every week to ensure consistent temperature at 103°C.

6. DI Water Quality

Tap water was treated with a carbon filter, Reverse Osmosis and nanofilter is termed as DI water, and is free from ionized impurities, organics, microorganisms, and particulate matter larger than 0.2 μm . The DI water was used to prepare standards. The quality of DI water was measured using a conductivity meter to ensure specific resistance below 18 Mohm-cm and monitored every week.

7. Sterilization

The vials used for collecting samples and storage were soaked in bleach and soap for 6 to 12 hours, rinsed with tap water, and triple rinsed with deionized water. The vials were air dried prior use. All glassware and glass beads, pipette tips and solutions were autoclaved to ensure no microbial contamination.

8. Safety Precautions and Waste Handling

Online trainings provided by the UNLV Environmental Health and Safety on Biosafety, Chemical Hygiene, and Personal safety were taken at the very beginning before starting experiments. Personal protection and exposure control measures were taken for handling microbial samples. Transfers of microbial samples to the agar plates and to the batch reactors

were done under the biological UV hood. The batch reactors with ethanol were prepared under the chemical hood. Lab coats and gloves were worn all the times in the laboratory.

Quality Control

Table 5.3 lists the quality controls for all the experiment, based on accuracy, precision, detection limit, and coefficient of determination (R^2) of the methodology. The accuracy of the data was determined by calibration of the instrument using the known standard solutions and obtaining R^2 value in each run, and the precision was determined by the duplicates for each sample. Detection limits for perchlorate and chloride were obtained based on the best fit of a wide range of standards.

Table 5.3: Accuracy, Precision, Detection Limit, and R^2 of the Methods Opted for Various Parameters

Parameter	Method	R^2	Precision (Confidence Limit)	Detection Limit	Calibration Range
Perchlorate	IC	0.9997	95 %	4 $\mu\text{g/L}$	1, 2, 3, 4, 5, 6, 7
Nitrate	HACH		95 %		
COD (Low and ultra-low ranges)	HACH	N/A	95 %	N/A	0-1500 ppm and 0- 40 ppm

5.3. Results

5.3.1 Characterization of Bacterial Community

5.3.1.1 PRB Enrichment Cultured at the UNLV Laboratory

The bacterial community analysis of the culture enriched at the UNLV- Environmental Engineering and Water Quality Laboratory (EWL) showed that the majority of the microbes were *Proteobacteria* (93.834%); out of which, 68.139% were *Betaproteobacteria* (Table 5.4). Table 5.4 includes only those bacteria that were hit for more than 1% of the total number of sequences. The entire results of the bacteria community analysis up to species level is presented in Appendix H 1.

Table 5.4: Bacterial Community in PRB Culture Enriched in UNLV Environmental and Water Quality Laboratory

Phylum	Class	Order	Family	Genus	Species
Proteobacteria (93.834%)	Beta- proteobacteria (68.139%)	Burkholderiales (67.447%)	Alcaligenaceae (67.356%)	Unknown (67.355%)	Unknown (67.355%)
	Gamma- proteobacteria (23.179%)	Pseudomonadales (23.020%)	Pseudomonadaceae (22.175%)	Pseudomonas (22.175%)	Pseudomonas sp. (22.175%)
Actinobacteria (4.809%)	Actinobacteria (4.809%)	Actinomycetales (4.809%)	Corynebacteriaceae (4.377%)	Corynebacterium (4.377%)	Unknown (4.377%)
Spirochaetes (1.309%)	Spirochaetia (1.309%)	Spirochaetales (1.309%)	Unknown (1.163%)	Unknown (1.163%)	Unknown (1.163%)

The majority of the bacteria within Betaproteobacteria were *Alcaligenaceae* which fall under *Burkholderiales*, but were not identified at the genus level (unknown circled in Figure 5.7). In the literature, these *Alcaligenaceae* has been associated with nitrate and uranium reduction (Spain, 2007). These unclassified bacteria at the genus level are likely the perchlorate reducers in the enrichment since perchlorate degradation was observed. Bacteria belonging to *Spirochaetales* order have been recently identified to comprise *Microcystis* biodegradation proteins (Kohler et al., 2014). These bacteria are also known for biodegradation of benzamide and roxarsone commonly used as feed additive to poultry (Falkow et al., 2006). Strains, *Pseudomonas sp.* are well studied for biodegradation of crude oil (Berekaa, 2013), nitrate reduction (Katz et al., 2000) and chlorate reduction (Xu et al., 2004). The *Pseudomonas strain, PDA*, was able to express chlorate reductase and chlorite dismutase, but was unable to respire perchlorate (Xu et al., 2004).

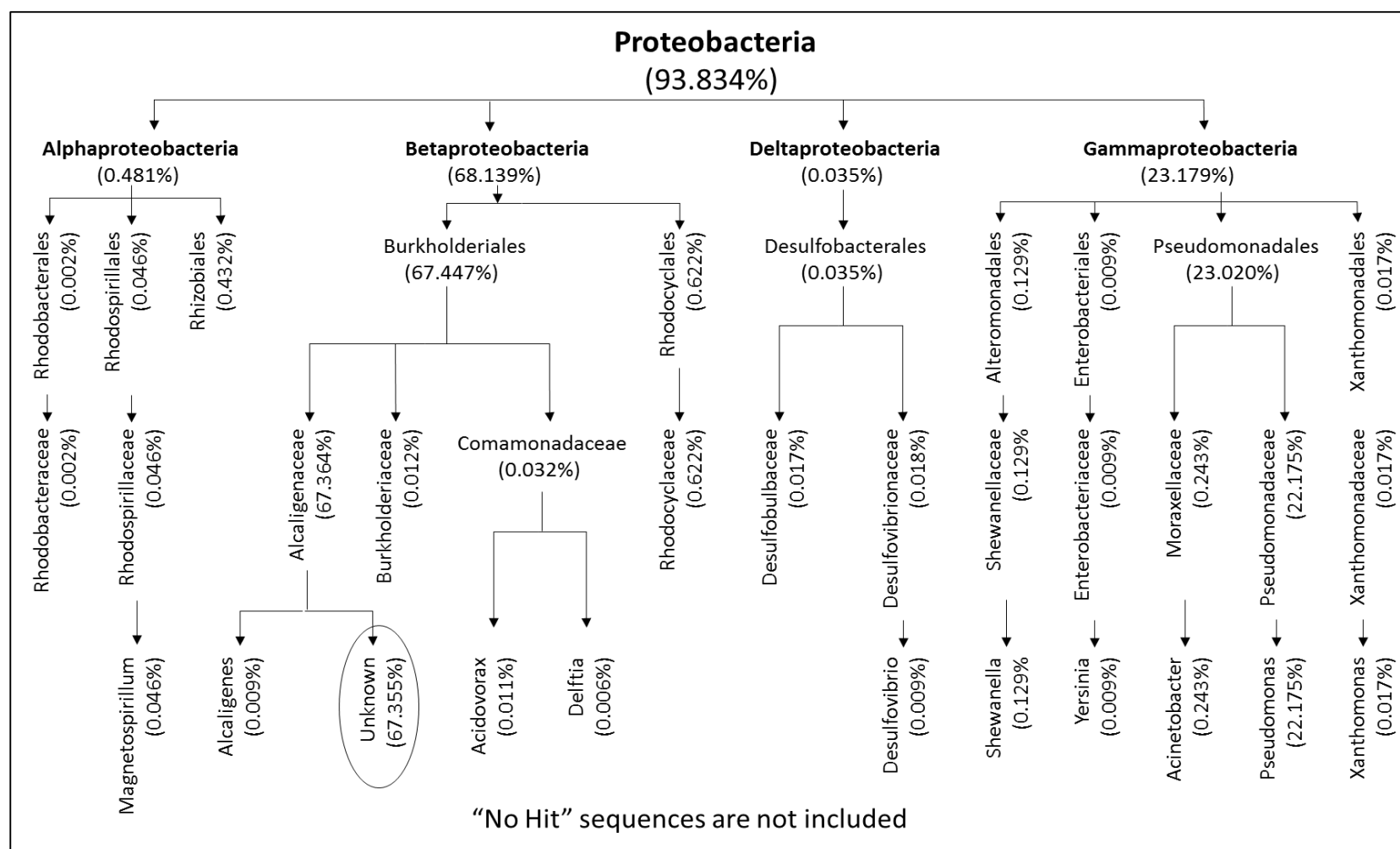


Figure 5.7: Bacteria under proteobacteria phylum identified in the culture enriched at the UNLV-Environmental Engineering and Water Quality Laboratory.

Even though the culture was capable of perchlorate degradation (98.8% in a week) and the majority of the bacteria identified in the culture are *beta* and *gamma proteobacteria*, at the genus level, the PRB present are not the same as the ones identified previously by other researchers. The presence of *Pseudomonas* strain, a chlorate reducer, suggests that at least two different groups of bacteria are present. *Pseudomonas* strain, *PDA* and *PDB* have been reported to see chlorate, but cannot respire perchlorate (Logan et al. 2001; Xu et al., 2004). Most perchlorate degrading bacteria degrade chlorate, but not all chlorate reducing bacteria reduces perchlorate (Xu et al., 2003; Logan et al., 2004).

An electrophoresis gel was running against *Dechloromonas agitata* (DA) as a positive control, water (negative control), and an environmental strain, which was capable of perchlorate reduction, *Pseudomonas aeruginosa* (PA). The result showed presence of perchlorate reductase band in the culture (Figure 5.8).



Figure 5.8: Electrophoresis gel ran for PCR products to identify presence of perchlorate reductase (Source: Touro University Laboratory, 2015).

The PRB culture is labeled as Sichu, *Dechloromonas agitata* as DA (positive control), water as H₂O (negative control), and *Pseudomonas aeruginosa* as PA (Sample that demonstrated possible perchlorate reduction at the Touro University Lab).

5.3.1.2 Bacterial and Eukaryotic Community Growing on the FBR Media

Table 5.5 lists the microorganisms identified in samples from the GAC media used in the FBRs. The media was sampled after running the reactor for 25 days with a perchlorate concentration of 100 ppm. The majority of the bacteria were *Proteobacteria* (77.83%); out of which, 52.69 % were *Betaproteobacteria* (Table 5.5). Betaproteobacteria have also been identified in the mixed enrichment culture used to inoculate the FBRs, therefore, it was expected to find such bacteria in the FBRs. At the species level, bacteria present at high percentages were different from those identified in the enrichment culture. A reason for that might be because the enrichment cultures were switched from suspended growth mode to a fixed film mode; only those bacteria which could be attached onto the GAC were advantaged. A recent study indicated that the bacterial community composition varies with surface type available for attached growth (Kim et al., 2014). Another study also speculates that the variation in bacterial community is influenced by surface material type and that media attachment might provide suitable environments for some microorganisms that would otherwise be washed out in suspended growth (Soondong et al., 2010).

The microaerobic and filamentous bacteria *Curvibacter lanceolatus*, which is found in wastewater treatment plants, was the major bacterial strain belonging to order *Burkholderiales*, detected in the FBRs (Figure 5.9). Another strain *Diaphorobacter sp.* belonging to *Burkholderiales*, a known nitrate reducing bacteria, was also found to be a dominating bacterium. *Sulfurospirillum sp.* (13.15%), a known nitrate reducer and known to respire tetrachloroethene (Hubert and Voordouw, 2007; Luijten et al., 2003) was also identified. A strain belonging to genus *Azospira* had the second highest counts (22%) and it is a known perchlorate reducer (Byrne-Bailey and Coates, 2012). The strains with percent ihts less than 1%

were not included as individual bacteria, instead, a cumulative value for the bacteria is shown in Figure 5.9 b.

Table 5.5: Bacterial Community on the FBR Media

K	Phylum	Class	Order	Family	Genus	Species
Bacteria (100%)	Bacteroidetes (3.59%)	Flavobacteriia (3.59%)	Flavobacteriales (3.59%)	Flavobacteriaceae (3.59%)	Chryseobacterium (1.17%)	Chryseobacterium sp (1.17%)
					Cloacibacterium (1.17%)	Cloacibacterium rupense (1.17%)
	Proteobacteria (77.83%)	Alpha-proteobacteria (2.03%)	Rhizobiales (2.03%)	Bartonellaceae (2.03%)	Bartonella (2.03%)	Candidatus Bartonella ancashi (2.03%)
		Beta-proteobacteria (52.69%)	Burkholderiales (30.70%)	Comamonadaceae (30.70%)	Curvibacter (21.73%)	Curvibacter lanceolatus (21.73%)
					Delftia (1.71%)	Delftia sp (1.71%)
					Diaphorobacter (7.25%)	Diaphorobacter sp (7.25%)
		Epsilon-proteobacteria (13.15%)	Rhodocyclales (22%)	Rhodocyclaceae (22%)	Azospira (22%)	Azospira sp (22%)
			Campylobacteriales (13.15%)	Campylobacteraceae (13.15%)	Sulfurospirillum (13.15%)	Sulfurospirillum sp (13.15%)
			Chromatiales (3.27%)	Chromatiaceae (3.27%)	Rheinheimera (3.27%)	Rheinheimera sp (3.27%)
		Gamma-proteobacteria (9.95%)	Pseudomonadales (6.68%)	Moraxellaceae (6.68%)	Acinetobacter (6.68%)	Acinetobacter sp (6.68%)
			Unclassified (10.98%)	Unclassified (10.98%)	Unclassified (10.98%)	Unclassified (10.98%)
	No Hit for bacteria (0.15%)	No Hit (0.15%)	No Hit (0.15%)	No Hit (0.15%)	No Hit (0.15%)	No Hit(0.15%)
Fungi (100%)	Ascomycota (100%)	Saccharomycetes (100%)	Saccharomycetales (100%)	Dipodascaceae (100%)	Dipodascus (0.38%)	Dipodascus ambrosiae (0.38%)
					Galactomyces (99.99%)	Galactomyces reessii (99.99%)
					Geotrichum (8.62%)	Geotrichum candidum (0.18%)
						Geotrichum klebahnii (7.89%)
						Geotrichum sp (0.54%)

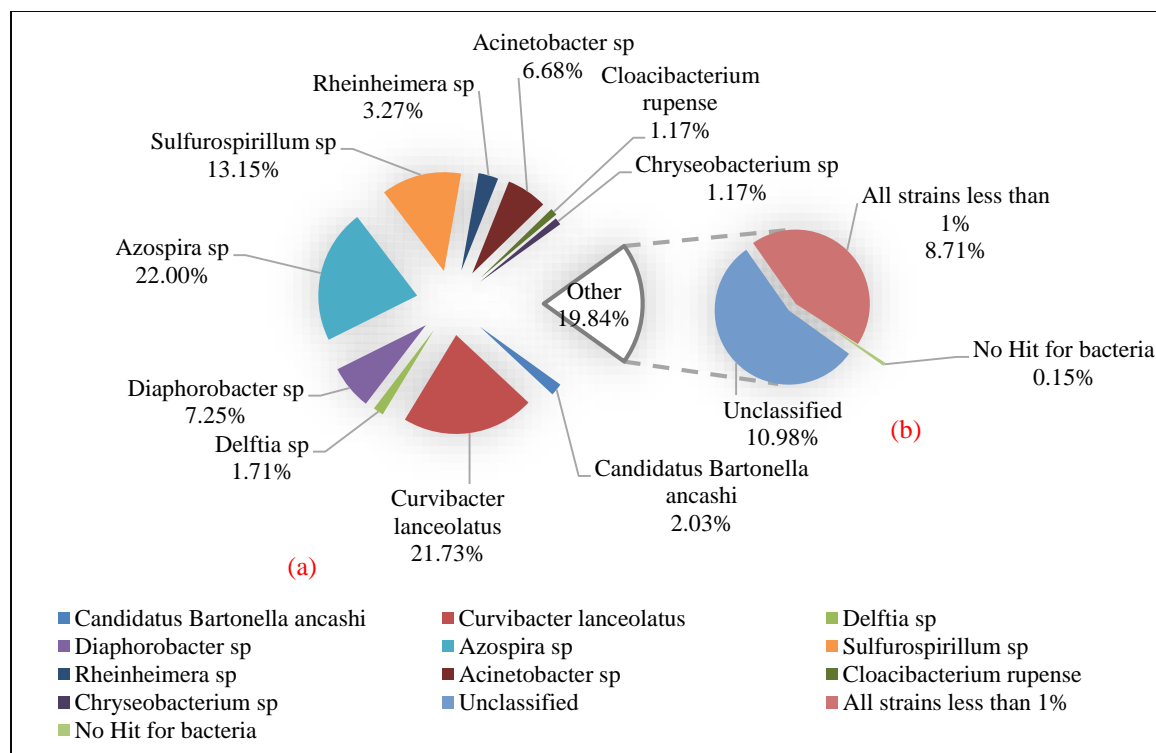


Figure 5.9: Bacteria at species level in the GAC FBR media fed with varying perchlorate concentrations.

The major bacteria are shown in (a) and the bacteria which were not classified, bacterial strain with less than 1% similarity and error (no hit) for bacteria is shown in (b).

5.3.2 Perchlorate Reduction at High (ppm) and Low (ppb) Concentrations by the Enrichment Culture in Batch Reactors

Perchlorate reduction kinetics in batch degradation tests with ppm level perchlorate was faster than in those with ppb level, as expected. The average residual perchlorate concentration with standard deviation over time in the batches is shown in Figure 5.10. The reduction rate (mg/hour) of the batches with ppb levels increase slowly and achieved maximum value (0.323 mg/hour) during the first four hours. The rate continued to decline after four hours until the perchlorate concentration reduced to below detection limit. The reduction rate (mg/hour) in batches with ppm levels had high removal rate in the first two hours (0.457 mg/hour), and the rate decreased in the following hours (Table E.1) to 0.267 mg/hour from four to eight hours. The

reduction rate from 17 to 24 hours in the ppm (0.017 mg/hour) and ppb (0.011 mg/hour) level reactors were comparable. After 24 hours, the concentration of perchlorate was below detection limit for ppm levels, whereas the batches with ppb levels required 30 hours to reach below detection limit.

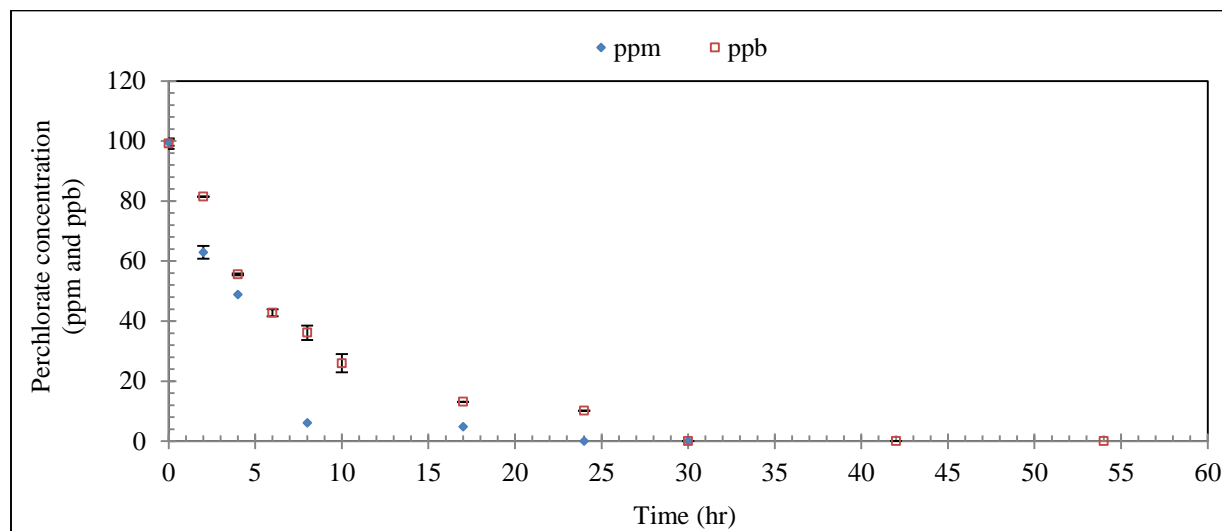


Figure 5.10: Residual perchlorate concentration for 100 ppm and 100 ppb batches with time.

It is well accepted that perchlorate reduction has first order kinetics related to perchlorate concentration. The reduction in perchlorate concentrations in ppm and ppb reactors are shown in Figure 5.10. The data were checked for first order kinetics by plotting the logarithmic (Ln) concentrations of perchlorate against time (Appendix E; Figure E.1). The ln C diagram for both ppm ($R^2=0.89$) and ppb ($R^2=0.90$) data resulted in a straight line. Further, plot between the perchlorate removal rate against concentration of perchlorate was also a straight line for both ppm ($R^2=0.92$) and ppb ($R^2=0.80$) reactors. Thus, the result indicates that the perchlorate removal rate (mg/hour) depends on the residual perchlorate concentration and has first order reaction kinetics. In a similar experiment performed in pure cultures of PRB (KJ and PDX) Logan et al. (2001 a) analyzed existing data on perchlorate degradation kinetics, compared with

KJ and PDX, and demonstrated that the perchlorate removal rate depends solely on the concentration of the perchlorate available for the bacteria and concluded that the perchlorate reduction is the first order reaction.

Optical density was measured to quantify the bacterial growth in the bioreactors. The optical density increased slightly in ppm level reactors, but decreased in ppb level reactors. These results confirm that the degradation of very low perchlorate concentrations is slow and generates very small amount of biomass. That is the case because the half saturation constant (K_s) for perchlorate is reported as 2.2 to 18 mg ClO_4^-/L when acetate was used as sole electron donor, 0.14-76.6 mg ClO_4^-/L in pure cultures and K_s values range between 0.1 to 20 mg ClO_4^-/L for acetate and 0.01 to 567.3 mg ClO_4^-/L for hydrogen as electron acceptor. In the ppb concentration range the amount of energy bacteria gain is very small and biomass formation is small. In the absence of sufficient electron donor or acceptor, bacteria tend to use the electrons for energy or cell maintenance rather than synthesis of new cells (Rittmann and McCarty, 2001).

5.3.3 Test of Biofilm Model to Determine Backwashing of FBR Based on Biofilm Kinetics

A biofilm model was developed based on the biofilm growth model described by McCarty and Meyers (2005) considering kinetics of substrate utilization, molecular diffusion of electron acceptors, and biomass loss due to shear (Rittmann and McCarty, 2001). The model considered biomass growth due to oxygen, nitrate and perchlorate so that it can be used for contaminated waters consisting of all or any of these three electron acceptors. All the parameters assumed and estimated for the model are presented in Chapter 2.7.4. Figure 5.11 shows the biofilm thickness generated by the model for 100 ppm, 100 ppb and 10 ppm. The threshold thickness is that after which the media in the FBR start to float and is shown in Figure 5.11 as a horizontal dotted line. For the model, the beginning thickness for 100 ppm perchlorate concentration was 0.00019 cm

corresponding to a 2000 mg/L culture (2L) inoculated in the FBR, 100 ppb was 0.0168 cm and for 10 ppm was 0.00703 cm.

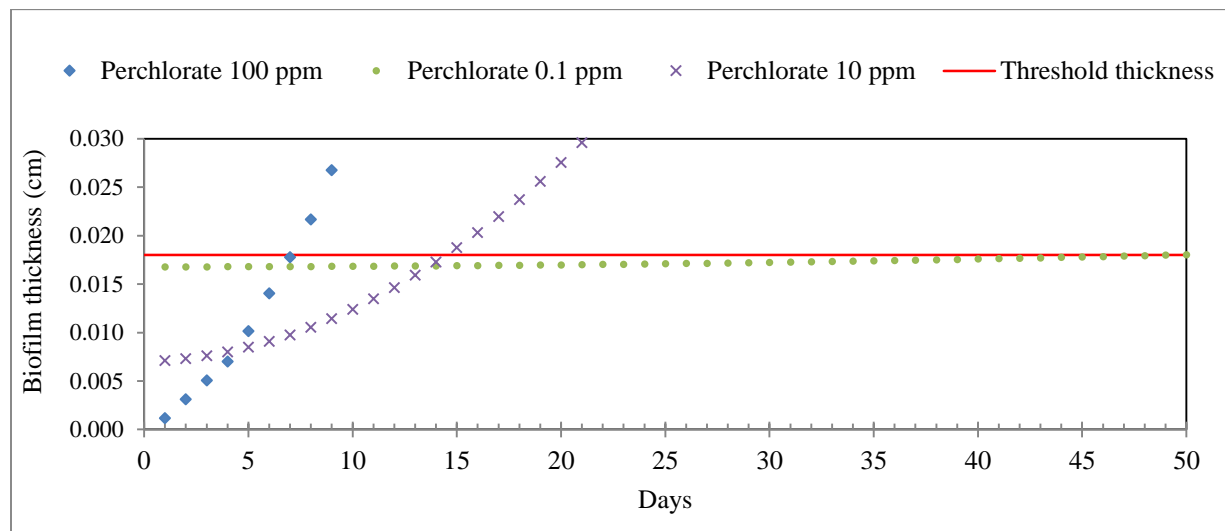


Figure 5.11: Biofilm thickness computed by the model for perchlorate, as the sole electron acceptor, at concentrations 100 ppm, 100 ppb, and 10 ppm. The horizontal line is the threshold biofilm thickness. The time for backwash corresponds to the time when the biofilm thickness exceeds the threshold thickness.

The backwash time from the model was estimated as the time when the biofilm thickness exceeded a threshold biofilm thickness. The threshold biofilm thickness (horizontal line in Figure 5.11) was calculated based on weighted average density of biofilm and the GAC. The GAC was assumed to be sphere, density of GAC 1.42 g/cm^3 (McCarty and Meyer, 2005), and density of biofilm assumed to be 0.8 g/cm^3 (van Veen, 1979). For example, for 100 ppm, the backwash time is day 8 when the biofilm thickness exceeded 0.018 cm (threshold thickness).

The increase in the biofilm thickness was curvilinear, concaving upwards (Figure 5.11). The curvilinear nature of biofilm observed in the model developed in this study was because the biofilm was not thick enough to follow a typical bacterial growth curve. Ai et al. (2016) also observed a similar curvilinear plot for biofilm thickness in laboratory scale sewer, under different

hydraulic shear stress, in the beginning (until day 25), later the biofilm thickness followed typical bacterial growth curve- growth phase, stationary phase and decay phase.

5.3.4 Preliminary Test to Estimate Biofilm Thickness Using Biomass Growth in Bioreactors

A preliminary test was conducted using batch bioreactors to estimate biofilm thickness in the GAC media. A total of four backwashes, two high rate backwashes (first and fourth; 75 rpm for 30 seconds, twice) and two low rate backwashes (second and third; 75 rpm for 10 seconds) were performed on the day when the biofilm thickness crossed the threshold thickness of 0.018 cm.

The result showed that the biomass increased gradually at a rate of 0.039 per day (biofilm thickness of 0.00069 cm/day) from second day (measured after 48 hours for acclimation) to the 9th day. The slow biomass growth (i.e. slow initial increase in biofilm thickness) might be because of bacteria required time for acclimation. Similarly, the biomass and the biofilm thickness increased at a slow rate after high rate backwashes on day 22nd (fourth backwash). The biomass growth rate was high (0.16 per day) after the low rate backwashes on the 14th day (second backwash) and 18th day (third backwash). It might be because the biofilm thickness, after the low intensity backwash, remained enough to prevent excessive loss of bacteria and regained growth faster. Figure 5.12 shows the biofilm estimated from biomass in batch bioreactors.

The growth rates obtained from the bioreactor are smaller than those found in literature. Most of the studies have represented specific growth rate in terms of hours whereas in this study, the growth rates were obtained as per day. Logan et al. (2001 a), which showed that the pure cultures of *KJ* and *PDX*, perchlorate reducing bacteria, had a growth rate of 0.14 and 0.21 per hour respectively in a reactor supplied with 500 mg/L perchlorate and varying amounts of acetate. The kinetics of *PDX* was dependent on carbon source; acetate was preferred by the

strain compared to lactate. Another study (Prata, 2014) observed a specific growth rate of 0.17 per hour for *Dechlorospirillum* sp. DB and *Dechlorosoma* sp. PCC with 20mM acetate and 10 mM perchlorate. The high growth rates were probably because the cultures used were pure strains of perchlorate reducer, unlike a mixed culture used in this study. Wang et al., (2008) observed a growth rate of 0.096 per day for a mixed culture, which is similar to the biomass growth obtained after the 4th backwash and was within the range 0.039 to 0.16 per day obtained in this study. Studies with mixed culture using electron donor other than acetate, however, have higher growth rates than those obtained in this study. Matos et al. (2006) obtained 0.13 per hour and Ricardo et al. (2012) obtained 0.082 per hour, both used ethanol as the electron donor. Urbansky (2000) observed a growth rate of 0.2 per hour in a system with high perchlorate concentrations.

In this study, it was observed that the biomass removal from the GAC, using magnetic stirring, during high backwash intensity was 5360 ± 75 mg/L (0.016 cm thick biofilm), and during low backwash was 1180 ± 89 mg/L biomass (0.0039 cm thick biofilm). These values were used for estimating biofilm thickness after backwash in the biofilm model.

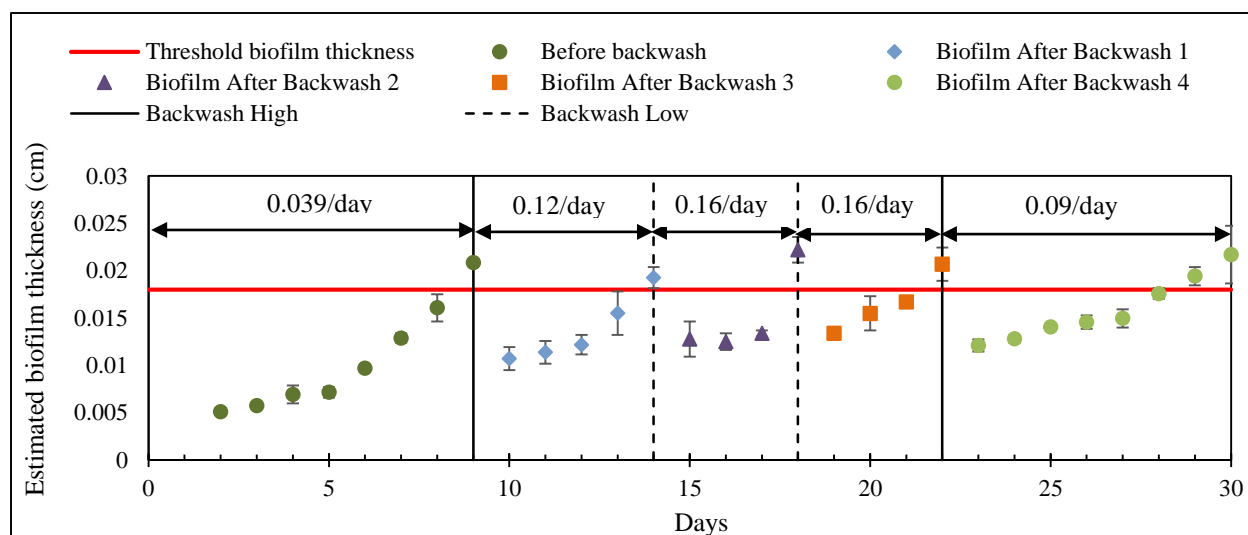


Figure 5.12: Biofilm thickness estimated from biomass growth on GAC media due to perchlorate degradation (100 mg/L). The growth rate is given for each segment above the data points. The solid-horizontal line represents the threshold biofilm thickness, solid-vertical lines represent high backwash rate, and dotted-vertical lines represent low backwash rate.

5.3.5 Perchlorate Removal in FBR: Use of Image Processing for Determining Backwash Time Coupled with Biofilm Model

5.3.5.1 Perchlorate Removal in the FBR

Preliminary test with 100 ppb and 100 ppm in batch bioreactors showed that the ppm level bioreactors had faster removal rate than ppb levels. The same perchlorate concentrations (100 ppm and 100 ppb) and 10 ppm were used to operate laboratory scale FBRs to investigate the loss of media at low and high perchlorate concentrations. FBRs were operated starting with 100 ppm, 100 ppb and lastly, 10 ppm –for about 25 days with each concentration. The operation with 100 ppm showed overall average removal of only 64% which might be because of insufficient hydraulic retention time. The reactors operated at 100 ppb showed much lower average removal (45%), which was expected because the microbial kinetics for perchlorate is slow at low concentrations. The highest removal was observed in the 10 ppm FBR (78%) compared to other two. This might be because the 10 ppm test was operated at the end of the

study period and perchlorate reducing bacteria were already acclimated to the reactor. Figure 5.13 shows the perchlorate removal for the varying influent perchlorate concentrations.

The FBRs operated at 100 ppm perchlorate concentrations showed higher effluent values for the first four days than in the influent concentration. This is attributed to residual perchlorate from the seed culture used for inoculation of the FBRs (Figure 5.14 a). On the sixth day no removal was observed in the second reactor because its pump head failed (shown by an arrow in Figure 5.14 a). By the eleventh day, the perchlorate removal was limited to 50% (i.e. removal rate is 3.4 mg/ minute). The low perchlorate removal might be because of insufficient retention time for degradation; the empty bed contact time (EBCT) was 8.2 minutes for the reactors. Hatzinger et al. (2000) observed a removal of 4.6 mg/minute in a FBR with expansion of 32% and 400 mg/L of influent perchlorate concentration and using ethanol as the electron donor. The flow, in the FBR, was reduced by half (0.8 mL/second) on the 12th day. The average perchlorate removal after flow reduction was more than 92% (i.e. removal rate is 9.2 mg/minute) (Figure 5.14 a). Miller and Logan (2000) observed 1.05 mg/minute removal in a fixed bed reactor with hydrogen as the electron donor and 740 mg/L of perchlorate concentration. Xiao et al. (2010) observed a removal of 22.4 mg/minute in a FBR fed with acetate as electron donor, despite a perchlorate lower concentration of perchlorate (70 mg/L) than this study.

The average percent perchlorate removal at the influent concentrations to 100 ppb was 20% (0.0014 mg/minute), operated at 0.8 mL/second. Only after day 6, perchlorate removal of about 40% (0.0057 mg/minute) was observed (Figure 5.14 b). The lower percent removals at the 100 ppb might be because of the slow kinetics at low perchlorate concentration. On the 10th day, flow was resumed back to designed flow rate (1.6 mL/second). The increase in flow rate did not affect the percent perchlorate removal. However, there were frequent breakdown of the pump

head causing introduction of air into the reactors increasing the dissolved oxygen levels in the reactor. Oxygen, a preferred electron acceptor over perchlorate, might have hindered the degradation of the perchlorate. Brown et al. (2003) achieved a removal of 0.262 $\mu\text{g}/\text{minute}$ in a mixed cultured biological activated carbon filter with 50 $\mu\text{g}/\text{L}$ perchlorate concentrations, when the EBCT was 5 minutes and complete degradation at 9 minutes. Another study using a FBR, inoculated with pure strain of *Dechlorosoma KJ*, also reported a similar removal of 0.275 $\mu\text{g}/\text{minute}$ in a reactor treating 77 $\mu\text{g}/\text{L}$ of perchlorate with acetic acid as the electron donor and a residence time of 18 to 30 minutes (Min et al., 2004). Giblin et al. (2000) however, reported 0.0037 mg/L in a FBR with 738 $\mu\text{g}/\text{L}$ of perchlorate fed with acetate and a residence time of 10 hours; the study used pure strain *perlance* for removal.

Lastly, the influent perchlorate concentration was increased to 10 ppm, and immediate removal was observed (from 2nd day). The average percent perchlorate removal was 80% (0.85 mg/minute) in the FBR (Figure 5.14 c). Despite of frequent pump head failure, the perchlorate removal was observed to be best in this operation period. However, on days with pump head failure, the effluent concentrations were elevated (shown by an arrow in Figure 5.14 c).

Hatzinger et al. (2000) reported perchlorate removal of 20.6 mg/minute in a FBR inoculated with mixed culture, and fed with ethanol and 10 mg/L perchlorate. Kim and Logan (2001) observed a removal of 0.04 mg/minute in a fixed bed reactor inoculated with mixed culture fed with 20 mg/L perchlorate and acetate, and 1.28 mg/minute in a reactor with pure culture (MS2).

The removal rates reported in the literature are in wide range and varied with concentration of perchlorate, electron donor, type of reactor, salinity, and bacteria inoculated in the reactor. The removal rates obtained in this study for all the concentrations were within the reported range.

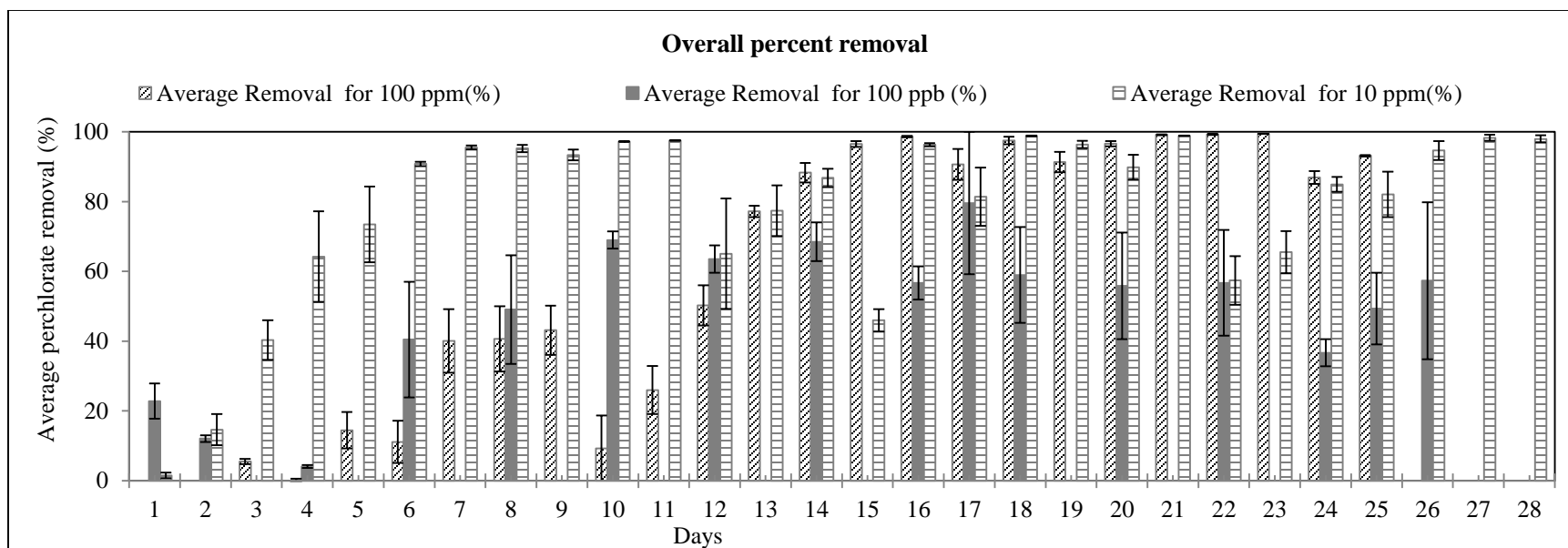


Figure 5.13: Average percent perchlorate removal in both FBRs for 100 ppm, 100 ppb, and 10 ppm for overall period.

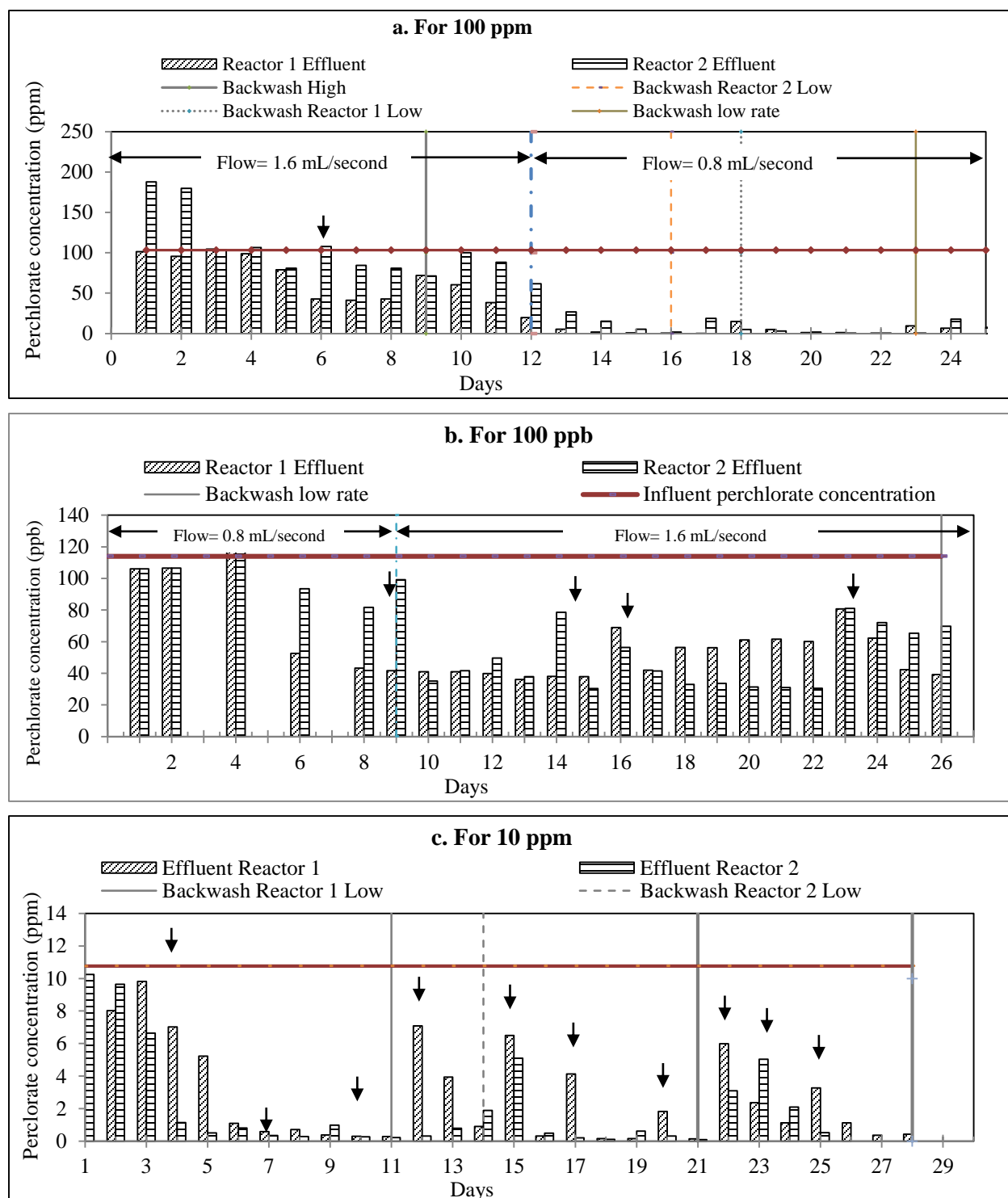


Figure 5.14: Average perchlorate effluent concentration (bars) in the FBRs operated at 100 ppm (a), 100 ppb (b), and 10 ppm (c) with average influent (horizontal line), pump head failures (arrows), and backwash (lines).

5.3.6 FBR Backwashing Frequency and Media Loss Evaluation Using Image Processing Technique

Preliminary investigation of images taken at the top portion of a FBR operated with 1 ppm perchlorate showed that the GAC in the FBR start to float as a block as the density of the media decreases due to bacteria growth, and therefore, backwash time could be estimated using the change in GAC depth. Results of preliminary study are shown in Appendix E. The ImageJ converts the digital pictures into grey-scale (black for GAC and white for empty operating zone).

At the start-up, the GAC media experienced hydraulic expansion only and the entire operational area was empty (white area). The ImageJ measured the empty operational area (percent area available for expansion, A_e) as 100%. As the bacteria started to form biofilm, the media started to move up, the pictures started to gain black area, thereby reduced the value of A_e . The ImageJ was used to calculate the percent area of the white and black areas. The analyzed picture has red color for the empty space and black for GAC. Figure 5.15 show the final images after processing using the ImageJ. The empty space has been termed 'percent area available for GAC expansion' (red color area in analyzed picture) in Figure 5.15.

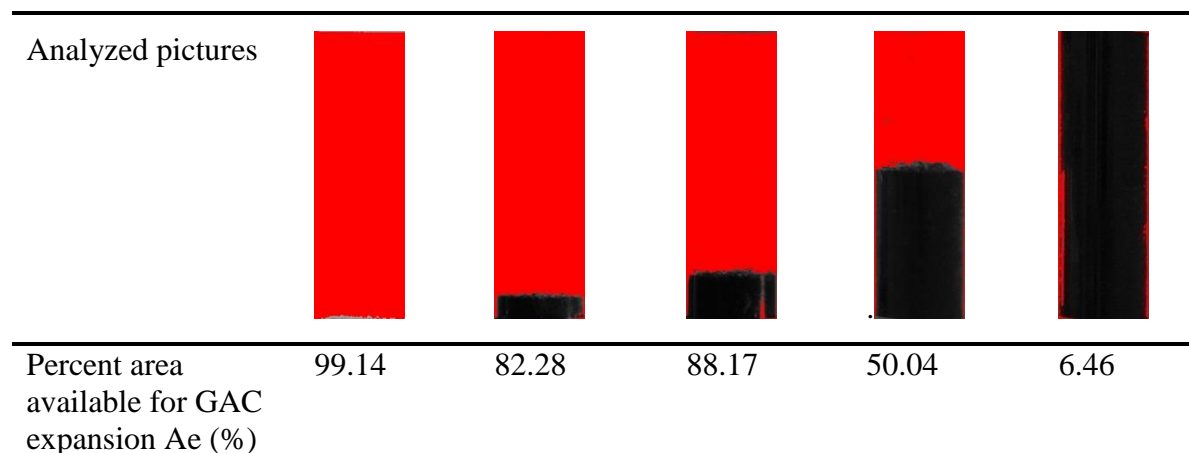


Figure 5.15 Final analyzed pictures of the operating zone using ImageJ.

Figure 5.16 (a, and b), show values of Ae as obtained from the ImageJ analysis for 100 ppm and 100 ppb, and 10 ppm is shown in Appendix E (Figure E.7). Ae was observed 100% in the beginning of the operation and the first day after backwash. No buoyancy of the media suggests that the FBR media has insufficient biofilm formation on the media. Figure 5.16 (b) suggests that perchlorate started to decline after 5th day for 100 ppm. The image processing also showed decreased value of Ae, which indicates that the biomass was enough for perchlorate degradation and floatation. The rapid rate of decrease in the Ae values from days 8 to 10 indicates sufficient biomass in the reactor by then. By day 8, the perchlorate degradation was more than 50% (Figure 5.16 b). Similarly, a slow decrease rate followed by a rapid decrease rate of Ae was observed after each backwash.

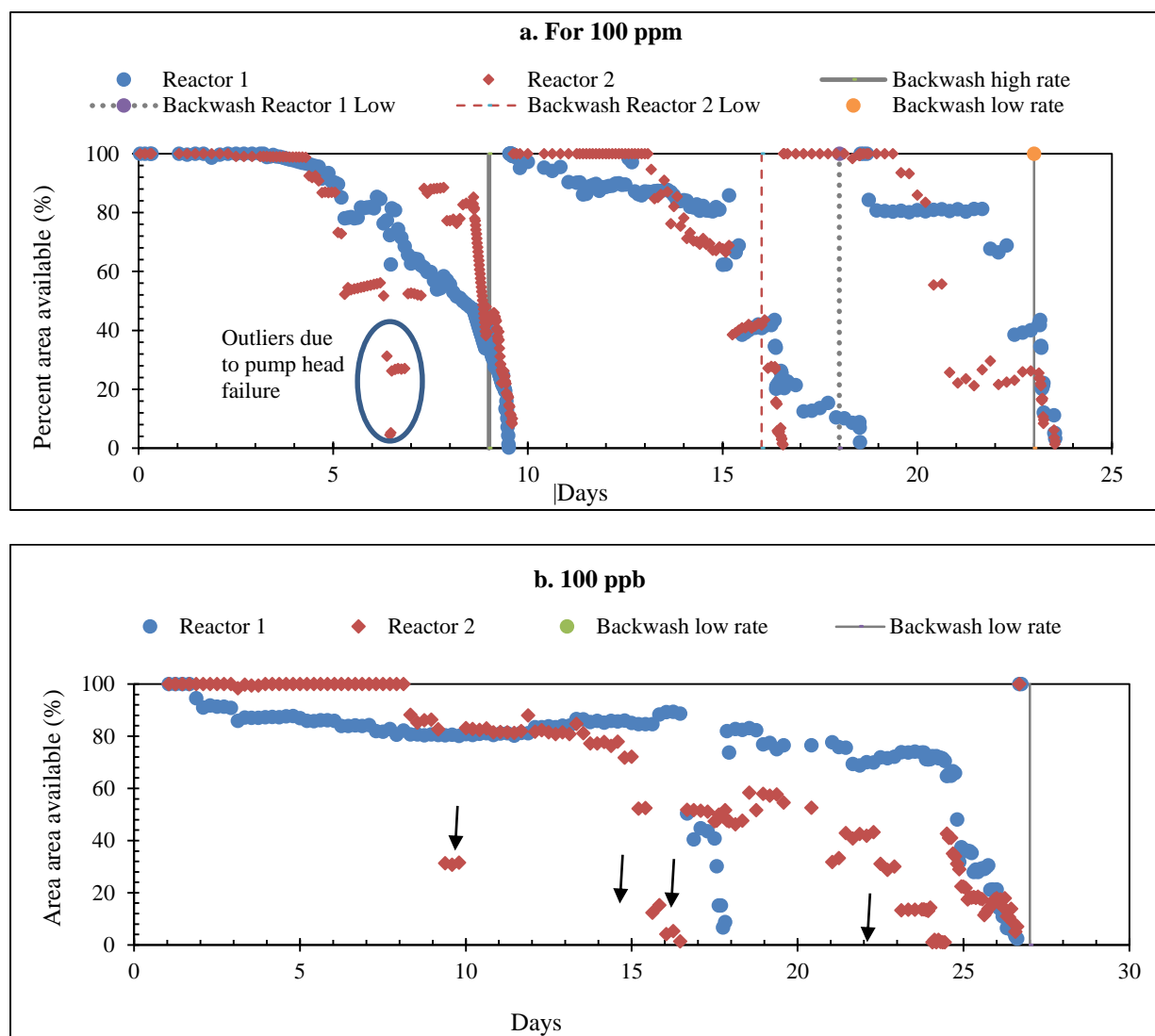


Figure 5.16: Percent area available for media expansion in the operating depth against time for FBRs operated at 100 ppm (a), and 100 ppb (b) . The vertical lines indicate backwash and the arrows indicate events with pump head failure.

5.3.7 Test of Biofilm Model to Determine Backwashing of FBR based on Image Analysis of Media Flootation in FBR

The FBRs were operated at 100 ppm at first and with an initial biofilm thickness of 1.93×10^{-3} cm. The GAC was backwashed at low rate before using for 100 ppb perchlorate concentrations and a strong backwash was performed before switching to 10 ppm. Therefore, the curves for 100

ppb and 10 ppm had some biofilm thickness prior operation. It was assumed that the high intensity backwash removed 5360 mg/L biomass (0.016 μm), and low intensity backwash removed 1180 mg/L biomass (0.0039 μm) from the GAC. The test was done for conditions with 100 ppm perchlorate. Figure 5.17 shows the backwash time corresponding to the biofilm thickness estimated by the model and backwash time required in the FBRs.

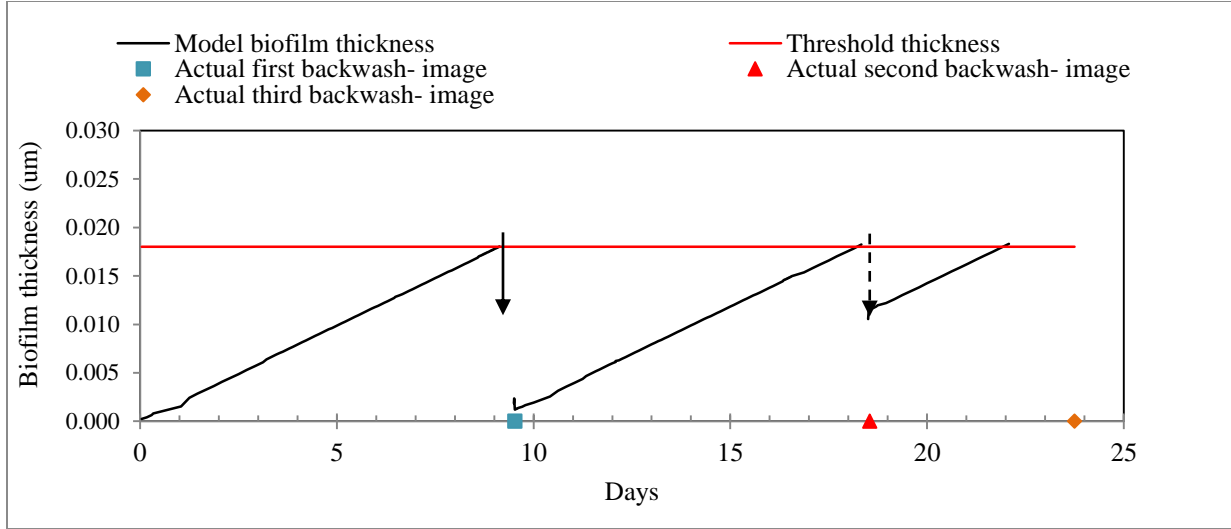


Figure 5.17: Biofilm thickness (cm) estimated using model, and actual biofilm thickness computed from biomass to obtain the appropriate backwash time. The actual backwash in FBRs as obtained after image processing is shown on the x-axis by square (1st backwash at high rate), triangle (2nd backwash at low rate) and diamond (3rd backwash at high rate).

For 100 ppm, the first backwash time obtained from the model was day 9.12, the second was day 18.33 and third was day 22.07. The backwashes estimated from the FBR image analysis were on days 9.5 for the first backwash, 18.54 for second and 23.75 for third. The backwash time estimated from FBR coincided with the actual biofilm computed from biomass model except for the last backwash. The actual biofilm computed from the batch bioreactors with 100 ppm showed that the first backwash required was on days 9, second on 14, third on 18, and finally on 22 (Figure 5.17). Therefore, the estimated backwashing time is close to actual

backwash time in the FBR. The batch bioreactors with 100 ppm required one extra backwash than real FBR and the model, which might be because the batch bioreactors lack of hydraulic shear that was the biofilm experienced in FBR.

5.4. Conclusions

In FBRs, maintaining the biomass to just enough to degrade perchlorate is very critical. Too much biomass growth will result in media flotation and loss. The most common method to clean the media is backwash, which is practiced based on visual inspection of the media depth. This research explores the use of imaging processing technique as a tool to forecast the appropriate backwashing time for FBRs treating perchlorate contaminated water. A biofilm model was also developed to test the suitability of image processing technique as an operation tool for FBRs treating perchlorate. There are very few studies focusing on appropriate backwashing frequency of FBRs. Most of the FBR studies for perchlorate removal have focused on removal efficiencies. Previous Biofilm models for perchlorate removal have focused on mass transfer of electron donor and acceptors. This study addresses the use of image processing as a tool to determine backwashing frequencies of FBR reactors treating perchlorate. The following can be concluded from the data obtained in this research.

1) This study confirmed that the degradation kinetics of perchlorate in ppb level is slower in bioreactors with ppm level. Perchlorate has a large half saturation constant (K_p) value that result in slow microbial kinetics at low perchlorate concentration (Logan, 1998; Dudley et al., 2008). In the bioreactors with perchlorate concentrations at 100 ppb did not generate much biomass due to slow kinetics; Optical density, used to quantify the bacterial growth in the bioreactors, increased slightly in ppm level reactors, but remained constant or decreased in ppb level reactors.

Hazinger (2009) observed increase in optical density, biomass growth per hour, in presence of high concentrations of perchlorate (25 to 100 mg/L), oxygen (8mg/L) and nitrate (25 to 1000 mg/L).

2) In this experiment with FBRs, operated at 100 ppm and 100 ppb, biomass growth was slow in 100 ppb concentrations. The biomass growth in the FBR during 100 ppm run required three backwashes within 25 days of operation due to excessive biomass growth, whereas during 100 ppb run required only one backwash after operating for 26 days.

3) The visual inspection and microbial community analysis of the GAC from the FBR obtained at the end of 100 ppm run, indicated presence of a filamentous bacteria (*Curvibacter lanceolatus*,) and yeast (*Galactomyces reessii*) with large and distinctive vacuoles. The presence of these microorganisms might have contributed to the uplifting of the media. However, it was not yet clear whether the media expansion in the FBRs was due to bacteria growth or eukaryotic organism enhanced the expansion.

4) This study shows that image processing technique can be used for identifying backwashing frequency. The backwash time estimated using image processing technique for FBRs operated at 100 ppm was same or a day earlier than the biofilm model. However, the backwash required for 100 ppb level was under estimated by the biofilm model. The biofilm model estimated 50 days as the time for backwash, but in the reality backwash was required on the 26th day. Similarly, for 10 ppm, the model identified day 15 as the backwash day, but in reality backwash was required on days 10 and 14 for FBRs 1 and 2, respectively. In these cases, image processing technique proved a better option. The limitation of image processing technique was that during events of pump failure media depth increased due to air trapped in the reactor, but such increase was also accounted as expansion of media due to biomass growth.

CHAPTER 6

CONCLUSIONS AND RECOMMENDATIONS

6.1 Conclusions

This dissertation is focused on two important, but not completely researched issues related to ex-situ and in-situ perchlorate biodegradation. The first objective was to evaluate use of digital images as a tool to determine an appropriate backwash time to avoid media loss in FBRs treating perchlorate. The second objective was to evaluate the feasibility of using emulsified oils as a slow release electron donor for in-situ perchlorate bioremediation.

In FBRs, maintaining sufficient biomass to degrade perchlorate is very critical. However, too much biomass accumulation promotes floating and loss of FBR media. Backwashing is used to remove excess biomass from FBRs. Currently FBR backwashing is practiced based on visual inspection of the media depth and this process has not yet been adequately characterized. This research explores the potential use of image processing as a tool to forecast an appropriate backwashing frequency for FBRs treating perchlorate. A biofilm model was also developed to test the suitability of image processing as an operation tool for FBRs. The following can be concluded from the data obtained in this research.

- 1) As forecasted, the FBR media started to float as the biomass grew on it. Most of the biomass was visible at the bottom 15 cm of the reactor. The GAC media observed under a phase contrast microscopy indicated presence of yeast, a eukaryotic community, in addition to bacteria. The yeast, *Galactomyces reessii*, a filamentous fungus, contains large vacuole(s), which might be an additional potential cause of uplifting of the media in FBRs. The assumption that the media floats due to sole bacterial growth requires further research.

- 2) The theoretical backwash times obtained by using the biofilm model were very close to the times obtained using digital images. The backwash time identified by using the biomass growth in perchlorate fed batch bioreactors, which was operated to simulate FBRs, was in agreement with the other two methods for the first backwash trial, but the operation of the biomass growth method could not simulate similar backwashes for the second and third backwash trials of the FBRs.
- 3) For full-scale applications, identifying a suitable place for mounting the camera to measure FBR bed expansion is still needed. One possibility is to mount the camera facing the inspection window that is used for maintenance. However, it should be noted that the analysis of the pictures taken from the inspection window will be different than shown in this study; in this study pictures of the entire operation depth were captured and analyzed. The pictures should also be evaluated for quality and suitability for use in an automated program to forecasting backwashing frequency. The inspection window should be build of transparent material that is resistant to microbial growth. Recently, special glass was used in the inspection window of an anaerobic digester in a wastewater treatment plant in California (Ackman and Le, 2006)

The second objective of this research was to explore the use of a slow releasing electron donor, emulsified oil, to serve as electron donor for in-situ bioremediation of high concentrations of perchlorate and nitrate. The research simulated aquifers of high and low hydraulic conductivities in four columns using soil and plastic media. There exist very few studies similar to the one reported here. Most perchlorate biodegradation studies have focused on the use of soluble substrates for ex-situ bioremediation. The following can be concluded from the research on EO use: 1) EO was proven to be an effective electron donor to degrade nitrate and perchlorate

under the investigated conditions. EO desorption, measured as COD, suggested that EO attached to the soil leached out in the effluent over a period of 30 days. After a month, when the COD levels dropped to 30 mg/L, nitrate removal ceased. Addition of more EO to the soil columns promoted immediate removal of perchlorate and nitrate. These results show the importance of providing enough EO to support the degradation of electron acceptors present. The results also point to the need to determine the amount of EO that can be sorbed and desorbed from soils depending on hydraulic conductivity of the groundwater, soil type, porosity, and concentration of EO applied. Such results would help establish the frequency of EO applications in full-scale bioremediation.

- 1) A negative impact of nitrate on perchlorate degradation was clearly observed in this study.

In the presence of nitrate, perchlorate removal in the EO microcosms was only 18%, but when the nitrate concentration reduced below 0.5 mg-N/L; perchlorate reduction increased up to 80% were observed. Similar results were observed in column bioreactors. Perchlorate reduction was observed after an acclimation period of 30 days. After the acclimation period, when the nitrate concentration in the groundwater was increased by four fold, the perchlorate removal was affected, but was recovered back to 98% within 5 days. Additionally, despite the incomplete removal of high level of nitrate in the column bioreactors, perchlorate reduction was observed after the acclimation period. This result suggests that in a consortium of bacteria that is able to degrade perchlorate.

- 2) The relative concentrations of nitrate and perchlorate, in groundwater of high hydraulic conductivity, impact the perchlorate removal when EO is used.
- 3) The second addition of EO, affected the hydraulic conductivities in the soil columns. The addition of EO itself has the potential to reduce hydraulic conductivity in soil column

bioreactors. However, it is believed that the growth of microbes as biodegradation proceeded was the major factor impacting hydraulic conductivity. Both factors may be detrimental to the implementation of bioremediation in areas of low hydraulic conductivities. While locations with high hydraulic conductivities will be less prone to a decreased in hydraulic conductivity (i.e clogging), their fast water flows result in less contact time between the contaminant and EO, resulting in less degradation.

6.2 Recommendations for Future Research

- 1) The biofilm thickness for FBRs were estimated from biomass formation in batch bioreactors with 100 ppm perchlorate that were operated simulating FBRs. Measuring biofilm thickness in the FBRs used for this study was not possible without disturbing the overall set-up. There is a need to develop a direct and non-invasive methods such as confocal microscopy to measure the biofilm thickness using in FBRs. An attempt made of such measurement in this research was not successful.
- 2) The GAC media observed under a phase contrast microscopy indicated presence of a eukaryotic community in addition to bacteria. *Galactomyces reessii*, a filamentous fungi containing large vacuole(s) might be an additional potential cause of uplifting of the media in FBRs. The assumption that the media floats due to sole bacterial growth requires further research.
- 3) Image processing technique provided more realistic results to obtain backwashing frequency in the FBRs. However, during events of pump failure and increased media depth due to air trapped in the reactor, the technique accounted as expansion of media due to biomass growth.

The reliability of the image processing techniques needs to be tested for large scale FBRs under actual FBR operation scenarios to validate the results.

- 4) Research is still needed to investigate the adsorption and desorption of EO to various type of soils. This information is needed to establish EO application frequencies in full scale in-situ bioremediation. In this study, when COD concentrations were below 30 mg/L, biodegradation was significantly impacted.
- 5) Although it was observed that the EO was reduced in the effluent with time, this research did not investigate if residual EO remains in the soil that is not desorbed for use by bacteria. This is also an area where research is still lacking

REFERENCES

- Abdo Z., Schuette U.M, Bent S.J., Williams C.J, Forney L.J. and Joyce P., 2006. Statistical methods for characterizing diversity of Microbial communities by analysis of terminal restriction fragment length polymorphisms of 16 S rRNA genes. *Environmental Microbiology*, 2006
- Achenbach, L. A., U. Michaelidou, R. A. Bruce, J. Fryman, and J. D. Coates. 2001. *Dechloromonas agitata* gen. nov., sp nov and *dechlorosoma suillum* gen. nov., sp nov., two novel environmentally dominant (per)chlorate-reducing bacteria and their phylogenetic position. *International Journal of Systematic and Evolutionary Microbiology* 51 (MAR 2001): 527-33.
- Achenbach. 2002. Sequencing and transcriptional analysis of the chlorite dismutase gene of *dechloromonas agitata* and its use as a metabolic probe. *Applied and Environmental Microbiology* 68 (10) (OCT 2002): 4820-6.
- Ackman, P., and Le, T. 2006. Installation of Radar Level Instruments in Anaerobic Digesters. *Water Environment Foundation*. 2006.
- Adham S., Gillogly, T., Lehman, G., Rittmann, B., and Nerenberg, R., 2004. Membrane Biofilm Reactor Process for Nitrate and Perchlorate Removal. Awwa Research Foundation, 2004.
- Ahn, Chang Hoon, Hyangkyun Oh, Dongwon Ki, Steven W. Van Ginkel, Bruce E. Rittmann, and Joonhong Park. 2009. Bacterial biofilm-community selection during autohydrogenotrophic reduction of nitrate and perchlorate in ion-exchange brine. *Applied Microbiology and Biotechnology* 81 (6) (JAN 2009): 1169-77 (Last accessed: 1/23/2014 6:44:58 PM).
- Arthur, R.D. 2011. Process Control Factors for Continuous Microbial Perchlorate Reduction in the Presence of Zero-Valent Iron. *Graduate Faculty of Auburn University in partial fulfillment of the requirements for the Degree of Masters of Science*. 2011.
- Attaway, Hubert, and Mark Smith. 1993. Reduction of perchlorate by an anaerobic enrichment culture. In *Journal of industrial microbiology & biotechnology*. Vol. 12, 408-412Springer Berlin / Heidelberg.
- Attaway, Hubert, and Mark Smith. 1994. Propellant wastewater treatment process. US 5302285.
- AWWaRF, 2004. Membrane Biofilm Reactor Process for Nitrate and perchlorate Removal, Report. 2004.

- Backlund, Anna S., and Thomas Nilsson. 2011. Purification and characterization of a soluble cytochrome c capable of delivering electrons to chlorate reductase in *Ideonella Dechloratans*. *FEMS Microbiology Letters* 321 (2) (AUG 2011): 115-20.
- Backlund, Anna Smedja, Jan Bohlin, Niklas Gustavsson, and Thomas Nilsson. 2009. Periplasmic c cytochromes and chlorate reduction in ideonella dechloratans. *Applied and Environmental Microbiology* 75 (8) (APR 2009): 2439-45.
- Bardiya, N., and J. H. Bae. 2005. Bioremediation potential of a perchlorate-enriched sewage sludge consortium. *Chemosphere* 58 (1) (JAN 2005): 83-90.
- Bardiya, 2004. Role of citrobacter amalonaticus and citrobacter farmeri in dissimilatory perchlorate reduction. *Journal of Basic Microbiology* 44 (2) (2004): 88-97.
- Bardiya, N., and Jae-Ho Bae. 2011. Dissimilatory perchlorate reduction: A review. *Microbiological Research* 166 (4) (2011): 237-54.
- Bardiya. 2008. Isolation and characterization of dechlorospirillum anomalous strain JB116 from a sewage treatment plant. *Microbiological Research* 163 (2) (2008): 182-91.
- Batista, J. R., F. X. McGarvey, and A. R. Vierira. 1999. Removal of perchlorate from waters using ion-exchange resins. *Abstracts of Papers of the American Chemical Society* 218 (AUG 22 1999): U551.
- Batista, J.R., Gingras, T.M., and Vieira, A.R., 2002. Combining Ion-Exchange (IX) Technology and Biological Reduction for Perchlorate Removal. *Remediation*. 20002.
- Batista, J.r., Amy, O., Papelis, L., Chang, Y., 2003. The fate and transport of perchlorate in a contaminated site in the Las Vegas Valley. Final report.
- Batista J.R., Papelis, L., Kesterson, K., and Amy, P., 2005. Potential for Bioremediation of the Perchlorate-Contaminated Sediments in the Las Vegas Wash Area, Henderson, Nevada. *Remediation*, 2005.
- Begum, Shamim A., and Jacimaria R. Batista. "Impact of butyrate on microbial selection in enhanced biological phosphorus removal systems." *Environmental technology* 35.23 (2014): 2961-2972.
- Bender, K.S., 2004. The Genetics of (Per)Chlorate Reduction. Southern Illinois University Carbondale, 2003.
- Bender, K.S., Rice, M.R., Fugate, W.H., Coates, J.D., and Achenbach, L.A. 2004. Metabolic Primers for Detection of (Per)chlorate-Reducing Bacteria in the Environment and Phylogenetic Analysis of cld Gene Sequences. *Applied and Environmental Microbiology*. 2004: 70 (9), 5651-5658.

- Bender, K. S., C. Shang, R. Chakraborty, S. M. Belchik, J. D. Coates, and L. A. Achenbach. 2005. Identification, characterization, and classification of genes encoding perchlorate reductase. *Journal of Bacteriology* 187 (15) (AUG 2005): 5090-6.
- Berekaa, M. M. 2013. Towards efficient crude oil degradation by *Pseudomonas* sp. strain-O2: Application of PlackettBurman design for evaluation of cultivation conditions. *Academic Journals*. 2013: 7(39), 4722-4729.
- Betancur-Corredor, B., Pino, N.J., Cardona, S., and Peñuela, G.A. 2015. Evaluation of biostimulation and Tween 80 addition for the bioremediation of long-term DDT-contaminated soil. *Environ Sci (China)*. 2015: 1, 28, 101-9.
- Bhattacharjee, S., Youtube video, (Last accessed: 2013).
- Blount B.C., Pirkle, J.L., Osterloh J.D., Valentin-Blasini, L., and Caldwell K.L, 2006. Urinary Perchlorate and Thyroid Hormone Levels in Adolescent and Adult Men and Women Living in the United States. *Environmental Health Perspectives*, 114 (12), 2006.
- Bohlin, Jan, Anna Smedja Backlunda, Niklas Gustavsson, Sara Wahlberg, and Thomas Nilsson. 2010. Characterization of a cytochrome c gene located at the gene cluster for chlorate respiration in *ideonella dechloratans*. *Microbiological Research* 165 (6) (2010): 450-7.
- Boralessa and Batista, 2000. Transport of Perchlorate in the Las Vegas Wash and Lake Mead, University of Nevada, Las Vegas.
- Borden, B., 2006. Protocol for enhanced In-Situ bioremediation using Emulsified Edible Oil. Solution-IES, 2006.
- Borden, R.C., 2007a. Effective distribution of emulsified edible oil for enhanced anaerobic bioremediation. *Contaminant Hydrology*. 2007: 94, 1-12.
- Borden, R.C., 2007b. Concurrent bioremediation of perchlorate and 1,1,1-trichloroethane in an emulsified oil barrier. *Contaminant Hydrology*. 2007: 94, 3-33.
- Borden, R. C., and Lieberman, M.T., 2009. Passive Bioremediation of Perchlorate Using Emulsified Edible Oils. *Environmental Remediation Technology*. 2009: 155-175.
- Borsodi, A.K., Micsinai, A., Kovács, G., Tóth, E., Schumann, P., Kovács, A.L., Böddi, B., and Márialigeti, K. 2003. *Pannonibacter phragmitetus* gen. nov., sp. nov., a novel alkalitolerant bacterium isolated from decomposing reed rhizomes in a Hungarian soda lake. *Int J Syst Evol Microbiol*. 2003: 53(Pt 2), 555-61.
- Bouwer, E. J., and P. L. Mccarty. 1984. Modeling of trace organics biotransformation in the subsurface. *Ground Water* 22 (4) (1984): 433-40.

- Bramucci, M. and Nagarajan, C.M., 2006. Genetic organization of a plasmid from an industrial wastewater bioreactor. *Appl Microbiol Biotechnol.* 71(1):67-74.
- Brown, J. C., Snoeyink, V. L., & Kirisits, M. J., 2002. Abiotic and biotic and biotic perchlorate removal in an activated carbon filter. *Journal American Water Works Association* 94 (2) (FEB 2002): 70–79.
- Brown, J. C., Snoeyink V. L., Raskin L., and Lin R. 2003. The sensitivity of fixed-bed biological perchlorate removal to changes in operating conditions and water quality characteristics. *Water Research* 37 (1) (JAN 2003): 206-14.
- Brown, J. C., R. D. Anderson, J. H. Min, L. Boulos, D. Prasifka, and G. J. G. Juby. 2005. Fixed bed biological treatment of perchlorate-contaminated drinking water. *Journal American Water Works Association* 97 (9) (SEP 2005): 70-81.
- Bruce, R. A., L. A. Achenbach, and J. D. Coates. 1999. Reduction of (per)chlorate by a novel organism isolated from paper mill waste. *Environmental Microbiology* 1 (4) (AUG 1999): 319-29.
- Byrne-Bailey, K.G. and Coates, J.D. 2012. Complete Genome Sequence of the Anaerobic Perchlorate-Reducing Bacterium *Azospira suillum* Strain PS. *Journal of Bacteriology*. (MAY 2012): 194, 10, 2767-2768.
- Cameron M.L., Robert C. B., 2006. Enhanced reductive dechlorination in columns treated with edible oil emulsion. *Contaminant Hydrology*. (2006): 87, 54-72.
- Careghini, A., Saponaro, S., and Sezenna, E. 2013. Biobarriers for groundwater treatment: a review. *Water Science and Technology*. 2013: 67.3, 453-468.
- Carucci, A., Ramadori, R., Rossetti, S. and Tomei, M.C. 1996. Kinetics of denitrification reactions in single sludge systems. *Science Direct*. (JAN 1996): 30, 1, 51-56.
- Chaudhuri, S. K., S. M. O'Connor, R. L. Gustavson, L. A. Achenbach, and J. D. Coates. 2002. Environmental factors that control microbial perchlorate reduction. *Applied and Environmental Microbiology* 68 (9) (SEP 2002): 4425-30.
- Characklis W.G. and Marshall K., C., 1990. *Biofilms*. New York: Wiley, - Wiley series in ecological and applied microbiology, 796 pages
- Chemtronic, 2015, http://www.chemtronic-gmbh.de/images/chemtronic/PDFe/Prospect%20AS3_AT3.pdf (Last accessed: 10/20/2015)
- Choi H. 2005. Reduction of perchlorate in a fixed biofilm process: Effects of perchlorate ion concentration, flow recirculation, and competing electron acceptors. Ph.D., University of Colorado at Boulder, <http://search.proquest.com/docview/305011815?accountid=3611>.

- Choi Y.C., and Silverstein J., 2007. Effluent recirculation to improve perchlorate reduction in a fixed biofilm reactor. *Biotechnology and Bioengineering* 98 (1) (SEP 1 2007): 132-40.
- Choi Y.C., Li, X., Raskin L., Morgenroth E., 2008. Chemisorption of oxygen onto activated carbon can enhance the stability of biological perchlorate reduction in fixed bed biofilm reactors. *Water Research* 42 (13) (JUL 2008): 3425-34.
- Choi Y.C., Li, X., Raskin L., Morgenroth E., 2007. Effect of backwashing on perchlorate removal in fixed bed biofilm reactors. *Water Research* 41 (9) (MAY 2007): 1949-59.
- Cheong, S.s., Lee S.H., Lee, J. W., Suh, C.W>, Nam, J.Y. and Shin, H.S., 2010. A comparative study of perchlorate degradation in acute toxicity and chronic toxicity. *Water Science and Technology-WST*,2010, 62 (5); 1143-8
- Chung, J., S. Shin, and J. Oh. 2010. Influence of nitrate, sulfate and operational parameters on the bioreduction of perchlorate using an up-flow packed bed reactor at high salinity. *Environmental Technology* 31 (6) (05/01; 2014/02): 693-704, <http://dx.doi.org/10.1080/09593331003621557>.
- Chung, J., S. Shin, and J. Oh. 2010. Biological reduction of nitrate and perchlorate in brine water using up-flow packed bed reactors. *Journal of Environmental Science and Health Part A-Toxic/hazardous Substances & Environmental Engineering* 45 (9) (2010): 1109-18.
- Clark I., Melnyk R.A., Engelbrektson A., and Coates, J. D., 2013. Structure and Evolution fo Chlorate Reduciton Composite Transposons <http://mbio.asm.org/content/4/4/e00379-13.full>
- Coates, J. D., K. A. Cole, R. Chakraborty, S. M. O'Connor, and L. A. Achenbach. 2002. Diversity and ubiquity of bacteria capable of utilizing humic substances as electron donors for anaerobic respiration. *Applied and Environmental Microbiology* 68 (5) (MAY 2002): 2445-52.
- Coates, J. D., U. Michaelidou, R. A. Bruce, S. M. O'Connor, J. N. Crespi, and L. A. Achenbach. 1999. Ubiquity and diversity of dissimilatory (per)chlorate-reducing bacteria. *Applied and Environmental Microbiology* 65 (12) (DEC 1999): 5234-41.
- Coates, J. D., and Achenbach, L. A., 2004. Microbial perchlorate reduction: rocket-fueled metabolism. *Nature Reviews Microbiology* 2, 569-580 (July 2004).
- Coulibaly, K. M., and Borden, R. C., 2004. Impact of edible oil injection on the permeability of aquifer sands. *Contaminant Hydrology*. 2004: 71, 219-237.
- Dasgupta, P. K., P. K. Martinelango, W. A. Jackson, T. A. Anderson, K. Tian, R. W. Tock, and S. Rajagopalan. 2005. The origin of naturally occurring perchlorate: The role of atmospheric processes. *Environmental Science & Technology* 39 (6) (MAR 15 2005): 1569-75.

- DasGupta, Purnendu K., Jason V. Dyke, Andrea B. Kirk, and W. Andrew Jackson. 2006. Perchlorate in the united states. analysis of relative source contributions to the food chain. *Environmental Science & Technology* 40 (21) (NOV 1 2006): 6608-14.
- de Geus, Daniel C., Ellen A. J. Thomassen, Peter-Leon Hagedoorn, Navraj S. Pannu, Esther van Duijn, and Jan Pieter Abrahams. 2009. Crystal structure of chlorite dismutase, a detoxifying enzyme producing molecular oxygen. *Journal of Molecular Biology* 387 (1) (MAR 20 2009): 192-206.
- De Long, S. K., X. Li, S. Bae, J. C. Brown, L. Raskin, K. A. Kinney, and M. J. Kirisits. 2012. Quantification of genes and gene transcripts for microbial perchlorate reduction in fixed-bed bioreactors. *Journal of Applied Microbiology* 112 (3) (MAR 2012): 579-92.
- Touro University Laboratory, Laboratory of Dr. Terry Else, 2015.
- Dudley, Margaret, Anna Salamone, and Robert Nerenberg. 2008. Kinetics of a chlorate-accumulating, perchlorate-reducing bacterium. *Water Research* 42 (10-11) (MAY 2008): 2403-10.
- Duffield, 2015. http://www.aqtesolv.com/aquifer-tests/aquifer_properties.htm (Last accessed: 04/21/2016).
- Eleuterio, L. 2007. Removal of the cyanobacterial toxin microcystin-LR by biofiltration: Identification of toxin-degrading bacteria and effects of backwashing. University of Nevada, Las Vegas, 2007.
- Emelko, M. B., Huck, P. M., Coffey, B. M., and Smith E. F., 2006. Effects of media, backwash, and temperature on full-scale biological filtration. *Journal (American Water Works Association)* Vol. 98, No. 12 (December 2006), pp. 61-73.
- Einsle O. and Kroneck, 2004. Structural basis of denitrification. *Biol Chem.* 2004 Oct; 385(10):875-83.
- En, C., Rong-Xin, Z., and Fei, Y. 2013. Automatic Detection and Assessment System of Water. Turbidity based on Image Processing. *TELKOMNIKA*. 2013: 11 (3), 1506 – 1513.
- Environ, 2014. <https://ndep.nv.gov/bmi/docs/nert/2014-06-19%20NERT%20RIFS%20Workplan%20Revision%202.pdf> (Last accessed: 3/21/ 2016).
- Envirogen, 2011, <http://www.envirogen.com/news/envirogen-news/showcase-installation-will-address-critical-groundwater-contamination-issue-in-california-s-rialto-colton-basin-with-high-efficiency-cost-effective-green-technology>; (Last accessed: Jan 2015).

- EOS, 2015. <http://www.eosremediation.com/eos-pro-product-information/#> (Last accessed: 10/21/ 2015).
- EPA, 2006. Perchlorate (ClO_4^-) Treatment Technologies Literature Review Operable Unit 1 Expanded Treatability Study. NASA. 2006.
- Ericksen G.E., 1983. The Chilean Nitrate Deposits: The origin of the Chilean nitrate deposits, which contain a unique group of saline minerals, has provoked lively discussion for more than 100 years. Vol. 71, No. 4 (July-August 1983), pp. 366-374.
- Falkow, S., Rosenberg, E., Schleifer, K.H., and Stackebrandt, E. 2006. The Prokaryotes: Vol. 2: Ecophysiology and Biochemistry. *Springer + Business Media. LLC*. 2006: 2, 3-15.
- Fernandez-Canque, H., Hintea, S., Csipkes, G., Pellow, A., and Smith, H. 2008. Machine Vision Application to the Detection of Micro-organism in Drinking Water. *Springer-Verlag Berlin Heidelberg*. 2008: Part III, LNAI 5179, 302 – 309.
- Frankenberger, W. T., and Herman D.C., 2000. Bacterial removal of perchlorate and nitrate. US Patent No. 6,077, 429.
- Fuller, M. E., Hatzinger, P. B., Condee, C. W., and Togna, A. P., 2007. Combined treatment of perchlorate and RDX in ground water using a fluidized bed reactor. *Ground Water Monitoring and Remediation* 27 (3) (2007): 59-64.
- Giblin, T. L., Herman, D. C., and Frankenberger, W. T., 2000. Removal of perchlorate from ground water by hydrogen-utilizing bacteria. *Journal of Environmental Quality* 29 (4) (2000): 1057-62.
- Gich F.B., Amer E., Fiqueras J.B. Abella C.A., Balaquer M.D. Poch M., 2000. Assessment of microbial community structure changes by amplified ribosomal DNA restriction analysis (ARDRA).
- Gingras, T. M., and Batista, J. R. 2002. Biological reduction of perchlorate in ion exchange regenerant solutions containing high salinity and ammonium levels. *Journal of Environmental Monitoring* 4 (1) (FEB 2002): 96-101.
- Ginsberg GL, Hattis DB, Zoeller RT, Rice DC. 2007. Evaluation of the U.S. EPA/OSWER preliminary remediation goal for perchlorate in groundwater; focus on exposure to nursing infants. *Environmental Health Perspectives* 115(3): 361-69.
- Gomez, M. A., E. Hontoria, and J. Gonzalez-Lopez. 2002. Effect of dissolved oxygen concentration on nitrate removal from groundwater using a denitrifying submerged filter. *Journal of Hazardous Materials* 90 (3) (MAR 29 2002): 267-78.

- Gu, B., Brown, G. M., and Chiang, C., 2007. Treatment of perchlorate-contaminated groundwater using highly selective, regenerable ion-exchange technologies. *Environmental Science & Technology* 41 (17) (SEP 1 2007): 6277-82.
- Gu, B., and Coates, J.D., 2006. *Perchlorate: Environmental occurrence, interactions and treatment*. New York: Springer.
- Gullick, R. Q., Lechvallier, M. W., and Barhorst, T. A. S. 2001. Occurrence of perchlorate in drinking water sources. *Journal American Water Works Association* 93 (1) (JAN 2001).
- Gurol, M. D., and Kim, K. 1999. Investigation of perchlorate removal in drinking water sources by chemical methods. *Abstracts of Papers of the American Chemical Society* 218 (AUG 22 1999): U554-.
- Hach, 2015. <http://www.hach.com/ph-orp-sensors/family?productCategoryId=35546331620> (Last accessed: 10/1/2015).
- Hanes, D.M., Vincent C.E., Huntley, D.A., and Clark T.L., 1988. *Acoustic measurements of suspended sand concentration in C2S2 experiment Stanhope Lane, Prince Edward Island*. Marine Geology (June 1988), Pages 185-196.
- Hatzinger, P., and Diebold, J. 2009. In Situ Bioremediation of Perchlorate in Groundwater. *ESTCP Project ER-0224*. 2009: Final Report.
- Hatzikioseyan, A., and Tsezos, M., 2006. Modelling of microbial metabolism stoichiometry: Application in bioleaching processes. *Hydrometallurgy* 83 (1–4) (9): 29-34.
- Hatzinger, P. B. 2005. Perchlorate biodegradation for water treatment. *Environmental Science & Technology* 39 (11) (JUN 1 2005).
- Hatzinger, P. B. 2010. Perchlorate: Overview and cleanup case studies., Shaw Environmental, Inc., Lawrenceville, NJ.
- Herman, D. C., and W. T. Frankenberger, 1999. Bacterial reduction of perchlorate and nitrate in water. *Journal of Environmental Quality* 28 (3) (MAY-JUN 1999): 1018-24.
- Herman, D. C., and W. T. Frankenberger, 1997. Bacterial reduction of perchlorate and nitrate in water. US Patent 6077429 A
- Herman, D. C. and W. T. Frankenberger, 1998. Microbial-mediated reduction of perchlorate in groundwater. *Journal of Environmental Quality* 27 (4) (JUL-AUG 1998): 750-4.
- Hernandez, D., and Rowe, J. J., 1987. Oxygen regulation of nitrate uptake in denitrifying *Pseudomonas aeruginosa*. *Appl Environ Microbiol.* (APR 1987): 53(4), 745–750.

- Higuchi, R., Dollinger, G., Walsh, P. S., and Griffith, R. 1992. Simultaneous amplification and detection of specific DNA sequences. *Bio/technology* 10: 413-417.
- Horn, H., and Lackner, S., 2014. Modeling of Biofilm Systems: A Review. *Advances in Biochemical Engineering/Biotechnology*. 2014: 146, 53-76.
- Hubert, C. and Voordouw, G. 2007. Oil field souring control by nitrate-reducing *Sulfurospirillum* spp. that outcompete sulfate-reducing bacteria for organic electron donors. *Appl Environ Microbiol.* (APR 2007): 73(8), 2644-52.
- Hunter, J. V., and Faust, S.D., 1971. *Organic compounds in aquatic environments*. New York: M. Dekker.
- Hunter, W. J., 2001. Use of vegetable oil in a pilot-scale denitrifying barrier. *Contaminant Hydrology*. 2001: 53, 119-131.
- Hyman, M. 2001. *Groundwater and soil remediation: Process design and cost estimating of proven technologies*. Reston, VA, USA: ASCE.
- ITRC, 2008. *Perchlorate Remediation Technologies*. Technical and Regulatory Guidance document: Remediation Technologies for Perchlorate Contamination in Water and Soil (PERC-2, 2008).
- ITRC, 2011. *Environmental molecular diagnostics fact sheets*. 50 F Street NW, Suite 350, Washington, DC 20001: The Interstate Technology & Regulatory Council Environmental Molecular Diagnostics Team, EMD-1.
- Jackson, W. A., Boehlke J. K., Gu, B., Hatzinger, P.B., and Sturchio, N. C., 2010. Isotopic composition and origin of indigenous natural perchlorate and co-occurring nitrate in the southwestern united states (vol 44, pg 4869, 2010). *Environmental Science & Technology* 44 (24) (2010): 9597.
- Jackson, W. A., Davila, A. F., Estrada, N., Lyons, W. B., Coates, J. D., and Priscu J. C., 2012. Perchlorate and chlorate biogeochemistry in ice-covered lakes of the McMurdo dry valleys, antarctica. *Geochimica Et Cosmochimica Acta* 98 (2012): 19-30.
- Jiménez, N., Viñas, M., Guiu-Aragones, C., Bayona, J. M., Albaiges, J., and Solanas, A.M., 2011. Polyphasic approach for assessing changes in an autochthonous marine bacterial community in the presence of Prestige fuel oil and its biodegradation potential. *Environmental Biotechnology*. 2011: 91:823–834.
- Jördening, Hans-Joachim, and Klaus Buchholz. 1999; 2008. Fixed film stationary bed and fluidized bed.

- Jung, Y., Coulibaly, K.M., Borden, R.C., 2006. Transport of edible oil emulsions in clayey-sands: 3-D sandbox results and model validation. *J. Hydrol. Eng.* 11 (3), 238–244.
- Katza, I., Greenb, M., Ruskolb, Y., and Dosoretz, C. G. 2000. Characterization of atrazine degradation and nitrate reduction by *Pseudomonas* sp. strain ADP. *Advances in Environmental Research*. 2000: 4(3), 211–218.
- Kengen, S. W. M., G. B. Rikken, W. R. Hagen, C. G. van Ginkel, and A. J. M. Stams. 1999. Purification and characterization of (per)chlorate reductase from the chlorate-respiring strain GR-1. *Journal of Bacteriology* 181 (21) (NOV 1999).
- Kengo, M., Kengo, K., Hideki, H., (2014). Molecular Diversity of Eukaryotes in Municipal Wastewater Treatment Processes as Revealed by 18SrRNA Gene Analysis. *Microbes Environ.* (2014). Vol. 29, No. 4, 401-407.
- Kesterson, K. E., P. S. Amy, and J. R. Batista. 2007. Limitations to natural bioremediation of perchlorate in a contaminated site. *Bioremediation Journal* 9 (3-4): 129-139.
- Kim, H. S., P. R. Jaffe, and L. Y. Young. 2004. Simulating biodegradation of toluene in sand column experiments at the macroscopic and pore-level scale for aerobic and denitrifying conditions. *Advances in Water Resources* 27 (4) (APR 2004): 335-48.
- Kim, K., and B. E. Logan. 2001. Microbial reduction of perchlorate in pure and mixed culture packed-bed bioreactors. *Water Research* 35 (13) (SEP 2001): 3071-6.
- Kim, K. 2000. Fixed-bed bioreactor treating perchlorate-contaminated waters. *Environmental Engineering Science* 17 (5) (SEP-OCT 2000): 257-65.
- Kimbrough, David Eugene, and Pankaj Parekh. 2007. Occurrence and co-occurrence of perchlorate and nitrate in california drinking water sources. *Journal American Water Works Association* 99 (9) (SEP 2007): 126-32.
- Kim et al., 2004. Technical Report.
http://www.geol.sc.edu/gvoulgar/TechReports/CPSD_TechReport_04_02.pdf (Last accessed: 10/1/2015).
- Kim, W., Rqcimo, F., Schluter, J., Levy, S.B., and Foster, K.R., 2014. Importance of positioning for microbial evolution. *Cross Mark*. <http://www.pnas.org/content/111/16/E1639.full.pdf>.
- Kohler, E., Villiger, J., Posch, T., Derlon, N., Shabarova, T., Morgenroth, E., Pernthaler, J., and Blom, J. F. 2014. Biodegradation of Microcystins during Gravity-Driven Membrane (GDM) Ultrafiltration. *PLoS ONE*. 2014: 9(11), e111794.
- Kounaves, S. P., Stroble, S.T., Anderson, R. M., Moore, Q., Catling, D. C., Douglas S., McKay C.P., Ming D.W., Smith P.H., Tamppari, L.K., and Zent A.P., 2010. Discovery of natural

- perchlorate in the antarctic dry valleys and its global implications. *Environmental Science & Technology* 44 (7) (APR 1 2010): 2360-4.
- Korenkov, V.N., V. Ivanovich, S.I. Kuznetsov, and J.V. Vorenov. 1976. Process for purification of industrial waste waters from perchlorates and chlorates. U.S. Patent No. 3,943,055.
- Kwon, S., Taek-Seung, K., Gi, J.Y., Joon-Hong, J., and Hee-Dung, P., 2010. Bacterial Community Composition and Diversity of a Full-Scale Integrated Fixed-Film Activated Sludge System as Investigated by Pyrosequencing. *J. Microbiol. Biotechnol.* (2010), 20(12), 1717–1723.
- Krauter, Paula, Bill Daily, Valerie Dibley, Holly Pinkart, and Tina Legler. 2005. Perchlorate and nitrate remediation efficiency and microbial diversity in a containerized wetland bioreactor. *International Journal of Phytoremediation* 7 (2) (04/01; 2014/02): 113-28, <http://dx.doi.org/10.1080/16226510590950414>.
- LaPara, T. M., C. H. Nakatsu, L. Pantea, and J. E. Alleman. 2000. Phylogenetic analysis of bacterial communities in mesophilic and thermophilic bioreactors treating pharmaceutical wastewater. *Appl Environ Microbiol.* 66 (9): 3951-9.
- Laurent, P., A. Kihn, A. Andersson, and P. Servais. 2003. Impact of backwashing on nitrification in the biological activated carbon filters used in drinking water treatment. *Environmental Technology* 24 (3) (MAR 2003): 277-87.
- Lehman, S.G., Badruzzamana M., Adham, S., Roberts, D.J., and Clifford, D.A. 2008. Perchlorate and nitrate treatment by ion exchange integrated with biological brine treatment. *Water Research*. 2008: 42, 969– 976.
- Levenspiel O., 1972. Chemical Reaction Engineering. Third Edition. John Wiley and Sons.
- Li, Xu, Wangki Yuen, Eberhard Morgenroth, and Lutgarde Raskin. 2012. Backwash intensity and frequency impact the microbial community structure and function in a fixed-bed biofilm reactor. *Applied Microbiology and Biotechnology*: 1-13.
- Liebensteiner, M. G., Martijn W. H. Pinkse, Peter J. Schaap, Alfons J. M. Stams, and Bart P. Lomans. 2013. Archaeal (per)chlorate reduction at high temperature: An interplay of biotic and abiotic reactions. *Science* 340 (6128) (APR 5 2013): 85-7.
- Liu J., 2000. MS. Thesis, University of Nevada, Las Vegas, NV.
- Liwarska-Bizukojc, E., 2005. Application of image analysis techniques in activated wastewater treatment processes. *Biotechnology Letters*. 2005: 25, 1427-1433.

- Liwarka-Bizukojc, E., Bizukojc, M., and Ledakowicz S. 2012. Denitrification in the activated sludge systems: study of the kinetics, *Architecture Civil Engineering Environment*. *Architecture Civil Engineering Environment*. (2012): 5, 2, 101-108.
- Logan, B. E., K. Kim, P. Mulvaney, J. Miller, J. Wu, and H. S. Zhang. 1999. Factors affecting biodegradation of perchlorate-contaminated waters. *Abstracts of Papers of the American Chemical Society* 218 (AUG 22 1999): U560-.
- Logan. 1998. A review of chlorate- and perchlorate-respiring microorganisms. *Bioremediation Journal* 2 (2): 69-79.
- Logan, B. E. 2001 a. Analysis of overall perchlorate removal rates in packed-bed bioreactors. *Journal of Environmental Engineering-Asce* 127 (5) (MAY 2001): 469-71.
- Logan, B. E., J. Wu, and R. F. Unz. 2001 b. Biological perchlorate reduction in high-salinity solutions. *Water Research* 35 (12) (AUG 2001): 3034-8.
- Logan, B. E., H. S. Zhang, P. Mulvaney, M. G. Milner, I. M. Head, and R. F. Unz. 2001 c. Kinetics of perchlorate- and chlorate-respiring bacteria. *Applied and Environmental Microbiology* 67 (6) (JUN 2001): 2499-506.
- Logan, B. E., and D. LaPoint. 2002. Treatment of perchlorate- and nitrate-contaminated groundwater in an autotrophic, gas phase, packed-bed bioreactor. *Water Research* 36 (14) (AUG 2002): 3647-53.
- London, M. R., De Long S.K., Strahota, M.D., Katz, L.E., and Speitel, G.E. Jr., 2011. Autohydrogenotrophic perchlorate reduction kinetics of a microbial consortium in the presence and absence of nitrate. *Water Research* 45 (19) (DEC 1 2011): 6593-601.
- Long, C. M., and Borden, R.C., 2006. Enhanced reductive dechlorination in columns treated with edible oil emulsion. *Journal of Contaminant Hydrology* 87 (2006) 54-72.
- Lybrand, R. A., Michalski, G., Graham, R.C., and Parker, D. R. 2013. The geochemical associations of nitrate and naturally formed perchlorate in the Mojave desert, California, USA. *Geochimica Et Cosmochimica Acta* 104 (MAR 1 2013): 136-47.
- Luijten, M.L., de Weert, J., Smidt, H., Boschker, H.T., de Vos, W.M., Schraa, G., and Stams, A.J. 2003. Description of *Sulfurospirillum halorespirans* sp. nov., an anaerobic, tetrachloroethene-respiring bacterium, and transfer of *Dehalosporillum multivorans* to the genus *Sulfurospirillum* as *Sulfurospirillum multivorans* comb. nov. *Int J Syst Evol Microbiol*. (MAY 2003): 53(Pt 3):787-93.
- Macdonald, D. V. 1990. Denitrification by an expanded bed biofilm reactor. *Research Journal of the Water Pollution Control Federation* 62 (6) (SEP-OCT 1990): 796-802.

- Madigan M.T., Matinko J.M., Dunlap P.V., Clark D.P., 2009. Brock Biology of Microorganisms.
- Mafla, S., Moraga, R., León, C. G., Guzmán-Fierro, V. G., Yañez, J., Smith, C. T., Mondaca, M. A., and Campos, V. L. 2015. *Springer Netherlands*. 2015: 31(8), 1267-77.
- Mafft, 2015. <http://mafft.cbrc.jp/alignment/software/>.
- Mallard, F., Le Bourlot, V., and Tully, T., 2013. An Automated Image Analysis System to Measure and Count Organisms in Laboratory Microcosms. *PLOS ONE*. 2013: 8 (5), e64387
- Malik, A., Grohmann, E. and Alves, M., 2013. Management of Microbial Resources in the Environment. *Springer Science + Business Media Dordrecht*. 2013.
- Metcalf and Eddy, 2006. Wastewater Engineering: Treatment and Reuse. Eighth reprint. Tata McGraw-Hill Publishing Company Limited.
- Malmqvist, A., T. Welander, and L. Gunnarsson. 1991. Anaerobic growth of microorganisms with chlorate as an electron-acceptor. *Applied and Environmental Microbiology* 57 (8) (AUG 1991): 2229-32.
- Malmqvist, A., T. Welander, E. Moore, A. Ternstrom, G. Molin, and I. M. Stenstrom. 1994. Ideonella-dechloratans gen-nov, sp-nov, a new bacterium capable of growing anaerobically with chlorate as an electron-acceptor. *Systematic and Applied Microbiology* 17 (1) (MAR 1994): 58-64.
- Marangon, J., Paes de Sousa, P.M., Moura, I., Brondino, C.D., Moura, J.J., and Gonzalez, p.J., 2012. Substrate-dependent modulation of the enzymatic catalytic activity: Reduction of nitrate, chlorate and perchlorate by respiratory nitrate reductase from marinobacter hydrocarbonoclasticus 617. *Biochimica Et Biophysica Acta-Bioenergetics* 1817 (7) (JUL 2012): 1072-82.
- Mardis, E. R., 2008. Next-Generation DNA Sequencing Method. <http://www.columbia.edu/cu/biology/courses/w3034/Dan/readings/6-12.pdf>.
- Marsh T.L., Saxman P., Cole J., and Tiedje J., 2000. Terminal Restriction Fragment Length Polymorphism Analysis Program, a Web-Based Research Tool for Microbial Community Analysis. *Applied and Environmental Microbiology*, 2000.
- Maltos, C. T., Velizarov, S., Crespo, J. G., and Reis, M. A. M., 2006. Simultaneous removal of perchlorate and nitrate from drinking water using the ion exchange membrane bioreactor concept. *Water Research* 40 (2) (JAN 2006): 231-40.
- Maphosa, F., van Passel, M.W., de Vos, W.M., and Smidt, H. 2012. Metagenome analysis reveals yet unexplored reductive dechlorinating potential of Dehalobacter sp. E1 growing in

- co-culture with *Sedimentibacter* sp. *Society for Applied Microbiology and Blackwell Publishing Ltd.* 2012: 4(6), 604-16.
- Marttila, H., Postila, H., and Klove, B., 2010. Calibration of turbidity meter and acoustic doppler velocimetry (Triton-ADV) for sediment types present in drained peatland headwaters: Focus on particulate organic peat. *River Research Applications*. Volume 26, Issue 8, pages 1019–1035, October 2010.
- McCarty, P. L. 1971. Energetics and kinetics of anaerobic treatment. *Advances in Chemistry Series* (105) (1971).
- McCarty, P. L., and Meyer, T. E. 2005. Numerical model for biological fluidized-bed reactor treatment of perchlorate-contaminated groundwater. *Environmental Science & Technology* 39 (3) (FEB 1 2005): 850-8.
- McLaughlin, C. L., Blake, S., Hall, T., Harman, M., Kanda, R., Hunt, J., and Rumsby, P.C., 2011. Perchlorate in raw and drinking water sources in england and wales. *Water and Environment Journal* 25 (4) (DEC 2011): 456-65.
- McVicar, M., Anderson, L., Zevenhuizen, E., Mackie, A. L., Walsh, M. E., and Gagnon, G. A., 2012. Water reclamation and reuse. *Water Environment Research* 84 (10) (OCT 2012): 1332-46.
- Miller, J. P., and Logan B. E., 2000. Sustained perchlorate degradation in an autotrophic, gas-phase, packed-bed bioreactor. *Environmental Science & Technology* 34 (14) (JUL 15 2000): 3018-22.
- Miltner T.J., Summers, R.S. and Wang, J.X., 1995 Biofiltration Preformance: Part 2, Effect of Backwashing, American Water Works Association, 87 (12) 64-70.
- Min, B., Evans, P. J., Chu, A. K., and Logan, B. E., 2004. Perchlorate removal in sand and plastic media bioreactors. *Water Research* 38 (1) (JAN 2004): 47-60.
- Motzer, W. E. 2001. Perchlorate: Problems, detection, and solutions. *Environmental Forensics* 2 (4) (01/01; 2012/10): 301-11, <http://www.tandfonline.com/doi/abs/10.1006/enfo.2001.0059>.
- Murga, R., Stewart, P.S., and Daly, D., 1995. Quantitative analysis of biofilm thickness variability. *Biotechnology and Bioengineering*, Vol. 45, Pp. 503-510.
- MWH, ed. 2005. *Water treatment: Principles and design*. Second ed. Hoboken, New Jersey: John Wiley & Sons, Inc.
- Vijaya Nadaraja, A. Gangadharan Puthiya Veetil, P. and Bhaskaran, K., 2013. Perchlorate reduction by an isolated *serratia marcescens* strain under high salt and extreme pH. *FEMS Microbiology Letters* 339 (2) (FEB 2013): 117-21.

- Nakhla, G., and Shaukat F., 2003. Simultaneous nitrification–denitrification in slow sand filters. *Journal of Hazardous Materials* 96 (2–3) (1/31): 291-303.
- NDEP, 2011. <http://ndep.nv.gov/bca/perchlorate05.htm>.
- Nerenberg, R., and Rittmann, B. E., 2004. Hydrogen-based, hollow-fiber membrane biofilm reactor for reduction of perchlorate and other oxidized contaminants. *Water Science and Technology* 49 (11-12) (2004): 223-30.
- Nerenberg, R., Rittmann, B. E., and Najm, I., 2003. Perchlorate reduction in a hydrogen-based membrane-biofilm reactor (vol 94, pg 103, 2002). *Journal American Water Works Association* 95 (2) (FEB 2003).
- Nerenberg, R., Yasunori K., and Bruce E. R., 2008. Microbial ecology of a perchlorate-reducing, hydrogen-based membrane biofilm reactor. *Water Research* 42 (4-5) (FEB 2008): 1151-9.
- Nerenberg, R., Yasunori K., and Rittmann, B. E., 2006. Kinetics of a hydrogen-oxidizing, perchlorate-reducing bacterium. *Water Research* 40 (17) (OCT 2006).
- NIH, 2015. <https://imagej.nih.gov/ij/>.
- Nor, Seong Jin, Sang Hyon Lee, Kyung-Suk Cho, Daniel K. Cha, Kang In Lee, and Hee Wook Ryu. 2011. Microbial treatment of high-strength perchlorate wastewater. *Bioresource Technology* 102 (2) (JAN 2011): 835-41.
- Nozawa-Inoue, M., Scow KM, and Rolston DE. Reduction of perchlorate and nitrate by microbial communities in vadose soil. - *Appl Environ Microbiol.* 2005 Jul;71(7):3928-34.
- O'Connor, S. M., and Coates, J. D., 2002. Universal immunoprobe for (per)chlorate-reducing bacteria. *Applied and Environmental Microbiology* 68 (6) (JUN 2002): 3108-13.
- Okeke, B. C., and Frankenberger, W. T., 2003. Molecular analysis of a perchlorate reductase from a perchlorate-respiring bacterium perclace. *Microbiological Research* 158 (4) (2003): 337-44.
- Okeke, B. C., Giblin, T., and Frankenberger, W. T., 2002. Reduction of perchlorate and nitrate by salt tolerant bacteria. *Environmental Pollution* 118 (3) (2002): 357-63.
- Okeke, B. C., Ma, G., Cheng, Q., Losi, M. E., and Frankenberger, W.T. Jr., 2007. Development of a perchlorate reductase-based biosensor for real time analysis of perchlorate in water. *Journal of Microbiological Methods* 68 (1) (JAN 2007): 69-75.
- Omoregie, E. O., Couture, R.M., Van Cappellen, P., Corkhill, C. L., Charnock, J.M., Polya, D.A., Vaughan, D., Vanbroekhoven, K. and Lloyd, J. R. 2013. Arsenic Bioremediation by Biogenic Iron Oxides and Sulfides. American Society for Microbiology. 2013.

- Ontiveros-Valencia, A., Tang, Y., Krajmalnik-Brown, R., and Rittmann, B.E., 2013. Perchlorate reduction from a highly contaminated groundwater in the presence of sulfate-reducing bacteria in a hydrogen-fed biofilm. *Biotechnology and Bioengineering* 110 (12) (DEC 2013): 3139-47.
- Oren, A. 1999. Bioenergetic Aspects of Halophilism. *Microbiology and Molecular Biology Reviews*. 1999: 63(2), 334-338.
- Ortiz-Bernad, I., Anderson, R.T., Vrionis, H.A., and Lovley, D. R. 2004. Resistance of Solid-Phase U(VI) to Microbial Reduction during In Situ Bioremediation of Uranium-Contaminated Groundwater. *Applied and Environmental Microbiology*. 2004. 70(12), 7558-7560.
- OSWER, December 2013. Introduction to In Situ Bioremediation of Groundwater. *United States Environmental Protection Agency*. December 2013: 542, R, 13-018.
- Palmer Jr, Robert J., and David C. White. 1997. Developmental biology of biofilms: Implications for treatment and control. *Trends in Microbiology* 5 (11) (11): 435-40.
- Parker, D. R., 2009. Perchlorate in the environment: The emerging emphasis on natural occurrence. *Environmental Chemistry* 6 (1) (2009): 10-27.
- Pester, M., Brambilla, E., Alazard, D., Rattei, T., Weinmaier, T., Han, J., Lucas, S., Lapidus, A., Cheng, J.F., Goodwin, L., Pitluck, S., Peters, L., Ovchinnikova, G., Teshima, H., Detter, J.C., Han, C.S., Tapia, R., Land, M.L., Hauser, L., Kyrpides, N.C., Ivanova, N.N., Pagani, I., Huntmann, M., Wei, C.L., Davenport, K.W., Daligault, H., Chain, P.S., Chen, A., Mavromatis, K., Markowitz, V., Szeto, E., Mikhailova, N., Pati, A., Wagner, M., Woyke, T., Ollivier, B., Klenk, H.P., Spring, S., and Loy, A., 2012. Complete genome sequences of *Desulfosporosinus orientis* DSM765T, *Desulfosporosinus youngiae* DSM17734T, *Desulfosporosinus meridiei* DSM13257T, and *Desulfosporosinus acidiphilus* DSM22704T. *J Bacteriol.* 2012: 194(22), 6300-1.
- Patel, A., Zuo, G., Lehman, S. G., Badruzzaman, M., Clifford, D. A. and Roberts, D. J., 2008. Fluidized bed reactor for the biological treatment of ion-exchange brine containing perchlorate and nitrate. *Water Research* 42 (16) (10): 4291-8.
- Pawley, J. B., 2006. Handbook of Biological Confocal Microscopy, 3rd ed., (Springer Science+Business Media, LLC, New York, 2006, pp.404–413
- Peyton, B.M. 1994. Statistical analysis of the effect of substrate utilization and shear stress on the kinetics of biofilm detachment. *Biotech. Bioengr.*, 41, 728–735.
- Peyton, B.M. 1996. Effects of Shear Stress and Substrate Loading Rate on *Pseudomonas Aeruginosa* Biofilm Thickness and Density. *Water Research*. 1996. 30(1), 29-36.

- Prata, F.C.P., 2014. Perchlorate and chlorate degradation by two organisms isolated from wastewater Microbial identification and kinetics. Instituto Superior Technico, 2014.
- Ricardo, A. R., Carvalho, G., Velizarov, S., Crespo, J.G., and Reis, M. A., 2012. Kinetics of nitrate and perchlorate removal and biofilm stratification in an ion exchange membrane bioreactor. *Water Research* 46 (14) (SEP 15 2012).
- Rikken, G. B., Kroon, A. G. M., and van Ginkel, C. G., 1996. Transformation of (per)chlorate into chloride by a newly isolated bacterium: Reduction and dismutation. *Applied Microbiology and Biotechnology* 45 (3) (APR 1996): 420-6.
- Rittmann, B. E., and McCarty, P.L. 1980 a. Evaluation of Steady-State-Biofilm Kinetics. *Biotechnology and Bioengineering*. 1980: XXII, 2359-2373.
- Rittmann, B. E., and McCarty, P.L. 1980 b. Model of Steady-State-Biofilm Kinetics. *Biotechnology and Bioengineering*. 1980: XXII, 2343-2357.
- Rittmann, B.E. 1981. The effect of shear stress on biofilm loss rate.
<http://onlinelibrary.wiley.com/doi/10.1002/bit.260240219/epdf>.
- Rittmann, B. E. 2006. The membrane biofilm reactor: The natural partnership of membranes and biofilm. *Water Science and Technology* 53 (3) (2006): 219-25.
- Rittmann, B. E. 2010. Environmental biotechnology in water and wastewater treatment. *Journal of Environmental Engineering-Asce* 136 (4) (APR 2010): 348-53 (Last accessed: 1/23/2014 6:44:58 PM).
- Rittmann, B. E., and McCarty, P.L. 2001. *Environmental biotechnology: Principles and applications*. McGraw-hill series in water resources and environmental engineering. Boston: McGraw-Hill.
- Robertson, W. J., Bowman, J.P., Franzmann, P.D., and Mee, B.J. 2001. Desulfosporosinus meridiei sp. nov., a spore-forming sulfate-reducing bacterium isolated from gasoline-contaminated groundwater. *Int J Syst Evol Microbiol*. 2001: 51(Pt 1), 133-40.
- Royce, 2015. http://www.roycetechnologies.com/refdocs/Royce_711Portable.pdf (Last accessed: 10/1/2015).
- Ryu, H. W., Nor, S., J., Moon, K., E., Cho, K.S., Cha, D. K., and Rhee, K.I., 2012. Reduction of perchlorate by salt tolerant bacterial consortia. *Bioresource Technology* 103 (1) (JAN 2012): 279-85.
- Sahu, A.K., Conneely, T., Nuesslein, K., and Ergas, S.J., 2009. Hydrogenotrophic denitrification and perchlorate reduction in ion exchange brines using membrane biofilm reactors. *Biotechnology and Bioengineering* 104 (3) (OCT 15 2009): 483-91.

- Schaefer, C.E., Fuller, M.E., Condee, C.W., Lowey, J.M, and Hatzinger, P. B., 2007. Comparison of biotic and abiotic treatment approaches for co-mingled perchlorate, nitrate, and nitramine explosives in groundwater. *Journal of Contaminant Hydrology*. 89 (2007) 231–250.
- Schneider, C. A., Rasband, W. S. and Eliceiri, K. W., 2012. NIH image to imageJ: 25 years of image analysis. *Nature methods*. 9, 671-675, 2012.
<http://www.nature.com/nmeth/journal/v9/n7/full/nmeth.2089.html>.
- Sellers, K., 2007. Perchlorate: Environmental problems and solutions. Boca Raton: CRC/Taylor & Francis, <http://www.library.unlv.edu/giving/bookplates/>.
- Servais P., Billen, G., Ventresque, C. and Bablon G.P., 1991. Microbial activity in GAC filters at the Choisy-le-Roi treatment plant. *Journal of American Water Works Association*. 83 (2), pp. 62-68.
- Shah, D. B., and Coulman, G. A. 1978. Kinetics of nitrification and denitrification reactions. *Biotechnology and Bioengineering*. (JAN 1978): 20, 1, 43-72.
- Sharbatmaleki, M., 2010. Investigation of potential pathways and multi-cycle bioregeneration of ion-exchange resin laden with perchlorate. University of Nevada, Las Vegas Thesis
- Sharbatmaleki, M., and Batista, J.R., 2012. Multi-cycle bioregeneration of spent perchlorate-containing macroporous selective anion-exchange resin. *Water Research* 46 (1) (JAN 1 2012): 21-32.
- Shen, L., Lu, Y., and Liu, Y., 2012. Mathematical modeling of biofilm-covered granular activated carbon: A review. *Journal of Chemical Technology and Biotechnology* 87 (11) (NOV 2012): 1513-20.
- Shendure J. and Ji H., 2008. Next-generation DNA sequencing.
<http://www.nature.com/nbt/journal/v26/n10/full/nbt1486.html>.
- Shiratori, H., Ikeno, H., Ayame, S., Kataoka, N., Miya, A., Hosono, K., Beppu, T., and Ueda, K., 2006. Isolation and Characterization of a New *Clostridium* sp. That Performs Effective Cellulosic Waste Digestion in a Thermophilic Methanogenic Bioreactor. *Applied and Environmental Microbiology*. 2006: 72(5), 3702–3709.
- Shrout, J. D., and Parkin, G. F., 2006. Influence of electron donor, oxygen, and redox potential on bacterial perchlorate degradation. *Water Research* 40 (6) (MAR 2006): 1191-9.
- Shrout, J. D., Williams, A. G. B., Scherer, M. M., and Parkin, G. F., 2005. Inhibition of bacterial perchlorate reduction by zero-valent iron. *Biodegradation* 16 (1) (FEB 2005): 23-32.

- Siddiqui, R. A., Warneckeberz, U., Hengsberger, A., Schneider, B., Kostka, S., and Friedrich, B., 1993. Structure and function of a periplasmic nitrate reductase in *alcaligenes-eutrophus* H16. *Journal of Bacteriology* 175 (18) (SEP 1993): 5867-76.
- Sohaskey, C.D. 2005. Regulation of nitrate reductase activity in *Mycobacterium tuberculosis* by oxygen and nitric oxide. *Microbiology*. (NOV 2005) 151(11), 3803-10.
- Solutions-IES, 2010. Edible Oil Barriers for Treatment of Chlorinated Solvent and Perchlorate-Contaminated Groundwater. *Environmental Security Technology Certification Program*. 2010: ER-0221.
- Song, Y. G., and Logan, B. E., 2004. Effect of O₂ exposure on perchlorate reduction by *dechlorosoma* sp KJ. *Water Research* 38 (6) (MAR 2004): 1626-32.
- Song, K.G., Cho, J., Cho, K.W., Kim S.D., and Ahn, K.H., 2010. Characteristics of simultaneous nitrogen and phosphorus removal in a pilot-scale sequencing anoxic/anaerobic membrane bioreactor at various conditions. *Desalination*, 250: 801-804.
- Spain A. M., Peacock, A.D., Istok, J. D., Elshahed, M.S., Najar, F.Z., Roe, B. R., White, D.C. and Krumholz, L.R., 2007. Identification and Isolation of a *Castellaniella* Species Important during Biostimulation of an Acidic Nitrate- and Uranium-Contaminated Aquifer. *Applied and Environmental Microbiology*, 2007, p. 4892–4904.
- Shapleigh, 2015 <https://micro.cornell.edu/research/shapleigh-lab>.
- Srinivasan, R., and Sorial. G.A., 2009. Treatment of perchlorate in drinking water: A critical review. *Separation and Purification Technology* 69 (1) (SEP 15 2009): 7-21.
- Stepanov, V. G., Xiao, Y., Tran, Q., Rojas, M., Willson, R. C., Fofanov, Y., and Roberts, D. J. 2014. The presence of nitrate dramatically changed the predominant microbial community in perchlorate degrading cultures under saline conditions. *BMC Microbiology*. 2014: 14, 225.
- Sutton, P. M., Greene, M., and Pitre, M. P., 1999. Treatment of groundwater containing perchlorate using biological fluidized bed reactors with GAC or sand media. *Abstracts of Papers of the American Chemical Society* 218 (AUG 22 1999): U557-.
- Sutton, P. M., 2006. Bioreactor configurations for ex-situ treatment of perchlorate: A review. *Water Environment Research* 78 (13) (DEC 2006): 2417-27.
- Tan, K., Anderson, T. A., and Jackson, W. A., 2005. Temporal and spatial variation of perchlorate in streambed sediments: Results from in-situ dialysis samplers. *Environmental Pollution* 136 (2) (JUL 2005): 283-91.
- Tan, K., 2004. Degradation kinetics of perchlorate in sediments and soils. *Water Air and Soil Pollution* 151 (1-4) (JAN 2004): 245-59.

- Tang, Y., Zhao, H. Marcus, A.K., Krajmalnik-Brown, R., and Rittmann, B. E., 2012. A steady-state biofilm model for simultaneous reduction of nitrate and perchlorate, part 1: Model development and numerical solution. *Environmental Science & Technology* 46 (3) (FEB 7 2012): 1598-607.
- Tang, Y., Zhao, H. Marcus, A.K., Krajmalnik-Brown, R., and Rittmann, B. E., 2012. A steady-state biofilm model for simultaneous reduction of nitrate and perchlorate, part 2: Parameter optimization and results and discussion. *Environmental Science & Technology* 46 (3) (FEB 7 2012): 1608-15.
- Tang, Y., Ziv-El, M., Zhou, C., Shin, J. H., Ahn, C. H., Meyer, K., Candelaria, D., 2010. Bioreduction of nitrate in groundwater using a pilot-scale hydrogen-based membrane biofilm reactor. *Frontiers of Environmental Science & Engineering in China* 4 (3) (SEP 2010): 280-5.
- Teefy, S.M., and Singer, P.C. 1990. Performance and Analysis of Tracer Tests to Determine Compliance of a Disinfection Scheme With the SWTR. AWWA. 1990.
- Thrash, J. C, Trump, J. I.V, Weber, K. A. Miller, E. Achenbach, L.A> and Coates, J. D., 2007. Electrochemical Stimulation of Microbial Perchlorate Reduction. *Environ,Sci. Technol.*, 2007, 41, 1740-1746.
- Theron, J. and Cloete, T.E., 2000. Molecular techniques for determining microbial diversity and community structure in natural environments. *Critical Reviews in Microbiology* 26: 37– 57
- Trulear, M.G., and Characklis, W.G. 1982. Dynamics of Biofilm Processes. *Water Pollution Control Federation*. 1982: 54(9), 1288-1301.
- Urfer, D., Huck, P., Booth, S., Coffey, B. (1997) Biological filtration for BOM and particle removal: a critical review. *Journal - American Water Works Association* 89 (12), 83-98.
- Urbansky, E. T., 1998. Perchlorate Chemistry: Implications for Analysis and Remediation. <https://clu-in.org/download/contaminantfocus/perchlorate/urbansky2.pdf>.
- Urbansky, E. T., 2000. *Perchlorate in the environment*. Environmental science research. Vol. 57. New York: Kluwer Academic/Plenum Publishers.
- van Ginkel, C. G., Plugge, C. M., and Stroo. C. A., 1995. Reduction of chlorate with various energy substrates and inocula under anaerobic conditions. *Chemosphere* 31 (9) (11): 4057-66.
- van Ginkel, Steven W., Chang Hoon Ahn, Mohammad Badruzzaman, Deborah J. Roberts, S. Geno Lehman, Samer S. Adham, and Bruce E. Rittmann. 2008. Kinetics of nitrate and perchlorate reduction in ion-exchange brine using the membrane biofilm reactor (MBfR). *Water Research* 42 (15) (SEP 2008): 4197-205.

- Van Ginkel, Steven W., Regina Lamendella, William P. Kovacik Jr., Jorge W. Santo Domingo, and Bruce E. Rittmann. 2010. Microbial community structure during nitrate and perchlorate reduction in ion-exchange brine using the hydrogen-based membrane biofilm reactor (MBfR). *Bioresource Technology* 101 (10) (MAY 2010): 3747-50.
- van Ginkel, Steven W., Chen Zhou, Michael Lien, and Bruce E. Rittmann. 2011. Hydrogen-based nitrate and selenate bioreductions in flue-gas desulfurization brine. *Journal of Environmental Engineering-Asce* 137 (1) (JAN 2011): 63-8 (Last accessed: 1/23/2014 6:44:58 PM).
- van Glinkel, C. G., G. B. Rikken, A. G. M. Kroon, and S. W. M. Kengen. 1996. Purification and characterization of chlorite dismutase: A novel oxygen-generating enzyme. *Archives of Microbiology* 166 (5) (NOV 1996).
- Venkatesan, A.K., 2010. Investigation of feasibility and potential mechanisms for the bioregeneration of perchlorate laden gel-type anion exchange resin. University of Nevada, Las Vegas.
- Venkatesan, A.K., Sharbatmaleki, M., and Batista, J.R. 2010. Bioregeneration of perchlorate-laden gel-type anion-exchange resin in a fluidized bed reactor. *Journal of Hazardous Materials*. 2010: 177, 730-737.
- Venkatesan, A.K., and Batista, J.R. 2011. Investigation of Factors Affecting the Bioregeneration Process for Perchlorate-Laden Gel-Type Anion Exchange Resin. *Bioremediation*. 2011: 15(1), 1–11.
- Wallace, W., Beshear, S., Williams, D., Hospadar, S. and Owens, M., 1998. Perchlorate reduction by a mixed culture in an up-flow anaerobic fixed bed reactor. *Journal of Industrial Microbiology & Biotechnology* 20 (2) (FEB 1998): 126-31.
- Wallace, W., Ward, T., Breen, A., and Attaway, H., 1996. Identification of an anaerobic bacterium which reduces perchlorate and chlorate as *Wolinella succinogenes*. *Journal of Industrial Microbiology* 16 (1) (JAN 1996): 68-72.
- Waller, A. S., Cox, E. E., and Edwards E. A., 2004. Perchlorate-reducing microorganisms isolated from contaminated sites. *Environmental Microbiology* 6 (5) (MAY 2004): 517-27.
- Wang, C., Lippincott, L. and Meng, K., 2008. Kinetics of biological perchlorate reduction and pH effect. *Journal of Hazardous Materials* 153 (1-2) (MAY 2008): 663-9.
- Wang, C., Meng, X., and Lippincott, L., 2006. Biological reduction kinetics of perchlorate and its effect by pH. *Abstracts of Papers of the American Chemical Society* 232 (SEP 10 2006): 680-.

- Watson, D.B., Wu, W., Mehlhorn, T., Tang, G., Earles, J., Lowe, K., Gihring, T. M., Zhang, G., Phillips, J., Boyanov, M. I., Spalding, B. P., Schadt, C., Kemner, K. M., Criddle, C. S., Jardine, P. M, and Brooks, S. C. 2013. In Situ Bioremediation of Uranium with Emulsified Vegetable Oil as the Electron Donor. *Environmental Science & Technology*. 2013: 47, 6440-6448.
- Webster, T. S., Guarini, W. J., and Wong H. S., 2008. Fluidized bed bioreactor treatment of perchlorate-laden groundwater to potable standards. *Journal American Water Works Association* 101 (5) (MAY 2009): 137.
- Webster T.S., and Togna P., 2009. Demonstration of a Full Scale Fluidized Bed Bioreactor for the Treatment of Perchlorate at Low Concentrations in Groundwater, ESTCP Project ER-0543.
- West Valley Water District (WVWD), 2012. Water news, Groundwater wellhead treatment system project. Volume 31.
- Westerman, P.W. 2008. Sludge Survey Methods for Anaerobic Lagoons. *North Carolina State University*. 2008, E09-51800.
- White, G., 2013. Automation Advantages. *Instrumentation*. September 2013: 102, 48.
- William J.H., 2005. Injection of innocuous oils to create reactive barriers for bioremediation: Laboratory studies. *Contaminant Hydrology*. 2014: 80. 31-48.
- Williamson, K., and McCarty, P. L., 1976. A model of substrate utilization by bacterial films. *Journal (Water Pollution Control Federation)* 48 (1) (Jan.): pp. 9-24, <http://www.jstor.org/stable/25038465>.
- Wolf D. and Resnick W., 1963. Residence Time Distribution in Real Systems Ind. Eng. Chem. Fundamen., 1963, 2 (4), pp 287–293. DOI: 10.1021/i160008a008. Publication Date: November 1963.
- Wolterink, 2004. Characterization of (per)chlorate-reducing bacteria. Thesis Wageningen University, The Netherlands.
- Wong, C. J., Matjafri, M. Z., Abdullah, K., Lim, H. S., and Low, K. L., 2007. Temporal air quality monitoring using surveillance camera. Paper presented at 2007 IEEE International Geoscience and Remote Sensing Symposium, IGARSS 2007, June 23, 2007 - June 28, <http://dx.doi.org/10.1109/IGARSS.2007.4423441>.
- Wong, L. T., Mui, K. W., and Hui, P. S., 2009. Evaluation on screening strategies for indoor air quality assessments in air-conditioned offices. *Building Services Engineering Research and Technology* 30 (3): 203-12, <http://dx.doi.org/10.1177/0143624409105452>.

- Wood, S. R., Kirkham, J., Marsh, P. D., Shore, R. C., Nattress, B. and Robinson, C., 2000. Architecture of intact natural human plaque biofilms studied by confocal laser scanning microscopy., *Biomaterials and Bioengineering. J Dent Res*, 79 (1): 21-27, 2000
- Xiao, Y., and Roberts, D. R., 2013. Kinetics analysis of a salt-tolerant perchlorate-reducing bacterium: Effects of sodium, magnesium, and nitrate. *Environmental Science & Technology* 47 (15) (AUG 6 2013): 8666-73.
- Xiao, Y., Roberts, D. J., Zuo, G., Badruzzaman, M., and Lehman, G. S., 2010. Characterization of microbial populations in pilot-scale fluidized-bed reactors treating perchlorate- and nitrate-laden brine. *Water Research* 44 (14) (JUL 2010): 4029-36.
- Xu, J. L., Song, Y. U., Min, B. K., Steinberg, L., and Logan, B. E., 2003. Microbial degradation of perchlorate: Principles and applications. *Environmental Engineering Science* 20 (5) (SEP-OCT 2003): 405-22.
- Xu, J. L., Trimble, J. J., Steinberg, L., and Logan, B. E., 2004. Chlorate and nitrate reduction pathways are separately induced in the perchlorate-respiring bacterium *dechlorosoma* sp KJ and the chlorate-respiring bacterium *pseudomonas* sp PDA. *Water Research*. 2004: 38 (3), 673-80.
- Ye, L., You, H., Yao, J., and Su, H., 2012. Water treatment technologies for perchlorate: A review. *Desalination* 298 (0) (7/16): 1-12.
- Yoon, I. H., Meng, X., Wang, C., Kim, K. W., Bang, S., Choe, E., and Lippincott, L., 2009. Perchlorate adsorption and desorption on activated carbon and anion exchange resin. *Journal of Hazardous Materials* 164 (1) (MAY 15 2009): 87-94.
- Yu, L.L., Jarrett J.M., Davis, W.C., Kilpatrick E.L., Oflaz, R., Turk, G.C., Leber, D.D., Valentin, L., Morel-Espinosa, M. and Blount, B.C., 2006. Characterization of Perchlorate in a New Frozen Human Urine Standard Reference Material. *Anal Bioanal Chem*. 2012 October; 404(0): 1877–1886. doi:10.1007/s00216-012-6263-5.
- Zhang, H., Logan, B. E., Regan, J. M., Achenbach, L. A., and Bruns, M. A., 2005. Molecular assessment of inoculated and indigenous bacteria in biofilms from a pilot-scale perchlorate-reducing bioreactor. *Microbial Ecology* 49 (3) (APR 2005).
- Zhao, H.P., Ontiveros-Valencia, A., Tang, Y., Kim, B. O., Ilhan, Z.E., Krajmalnik-Brown, R., and Rittmann, B., 2013. Using a two-stage hydrogen-based membrane biofilm reactor (MBfR) to achieve complete perchlorate reduction in the presence of nitrate and sulfate. *Environmental Science & Technology* 47 (3) (FEB 5 2013): 1565-72.
- Zhao, H. P., Van Ginkel, S., Tang, Y., Kang, D.W., Rittmann, B., and Krajmalnik-Brown, R., 2011. Interactions between perchlorate and nitrate reductions in the biofilm of a hydrogen-

based membrane biofilm reactor. *Environmental Science & Technology* 45 (23) (DEC 1 2011): 10155-62.

Zhu, I. X., Getting, T., and Bruce, D., 2010. Review of biologically active filters in drinking water applications. *Journal American Water Works Association* 102 (12) (DEC 2010): 67-77.

APPENDIX A

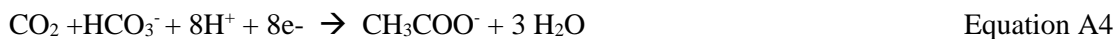
CALCULATION OF STOICHIOMETRIC EQUATION

Equations A1-A3 are the half reactions for electron acceptors; Equation A4 represents the reaction for acetate as donor and carbon source; and Equation A5 represents cell synthesis using nitrate as nutrient (Rittman and McCarty, 2001).

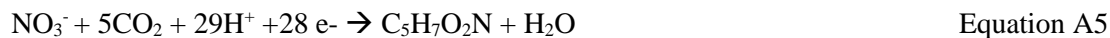
For electron acceptor (oxygen, nitrate and perchlorate) R_a :



For carbon source/electron donor (acetate) R_c :



For cell synthesis, assuming nitrate as source of nitrogen for the organisms R_c :



The total reaction is given by:

$$f_e R_a + f_s R_c - R_d \quad \text{Equation A6}$$

The coefficients (f_e and f_s) in Equation A6 are the actual fraction of electron used for energy generation, and biomass synthesis respectively. The f_s value represents the biomass yield as mole of cells/mole of electron acceptor or as e-eq of cells/ e- eq of electron acceptor. The values of these fractions for various microorganisms are listed by Rittman and McCarty (2001).

The fraction, f_s , can be calculated from the reaction energetic and biological solid retention time as given below.

$$f_s = f_s^0 * \frac{1 + (1 - f_d) b \theta_x}{1 + b \theta_x} \quad \text{Equation A7}$$

Where, f_s^0 =maximum fraction synthesized for electron acceptor, f_d = degradable portion of bacteria and θ_x = biological solids retention time (d)

Wang et al. (2008) observed maximum yield (Y) of 0.2 mg DW/mg perchlorate (Table 2.4). Considering ammonium as source of nitrogen, f_s can be calculated to be 0.44 using Equation A7 (Rittman and McCarty, 2001). However, the same calculation will have f_s value of 0.62 if the nutrient source was considered to be nitrate.

$$Y = 0.2 \frac{\text{mg DW}}{\text{mg ClO}_4^-} = 0.2 \frac{\text{mg DW}}{\text{mg ClO}_4^-} * \frac{20 \text{ e-eq}}{113 \text{ g DW}} * \frac{99.5 \text{ g}}{8 \text{ e-eq}} = 0.44 \quad \text{Equation A8}$$

For pure culture of KJ has high yield same study has reported 10 to 50 times more yield for pure cultures of perchlorate reducing strains. Ricardo et al. (2012) observed very high yield for perchlorate reducing (3.64 mgVSS/mgClO₄⁻) and 0.18 mgVSS/mg NO₃⁻.

APPENDIX B

CULTURE DEVELOPMENT

Table B.1: Calculation of Chemicals for Two-Liter Culture Preparation

Stock	Concentration of Stock	Target Concentration	Total Volume(L)	mL added
Acetate (mg/L)	120,000	3,000	1	25
Perchlorate (mg/L)	40,000	1,000	1	25
Nutrient	100X	X	1	10
Buffer	10X	X	1	100

Table B.2: Amounts of Chemicals Needed for Wasting-Feeding Mode

Wasting volume (L)	Amount Added (mL)			
	Acetate	Perchlorate	Nutrients	Buffer
0.5	12.5	12.5	5	50
1.5	37.5	37.5	15	150

Table B.3: Schedule for Culture Development

	Day I	Day II	Day III	Day IV	Day V	Day VI	Day VII	Day VIII	Day IX	Day X
Seed mL	200									
Nutrient	5	5	5	5						
Buffer	50	50	50	50						
Acetate (Stock of 120 g/L)	3	3	4	5	6	6	6	6	6	1.5
Perchlorate (Stock of 40 g/L)	0.02	0.08	2	5	6	6	6	6	6	1.5
DI	600	100	100	100	100					

APPENDIX C

OPTICAL DENSITY VS. TOTAL SUSPENDED SOLIDS

The culture was diluted serially. For each diluted culture, OD and TSS were measured. To account bacteria growth, OD was measured. TSS was calculated using the equation $y = 1967.3x - 41.62$.

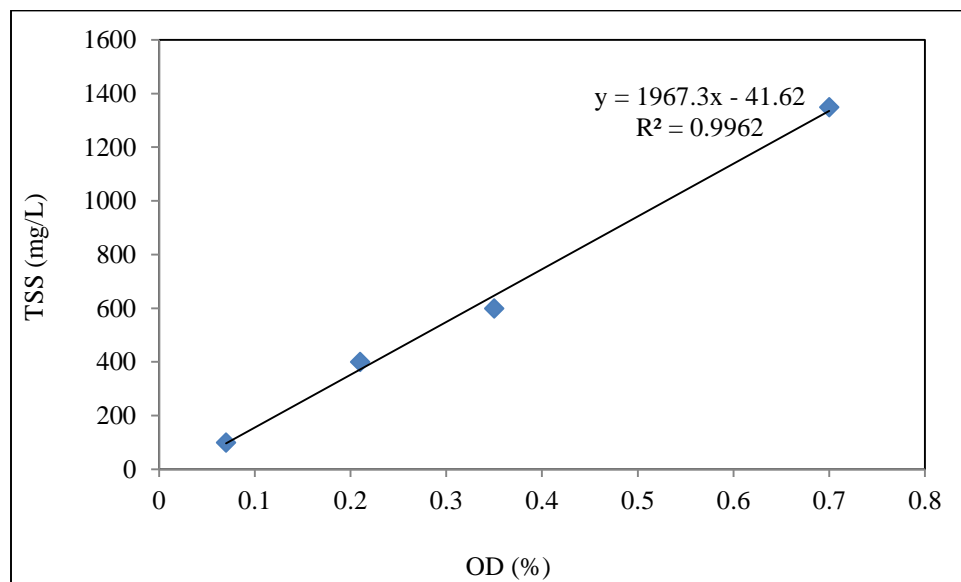


Figure C.1: Relation between TSS (mg/L) and OD (%)

APPENDIX D

GAC TESTS

D.1 GAC Adsorption Test

Abiotic reduction of perchlorate by adsorption in GAC is known to be negligible. Miller and Logan (2000) cited that the abiotic perchlorate degradation was not significant enough as compared to biodegradation. In contrast, Brown et al. (2002) observed 50-90% abiotic perchlorate removal by the GAC. In the abiotic test, the authors used two different types of GAC (extruded peat and bituminous coal), either virgin or treated with acid wash out-gassing procedure, and diameters (0.8 mm and 0.5mm). The study concluded that perchlorate removal by the GAC was due to ion-exchange rather than abiotic degradation, and the exchange capacity is 0.172 mg perchlorate/g GAC (Brown et al., 2002). AWWA (2001) also attributed adsorption as the phenomenon in removing perchlorate by GAC, and indicated that the reactivity of the carbon particle depends on the size and the treatment process used in preparing the carbon.

Prior to using GAC in the FBR reactors, batch experiments were performed to determine if the GAC selected adsorbed perchlorate. The objective of this experiment was to evaluate the perchlorate removal by adsorption in GAC. The GAC adsorption test were conducted in 125 mL batch reactors at perchlorate concentrations 0 (control, DI only), 100, 200, and 500 ug/L. In each reactor, 2 g of fresh baked GAC (550°C for 1 hour) were added. The batch reactors were sealed with rubber caps and were kept on the Orbital shaker to ensure continuous mixing. Samples were collected at 20, 60, 80, 120, and 180 minutes using a 10 mL syringe. No DI water was added after sample collection.

Table D.1 shows the removal of perchlorate per gram of GAC at each perchlorate concentration and Figure D.1 shows the decrease in perchlorate concentration. The adsorption of perchlorate by the GAC observed in this study supported removal in Brown et al. (2002). However, the average removal in this study was 4.4843 ± 0.5986 ug/g GAC, which is one-hundredth time lower than reported values for GAC.

Table D.1: Average Perchlorate Removed by GAC (ug/g GAC)

DI	100 ug/L	200 ug/L	500 ug/L
0	3.2588	5.0109	4.0706
0	3.8329	5.1799	6.3284
- 0.1378	3.8393	4.9596	4.1870
0.2766	3.6487	4.8491	4.6466

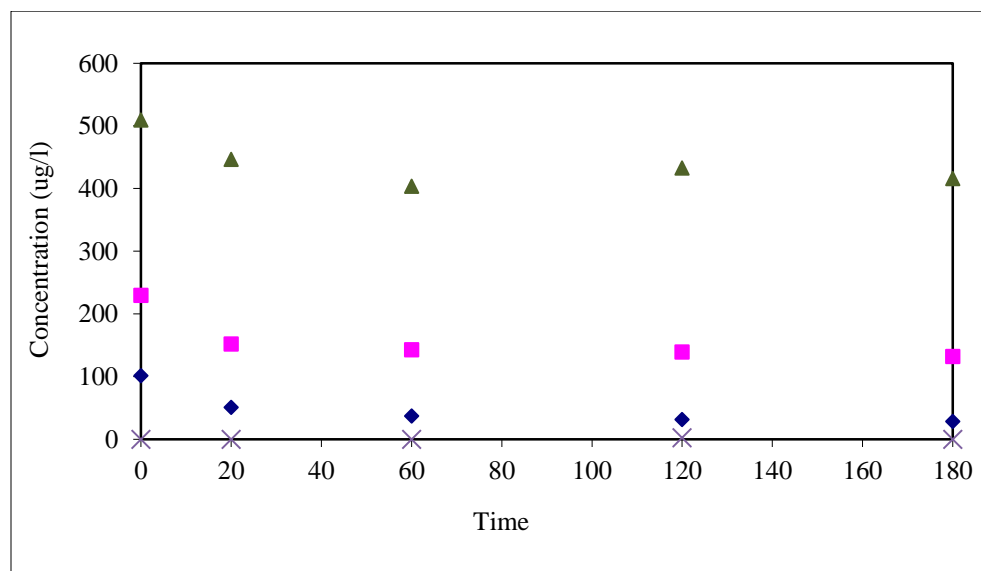


Figure D.1: Perchlorate concentration in a batch reactor with GAC; Triangle represent data for 500 ug/L, Squares represent 200 ug/L, Diamonds represent 100 ug/L and Cross represent DI water (control).

Figure D.1 shows that the perchlorate concentration at the time of sampling. The perchlorate concentration for all reactors decreased with time in the bulk liquid except for DI water batch reactor (control). The perchlorate concentration in reactor with 500 ug/L showed the least decrease.

Figure D.2 shows the ratio of perchlorate concentration at the time of sampling to its initial concentration over time. Figure D.2 shows that within 180 minutes, only 50% of the perchlorate was available for bacteria in the reactors with 100 $\mu\text{g/L}$ perchlorate, 60% perchlorate were available in the reactors with 200 $\mu\text{g/L}$, and 80% in the reactors with 500 $\mu\text{g/L}$ reactors.

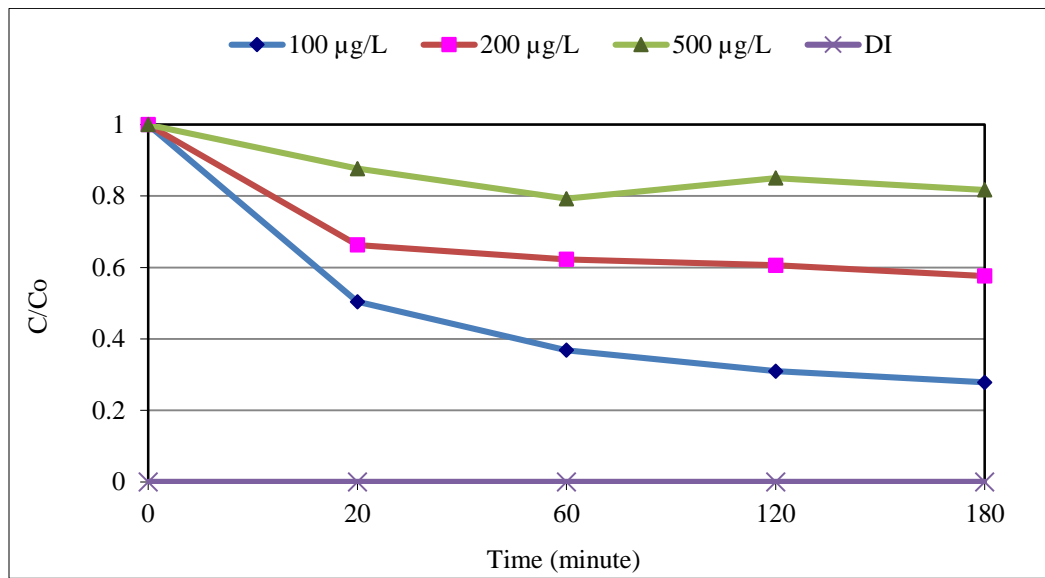


Figure D.2: Ratio of perchlorate concentration in a batch reactor with GAC.

Triangle represent data for 500 $\mu\text{g/L}$, Squares represent 200 $\mu\text{g/L}$, Diamonds represent 100 $\mu\text{g/L}$ and Cross represent DI water

The GAC was sieved through US standard testing sieve of opening sizes 1.4 mm, 0.85 mm and 0.71mm. The GAC passing through sieve with opening of 14 mm, and retaining on sieve with opening 0.85 mm were selected for this study.

D.2 GAC Density and Porosity

The density of GAC used in the FBR design was the average of three density calculations. The density is the ratio of mass of GAC to volume of GAC. The volume of measured GAC was calculated from the volume of water that the dish could hold. The calculation is shown below.

$$\text{Density of GAC } \text{kg/m}^3 = \frac{(\text{mass of GAC + dish}) - (\text{mass of dish})}{\text{Maximum amount of water in the dish} - \text{Volume of water added to the GAC}}$$

Table D.2: Density Calculation for the GAC

Weight of GAC			
	Trial1	Trial 2	Trial 3
Mass of aluminum dish g	0.9699	0.9704	0.9806
Mass of dish + GAC g	26.2929	26.9674	27.6872
Volume calculation			
Water added to the GAC in the aluminum dish mL	27	31	28
Maximum amount of water in the aluminum dish mL	45	50	46
Density (kg/m ³)	1406.83	1368.26	1483.7
Porosity (%)	0.6	0.62	0.61

Average density of GAC = 1419.599 kg/m³ is comparable to 1300-1700 kg/m³, density of GAC in literature (MWH, 2005).

Average porosity of GAC obtained = 0.61

The variation among the calculated density may be due to various errors during the experiment. It was challenging to add the same amount of water in each trial due to possible surface tension developed over the GAC. The size of GAC used varied between 0.85-1.4 mm and pore size within the GAC changed accordingly. Water added to the GAC filled the internal pores and expanded the content in the dish. The expansion of GAC further increased the surface tension of water.

APPENDIX E

FBR REACTOR DESIGN

E.1 Parameters for Reactor Design

The reactor was designed for treating perchlorate 100 mg/L to below 15ug/L (EPA recommendation for drinking water). Table E.1 shows the parameters and their respective values assumed for the design.

Table E.1: Parameters Used for Reactor Design

Assumed Parameters		Measured Parameters of GAC	
Dynamic viscosity μ N-s/m ² at 20°C	0.001002	Diameter of GAC mm	0.5 ^c
kv	210 ^a	Density of GAC kg/m ³	1483.7 ^c
Ki	3.5 ^a	Porosity of fixed bed GAC (without fluidization) ϵ_F	0.69 ^d
Fluidization (25-30) ^b %	25	Porosity of GAC after fluidization ϵ	0.70
		β	770.46

^a MWH, 2005

^b Webster et al., 2009

^c measured/seived

^d Calculated

Table E.2: Equations Used for the FBR Design

Expanded media depth $L_E = L_F + 0.3 * L_F$; Where, L_F = Fixed or initial media depth

$\epsilon =$	$1 - \left(\frac{L_F}{L_E} (1 - \epsilon_F) \right)$
$\beta =$	$\frac{g \rho_w (\rho_p - \rho_w) d^3 \epsilon^3}{\mu^2}$
Renolds number $Re =$	$\frac{-K_V(1-\epsilon)}{2K_I} + \frac{1}{2K_I} \sqrt{K_V^2(1-\epsilon)^2 + 4K_I\beta}$
Kinematic viscosity $\nu =$	$\frac{\mu Re}{\rho_w d}$

Table E.3 FBR Configuration and Design

Parameters	Value	Unit
Diameter of reactor	2.5	cm
Surface area	4.91	cm ²
Desired fluidization of media (25-35%)	25	%
Actual flow rate required to obtain the fluidization	1.6	mL/s
Flow rate Q	96	mL/min
Desired contact time Ct	9	min
Actual bed depth of FBR	117	cm
Volume of fixed bed media	574.4	mL
Fluidized bed volume	718	mL
EBCT time	9.2	minutes
Contact time	7.48	minutes

Table E.4: Average Flow from Each Pump Head in the Pump Setting for FBR

		Volume (mL)	Time (s)	Flow (mL/s)
All combined	Reactor 1	16	10	1.60
	Reactor 2	31.5	20	1.56
Acetate	Reactor 1	25	61	0.41
	Reactor 2	25	60.2	0.42
Perchlorate	Reactor 1	10	28	0.36
	Reactor 2	10	27.9	0.36
DI	Reactor 1	10	12	0.83
	Reactor 2	10	13.5	0.74

E. 2 Preliminary FBR design

A lab scale FBR was designed and operated at 25% fluidization. The reactor was filled with 500 μm , clean GAC, which has a relative density (using the water displacement method) of 1419 kg/m^3 respectively. The hydraulic equations used for the calculation of fluidized bed depth and porosity are shown in Appendix D. Table E.5 shows the reactor configuration and design for this study.

Table E.5: Preliminary Reactor Configuration and Design

Length (m)	0.68
Diameter of reactor (m)	0.025
Media depth (m) (unfluidized)	0.35
Porosity	0.61 ^a
Empty bed contact time (min)	3.5
Fluidized bed depth (m)	0.44
Fluidized porosity	0.69
Flow (mL/min)	96 (1.6 mL/s)
Contact time achieved (min)	2.24

^a McCharty and Meyers, 2005

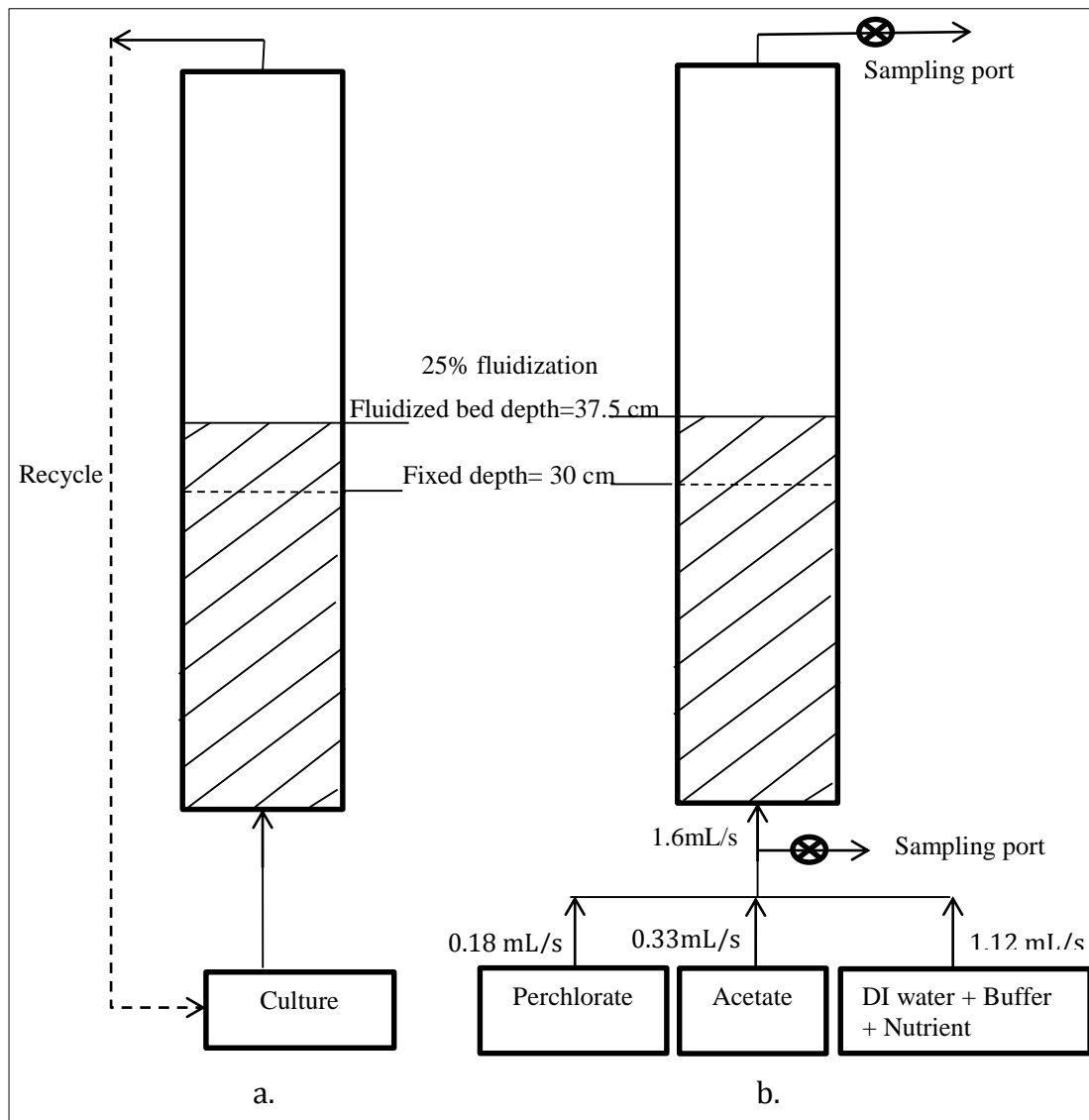


Figure E.1: Schematic diagram of inoculation of the culture for a week (a), and operation of the reactor (Ex-situ treatment) (b).

Table E.6: Average Flow from Each Pump Head in the Pump Setting for Preliminary FBR

	Volume (mL)	Time (s)	Flow (mL/s)	Avg Flow (mL/s)
All combined	50	28.4	1.76	1.76
	50	28.4	1.76	
	50	28.6	1.75	
DI	50	39.7	1.26	1.25
	50	40.1	1.25	
	50	40	1.25	
Perchlorate	10	48.9	0.20	0.21
	10	48.2	0.21	
	10	48.2	0.21	
Acetate	10	30.8	0.32	0.33
	10	30.3	0.33	
	10	30	0.33	

E.2.1 Perchlorate Degradation in the FBR

The perchlorate removal in the reactor was only 25% by the end of three weeks. The reactor was shut down in three weeks due to pump failure.

E.2.2 Analysis of Media Loss/Backwashing in FBR Reactors Using Image Processing Technique

Figure E.2 shows the media expansion due to microbial growth. The media expanded uniformly with time during three-week period.

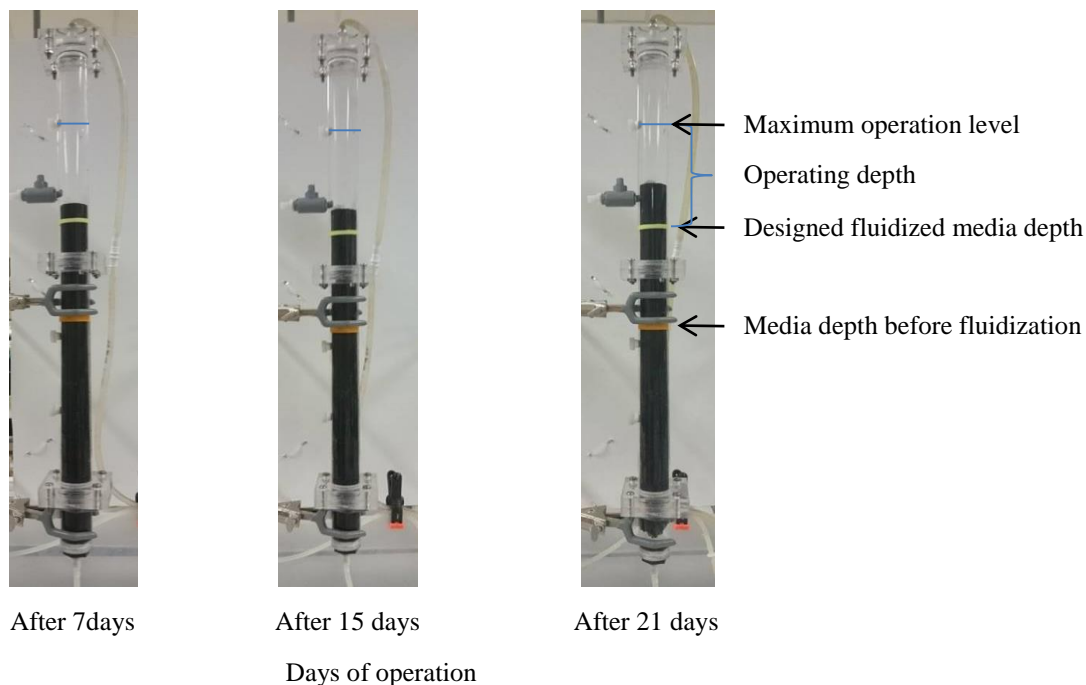


Figure E.2: Media expansion in the reactor due to microbial growth.

The pictures were analyzed for the section of the reactor above the designed fluidized media depth, the top portion of the reactor above the yellow mark in Figure E.2. Only the operation zone (between the designed fluidized media depth and the maximum operation level) of the reactor was used for image processing. The image J processed the picture into two colors: red for space above the media and black for media. As shown in Figure E.3, as the media started to float, the media depth (black color) increases, decreasing the operation zone (red color). The software calculates the area of the operating zone as shown in Figure E.3.

The software analyzes the picture as 2-D diagram and calculates the area (%). The area (%) is the ratio of area above the media to the actual area of the operating zone. Once the area approaches zero, indicates that the media reached the maximum operating depth and should be backwashed.

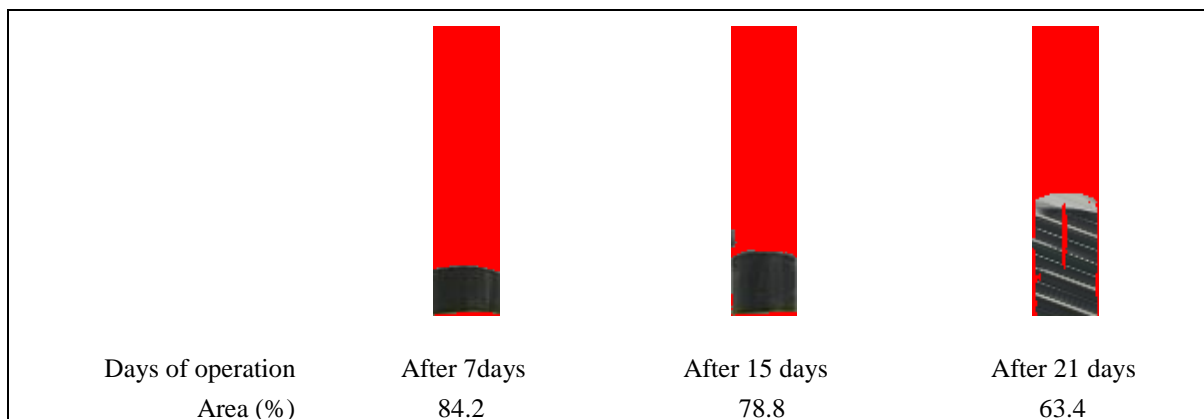


Figure E.3: Picture of the top portion of the reactor processed by Image J.

The red portion is the space above the media and the black portion is the media. The area (%) represents the area of red portion to the entire picture.

E.4 Tracer Test

Figure E.4 shows the tracer (NaNO_3) response curve in the reactor with respect to time. The arrow in Figure E.4 indicates samples were collected up to 70 min (beyond 30 min), those data not shown here remained between 0.001 to 0.004 $\text{mg NO}_3^-/\text{L}$.

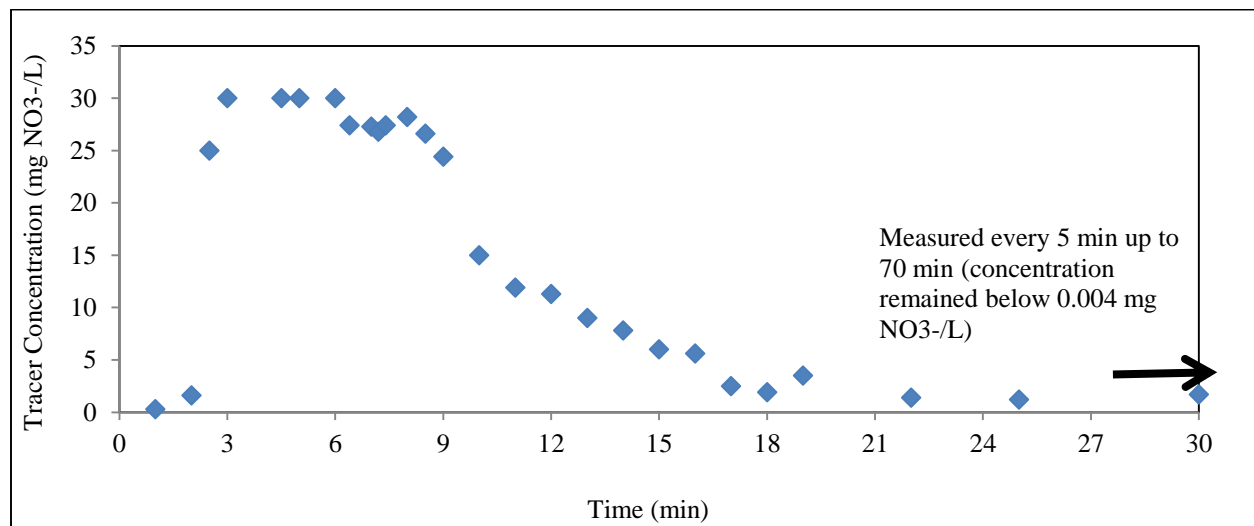


Figure E.4: Tracer test results for flow rate 1.6 mL/s.

The tracer data was normalized with respect to residence time and output concentration.

Figure E.5 shows the distribution curve for normalized concentration and normalized time (Θ).

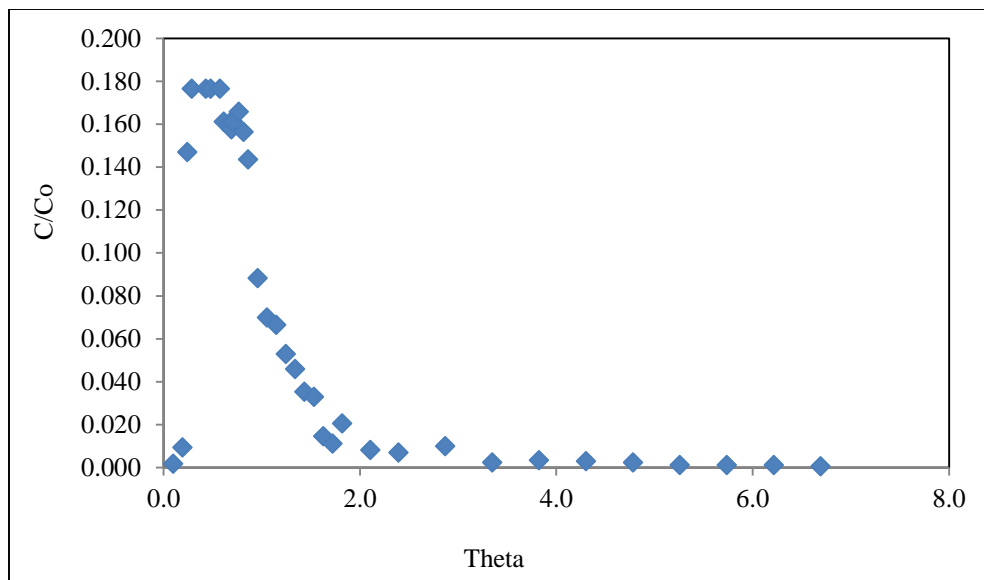


Figure E.5: Normalized concentration vs normalized time.

Figure E.6 shows the cumulative exit age distribution of the tracer. The Θ corresponding to 10% recovery of the tracer was 0.5 and 90% recovery was 2.1. The dispersion index for the reactor is 4.2, indicates that the reactor is not a plug flow.

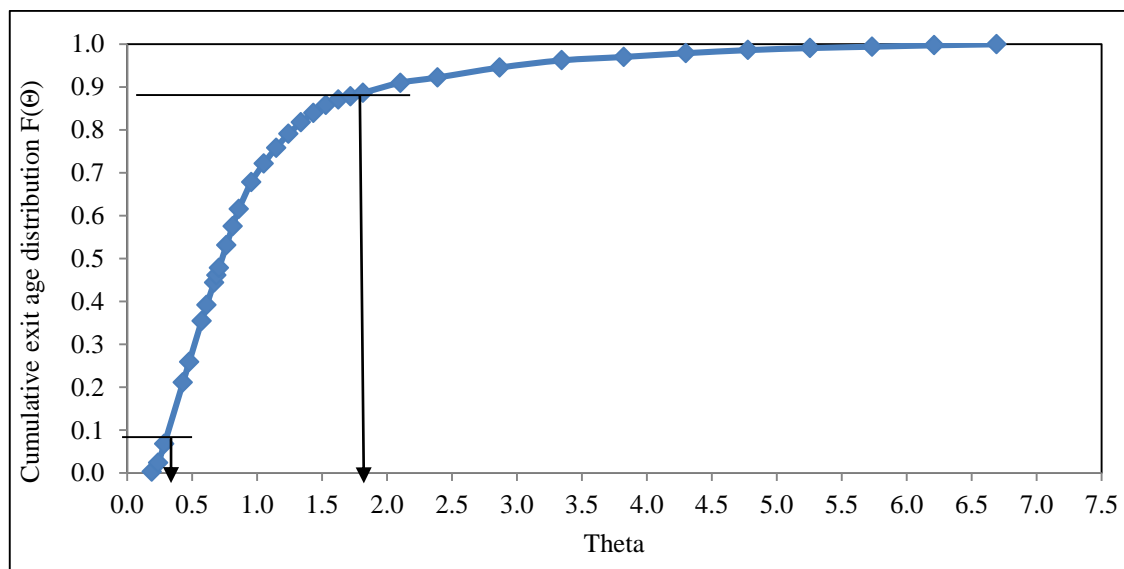


Figure E.6: Cumulative exit age distribution ($F(\Theta)$) for flow rate 1.8 mL/s.

During 75 min sample collection period, 92.3 % of the tracer test was recovered. The tracer test data were analyzed using Dispersed Flow Model (DFM). Table E.7 shows the hydraulic characteristics of the reactor, and Peclet number (ratio of rate of transport by advection to dispersion) and dispersion number obtained from the DFM analysis.

Table E.7: Analysis of Tracer Test

HRT (min)	Actual Residence Time t (min)	C_N	Variance (t)	Std. Dev. (t)	P_e	d
9	20.46	29.9	94.6	9.72	3.50	0.286

The HRT of the reactor is one third of the actual resident time (t), suggesting no short circuiting in the reactor. Higher value of over HRT is preferred for proper operation of a reactor. A small value of dispersion number (d) indicates that the reactor is well dispersed (Metcalf and Eddy, 2005). Metcalf and Eddy (2005) tabulated “d” values for various reactors; for a complete mix activated sludge aeration reactor dispersion number (d) is 3-4 and indicated that reactors with value of $d > 0.25$ means high dispersion in the reactor.

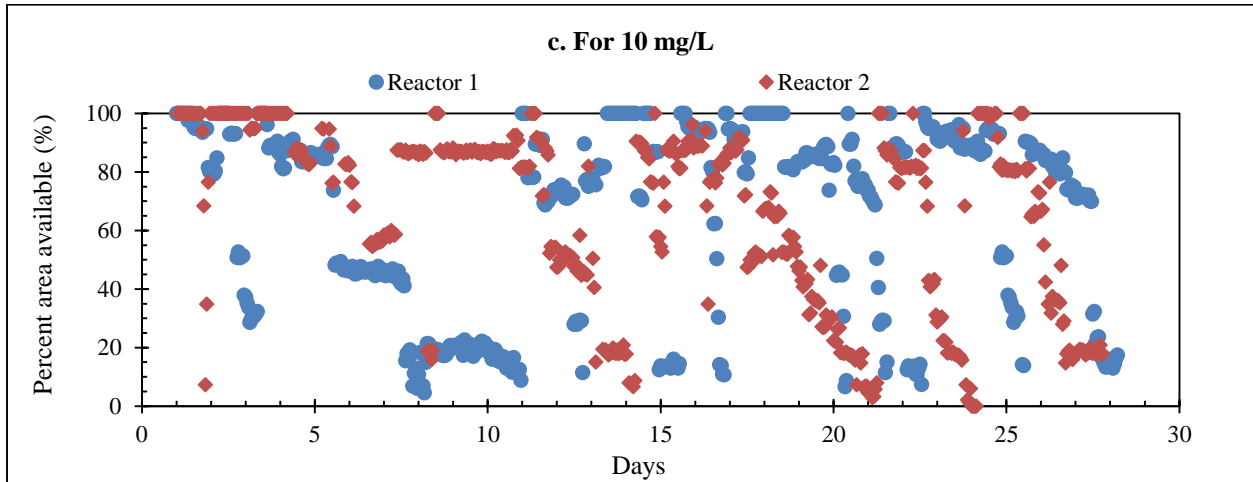


Figure E.7: The percent area available above the media in the FBRs operated with 10 ppm perchlorate.

APPENDIX F

COLUMN BIOREACTOR DESIGN FOR TESTING SLOW RELEASE ELECTRON DONOR (EMULSIFIED OIL)

F.1 Preliminary Column (Beta-Column) Testing

Figure F.1 shows the effluent concentration of COD, nitrate, perchlorate and pH of the Beta column. The COD on the Day 1 (6/30/2015) was 43 mg/L, but the second sample on the same day, after 12 hours of operation, the COD increased to 820 mg/L. The COD further increased to 1070 mg/L on Day 2 (7/1/2015) which might be because of leaching of the EOS-PRO mixed in the soil media. The effluent COD gradually decreased, but remained above 199 mg/L throughout the study period. The nitrate concentration also increased from 10.4 mg-N/L to 18.8 mg-N/L after 12 hours of operation on the first day, and reduced to 1.4 mg-N/L within five days (7/4/2015). However, the nitrate concentration increased to an average concentration at 3.3 ± 0.76 mg-N/L on Day 7. The nitrate concentration decreased to 0.3 ± 0.05 mg-N/L on Day 21. The pH of the effluent remained between 7.5 to 8. No perchlorate degradation was observed during the Beta column operation. Further, the column never achieved 18.4 mL/min flow and got clogged within a month of operation. Thus, for soil column packing purposes, the amount of fines was reduced to 0.5%.

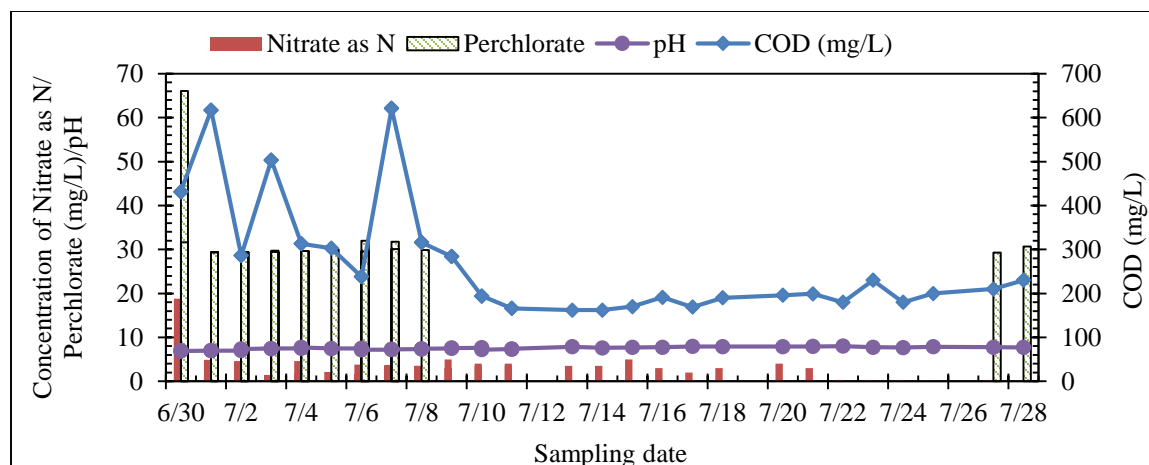


Figure F.1: Effluent concentration of COD, nitrate, perchlorate and pH of the Beta column

Table F.1: Characteristic of Emulsified Oil, EOS-PRO (EOS, 2015)

Parameter	Value
Refined and Bleached US Soybean Oil (% by wt.)	59.8
Rapidly Biodegradable Soluble Substrate (% by wt.)	4
Other Organics (emulsifiers, food additives, etc.) (% by wt.)	10
Specific Gravity	0.96-0.98
Organic Carbon (% by wt.)	74
Mass of Hydrogen Produced (lbs. H ₂ per lb. EOS PRO)	0.25
COD (mg/mL)	2000*

*measured in Water and Environmental Laboratory, UNLV

Table F.2: Major Characteristic of Saturated soil and Groundwater

Soil Characteristic		Groundwater quality	
Moisture	12-20%	Nitrate (mg N/L)	16
Porosity	28.2- 31.3%	Perchlorate (mg/L)	30
Bulk density of coarse solids:		Chlorate (mg/L)	30
Wet=135.895 lb/Cuft			
Dry=118.87 lb/Cuft			

Table F.3: Chemical Composition from the Saturated Soil Extract

Chemical Composition Soil Extract Using DI Water	
Nitrate (mg N/L)	2
Perchlorate (mg/L)	48
Chlorate (mg/L)	48

Table F.4: Computation of Empty Bed Contact Time (EBCT) of the Column Bioreactors

diameter (ft) = 0.167
Media height (ft) = 5.6
Surface area (Sq ft) = 0.02
Volume (Cu ft) = 0.12
Soil required to fill up the soil columns = 5.1 kg
Assumed velocity of groundwater in the column bioreactor ft/d = 15 (Reported range at the BMI site 16-30 ft/d)
EBCT min =528
Total amount of groundwater treated in the column Q (L/d) = 9.265~10 L/d = 2.5 gallons/day

Table F.5: Computation of Oil Dosage to Be Added to the Soil Media for Soil Column and Feed Water For Plastic Column

For Soil Column	For Plastic Columns
Assuming,	Amount of feed water required for two plastic columns
Porosity = 30%	= 5 gallons/day
Moisture =16%	Based on previous oil adsorption microcosm test,
Amount of oil needed to remove electron donors	COD needed= 400 mg/L
nitrate, chlorate and perchlorate	COD in feed water to remove nitrate and perchlorate =
= 0.5 mL oil per 40 gram wet soil	7570 mg
= 15 mL/ kg dry soil	COD of EOS-PRO= 2000000 mg/L
	Thus, Amount of EOS-PRO = 3.785 mL
	~ 4 mL in 5 gallon of groundwater

APPENDIX G

BATCH TESTS

Table G.1: Comparison between perchlorate removal rates (mg/hr) for batches with ppm and ppb initial perchlorate concentration

Time (hour)	Batch with Initial Perchlorate Levels in ppm		Batch with Initial Perchlorate Levels in ppb	
	Average Residual Perchlorate (ppm)	Degradation Rate (mg/hour)	Average Residual Perchlorate (ppb)	Degradation Rate (mg/hour)
0	99.521		99.123	
2	62.925±1.137	0.457	81.486±1.788	0.22
4	50.976±2.136	0.176	71.504±0	0.323
6			42.802±0.358	0.160
8	6.135±0.963	0.267	36.128±1.164	0.083
10			25.972±2.404	0.127
17	4.836	0.002	13.096±3.020	0.046
24	<1	0.017	10.104±0.028	0.011
30			<0.004	0.042

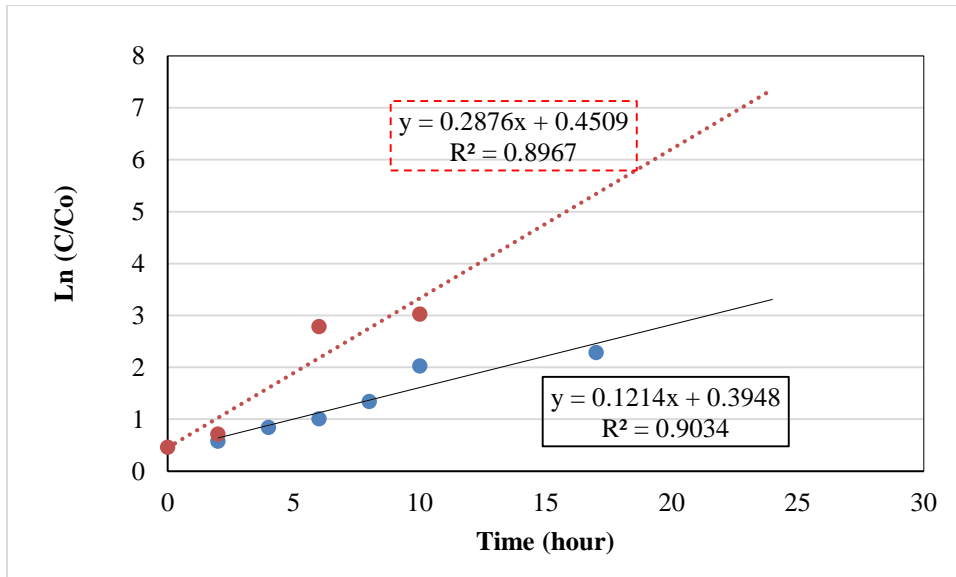


Figure G.1: Logarithmic concentration of perchlorate for ppm and ppb concentrations against time.

APPENDIX H

IDENTIFIED LIST of BACTERIA

Table H.1: Bacteria Identified in the PRB Culture Enriched in UNLV Laboratory Bacteria

Phylum	Class	Order	Family	Genus	Species	%
Acidobacteria	Acidobacteriia	Unknown				
Bacteroidetes	Flavobacteriia	Flavobacteriales	Flavobacteriaceae	Muricauda	Unknown	5.409
				Unknown		0.011
	Sphingobacteriia	Sphingobacteriales	Sphingobacteriaceae	Pedobacter	Unknown	0.137
Firmicutes	Clostridia	Clostridiales	Clostridiaceae	Geosporobacter	Geosporobacter sp	0.033
			Clostridiales Family XIII Incertae Sedis	Anaerovorax	Unknown	0.011
			Unclassified			0.680
				Caulobacter	Caulobacter sp	8.544
Proteobacteria	Alphaproteobacteria	Caulobacterales	Caulobacteraceae	Phenylobacterium	Phenylobacterium sp	1.293
					Unknown	0.219
				Unknown		0.153
		Rhizobiales	Methylocystaceae	Methylosinus	Methylosinus sp	0.022
			Rhizobiaceae	Agrobacterium	Agrobacterium tumefaciens	0.280
				Rhizobium	Rhizobium gallicum	0.027
			Unclassified			0.005
		Rhodobacterales	Rhodobacteraceae	Pannonibacter	Unknown	1.392
				Unknown		6.303
			Unknown			0.000
		Rhodospirillales	Rhodospirillaceae	Azospirillum	Unknown	0.000
				Magnetospirillum	Unknown	0.049
				Tistrella	Tistrella mobilis	0.011
				Unknown		1.600
		Rickettsiales	Unknown			0.011
		Sphingomonadales	Sphingomonadaceae	Blastomonas	Blastomonas natatoria	0.126
				Novospingobium	Novospingobium sp	0.000

Phylum	Class	Order	Family	Genus	Species	%			
	Betaproteobacteria			Spingobium	Sphingobium sp	0.263			
				Sphingomonas	Shpingonomas sp	1.266			
				Sphingopyxis	Sphingopyxis alaskensis	0.077			
				Burkholderiaceae	Burkholderia	Unknown	0.011		
			Burkholderiales	Comamonadaceae	Limnobacter	Limnobacter sp	0.005		
					Acidovorax	Acidovorax sp	0.016		
				Unclassified	Aquabacterium	Aquabacterium	0.137		
			Rhodocyclales	Rhodocyclaceae	Unknown		0.022		
					Denitromonas	Denitromonas sp	0.362		
				Zoogloea	Unknown	0.011			
		Unknown			0.027				
		Deltaproteobacteria	Desulfobacterales	Desulfobacteraceae	Desulforegula	Desulforegula conservatrix	0.077		
			Gammaproteobacteria		Aeromonadales	Aeromonadaceae	Aeromonas	Aeromonas hydrophila	0.033
					Alteromonadales	Shew anellaceae	Shew anella	Shew anella sp	0.011
					Enterobacteriales	Enterobacteriaceae	Unknown		0.444
Pseudomonadales	Moraxellaceae				Acinetobacter	Acinetobacter sp	11.274		
				Unknown		0.027			
	Pseudomonadaceae			Pseudomonas	Pseudomonas alcaligenes	0.027			
					Pseudomonas sp	44.547			
Unknown					10.183				
Xanthomonadales	Unknown				0.159				
	Xanthomonadaceae			Pseudoxanthomonas	Pseudoxanthomonas sp	3.184			
	Unclassified					0.882			
Unknown						0.636			

Table H.2: Bacteria Identified in the Plastic Media from Plastic Column Bioreactor 1

Phylum	Class	Order	Family	Genus	Species	%
Acidobacteria	Acidobacteriia	Unknown				
Bacteroidetes	Flavobacteriia	Flavobacteriales	Flavobacteriaceae	Muricauda	Unknown	5.409
				Unknown		0.011
	Sphingobacteriia	Sphingobacteriales	Sphingobacteriaceae	Pedobacter	Unknown	0.137
Firmicutes	Clostridia	Clostridiales	Clostridiaceae	Geosporobacter	Geosporobacter sp	0.033
			Clostridiales Family XIII Incertae Sedis	Anaerovorax	Unknown	0.011
			Unclassified			0.680
Proteobacteria	Alphaproteobacteria	Caulobacterales	Caulobacteraceae	Caulobacter	Caulobacter sp	8.544
				Phenylobacterium	Phenylobacterium sp	1.293
				Unknown	Unknown	0.219
				Unknown		0.153
		Rhizobiales	Methylocystaceae	Methylosinus	Methylosinus sp	0.022
			Rhizobiaceae	Agrobacterium	Agrobacterium tumefaciens	0.280
				Rhizobium	Rhizobium gallicum	0.027
			Unclassified			0.005
		Rhodobacterales	Rhodobacteraceae	Pannonibacter	Unknown	1.392
				Unknown		6.303
			Unknown			0.000
		Rhodospirillales	Rhodospirillaceae	Azospirillum	Unknown	0.000
				Magnetospirillum	Unknown	0.049
				Tistrella	Tistrella mobilis	0.011
				Unknown		1.600
		Rickettsiales	Unknown			0.011
		Sphingomonadales	Sphingomonadaceae	Blastomonas	Blastomonas natatoria	0.126
				Novospingobium	Novospingobium sp	0.000
				Spingobium	Sphingobium sp	0.263
				Sphingomonas	Shpingonomas sp	1.266
				Sphingopyxis	Sphingopyxis alaskensis	0.077
	Betaproteobacteria	Burkholderiales	Burkholderiaceae	Burkholderia	Unknown	0.011
				Limnobacter	Limnobacter sp	0.005

Phylum	Class	Order	Family	Genus	Species	%	
			Comamonadaceae	Acidovorax	Acidovorax sp	0.016	
			Unclassified	Aquabacterium	Aquabacterium	0.137	
				Unknown		0.022	
		Rhodocyclales	Rhodocyclaceae	Denitromonas	Denitromonas sp	0.362	
				Zoogloea	Unknown	0.011	
		Unknown			0.027		
		Deltaproteobacteria	Desulfobacterales	Desulfobacteraceae	Desulforegula	Desulforegula conservatrix	0.077
	Gammaproteobacteria	Aeromonadales	Aeromonadaceae	Aeromonas	Aeromonas hydrophila	0.033	
		Alteromonadales	Shew anellaceae	Shew anella	Shew anella sp	0.011	
		Enterobacteriales	Enterobacteriaceae	Unknown		0.444	
		Pseudomonadales	Moraxellaceae	Acinetobacter	Acinetobacter sp	11.274	
					Unknown	0.027	
			Pseudomonadaceae	Pseudomonas	Pseudomonas alcaligenes	0.027	
					Pseudomonas sp	44.547	
					Unknown	10.183	
		Xanthomonadales	Unknown			0.159	
			Xanthomonadaceae	Pseudoxanthomonas	Pseudoxanthomonas sp	3.184	
		Unclassified					0.882
		Unknown					0.636
		Total:					100.000

Table H.3: Bacteria Identified in the Plastic Media from Plastic Column Bioreactor 2

Phylum	Class	Order	Family	Genus	Species	%	
Bacteroidetes	Flavobacteriia	Flavobacteriales	Flavobacteriaceae	Muricauda	Unknown	2.069	
				Unknown		0.005	
			Unknown			0.002	
	Sphingobacteriia	Sphingobacteriales	Sphingobacteriaceae	Pedobacter	Unknown	0.084	
Firmicutes	Bacilli	Bacillales	Bacillaceae	Vulcanibacillus	Vulcanibacillus modesticaldus	0.014	
	Clostridia	Clostridiales	Clostridiaceae	Clostridium	Clostridium sp	0.029	
				Geosporobacter	Geosporobacter sp	0.101	
			Clostridiales Family XIII Incertae Sedis	Anaerovorax	Unknown	0.007	
			Peptococcaceae	Desulfosporosinus	Desulfosporosinus sp	0.010	
			Unclassified			0.856	
			Unknown			0.022	
			Unclassified			0.012	
			Proteobacteria	Alphaproteobacteria	Caulobacterales	Caulobacteraceae	Brevundimonas
	Caulobacter	Caulobacter sp					5.909
	Phenylobacterium	Phenylobacterium sp					0.890
	Unknown	Unknown					0.043
	Unknown						0.087
Methylocystaceae	Methylosinus	Methylosinus sp					0.010
Rhizobiaceae	Agrobacterium	Agrobacterium tumefaciens					0.174
	Rhizobium	Rhizobium gallicum					0.041
Rhodobiaceae	Parvibaculum	Parvibaculum lavamentivorans					0.010
Unclassified							0.012
Rhodobacterales	Rhodobacteraceae	Pannonibacter			Unknown	2.467	
	Unknown				5.906		
Rhodospirillales	Rhodospirillaceae	Unknown				0.675	
	Erythrobacteraceae	Porphyrobacter			Porphyrobacter sp	0.005	
Sphingomonadales	Sphingomonadaceae	Blastomonas			Blastomonas natatoria	0.125	
		Novosphingobium			Novosphingobium sp	0.005	
		Spingobium			Sphingobium sp	0.837	
		Sphingomonas			Shpingonomas sp	1.647	
		Sphingopyxis			Sphingopyxis alaskensis	0.094	
		Unknown				0.010	
		Unclassified			Candidatus Nucleicultrix	Candidatus Nucleicultrix Amoebiphilla	0.017

Phylum	Class	Order	Family	Genus	Species	%		
	Betaproteobacteria	Burkholderiales	Burkholderiaceae	Burkholderia	Unknown	0.029		
			Comamonadaceae	Acidovorax	Acidovorax sp	0.012		
			Unclassified	Aquabacterium	Aquabacterium	0.147		
				Unknown		0.024		
		Rhodocyclales	Rhodocyclaceae	Azospira	Azospira sp	0.007		
				Dechloromonas	Dechloromonas sp	0.002		
					Unknown	0.019		
				Denitromonas	Denitromonas sp	1.360		
				Thauera	Thauera sp	0.005		
				Unknown		0.046		
	Deltaproteobacteria	Desulfobacterales	Desulfobacteraceae	Desulforegula	Desulforegula conservatrix	0.176		
		Desulfovibrionales	Desulfovibrionaceae	Desulfovibrio	Unknown	0.012		
	Gammaproteobacteria	Aeromonadales	Aeromonadaceae	Aeromonas	Aeromonas hydrophila	0.051		
					Shew anella	Shew anella sp	0.043	
					Enterobacteriales	Enterobacteriaceae	Unknown	0.818
		Pseudomonadales	Moraxellaceae	Acinetobacter	Acinetobacter sp	16.159		
					Unknown	0.027		
			Pseudomonadaceae	Pseudomonas	Pseudomonas alcaligenes	0.014		
					Pseudomonas sp	41.360		
Unknown					11.133			
Xanthomonadales	Xanthomonadaceae	Pseudoxanthomonas	Pseudoxanthomonas sp	4.245				
Unclassified					1.399			
Unknown					0.424			
Unknown					0.005			
No Hit					0.010			
Total:						100		

Table H.4: Bacteria Identified in the Soil Media from Soil Column Bioreactor 1

Phylum	Class	Order	Family	Genus	Species	%	
Actinobacteria	Actinobacteria	Actinomycetales	Propionibacteriaceae	Propionibacterium	Propionibacterium sp	0.013	
			Unknown			0.325	
			Cyclobacteriaceae	Algoriphagus	Unknown	0.023	
Bacteroidetes	Cytophagia	Cytophagales	Cytophagaceae	Unknown		0.028	
			Unknown			0.025	
			Flavobacteriaceae	Flavobacterium	Unknown	0.005	
	Flavobacteriia	Flavobacteriales	Muricauda	Unknown		0.672	
			Unknown			0.051	
			Unknown			0.101	
	Sphingobacteriia	Sphingobacteriales	Sphingobacteriaceae	Pedobacter	Unknown	0.269	
			Unknown			0.013	
	Firmicutes	Bacilli	Bacillales	Bacillaceae	Vulcanibacillus	Vulcanibacillus modesticaldus	0.119
					Clostridium	Clostridium sp	3.315
Clostridia		Clostridiales	Clostridiaceae	Geosporobacter	Geosporobacter sp	0.741	
			Clostridiales Family XI Incertae Sedis	Sedimentibacter	Sedimentibacter sp	4.251	
			Clostridiales Family XIII Incertae Sedis	Anaerovorax	Unknown	0.015	
			Peptococcaceae	Desulfosporosinus	Desulfosporosinus sp	2.361	
			Unknown			2.645	
			Proteinivoraceae	Anaerobranca	Anaerobranca sp	0.036	
			Ruminococcaceae	Ruminococcus	Ruminococcus sp	0.066	
			Unclassified			7.160	
			Unknown			0.923	
			Unclassified			0.715	
			Unknown			0.015	
			Unknown			0.061	

Phylum	Class	Order	Family	Genus	Species	%	
Gemmatimonadetes	Gemmatimonadetes	Gemmatimonadales	Gemmatimonadaceae	Gemmatimonas	Gemmatimonas sp	0.921	
Proteobacteria	Alphaproteobacteria	Caulobacterales	Caulobacteraceae	Asticcacaulis	Asticcacaulis excentricus	0.434	
				Brevundimonas	Brevundimonas sp	0.596	
				Caulobacter	Caulobacter sp	0.718	
				Phenylobacterium	Phenylobacterium sp	0.670	
					Unknown	1.542	
				Unknown	0.982		
			Rhizobiales	Bradyrhizobiaceae	Bradyrhizobium	Bradyrhizobium sp	0.061
					Unkown	0.046	
		Rhizobiaceae		Agrobacterium	Agrobacterium tumefaciens	0.013	
				Rhizobium	Rhizobium gallicum	0.195	
		Rhodobiaceae		Parvibaculum	Parvibaculum lavamentivorans	0.525	
		Unclassified		0.020			
		Unknown		0.063			
		Rhodobacterales		Rhodobacteraceae	Pannonibacter	Unknown	0.008
			Rhodobacter		Rhodobacter sp	0.030	
			Unknown		1.273		
			Unknown	0.018			
			Rhodospirillales	Rhodospirillaceae	Azospirillum	Unknown	0.180
					Magnetospirillum	Unknown	0.530
					Tistrella	Tistrella mobilis	0.013
					Unknown	0.005	
		Unclassified		0.043			
		Unknown		0.178			

Phylum	Class	Order	Family	Genus	Species	%		
		Rickettsiales	Rickettsiaceae	Rickettsia	Rickettsia peacockii	0.005		
			Erythrobacteraceae	Erthyromicrobium	Erythromicrobium sp	0.010		
				Porphyrobacter	Porphyrobacter sp	2.229		
					Unknown	0.061		
				Unknown	2.726			
			Sphingomonadales	Sphingomonadaceae	Blastomonas	Blastomonas natatoria	0.342	
					Novosphingobium	Novospingobium sp	0.015	
					Spingobium	Sphingobium sp	0.010	
					Sphingomonas	Shpingonomas sp	0.530	
		Sphingopyxis			Sphingopyxis alaskensis	0.614		
		Unknown	0.023					
		Unclassified		Candidatus Nucleicultrix	Candidatus Nucleicultrix Amoebiphilla	0.071		
		Unknown				0.053		
		Betaproteobacteria		Burkholderiales	Burkholderiaceae	Burkholderia	Unknown	0.015
						Limnobacter	Limnobacter sp	0.003
					Comamonadaceae	Acidovorax	Acidovorax sp	0.497
						Hydrogenophaga	Hydrogenophaga sp	1.877
				Unclassified	Aquabacterium	Aquabacterium	0.084	
					Methylibium	Unknown	0.033	
					Unknown	0.003		
Methylophilales	Methylophilaceae			Methylophilus	Methylophilus sp	0.038		
Rhodocyclales	Rhodocyclaceae			Azoarcus	Azoarcus sp	0.129		
				Azospira	Azospira sp	0.013		
				Dechloromonas	Dechloromonas sp	0.606		

Phylum	Class	Order	Family	Genus	Species	%
					Unknown	0.591
				Denitromonas	Denitromonas sp	9.990
				Thauera	Thauera sp	0.091
			Unknown			0.266
	Deltaproteobacteria	Desulfobacterales	Desulfobacteraceae	Desulforegula	Desulforegula conservatrix	8.976
		Desulfovibrionales	Desulfovibrionaceae	Desulfovibrio	Unknown	0.056
		Desulfuromonadales	Unknown			0.010
		Unknown				0.038
	Gammaproteobacteria	Alteromonadales	Shewanellaceae	Shewanella	Shewanella sp	0.185
		Enterobacteriales	Enterobacteriaceae	Unknown		1.304
		Legionellales	Legionellaceae	Legionella	Unknown	0.068
			Unclassified			0.018
		Oceanospirillales	Alcanivoracaceae	Alcanivorax	Alcanivorax sp	0.010
			Moraxellaceae	Acinetobacter	Acinetobacter sp	0.008
		Pseudomonadales	Pseudomonadaceae	Pseudomonas	Pseudomonas alcaligenes	0.096
					Pseudomonas sp	24.107
					Unknown	7.652
					Unclassified	0.023
		Unknown				0.048
		Xanthomonadales	Unknown			0.304
			Xanthomonadaceae	Pseudoxanthomonas	Pseudoxanthomonas sp	1.534
		Unclassified				0.068
		Unknown				0.071
Unclassified						0.071
Unknown						0.309
No Hit						1.108
Total:						100

Table H.5: Bacteria identified in the soil media from Soil Column Bioreactor 2

Phylum	Class	Order	Family	Genus	Species	%
Acidobacteria	Acidobacteriia	Unknown				0.020
	Cytophagia	Cytophagales	Cyclobacteriaceae	Algoriphagus	Unknown	0.085
			Unknown			0.039
Bacteroidetes	Flavobacteriia	Flavobacteriales	Flavobacteriaceae	Flavobacterium	Unknown	0.013
				Muricauda	Unknown	0.411
				Unknown		0.098
			Unknown			0.117
	Sphingobacteriia	Sphingobacteriales	Sphingobacteriaceae	Pedobacter	Unknown	0.736
				Geosporobacter	Geosporobacter sp	0.378
Firmicutes	Clostridia	Clostridiales			Desulfosporosinus sp	0.007
			Peptococcaceae	Desulfosporosinus	Unknown	0.215
Gemmatimonadetes	Gemmatimonadetes	Gemmatimonadales	Gemmatimonadaceae	Gemmatimonas	Gemmatimonas sp	0.124
				Asticcacaulis	Asticcacaulis excentricus	0.046
				Brevundimonas	Brevundimonas sp	0.209
		Caulobacterales	Caulobacteraceae	Caulobacter	Caulobacter sp	3.565
				Phenylobacterium	Phenylobacterium sp	1.154
				Unknown	Unknown	1.232
				Unknown		0.587
		Rhizobiales	Rhizobiaceae	Agrobacterium	Agrobacterium tumefaciens	0.033
				Rhizobium	Rhizobium gallicum	0.391
			Rhodobiaceae	Parvibaculum	Parvibaculum lavamentivorans	0.091
			Unclassified			0.026
				Pannonibacter	Unknown	0.020
Proteobacteria	Alphaproteobacteria	Rhodobacterales	Rhodobacteraceae	Rhodobacter	Rhodobacter sp	0.020
				Unknown		0.007
		Rhodospirillales	Rhodospirillaceae	Magnetospirillum	Unknown	0.098
				Unknown		0.033
				Erthyromicrobium	Erythromicrobium sp	0.013
			Erythrobacteraceae	Porphyrobacter	Porphyrobacter sp	1.962
				Unknown	Unknown	0.007
		Sphingomonadales		Unknown		0.697
				Blastomonas	Blastomonas natatoria	0.358
			Sphingomonadaceae	Spingobium	Sphingobium sp	0.007
				Sphingomonas	Shpingonomas sp	0.665
				Sphingopyxis	Sphingopyxis alaskensis	0.652

Phylum	Class	Order	Family	Genus	Species	%
			Unknown			0.013
		Unclassified		Candidatus Nucleicultrix	Candidatus Nucleicultrix Amoebiphilla	0.052
		Unknown				0.046
			Burkholderiaceae	Limnobacter	Limnobacter sp	0.059
			Comamonadaceae	Acidovorax	Acidovorax sp	0.939
		Burkholderiales		Hydrogenophaga	Hydrogenophaga sp	1.466
			Unclassified	Aquabacterium	Aquabacterium	0.117
				Unknown		0.013
	Betaproteobacteria	Methylophilales	Methylophilaceae	Methylophilus	Methylophilus sp	0.020
				Azoarcus	Azoarcus sp	0.026
					Dechloromonas sp	0.339
		Rhodocyclales	Rhodocyclaceae	Dechloromonas	Unknown	0.150
				Denitromonas	Denitromonas sp	23.216
		Unknown				0.332
		Alteromonadales	Shew anellaceae	Shew anella	Shew anella sp	0.039
		Chromatiales	Chromatiaceae	Rheinheimera	Rheinheimera sp	0.039
		Enterobacteriales	Enterobacteriaceae	Unknown		2.242
		Legionellales	Legionellaceae	Legionella	Unknown	0.007
		Oceanospirillales	Alcanivoracaceae	Alcanivorax	Alcanivorax sp	0.600
			Moraxellaceae	Acinetobacter	Acinetobacter sp	0.026
					Pseudomonas alcaligenes	0.059
	Gammaproteobacteria	Pseudomonadales	Pseudomonadaceae	Pseudomonas	Pseudomonas sp	37.529
					Unknown	13.348
		Unclassified				0.274
		Unknown				0.156
			Unknown			1.147
		Xanthomonadales	Xanthomonadaceae	Pseudoxanthomonas	Pseudoxanthomonas sp	2.842
	Unknown					0.078
Unknown						0.202
No Hit						0.515
Total:						100

Table H.6: Bacteria Identified in the culture enriched from wastewater at UNLV-Laboratory

Phylum	Class	Order	Family	Genus	Species	%
Actinobacteria	Actinobacteria (class)	Actinomycetales	Corynebacteriaceae	Corynebacterium	Unknown	4.377
			Nocardiaceae	Rhodococcus	Unknown	0.159
			Nocardiodaceae	Unknown		0.048
			Unknown			0.225
Bacteroidetes	Bacteroidia	Bacteroidales	Bacteroidaceae	Bacteroides	Bacteroides sp	0.202
					Unknown	0.011
			Marinilabiliaceae	Anaerophaga	Anaerophaga sp	0.002
				Dysgonomonas	Dysgonomonas sp	0.035
			Porphyromonadaceae	Proteiniphilum	Proteiniphilum sp	0.120
			Unknown			0.109
	Flavobacteriia	Flavobacteriales	Flavobacteriaceae	Myroides	Myroides odoratus	0.002
				Unknown		0.047
	Unknown					0.025
Chloroflexi	Anaerolineae	Anaerolineales	Anaerolineaceae	Levilinea	Levilinea sp	0.010
				Unknown		0.004
Deferribacteres	Deferribacteres (class)	Deferribacterales	Deferribacteraceae	Geovibrio	Geovibrio thiophilus	0.055
Firmicutes	Bacilli	Bacillales	Bacillaceae	Bacillus	Bacillus sp	0.004
			Clostridiaceae	Clostridium	Clostridium sp	0.019
	Clostridia	Clostridiales	Clostridiales (family)	Fusibacter	Fusibacter sp	0.016
			Eubacteriaceae	Eubacterium	Eubacterium sp	0.098
			Unknown			0.225
	Erysipelotrichia	Erysipelotrichales	Erysipelotrichaceae	Erysipelothrix	Unknown	0.005
	Negativicutes	Selenomonadales	Acidaminococcaceae	Acidaminococcus	Acidaminococcus intestinalis	0.020
					Unknown	0.006
Proteobacteria	Alphaproteobacteria	Rhizobiales	Unknown			0.432
		Rhodobacterales	Rhodobacteraceae	Unknown		0.002

Phylum	Class	Order	Family	Genus	Species	%
	Betaproteobacteria	Rhodospirillales	Rhodospirillaceae	Magnetospirillum	Magnetospirillum sp	0.046
		Burkholderiales	Alcaligenaceae	Alcaligenes	Unknown	0.009
			Unknown			67.356
			Burkholderiaceae	Unknown		0.012
			Comamonadaceae	Acidovorax	Unknown	0.011
				Delftia	Unknown	0.006
				Unknown		0.015
			Unknown			0.039
		Rhodocyclales	Rhodocyclaceae	Unknown		0.622
		Unknown				0.070
	Deltaproteobacteria	Desulfobacterales	Desulfobulbaceae	Unknown		0.017
			Desulfovibrionaceae	Desulfovibrio	Desulfovibrio sp	0.009
		Unknown			0.009	
	Gammaproteobacteria	Alteromonadales	Shewanellaceae	Shewanella	Shewanella putrefaciens	0.129
		Enterobacteriales	Enterobacteriaceae	Yersinia	Unknown	0.009
		Pseudomonadales	Moraxellaceae	Acinetobacter	Unknown	0.243
			Pseudomonadaceae	Pseudomonas	Pseudomonas sp	22.175
				Unknown		0.601
		Unknown			0.004	
		Xanthomonadales	Xanthomonadaceae	Xanthomonas	Unknown	0.017
Spirochaetes	Spirochaetia	Spirochaetales	Spirochaetaceae	Spirochaeta	Spirochaeta sp	0.147
			Unknown			1.163
				Aminobacterium	Aminobacterium sp	0.750
				Thermanaerovibrio	Thermanaerovibrio sp	0.073
				Thermovirga	Thermovirga sp	0.118
				Unknown	Unknown	0.046
				No Hit	No Hit	No Hit

APPENDIX I

REPORTED KINETICS AND EFFECT OF ELECTRON ACCEPTORS ON THE PERCHLORATE REDUCING BACTERIA, AND TYPES OF REACTORS USED IN PERCHLORATE BIOREMEDIATION FROM LITERATURE

Table I.1: Kinetic Parameters of Pure/Mixed Cultures Used for Perchlorate Reduction from Literature

Culture	Electron Donor	Electron Acceptor	q _{max} (mg ClO ₄ ⁻ /mg DW-d)	μ _{max} h ⁻¹	K _p (mg ClO ₄ ⁻ /L)	Y (g VSS/g Acetate)	g Decay Constant d ⁻¹	Reference
Vibrio dechloratans	Acetate	Perchlorate	1.67					Calculated from Korenkov et al. 1976
Mixed		Perchlorate	2.57					Attaway and Smith, 1993
Dechlorosomanas CKB		Perchlorate						Bruce et al., 1999
Dechlorimonas sp. JM Isolates	Hydrogen	Perchlorate	2.15		14.9			Miller and Logan, 2000
GR-1	Acetate	Perchlorate Chlorate	5.65 7.48	0.1		0.24		Rikken et al., 1996
Wolinella succinogenes HAP-1	Acetate	Perchlorate	1.49	0.07				Wallace et al. 1996, 1998; Frankenberger and Herman, 2000
Mixed	Acetate	Perchlorate		0.2	20	0.5	0.01	Urbansky, 2000
KJ	Acetate	Perchlorate Chlorate	1.32*	0.2 (0.14) ^a 0.26	33±9	0.5 0.44		Logan et al., 2001
PDX	Acetate Lactate	Perchlorate Chlorate	0.41*	0.24 (0.21) ^a 0.15	12±4			Logan et al., 2001
<i>C. amalonaticus</i> JB101	Acetate	Perchlorate				0.09 ^b		Bardiya and Bae, 2004
<i>C. farmeri</i> JB109	Acetate	Perchlorate				0.11 ^b		Bardiya and Bae, 2003
SN1A	Acetate	Perchlorate	4.6	0.069	2.2	0.36		Waller et al., 2004

Culture	Electron Donor	Electron Acceptor	q _{max} (mg ClO ₄ ⁻ /mg DW-d)	μ _{max} h ⁻¹	K _p (mg ClO ₄ ⁻ /L)	Y (g VSS/g Acetate)	g Decay Constant d ⁻¹	Reference
ABL1	Acetate	Perchlorate	5.42	0.086	4.8	0.38		Waller et al., 2004
INS	Acetate	Perchlorate	4.35	0.067	18	0.37		Waller et al., 2004
RC1	Acetate	Perchlorate	6	0.085	12	0.34		Waller et al., 2004
Dechlorosoma suillum PS	Acetate	Perchlorate				0.31 ^c		Waller et al., 2004
Mixed heterotrophic	Acetate	Perchlorate		0.1				Bardiya and Bae, 2004
Mixed	Ethanol	Perchlorate	0.002	0.13				Matos et al., 2006
GR-1	Acetate	Perchlorate	5.65	0.1		0.42 ^d		Nerenberg et al., 2006
		Chlorate	7.48					
PC1	Hydrogen	Perchlorate	3.1		0.14	0.23	0.055	Nerenberg et al., 2006
		Chlorate	6.3		<0.014	0.22		
Dechloromonas sp. HZ	Hydrogen	Perchlorate	0.22		8.9			Yu et al., 2000
HCAP-C	Hydrogen	Perchlorate	4.39		76.6 ^e	0.36		Dudley et al., 2008
		Chlorate	8.3		58.3 ^e	0.30		
Mixed	Acetate	Perchlorate	0.49	0.004 ^e	<0.1	0.2	0.05	Wang et al. 2008
JB116	Acetate	Perchlorate				0.08 ^b		Bardiya and Bae, 2008
Mixed	Hydrogen	Perchlorate	2.92		567.3			Cheong et al., 2010
	Hydrogen	Perchlorate	0.27		25.6			
Mixed	Hydrogen	Perchlorate	0.043		0.03			London et al., 2011
Mixed	Ethanol	Perchlorate	0.3	0.082	4.97	3.64		Ricardo et al., 2012
		Nitrate	10.79	60	1.05	0.18		
P4B1	Acetate	Perchlorate	1.176	0.005	18	0.1		Xiao and Robers, 2013

^a Specific growth μ

^b Values expressed as mg protein/mg Ac

^c Y from fs assuming NH₄⁺ as source of nutrient (20 e- eq) (Rittman and McCarty, 2001)

^d Calculated using: u=q*Y

^e Higher kinetics were observed due to presence of another chlorate reducing strain in addition to pure culture of HCAP-C

* values expressed as mg ClO₄⁻/ mg protein-hr

Table I.2: Reported Effects of Oxygen and Nitrate on Perchlorate Reduction

Competitive electron acceptor/ Concentration	Perchlorate concentration	Culture	Degradation rate of perchlorate (mg ClO ₄ /mg VSS-d)	Degradation rate of nitrate (mg NO ₃ /mg VSS-d)	Findings	Reference
Oxygen						
< 2 mg/L					inhibited chlorite dismutase	Chaudhuri et al., 2002
6-7 mg/L		<i>Dechlorosoma</i> sp KJ			Exposure for > 12h ceased biodegradation	Song and Logan, 2003
6-7 mg/L					Exposure for < 12h perchlorate degradation observed	
4 mg/L					no perchlorate degradation	
1 mg/L		mixed			regained perchlorate degradation	Choi et al., 2007
Nitrate						
640	1000	mixed			Simultaneous degradation was observed	Attaway and Smith, 1993
122	122				Simultaneous degradation was observed; both reduced within 48 hr	Herman and Frankenberger, 1998
62	0.089	Perlace			Nitrate was reduced within 24 hr and perchlorate reduction in present of nitrate required 48 hr; Perchlorate alone was reduced within 36 hr	
310	310	D. suillum	0.35	0.3	Perchlorate reduction occurred only after complete nitrate reduction disregards to culture	
310	310	D.agitata			Both rate and extent of perchlorate utilization were lower in presence of nitrate; nitrite accumulation was observed	Chaudhuri et al., 2002

Competitive electron acceptor/ Concentration	Perchlorate concentration	Culture	Degradation rate of perchlorate (mg ClO ₄ /mg VSS-d)	Degradation rate of nitrate (mg NO ₃ /mg VSS-d)	Findings	Reference
11700	100	Perclace/Citrobacter coculture	0.017	0.79	Perchlorate removal of 46.4% was observed and 16.4% nitrate removal	Okeke et al., 2002
600	600	Citrobacter sp. JB 101 and JB 109	4.68	0.26	perchlorate grown culture reduced perchlorate completely within 40 hr whereas nitrate was reduced only 20% in 150 hr.	Bardiya and Bae, 2004
60	20	mixed	0.006-0.17	14.64	perchlorate reduction was realized only after complete reduction of nitrate and nitrite	Ricardo et al., 2012
500 ⁺	Gradually increased from 4 to 15	mixed	0*	100*	nitrite accumulation observed initially, but after 70 days of operation, no nitrite was observed	Xiao et al., 2010
negligible	increased to 70 mg/L		20-30*		Perchlorate reduction observed as nitrate reduced to zero	
6.2	0.0005	P4B1			culture grown in both nitrate and perchlorate medium resulted in better perchlorate reduction, but the same culture had limited perchlorate reduction when grown in nitrate only	Xiao and Robers, 2013

* Values removed in %

⁺ Unit as mgN/L

Table I.3: Configuration of Reported Reactors Used for Perchlorate Removal

Reactor configuration	Media bed depth (m)	Microbes	Flow (mL/min)	HRT (h)	Electron donor	Electron acceptor	Influent conc	Perchlorate removal (mg/min)	Reference	
Upflow bioreactor										
1.17 m length and 7.6 m internal dia with diatomaceous earth pellet (1.17 m depth)	Waste stream from rocket motor wash	W. succinogenes HAP1	0.5	1.17	Brewers yeast extract (BYF-100)	ClO ₄ ⁻	1500	0.6	Wallace et al., 1998	
			0.5	0.46			500	0.2		
0.18 m long and 0.052 m internal diameter with diatomaceous earth pellet (0.18 m depth)	Ground water	Perlance	0.5	10	Acetate	ClO ₄ ⁻ (ug/L)	738	0.00037	Giblin et al., 2000	
			1	5			738	0.00073		
			2	2.5			738	0.00134		
			2	2.5		NO ₃ ⁻	26	0.00005		
			3	3.3			26	0.00008		
Sand (32% expansion)	Ground water from Nevada	Mixed, dentirifying	11.5	2.1	Ethanol	ClO ₄ ⁻	400	4.595	Hatzinger et al., 2000	
						NO ₃ ⁻	20	0.219		
GAC (full scale plant)	Ground water from California		2574	ClO ₃ ⁻		480	5.474			
				ClO ₄ ⁻		8	20.582			
				NO ₃ ⁻		1.5	3.861			
				ClO ₃ ⁻		20	51.480			
0.1m * 0.61m * 0.30 m with 1 mm size sand (1.2 m depth)	Ground water	Dechloraosoma sp. KJ	3780	18-30 min	Acetic acid and ammonium phosphate	ClO ₄ ⁻ ug/L)	77	275.940	Min et al., 2004	
			7560			NO ₃ ⁻	4	30.240		
0.1m ht, 0.61m width, 0.30 m length with plastic(1.2 m depth)			3780			O ₂	7.5	0.000		
						7560	ClO ₄ ⁻ (ug/L)	75		283.500
							NO ₃ ⁻	4		30.240
							O ₂	7.5		56.700
0.7 m long and 0.15 m internal diameter with plastic media (0.63 m depth)	Synthetic water	Mixed	26	8	Acetate	ClO ₄ ⁻ only (ug/L)	1000	25.896	Choi and Silverstein, 2008	
						ClO ₄ ⁻ (ug/L)	1000	25.636		
						NO ₃ ⁻	10 to 16	0.416		
0.92 m* 5.2m dia w/ 0.9 mm – 1.1 mm GAC (28% expansion)			348000	0.203		ClO ₄ ⁻ only (ug/L)	52.5	18270.000	Weber et al., 2008	
						NO ₃ ⁻	27.01	9400.971		

10 cm diameter, 2.44 m height with GAC (0.91 m depth)	0.91	Mixed, salt tolerant	1600	0.2	Acetate	O ₂	8.1	2818.800	Xiao et al., 2010
						ClO ₄ ⁻	4.6	0.000	
						ClO ₄ ⁻	70	22.400	
						NO ₃ ⁻	500	800.000	
76.2 cm long and 5 cm diameter with Anion-exchange resin						ClO ₄ ⁻	10926	13166.400	Venkatesan et al., 2010
						ClO ₄ ⁻	7782	6787.200	
						ClO ₄ ⁻	4743	6635.200	
1.27 m *7.6 cm dia with ion-exchange resin (30-40% expansion)		Mixed	210		Acetate	ClO ₄ ⁻ (mg/Lresin)	10,000	1449.000	Sharbatmal eki and Batista, 2012
Fixed bed reactor									
0.125 m and 0.025 m internal dia with 3 mm dia glass beads (0.1 m depth)	0.1	Mixed	2.3	0.018-0.022	Hydrogen		740	1.055	Miller and Logan, 2000
28 cm long 2.5 cm dia with sand (0.28 m depth)	0.28	Pure (MS2)	50	0.035	Acetate	ClO ₄ ⁻	25.6	1.280	Kim and Logan, 2001
14 cm long, 2.5 cm dia with sandy soil (0.14 m depth)	0.14	Mixed	2.2	0.5	Acetate	ClO ₄ ⁻	20	0.044	
Biologically activated carbon		Mixed	5.7	0.42	Acetate, lactate, pyruvate	ClO ₄ ⁻	50	0.262	Brown et al., 2002
0.25m long and 0.025m internal diameter (0.25 m depth)	0.25	Mixed	2.3	0.018-0.022	H ₂	ClO ₄ ⁻ (ug/L) ClO ₄ ⁻	73	0.044	Logan and Lapoint, 2002
			2.3				18,000	41.248	
							22	0.051	
						NO ₃ ⁻	21	0.048	

14 cm and 2.4 cm dia with 3 mm dia glass beads		Mixed	13.5	23.4	ClO ₄ ⁻ (ug/L)	50	0.675	Choi et al., 2007
Membrane bioreactor								
Hollow-fiber				Hydrogen	ClO ₄	1000-2500	0	Rittman, 2000
sand		mixed		Lactate	ClO ₄	100,000	0	Liu, 2000
Hollow-fiber				H2	ClO ₄	100	0	Nerenberg et al., 2002
Ion exchange membrane bioreactor (IEMB)	mixed		8.3	Ethanol (> 375 ppm)	ClO ₄	100	0	Maltos et al., 2006
					NO ₃ ⁻	60	0	

APPENDIX J

CHECKING THICKNESS OF THE BIOFILM

Diffusion coefficient of perchlorate using Wilke-Chang equation:

D ClO ₄ ⁻ (cm ² /s)	1.06x E ⁻⁰⁵	= 0.91 cm ² /d	
Feed rate (mL/s)	1.6	mL/s	= 138240 cm ³ /d
μ N-s/m ² at °C (N-s/m ²)	0.001002		= 865.72 g/cm-d
Τ= 0.0059			
Re	2.08		
S _c	946.61		
u	7040.48	cm/d	0.081 cm/s
Shear stress σ	1.372		

B_{det} = 0.101 /day b_{det} is larger than b so, S_{min} and S*_{min} bioaccumulation and substrate flux depend on factors controlling detachment

Assuming steady state assumption

S* 10

K* = 1.92 K* > 1 indicate external mass transport is not dominant control, diffusion controls the mass transport.
K* < 1 indicates high growth potential and will not be limited by biofilm accumulation unless S approaches S_{min}

S* _{min}	0.14	
alpha	1.84	
beta	0.52	
f	0.46	
S _s *	0.1	(Assumed)
S _s * _{new}	4.37	Computed
J*	10.79	
J	13.21	
L _f (for buoyancy)	0.018	cm

Assuming non-steady state assumption:

L*	0.65
L _f *	3.01
D _f *	0.8
η	0.33
S _s *	9.53
J*	0.72

check

S _s *'	9.53
φ	0.67

$$\eta' \quad 0.95$$

$$\eta - \eta' = -0.621$$

Percent accuracy 1% acceptable = 0.02

Recalculating parameters

$$S_s^* \quad 8.65$$

$$J^* \quad 2.57$$

check

$$S_s^{*''} \quad 8.32$$

$$\varphi \quad 0.72$$

$$\eta'' \quad 0.94$$

$$\eta' - \eta'' = 0.006 \quad \text{OK}$$

Percent accuracy 1% acceptable = 0.01

Thick biofilm has $\eta = 1.79$

Shallow biofilm has η close to 1

Since η is close to 1, the media starts floating when the biofilm is shallow.

CURRICULUM VITAE

Graduate College
Univeristy of Nevada, Las Vegas

Sichu Shrestha

Local Address:

1600 E Rochelle Ave
Las Vegas, NV 89119

Degrees:

Bachelor of Engineering in Civil Engineering, 2004
Tribhuvan University, Nepal

Master of Science in Civil and Environmental Engineering, 2011
Carnegie Mellon University, Pittsburgh, Pennsylvania

Dissertation Title: Perchlorate Bioremediation: Controlling Media Loss In Ex-situ Fluidized Bed Reactors and In-situ Biological Reduction by Slow-Release Electron Donor

Dissertation Examination Committee:

Chairperson, Dr. Jacimaria Batista, Ph.D.
Committee Member, Dr. Sajjad Ahmad, Ph.D.
Committee Member, Dr. Daniel Gerrity, Ph.D.
Committee Member, Dr. David James, Ph.D.
Graduate College Representative, Dr. Eduardo Robleto, Ph.D.